2022

UNDERSTANDING STRENGTH OF DRIED IRON ORE PELLETS

Victor Claremboux
Michigan Technological University, vjclarem@mtu.edu

UNDERSTANDING STRENGTH OF DRIED IRON ORE PELLETS

By

Victor Claremboux

A DISSERTATION

Submitted in partial fulfillment of the requirements for the degree of

DOCTOR OF PHILOSOPHY

In Chemical Engineering

MICHIGAN TECHNOLOGICAL UNIVERSITY

2022

This dissertation has been approved in partial fulfillment of the requirements for the Degree of DOCTOR OF PHILOSOPHY in Chemical Engineering.

Department of Chemical Engineering

Dissertation Co-Advisor:	*S. Komar Kawatra*
Dissertation Co-Advisor:	*Timothy Eisele*
Committee Member:	*Gowtham*
Committee Member:	*Lei Pan*
Committee Member:	*Tony Rogers*
Department Chair:	*Pradeep Agrawal*

Table of Contents

List of Figures

List of Tables

Acknowledgements

I would like to thank Professor Komar Kawatra for his support and guidance of my research on this project. I would like to thank the other members of my research team for their support and discussions. I would like to thank Natalia Parra-Álvarez especially helping me finalize experimental work near the end of this project. I would also like to thank Robert Lovett, who helped me with numerous things outside of academia so that I could remain focused during this time. Finally, I would like to thank my mother, who has unfalteringly supported me through my entire time at Michigan Technological University.

Abstract

After an extensive literature review, it was found that there was no reliable way for predicting the impact of binders or mixtures of binders on iron ore pellets. This is a challenging problem because iron ore pellets are a complex product of an agglomeration process which is typically controlled only to the extent that is necessary to form a quality product for ironmaking. This work identifies the resistance of a dried pellet to abrasion as a prime variable to record and analyze to understand the influence of combined pellet binders. A consistent method of measuring abrasion resistance is identified and via novel analysis shown to be highly supported by theory. In turn, this theory is used to connect abrasion resistance to compressive strength and for mixing results for application to other binder dosages. Furthermore, compatibilities and incompatibilities between a group of dispersant based binders are identified, and a methodology of understanding, categorizing, and making qualitative predictions this compatibility is also proposed. The most major conclusion is that a one-parameter model based on abrasion kinetics allows for the accurate understanding of abrasion data, which can in turn be correlated to other abrasion data with good reliability for determining the properties of mixed binders, or which can be used to estimate other mechanical properties of the pellet such as compressive strength. This provides novel insight into mixed binders using a simple test by isolating the strength contribution of the binders in the abrasion resistance.

1 Introduction

This dissertation seeks to develop an understanding of the strength of dried iron ore pellets, which is a critical stage in the pelletizing of iron ore. This work is divided into six chapters, which are intended to build onto each other to allow for as complete of a picture as possible to combine existing and new knowledge together into a completed whole.

Chapter 1 is an introduction, meant to provide sufficient information about iron ore processing as a whole to identify both the importance of pelletization and the value of creating strong pellets.

Chapter 2 goes into detail on the background of modeling pellet strength and the pelletization process overall, along with a review of the types of binders which have been previously tried. The goal of chapter 2 is to highlight the sorts of questions which arise while trying to understand the strength of iron ore pellets.

Chapter 3 covers the goals and hypotheses which apply to this work specifically. It includes the development of novel strategies for understanding iron ore pellet strength and the development of a framework to confirm these ideas.

Chapter 4 is the methods and materials section, which describes the form of the experimental work which was undertaken to confirm the results of Chapter 3. This includes a modified test for determining the abrasion resistance which is shown to have good repeatability and insight into the behavior of abrasion resistance.

Chapter 5 is the results and discussion section, which reports on and discusses the results of the work described in Chapter 4.

Chapter 6 is the conclusions, summarizing the work overall, highlighting the key results, and describing what we now know about iron ore pelletizing.

This work is in many ways only a partial examination of all the aspects of iron ore processing which I have looked at during my time at Michigan Tech. I have been blessed to have one of my papers already have been cited 62 times on Google Scholar reviewing the flotation of iron ore. I have also assisted in our group's work in CO_2 capture and utilization, which has been presented at conferences and resulted in another publication having been cited 33 times since its publication earlier this year. The focus on the dry strength of iron ore pelletization is thus, in many ways, to keep the scope narrow enough to create a singular work.

1.1 About iron ore processing

The concentration of low-grade iron ores is vital to the continued availability of iron and steel in our everyday lives (Eisele and Kawatra, 2003; Kawatra and Claremboux, 2021a; Zhang et al., 2021). The pelletization process is a vital part of the concentration of iron ore in the United States (Meritt, 1965; Society of Mining Engineering, 1966; Meyer, 1980; Mourão, 2008), South America (Stetler, 1970; Erdemli, 1982; Bandeira de Mello et al., 1996; Mourão, 2008; De Moraes and Ribeiro, 2019), and Europe (e.g. the Kiruna concentrator at LKAB). A typical iron ore concentration process involves three major steps:

1. Liberation: The iron-bearing material is crushed down until the iron-bearing minerals are physically broken away from the gangue materials, allowing them to be separated.
2. Separation: The iron-bearing materials are selectively subjected to forces which move the iron-rich minerals away from the gangue minerals. This is typically accomplished via flotation (Zhang et al., 2021).
3. Agglomeration: The concentrated iron-bearing materials are prepared for shipping, handling, and utilization in blast furnaces or in other reduction processes where it is transformed into metallic iron. This often includes an induration step (Yamaguchi et al., 2010), but which is not strictly necessary if cold-bonding routes are taken instead (Halt et al., 2015a; Devasahayam, 2018; Kotta et al., 2019).

The processing of low-grade ores is important as despite iron being the fourth most abundant element in the Earth's crust, deposits which are high enough grade to be processed directly are only sparingly available. The exploitation of these deposits have typically quickly exhausted the highest grades of available material, and prior to World War II the lower grades of these deposits were difficult to make any use of. High-Some high grade ores are still exploited and directly sold in places like Australia, but in many places these rich deposits have already been exploited and exhausted. It was in part due to the pressures of the second world war combined with the U.S.'s dwindling iron reserves at the time that pushed the development of the iron ore concentration process forward so that low grade ores like the banded hematite formations could be utilized (Kakela, 1981). In particular, because of the requirement for the upgrading of the iron ore, the small liberation sizes required to achieve that upgrading, and the unsuitability of such fine materials for other agglomeration processes, pelletization's importance soared (Meyer, 1980; Kakela, 1981; Yamaguchi et al., 2010; Kawatra and Claremboux, 2021a). In the United States most iron ores available today are low grade iron ores such as taconites, like those found in banded iron formations in the Iron Range in the Midwest and which are pelletized to make a reducible product for blast furnace processing (Meyer, 1980).

Hematite (Fe_2O_3) and magnetite (Fe_3O_4) are the most common minerals targeted for iron ores. Both are often found with silica or alumina as gangue materials, with silica being the most prominent gangue material in iron ore processed in the United States. These minerals have well established routes for concentration and reduction and are

undoubtedly the primary minerals to consider in the overall picture of iron ore production.

Goethite (FeO_2H) can also occur in iron ore formations due to the hydration of other iron-bearing species. In flotation and pelletization, goethite behaves well if accounted for as it has good interactivity with many pellet binders and flotation reagents, due to its abundance of -OH groups for bonding (De Moraes et al., 2020), but the chemically bound water means that it requires more energy to indurate and can lose more strength than the other iron ore minerals during induration (Ooi et al., 2014; Ammasi, 2019; Kawatra and Claremboux, 2021b).

Siderite is also an important iron bearing mineral and has been investigated significantly and especially in Asia. Siderite ($FeCO_3$) has significantly different surface chemistry than the other iron-bearing minerals, requiring that flotation be specialized for its presence (Zhang et al., 2021). Like goethite, siderite pellets lose more strength during induration as the carbon dioxide is calcined away (Kawatra and Claremboux, 2021b). Additionally, siderite's density is among the lowest of iron-bearing ore minerals. When calcined, it experiences a significant volume contraction which can pull the pellet away from itself. Of these minerals the overall most important industrially are undoubtedly hematite and magnetite.

For successful blast furnace processing, the barest minimum iron ore content required is around 58wt% (Meyer, 1980). Often, pellets are held to much more stringent requirements, of 62wt% iron or higher (Eisele and Kawatra, 2003). The iron content of

pure hematite is around 68wt% and the iron content of pure magnetite is around 70wt%, so in essence the portion of the material which must be an iron bearing mineral often needs to be >91wt%. Furthermore, the content of silica and alumina should be minimized, and the presence of adverse elements such as phosphorous and sulfur must be avoided. Excess silica and alumina can require additional flux to ensure good slag separation (Chen et al., 2018), and other elements can. Adverse elements such as sulfur and phosphorous interfere with the successful formation of a metallic iron product after reduction and are not easily removed. Silica is often added with common bentonite binders, which, combined with limited availability and fluctuating market conditions, has sparked interest in alternative binders (De Souza et al., 1981; Haas et al., 1989a,b; Goetzmann et al., 1988; Eisele and Kawatra, 2003; Halt and Kawatra, 2017a).

A typical taconite deposit will have an iron grade of somewhere around 25-40wt%, composed primarily of hematite or magnetite. In banded iron formations like in the Midwest, this material is finely interspersed with typically silica gangue materials, with liberation sizes of <75 μm (Meyer, 1980). These size ranges are also typical of other low-grade ores typically processed around the world (Casagrande et al., 2017; Chen et al., 2018; Zhou et al., 2018). These iron ores are among the finest materials to be processed with mineral processing techniques. An example of a typical concentration procedure proceeds as something like:

1. Crushing and grinding – gyratory/jaw crushing followed by semiautogenous or pebble milling combined with cone crushing to crush critically sized material

2. Deslime thickening – removal of extremely fine (<5 μm) materials from processing via settling, gravity separation or selective flocculation and dispersion. These materials represent an unmanageable burden on further processing steps if not removed promptly (Haselhuhn et al., 2012; Zhang et al., 2021).
3. Flotation or magnetic separation – to separate iron-bearing material via hydrophobic or magnetic characteristics of the ore. Magnetic separation is very useful for streams which are primarily magnetite, but flotation is applicable to streams containing hematite, goethite, or magnetite. Siderite requires special consideration in flotation, but it is possible to separate (Zhang et al., 2021).
4. Drying – usually by filtration, the concentrated ore is reduced to a moisture content suitable for agglomeration, which is typically 7.5-9.5wt%. Some thermal drying may be needed to reach the lower end of this moisture range. Flocculating the ore increases filtration rate but usually at the cost of higher moisture contents (Besra et al., 1998; Haselhuhn and Kawatra, 2015; Huttunen et al., 2017).
5. Pelletization – the concentrated ore is mixed with binders, fluxes, and other useful materials, and then rolled in a disk or drum while wet to form spherical pellets.
6. Induration – the green (wet) pellets are sized, dried, and heat treated to create a strong (compression strength >400 lbf or >1780 N) pellet product which is ready to be shipped to a blast furnace. Some other processes have different requirements for pellet strength and composition, but the numbers here are typical of most pellets.

An example of this kind of process is presented visually in Figure 1.1. The process shown here is specific to a hematite-rich taconite feed, such as the material which is primarily used for examination in this work.

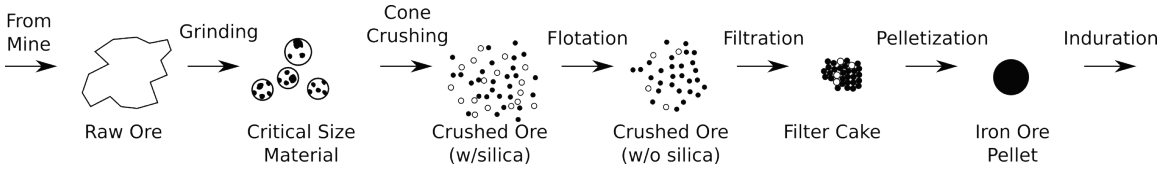

Figure 1.1 Overview of the steps in the concentration of iron ore.

Pelletization is necessary to make the finely ground concentrate easy to handle. The final diameter of iron ore pellets is typically in the range of 3/8” to ½” (9.5mm to 12.7mm). Some facilities produce larger pellets, with 5/8” occasionally being used and larger pellets still being technically possible. Laboratory pelletization usually aims for a narrower size distribution, such as 7/16”x1/2”. Industrial pellets of all sizes are typically made to have a final compressive strength of over 400 lbf (1780 N) to allow them to survive transport and to be able to be added in a structured fashion to the blast furnace.

1.2 Pellet requirements

Pellets are required to meet certain requirements relating to their physical structure. Some typical examples of such requirements shown in Table 1.1, which is also presented in my M.S. thesis (Claremboux, 2020). These properties listed in Table 1.1 are indicative of critical questions pertaining to the usability of the pellets. The numerical requirements for these tests are thus defined by the user of the pellet at each stage, up to and including the end consumer.

Each of these properties is important to the construction of a strong pellet, and each will be detailed here, but for this work the properties of interest will be the abrasion resistance and the compression strength of dry pellets. With organic binders, the conditions between the drying of the pellets and the induration of those same pellets represent the harshest conditions that a pellet will typically be subjected to. These properties are vital to the formation of a good pellet in the pelletizer, and a good understanding of how binders affect these properties leads to the ability to choose and evaluate binders more efficiently.

The final compression strength requirement is required by the consumer of the pellets. The most common number of 400lbf is required by blast furnaces so that the pellets can be loaded into the blast furnace without breaking prematurely. Weak pellets breaking can form airborne dusts which can inhibit the upward flow of the hot blast, leading to poor reduction performance and/or material losses. Therefore, final compression strength is a key parameter required by blast furnaces. Earlier pellet strengths are important for ensuring the pellet can survive induration (Athayde et al., 2018) and handling. Other reduction routes do not always require such compression strength, but higher strength typically lends itself to easier transportation either way.

Wet and dry compression strengths are vital to the process of creating the pellets in the first place. In both cases, the relatively small strengths required in these cases are so that the pellet can survive being transported to and through the induration process. For the final consumer, these properties are not particularly impactful, as they receive the final fired product instead. For the pelletizing facility itself though, meeting these strength requirements greatly improves the chances of a pellet surviving induration.

The size distribution of the pellets is important to maintaining a good stacking of pellets in any reduction process. The material in the pellets is made readily available during reduction by the proper stacking of a narrow, uniform size distribution of pellets. The narrow sizing ensures sturdy but somewhat loose packing and is one of the major advantages of using spherical pellets over other agglomerates or raw ores. Additionally, a narrow and small size distribution appears to improve induration efficiency as well (Athayde et al., 2018).

The wet drop number of the pellets is only of use to the pelletizing facility itself, as it concerns only green pellets. These pellets need to be able to survive a certain, minimal amount of handling between being formed in the pelletizing disk or drum and being transported to the induration step. Once a pellet has undergone induration, it is usually far too strong to be broken by incidental drops during routine handling. Thus, there is no particular pressure from the final consumer to develop pellets with high wet drop numbers, only from the pelletizing plant itself to avoid unnecessary material loss. Drops and impacts are still a primary factor in the chipping and abrasion of dried and fired pellets, however, even though complete breakage becomes very rare.

The thermal shock requirements of the pellet are similarly primarily of interest to the pelletizing facility itself, as the pellets only particularly need to survive thermal shock as they move from the pelletizing drum into the induration step. Several factors play into making a pellet which can survive rapid heating, including controlling the moisture content and ensuring the composition will not undergo large size changes.

Abrasion resistance, however, is of interest to anywhere that handles the pellets, as abrasion can occur even on otherwise very strong pellets. Abrasion results in loss of material to the environment in the form of very fine, potentially irritating dusts which can pose a hazard to the environment and to workers. Creating abrasion resistant pellets helps to minimize the exposure of workers to potentially harmful dust, the amount of resources required to suppress dust, and the amount of valuable material lost in the form of dust throughout the entire life of the pellet. A considerable amount of work has been put into understanding and minimizing the dustiness of both the final fired pellets and in the process overall (Copeland and Kawatra, 2005; Nabeel et al., 2016; Copeland et al., 2009, 2018; Halt and Kawatra, 2017a; Najafabadi et al., 2018).

The reducibility of pellets is a key measure of how useful the pellet is for producing metallic iron and is essentially related to the availability of the iron oxides within the surfaces of the pellets. This is helpful for all reducing processes, as highly reducible pellets ensure that metallic iron can be formed relatively quickly with good separation. Poor reducibility, on the other hand, may require that the pellet be completely melted before reduction can take place. This is particularly important in processes where slag separation is limited.

Reducibility is usually determined by the ability of the reducing gas to penetrate into the pellet without being blocked from the iron-bearing materials. For this reason, it is usually benefited by the use of organic binders (Eisele and Kawatra, 2003) which burn away during induration. Athayde et al. (2018) also suggests that smaller size distributions see more consistent oxidation of magnetite during induration, which may also correlate with

better reduction in a blast furnace. Reducibility is usually hampered by an excess of silica or slag bonding occurring during induration (). Composite pellets which can introduce the reducing agent into the pellet also tend to have better results ().

Low-temperature breakdown is a thermal shock test under reducing conditions followed by a dynamic tumble test. This is relevant to the performance of pellets as they undergo heating in the reduction furnace, and for their survivability immediately following induration.

Porosity is a measure of the void space within the pellet, which relates compression strength, abrasion resistance, and reducibility. A high porosity is correlated to high reducibility and low strengths, while low porosity may mean that it is difficult or impossible for reducing gases to permeate into the pellet. If reducibility and strength requirements are met, lower porosity would typically be desired because it allows the pellets to contain more valuable iron per unit volume.

Again, these measures are summarized and explained in Table 1.1 for convenience.

These requirements present the fundamental problems in iron ore pelletization: How do we develop a process so that pellets meeting all these requirements can be made consistently? The most important decision for most of these pellet properties is the composition of the pellet, including the binders which are used. The binders, despite being a relatively small fraction of the pellet by mass, can help determine almost all these pellet properties directly or indirectly. So how do we effectively choose a binder?

Naturally, it is best to choose a binder which creates pellets which have good structure and stability through each phase of the pellet's life. We also may be interested in using two or more binders together if they have advantageous properties: being less expensive, having a useful composition such as recycled iron-bearing fines, or having good synergy with the other binders. This motivates us to understand how to evaluate and relate the strengths of pellets to the dosage of potentially multiple binders, and how to evaluate the strength provided by the binders directly.

Table 1.1 Typical industry requirements for pellets (based on Halt and Kawatra, 2014; Kawatra and Claremboux, 2021a)

Pellet Property	**Test Procedure**	**Desired Values**
Compression strength	Green (wet), dry, or fired pellets are crushed with a compression rate of 40mm/min. The maximum load before pellet failure is recorded. The testing procedure is standardized in ISO 4700.	>22 N/pellet, green or dry >1780 N/pellet, fired
Size distribution	Pellets are sieved with screens between 6.3mm and 15mm. The testing procedure is standardized in ISO 4701.	>90% 9-12mm
Drop number	Green balls are dropped 18in (45cm) onto a steel plate repeatedly until they break. The number of drops required is recorded.	>4-5 drops (But also usually <10 drops.)
Thermal shock	Green balls heated in a preheated furnace at various temperatures between (100-1000°C) for 10min. Pellets are then removed and checked for cracks. The temperature where 90% of the pellets survive without cracking is the shock temperature recorded.	>350°C
Tumble and abrasion indices	Tumble pellets in a standard pelletization drum. Sieve on 500 mesh and 6.3mm screens. Tumble Index is the percent of pellets retained at 6.3mm. Abrasion Index is the percent of mass passing 500 mesh. Procedure is standardized in ISO 3271.	>90% pellets +6.3mm (Tumble) <5% pellets -500mesh (Abrasion)
Reducibility	Record weight loss of pellets as they are heated in the presence of a standardized temperature and reducing gas according to ISO 4695.	>0.5% min^{-1} $(dR/dt)_{40}$
Low-temperature breakdown	Size distribution of pellets is measured after a static reduction test and dynamic tumble test. Procedure is standardized in ISO 4696.	>80% pellets +6.3mm
Porosity	Can be measured in a porosimeter. (Forsmo, 2005)	Ore dependent, always <33%.

1.3 Motivation for modelling pellet strength

The importance of modeling pellet strength stems from the need to understand the impact of binders in pelletization. Pellets are required to meet a certain minimum pellet strength, which often requires adding binders to the pellet – but in turn this can add impurities to the pellet, impact its ability to indurated or reduced, increase or decrease material loss due to pellet losses and breakage, and directly impact the economics of the process. Of particular importance is that the cost of binder is second only to the cost of induration in the preparation of the pellet.

In the United States, most iron ore pellets are made with sodium bentonite, which is a phyllosilicate clay material and therefore contains silica. Since silica is also the most common gangue material removed from iron ore during concentration, and a pellet value can be significantly impacted by precisely how much silica is included in it, the addition of bentonite can negatively impact pellet value (Eisele and Kawatra, 2003; McDonald and Kawatra, 2017; Halt and Kawatra, 2017a; Kawatra and Claremboux, 2021a; Claremboux and Kawatra, 2022).

Additionally, the availability of high-quality sodium bentonite is largely restricted to the western hemisphere. High quality sodium bentonite is also used in several other industries, some of which have large, public-facing demands such as cat litter (Sposito et al., 1983; Eisele and Kawatra, 2003). As a result, there is considerable interest in the development of alternative binders to sodium bentonite.

Calcium bentonites are more widely available but are considerably less effective than sodium bentonites. This is because calcium bentonites cannot expand to the same extent as sodium bentonites as they absorb water within the pellet (Eisele and Kawatra, 2003; Kawatra and Claremboux, 2021b). Usually, a suitable dose of calcium bentonite is around double or more what the dosage would be for sodium bentonite (Forsmo et al., 2006; Zhou et al., 2016). There are methods to convert calcium bentonite to sodium bentonite, the most straightforward of which is treating it with sodium hydroxide, but due to the expense of the required reagents the cost increases significantly. This is particularly troublesome, as the relatively low cost of bentonites is a major contributor to its usefulness as a binder.

Note also that sodium bentonites readily convert into calcium bentonites in the presence of calcium ions. Bentonites can similarly adsorb magnesium, but the literature does not distinguish much between the characteristics of calcium and magnesium bentonites (Sposito et al., 1983).

Major existing alternatives often used outside the U.S. include modified starches (e.g. acid modified corn starches) or modified celluloses (e.g. carboxymethylcellulose a.k.a. CMC) (Eisele and Kawatra, 2003; Claremboux and Kawatra, 2022). These are organic binders, which can achieve similar binding strengths to sodium bentonite at significantly lower binder dosages by mass. However, they are typically more expensive to manufacture per unit mass than bentonite, so there is a trade-off between lower shipping costs (due to the lower mass and volume required) and higher product costs. Both

starches and CMC binders have a reputation for producing dustier pellets than sodium bentonite, despite achieving similar pellet strength.

Other major binders include humic acid based binders (Qiu et al., 2004; Han et al., 2012; Huang et al., 2013; Zhou et al., 2015, 2016, 2017; Zhou and Kawatra, 2017a,b; Zhang et al., 2020), or cementitious binders such as fly-ash based binders (Kawatra et al., 1998, 1999; Ripke and Kawatra, 2000; Kawatra and Ripke, 2002), molasses (Halt and Kawatra, 2014; Kotta et al., 2019), or epoxies (Devasahayam, 2018). These binders have been extensively discussed in several papers (Kawatra and Claremboux, 2021a,b; Claremboux and Kawatra, 2022).

Pelletization has often been described as an empirical process, or more of an art than a science. The value of the formation of iron ore pellets is undeniable. Iron ore pellets are in many places the primary raw material from which metallic iron is created. Thus, the development of high-quality pellets which are well-suited to forming metallic iron is important.

However, if these procedures have been successfully applied for several decades now, despite apparently relying primarily on empirical wisdom, what is the need to model their properties? Perhaps most importantly, modelling allows us to connect the empirical wisdom of pellet formation to fundamental physics, which could help pave the way for a guided approach for process optimization and the selection of pellet binders.

In addition to that, there is an open question which has not been generally addressed: how can we understand which types of composite binders will work? If someone attempts to

use two different binders instead of one in a pellet, will these binders perform better, worse, or the same as they would if they were used individually? Can we make stronger pellets with composite binders than we could with individual binders, what intuition would allow us to understand that process?

Composite binders are particularly of interest as certain materials have been found to promote or suppress the activity of existing binders, and while individually most of these processes appear to be straightforward there is little to no literature explaining the nuances of these interactions as generalities.

For example, Kawatra and Ripke (2003) tried a fly-ash based binder and succeeded at making strong iron ore pellets with it. However, when mixed with sodium bentonite, the strength of the pellets was lower than with either fly-ash or bentonite alone. This property was attributed to the necessity of fly-ash to be activated with soluble calcium, which transforms sodium bentonite into less effective calcium bentonite.

Meanwhile, mixtures of bentonite and organic binders like starch (McDonald and Kawatra, 2017), carboxymethylcellulose (Li et al., 2019), and such have been observed to have positive interactions. Li et al. (2019) reports that organic binders help both disperse and interconnect the bentonite layers and thus improving the bonding overall.

The development of a good intuition on the behavior and strengths of pellets allows for the efficient choosing of binders and materials to put in the pellet, and a keen understanding of what changes to be wary of in the pellet feed and why. Both scenarios can be leveraged to great effect when designing pellets to meet stringent grade or strength

requirements. However, a failure in understanding the situation in either of these scenarios can lead to sudden poor pelletization performance or significant loss of material. Often, issues that occur early in pelletization will become apparent after the induration step, after a huge amount of thermal energy has already been spent to try and finalize the pellets.

Having an appropriate understanding of iron ore pelletization thus has real value, at least in the sense of being able to design high quality iron ore pellets.

Another major motivating point is that historical approaches to iron ore pellet models and modern knowledge of pelletization do not readily agree on how to make good pellets. Furthermore, the most well-known models applied for pelletization in general and for pellets specifically do not implicate the effects of binders directly in any way. It should go without saying that since binders are required to form pellets which are strong enough to meet the strength requirements, that binders are inevitable in iron ore pellets. Yet, there is a distinct lack of mechanisms by which to apply our fundamental understanding of what binders are to how they will perform in pelletization. Some works do dive into specific opportunities regarding predicting and quantifying organic binder behaviors (Qiu et al., 2003), but there are several results in individual composite binders which extend past the scope of the available literature.

Some interesting results which have been noted which do not correlate well with previously available models are:

1. The utilization of dispersants to improve pellet strength (Halt and Kawatra, 2017a). This is notable because dispersants introduce repulsive forces within the pellet that should actively prevent bonding during the formation of the pellet, and thus in traditional models would be expected to decrease pellet strength.
2. The addition of calcium chloride reduces the formation of fine dust without increasing the strength or durability of the pellet (Halt and Kawatra, 2017a). This dust prevention ability is typically attributed to its hygroscopic nature, but in general abrasion behavior is ill-explained.
3. Improving the mechanical dispersion of sodium bentonite binder through the pellet significantly improves the performance of the bentonite (Kawatra and Ripke, 2002b), but chemically dispersing it before adding it to iron ore does not (McDonald, 2017). Adding sodium bentonite in addition to a dispersant improves pellet strength, but so does adding a dispersant alone (Claremboux, 2020). Existing models have difficulty explaining individual binders, never mind combinations of binders.
4. Starch can partially replace bentonite (McDonald and Kawatra, 2017), starch can be combined with dispersants (Halt and Kawatra, 2017a), bentonite can be combined with dispersants (Claremboux, 2020), but fly-ash based binders cannot be combined with bentonite (Ripke and Kawatra, 2000). What are the requirements for binders to exhibit compatibility with each other?
5. Some binders result in the formation of stronger pellets continuously as more are added, such as starch, molasses, and even bentonite (Claremboux and Kawatra,

2022). However, some binders such as sodium metasilicate improve pellet strength up to a certain point and then no more (Claremboux, 2020).

While each of these can be individually explained, these explanations are typically only narrowly applicable to the situations at hand. However, each of these results are results obtained from the same basic system, of an iron ore pellet formed by rolling concentrate in a drum. The bonding properties of each of these materials have more in common than they have differences. Ideally, these binders and their interactions can be explained in a general sense.

The goal of a useful model of pelletization is primarily to explain in a way where the natural predictions of the model provide correct insight into many different aspects of pellet formation. In this work, the focus will be on understanding how binders work to form strong pellets, primarily in the region of dried pellets before induration. This portion of the pellet's life is where most pellets are at their weakest and exposed to the greatest stresses. If a pellet can survive to and through induration, then the goal of any binder additive has been achieved.

In particular, the focus is to develop understanding which relates immediately useful pellet properties to each other and can be fed information which can be readily determined in an industrial environment. This second part heavily restricts what kinds of information can be reasonably used, as the behavior of real ores is uncontrollable and often presents very time sensitive problems to be resolved. The mathematical intuition should also, if possible, be able to be resolvable to fairly simple ideas – for example a

simple mixture of materials should be predicted by a simple mixture of a specific metric. This is, again, to provide a tool which is industrially usable, such that it is simple enough to be explained to others.

2 Background

The main questions that this work seeks to address are:

1. Can we understand how the strength of iron ore pellets are affected by binders and use that understanding to explain observations which escape traditional pellet strength models?
2. Can we isolate the impact of binders on the pure strength of the binding of the pellet material from effects which combine the strength and structure of the pellet?
3. Can we use this information to understand and predict the behavior of iron ore pellets, especially those with mixed binder compositions?

It will turn out that the key to isolating the effect of binders on the bonding strength is in understanding the kinetics of the abrasion strength, which will be discussed in full in Chapter 3. This chapter is to serve as the literature review which leads up to why the abrasion strength is an ideal metric for understanding the strength of the pellets.

There is quite a bit of information which is useful to help understand the formation of iron ore pellets and which properties can be expected to lead into high pellet strengths. The following sections focus on the critical aspects of pelletization as is required to understand the strength of the pellets. This includes:

1. The process by which pellets are formed.
2. How pellet strengths have been determined previously.

3. How abrasion breaks down pellets.
4. What kinds of pellet binders are used and why.
5. Other options for modeling the behavior of iron ore pellets during handling and under stress.

The level of detail here is targeted at providing sufficient information to allow a sense of understanding about the pelletization process as a whole and the challenges involved with modeling the behavior of binders.

There is, of course, quite a bit more information available in the literature than is presented here. However, in the specific field of understanding the impacts of iron ore pellet binders, the most pertinent works are highlighted here and in a series of review papers discussing the binders themselves in detail (Kawatra and Claremboux, 2021, 2022; Claremboux and Kawatra, 2022). Additionally, the number of papers which focus very specifically on the idea of mixing binder strengths together is quite limited – with modeling binders already being a relatively recent topic in the literature (e.g. Qiu et al., 2003, 2004), and the behavior of composite binders being a still relatively open question. Again, developing understanding composite binders is one of the fundamental points this work seeks to address.

2.1 Background of pellet formation

Iron ore pellets are formed by rolling fine iron ore concentrate around in a disk or drum. During this rolling, the water present in the concentrate forms capillary bridges between different particles within the concentrate. These capillary bridges are responsible for the rapid coalescence of disparate material into a coherent pellet seed or onto an existing pellet.

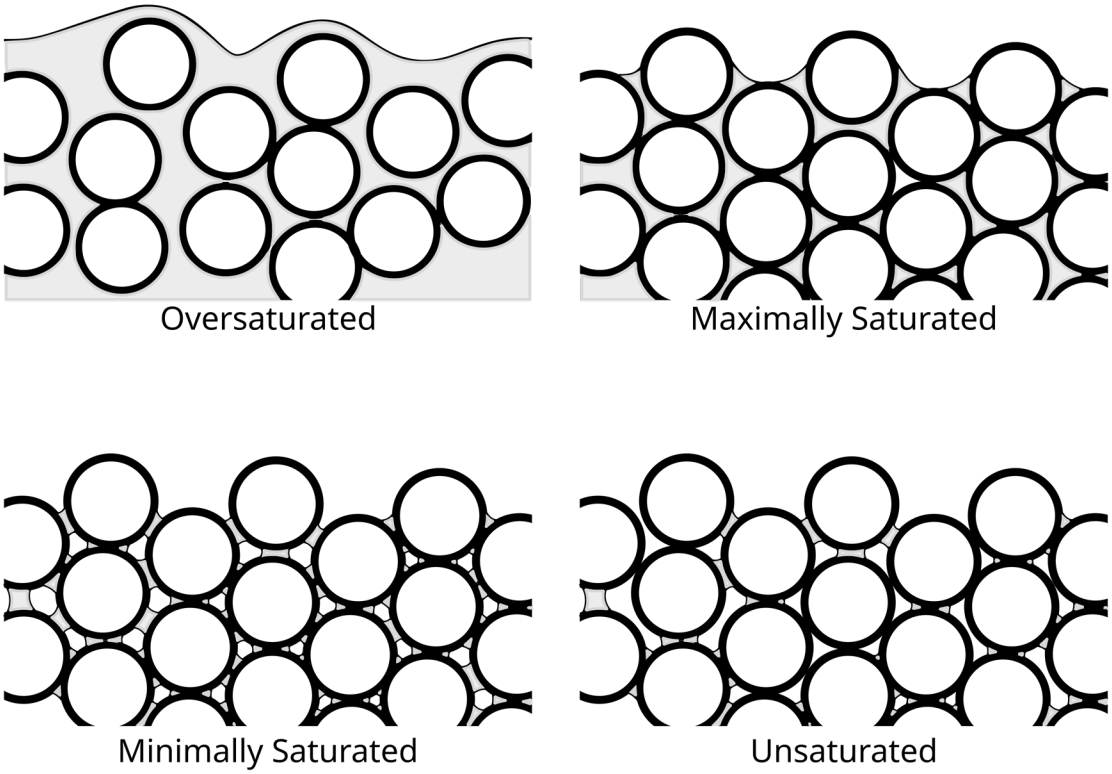

Figure 2.1: Examples of varying water saturation in a pellet. The top right scenario is ideal for growing pellets and the bottom left scenario is ideal for wet strength. The top left scenario prevents any capillary bonding from occurring.

In a wet pellet, the pore space within the pellet is partially or completely filled with a liquid binder, which is almost always water. The forces which bring a wet pellet together are the cohesion of the water and the capillary forces it provokes at the surface of the pellet (Forsmo et al., 2006).

The coalescence of the pellet is driven by these capillary actions, which allow the formation of bridges between the bulk of the pellet and new material, drawing the new material inwards. These capillary forces are present primarily where there are liquid-air interfaces in contact with the particles. As shown in Figure 2.1, an excess of water causes these interfaces to vanish.

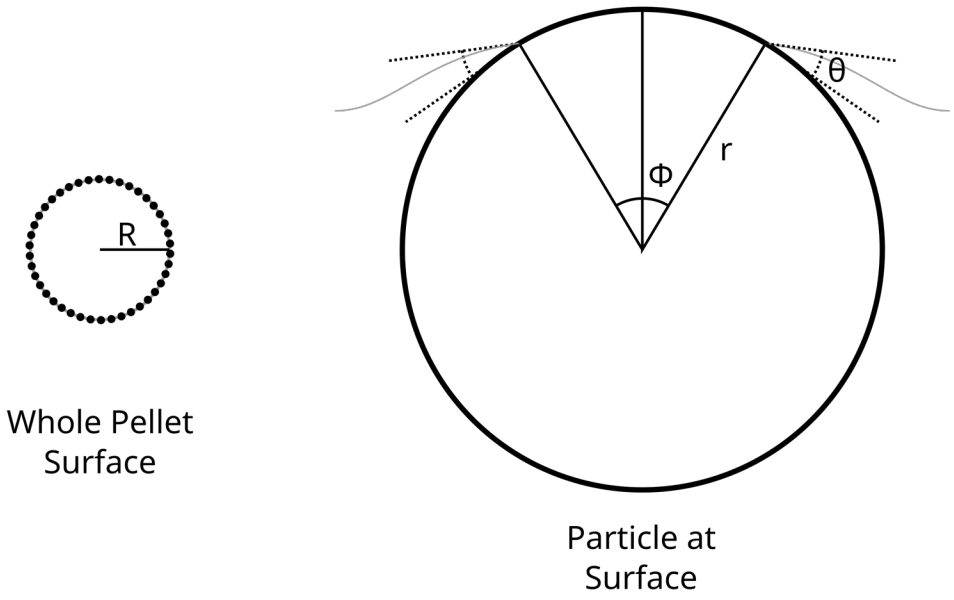

Figure 2.2: On the left, the pellet's surface is made up of many particles while on the right the interaction geometry of a single particle is shown. These particles interact with the surface via surface tension and hold the wet pellet together.

The capillary interaction occurs primarily at the surface of the pellet's water content. Specifically, the attractive force occurs where the water, solids, and the air all come into contact. The strength of this interaction is consistent for an unchanging material, and as a result the overall magnitude of the binding energy is proportional to the total perimeter of these intersections.

By assuming that the porosity is representative also of how much of the pellet's surface is exposed solid vs. exposed liquid, it is possible to derive a formula which collects the magnitude of these surface capillary interactions within the pellet. To accomplish this, we will use a geometry as shown in Figure 2.2.

First, we assume that the fraction of surface area A which must be accounted for by particles on the surface of a pellet of radius R and porosity ε is equal to Equation 2.1.

$$A = (4\pi R^2)(1-\varepsilon) \tag{2.1}$$

Then we note that the area A covered by smaller spheres of radius r at the surface is approximately the same as the area of a circle of the same radius modified by the azimuthal contact angle ϕ:

$$A = \pi(r\,sin\,\phi)^2 \tag{2.2}$$

Thus, the number n of pellets at the surface is approximated by:

$$n = \frac{(4\pi R^2)(1-\varepsilon)}{\pi(r\,sin\,\phi)^2} = \left(\frac{2R}{r\,sin\,\phi}\right)^2 (1-\varepsilon) \tag{2.3}$$

Along the perimeters of each of these smaller spheres, an inward force is applied due to capillary interactions with surface tension γ occurring along the surface of the particles at azimuthal angle ϕ and contact angle θ:

$$F = (2\pi r\, sin(\phi))\gamma\, cos(\theta) \tag{2.4}$$

This force can be multiplied by the number of particles involved and divided by the surface area of the pellet to get a binding pressure from the surface capillary effects.

$$P = \frac{2(1-\varepsilon)}{r\, sin\, \phi}\gamma\, cos\, \theta \tag{2.5}$$

This results in a formula along the lines of Equation 2.5, where P is the binding pressure, ε is the porosity of the pellet, ϕ is the azimuthal angle on the particle where the liquid line is, r is the diameter of a characteristic particle within the pellet, γ is the magnitude of the relevant interfacial tensions at the perimeter, and θ is the contact angle of the water with the solid surface.

Note that most of this result is purely geometric information about the nature of the pellet. The only binder material which plays a governing role in the formation of iron ore pellets is water, as only the capillary interactions water causes respond fast enough to have much of an impact on the growth of the pellet. While other liquid binders could be used, the economics of using any chemical besides water for this role ensures that any other choice is irrelevant for industrially produced pellets.

This result has a variety of features which align well with empirical wisdom regarding the pelletization of iron ore.

- The porosity of pellets should be minimized to form tightly bound pellets. Interestingly this means that tighter pellets are in general subject to stronger cohesion and compaction, allowing for further compaction. This is necessarily resisted by the interior structure of the pellet, of course.
- The radius of individual particles should be minimized to quickly form strong pellets. This is observationally observed even just working with different pelletizing materials. The finest pelletizer feeds can be balled successfully even with fairly little water and even entirely without binder, though the resulting pellets are not typically very strong.
- The surface tension should be maximized to ensure strong capillary interactions. This is not typically something that is strongly controlled for or observed simply because the most typical liquid binder used is water.
- The contact angle of the liquid phase should be minimized to ensure that the liquid rapidly and effectively wets the solid and ensure that capillary action is promoted well.
- Most importantly, to ensure a continuous driving force to grow the pellet, the availability of water at the surface of the pellet must be maintained. That is, the water line along the particle should maintain an azimuthal angle as close to 90° as possible.

There are also some interesting omissions from this same expression. These omissions also are well supported by empirical observations.

- The coordination number, nor any other specific measure of the geometry of the interior of the pellet, has no impact whatsoever on whether or not the pellet grows. Very bad pellets can be made during the pelletizing phase because the binding force from the capillary activity is considerably more potent than the forces available to break the pellet apart. On the scale of the pellet moving its own length, gravity provides only a very modest amount of energy. Therefore, the successful formation of a pellet cannot be taken as an indication of its quality.
- The radius of the pellet as a whole has no influence on the binding pressure. Interestingly, the forces holding a wet pellet together grow at the same rate as the gravitational forces which are providing energy to tear it apart. This means that practically there is no necessary upper limit on the size of a pellet where it will cease to grow in the pelletizer, a fact which has been observed around the world in operating plants. Occasionally, large boulder-sized pellets do form from the concentrate feed and being too large and strong to process normally must be broken up separately.

This formula is similar to formulas for strength due to capillary bonding networks shown in literature, such as in Forsmo et al. (2006):

$$\sigma_c = a\frac{1-\varepsilon}{\varepsilon}\gamma\frac{1}{d}cos\,\theta \tag{2.6}$$

Where in Equation 2.6, σ_c measures the strength of a pellet evolved due to capillary interactions, a is a constant, and d is the diameter of the particles within the pellet. One of the major distinctions here is that pellet strength is entirely independent of the diameter of the pellet. Therefore, while the driving force described in Equation 2.5 may continue to support pellet growth indefinitely, eventually the pellet will become heavy enough that it will no longer withstand its own weight. If Equation 2.5 is used to predict the pellet strength based on the critical force being equal to the binding pressure times the fracture area, then we acquire a formula as in Equation 2.7.

$$F_c = \frac{(1-\varepsilon)}{2r}\gamma\, cos(\theta)\left((1-\varepsilon)\pi R^2\right) \tag{2.7}$$

Where R is the radius of the whole pellet. If the constant and correlated terms are collected, then this differs from Equation 2.6 by a factor of $(1-\varepsilon)R^2/(\varepsilon \sin\phi)$, assuming that the radius term is not collected into the constant term in the previous equation. These differences appear to arise only from the slightly differing choices of emphasis in the geometries and treatments of the interior void spacing. The $1/\varepsilon$ term in particular arises from the treatment of internal capillary bridges in addition to the surface tension effects which arise at the surface. This is useful for discussing the overall strength of the wet pellet due to capillary bonding, as opposed to the motive force which causes pellet growth via capillary bridging.

The key takeaway here is that making pellets is easy, but that simply making pellets does not provide any reason to believe that they will be of high quality.

We also see that the ability of any binder to influence the growth behavior of pellets should be limited to a handful of possible mechanisms.

- Binders which promote the formation of pellets with lower porosities should result in faster pellet growth. Skipping ahead, this is likely achieved by the addition of dispersing compounds.
- Binders which increase the total binding pressure (such as by making the hematite more hydrophilic) should likely create smoother, rounder pellets, as the wet binding pressure is what is competing against gravity and other mechanical forces to form the pellet into a sphere. This would also typically suggest that strong dispersants likely make the pellets more spherical.
- Binders which moderate the availability of water can likely achieve more stable pellet formation. The rate of pellet growth is based primarily on the available water on the available surface of the pellet, so given optimal water conditions the growth of pellets can increase quadratically, making the system difficult to control precisely.
- Binders which make finer particles available to participate in the pellet's structure should improve pellet formation, while binders which create stable flocculated structures should hinder pellet formation.
- Binders which alter the wetting of the particle surfaces should correspondingly affect the formation of the pellets.

We can observe some of these effects during the formation of pellets. For instance, when forming pellets using calcium chloride or magnesium chloride as an additive in our own work, it was observed that it was very difficult to get the pellets to form. Calcium and magnesium ions can specifically adsorb to the surface of hematite, magnetite, and silica. In the pelletizing conditions used in the U.S., these surfaces typically have a negative surface charge on their surfaces, so the addition of these positively charged adsorbed ions results in a neutralization of this charge, allowing for coagulation to occur. This coagulation results in the characteristic size of a binding particle being greatly increased, and thus correspondingly reducing the driving force of pellet formation. The effective flocculation of the pellet material also restricts the ability of water to be removed from the pellet.

Similarly, sodium bentonite is particularly effective in pelletization because of its ability to absorb and slowly release a large quantity of water within the pellet, moderating the availability of water within the pellet's pores (Eisele and Kawatra, 2003). Bentonite allows the pelletization process to proceed more slowly and more smoothly.

The addition of dispersants to other binders does not hinder the initial growth and formation of pellets, but admittedly the overall improvement in pelletization efficiency is difficult to even be qualitatively certain of. Our current understanding of the action of dispersants is that they should decrease the pellet porosity slightly, up to around 10% (Halt and Kawatra, 2017a), so the resulting difference in pelletization efficiency should be correspondingly limited. This is in stark contrast to the immediately obvious effects of coagulants like calcium chloride.

Again, the growth of pellets is governed by the action of the surface water content. Pellets can be successfully grown without binders or other additives, but such steps are not sufficient to ensure that the pellets will be strong and resilient.

Furthermore, it should be emphasized very clearly that the binding strength of wet pellets containing binders is not derived from this same sort of capillary interaction. The binding of for example starch between particles in the pellet is quite a bit stronger than the capillary interactions between those same particles (Qiu et al., 2003). However, these same interactions can potentially hamper the growth of a strong pellet structure, as they can lock parts of the pellet in place relative to each other. This is observed directly in the work of Halt and Kawatra (2017a) and Claremboux (2020) where coagulant compounds had a strong negative impact on pellet strengths despite technically allowing the material to bind to itself more readily. Conversely from the same works, the addition of dispersants, which should actively prevent direct binding between the particles, had a strongly positive impact on pellet strength.

To summarize:

- The growth of the pellets is very important to the formation of a good structure within the pellets, but that the pellets grow is not evidence of strong long-term binding.
- The addition of modifying reagents can strongly impact the growth of pellets, and the results of such growth can be as important or more important than the actual ability of the modifier to connect different sections of the pellet together.

It is worth remembering that one of the most often cited advantages of sodium bentonite is that it helps to control the movement of water within the pellet (Eisele and Kawatra, 2003; Forsmo et al., 2006). The rapid growth of pellets, the controlled growth of pellets, and the growth of strong pellets are all separate end goals. Essentially any iron ore can be pelletized if it is fine enough and hydrophilic enough, but only with the addition of binders is good control and good strength achieved.

2.2 Background on pellet strength

Unlike the growth of pellets, which largely depends on the capillary action at the surface of the pellet, the strength of pellets largely depends on the presence of more permanent bonds internal to the pellet.

Rumpf's (1962) equation is perhaps the most well-known micromechanical model for describing the strength of pellets, relying on a handful of assumptions to provide an estimate of the tensile strength of a pellet. There are many newer models inspired by Rumpf's model, but the core analysis remains largely unchanged (Bika et al., 2001). The major differences between Rumpf's equation and newer models are different approaches to modeling the binding force magnitude, and differing treatment of geometries typically based on accounting for cracking microstructures.

Rumpf's equation is a micromechanical model that relates the tensile fracture strength of a pellet to its physical structure (Rumpf, 1962). Rumpf's equation considers the coordination number (Q), the bonding force (F), the porosity (ε), and the particle diameter (d) as the core physical variables determining the strength of the pellet (σ_T), and is presented as Equation 2.8 (Rumpf, 1962; Bika et al., 2001).

$$\sigma_T = \left(\frac{1-\varepsilon}{\pi}\right)\left(\frac{QF}{d^2}\right) \tag{2.8}$$

The primary goal of pelletization is to create a product which maintains a specific size and shape, even under considerable stresses and during shipping and handling, until it can

be effectively reduced to metallic iron. As a result, predicting the factors that go into the pellet strength is very useful for optimizing the pelletization process.

Equation 2.8 is derived by assuming that the pellet can be represented as a packing of uniformly sized spheres of diameter d and coordination number Q and porosity ε. These spheres are bridged by bonds with bonding force F. Then, for a maximal cross section across the pellet, the total strength of the pellet is determined by the force required to break every bond crossed.

In Rumpf's original derivation, the coordination number is assumed to be inversely correlated to the porosity, based on an empirical model of jarred uniform sphere packings (Rumpf, 1962). Notably, this empirical model is not entirely consistent with the rest of Rumpf's assumptions on the relevant geometry (Bika et al., 2001).

The binding force in the most often quoted version of Rumpf's equation is taken to be the capillary bridging force that occurs between wetted surfaces (Rumpf, 1962). However, the equation can also be applied to solid bridges or electrostatic interactions.

The particle diameter assumed in the original analysis is that of the most present particle species (Rumpf, 1962). These are typically finest particles in the pellet and are responsible for the numerical majority of bonds present within the pellet. The larger particles have relatively limited interactions with each other and chains of fine particles, and thus largely do not contribute to the pellet's overall strength.

Rumpf's (1962) assumption that particles are uniform spheres is also problematic. While in reality this assumption is workable for static strength analysis, the intuition it provides for the dynamics of pellet compaction during pelletization can be highly inaccurate. Perfect spheres can roll with any infinitesimal torque (Matuttis and Chen, 2014), but real particles are rough and can become caught on each other's surfaces. The compaction of real pellets can thus be highly limited by particles interlocking with each other. This affects the kinetics of the compaction, which is outside of the scope of what Rumpf's equation models but can have a significant impact on pellet strength (Halt and Kawatra, 2017; Claremboux, 2020).

Rumpf's equation is very well recognized for providing an understanding of the strength of iron ore pellets, but it also has difficulties providing quantitatively accurate results (Iveson et al., 2001). It also provides at best only very indirect and potentially misleading insight into the behavior of binders (Claremboux, 2020).

For example, when adding sodium bentonite to the pellet, which terms of Rumpf's equation are affected? Sodium bentonite is formed from small leafy platelets with small characteristic diameters, so perhaps the most appropriate place to incorporate it is in the particle diameter term. However, the amount of sodium bentonite typically added (usually around 0.66wt%) is not necessarily enough to guarantee that it has become the numerically most populous and representative species of the pellet. We can check such an assumption by considering some historical data.

It should be emphasized that while the data is historical, the data's use in explaining the shortcomings of Rumpf's equation for this scenario is novel. These works were performed with entirely different goals in mind.

Kawatra and Halt (2011) investigated the effects of increasing bentonite dosage on varying sizes of hematite and magnetite ore, including a hematite sample with an 80% passing size of 30 μm, a magnetite sample with an 80% passing size of 49 μm, and the same magnetite dry ground down to have the same 80% passing size as the hematite. The pellet behaviors of the similarly sized material were quite similar, and the coarser material performed worse in general in pelletization. The particle size of the bentonite platelets was not reported in this work. However, typically bentonite is somewhat finer than hematite or magnetite is usually ground to.

Kawatra and Halt (2011) report that an increasing bentonite dosage results in a linear increase of approximately the same magnitude in the strengths of both the fine hematite and coarse magnetite pellets. However, using a weight average of "numerically most populous" means that the coarser magnetite should be overshadowed by the presumably finer bentonite's properties far more rapidly. That the strength increase is about the same means that the fact that in the mentioned work about 6 hematite particles can be placed in the same space as 1 magnetite particle is not a major influencing factor. This is a general conclusion: if bentonite were simply supplementing the fine sized particles, then it should be far more effective with coarser ores than finer ones. Furthermore, it would not be the case that a clay-based binder needs to be an expanding or water absorbent clay. Any supplementary fine material should do, after all. Furthermore, in the alternative

interpretation that in these materials super fine hematite or magnetite is always responsible for the principle binding, then the addition of bentonite should have no impact on pellet strength, as there is no way for the bentonite to decrease the effective particle size within the pellet.

So where does the effect of bentonite appear? It would appear that the effect of the bentonite is either being counted among the geometry implied in the coordination number term, or that it is being concealed away in the magnitude of the force term. In either case, Rumpf's equation provides essentially no insight into how to handle such things as differing bentonite dosages.

How about if a soluble starch is added instead? This somewhat clearly must appear in the force term, as it does not make much sense for a soluble compound in the aqueous phase to appear in the diameter or porosity terms. More interestingly, the effects that starch has on the porosity or effective particle diameter should both be detrimental to the strength of the pellet, but it is well known that adding starch consistently improves pellet strength. The coordination number also can only vary so much (from 0 to about 12 for uniform spheres), while the continued addition starch leads to continuously improved pellet strengths (McDonald and Kawatra, 2017). Again, this is a location where Rumpf's equation does not help to make a clear and distinct decision.

What if we add a dispersant instead? In this case, the impact in the force term should be negative. When adding a dispersant to starch pellets, the impact on porosity is observed to be fairly small though significant while the pellet strength typically increases by

almost a factor of two (Halt and Kawatra, 2017a). In this case the only possible places where these effects could be accounted for is the effective particle radius from breaking up coagulated iron ore particles, or from an increase in coordination number due to better packing being achieved during the formation of the pellet. It has previously been shown that this is well explained as specifically a difference in the coordination number term (Claremboux, 2020).

This is further supported by re-examining Halt and Kawatra's (2017a) data, and accounting for each of the factors in Equation 2.8 to isolate the effects of the coordination number. The zeta potential, porosity, particle diameter, and compressive strength are all reported in Halt and Kawatra's (2017a) work, so only the binding force needs to be estimated.

In dried pellets, the binding force is typically solid bridges between particles which are formed from precipitating ionic solutes within the pellet moisture (Rumpf, 1972; Delenne et al., 2011). The strength of these bridges could plausibly depend on the ions present within solution but considering the low quantity of additives added in Halt and Kawatra's (2017) work, it seems unlikely that large variations in pellet strength could be expected. Thus, assuming that the binding force is essentially constant across all pellet configurations allows the pellets to be normalized against any single baseline case, as is shown in Figure 2.3.

Interestingly, it is not merely the impact of zeta potential alone which results in the distinction between dispersing and flocculating conditions. As I modeled in my M.S.

work, the valence of the anionic component of the anionic dispersants greatly amplifies the effect of the surface charge interactions caused at a given zeta potential. Therefore, pH modifiers which are primarily monovalent anions have a lesser impact than dedicated dispersants which are almost universally polyvalent or polymeric anionic compounds. Examples of effective dispersants shown in Figure 2.3 are listed in Table 2.1.

The most notable oddity in Table 2.1 is EDTA, as it should also potentially be a potent dispersant, especially with the amount of sodium hydroxide added. The 50:50 mixture of

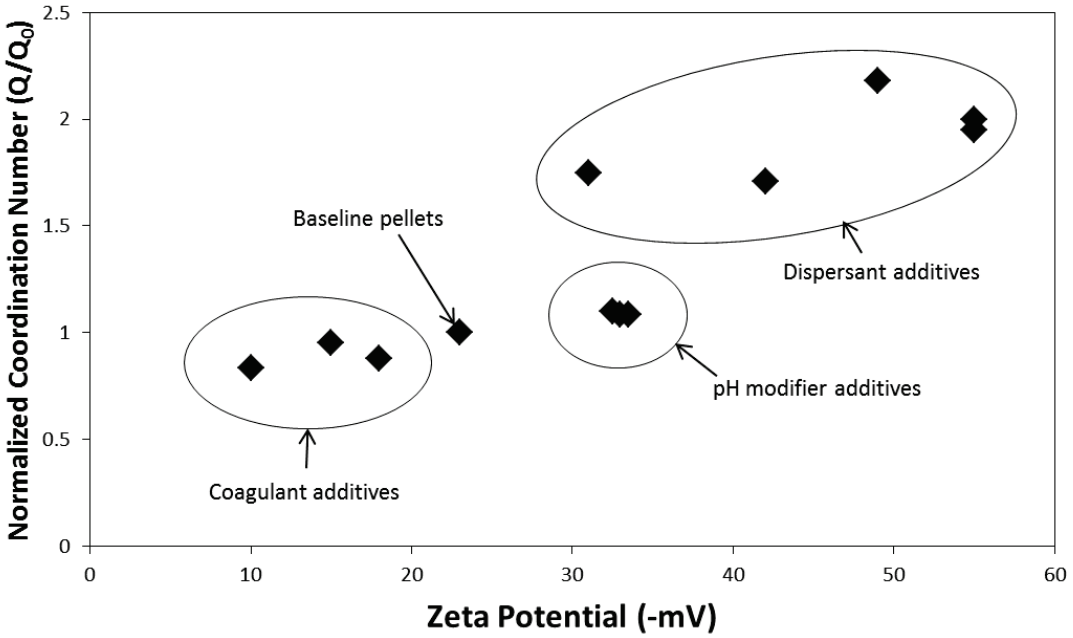

Figure 2.3 Coordination number extracted from Halt and Kawatra's (2017) data making fine hematite pellets with a starch binder and variety of coagulants, pH modifiers, and dispersants. A variety of additives was used for each category at 1kg additive/t ore dosages. A zeta potential of <30 is usually considered flocculating, while a zeta potential >30 is usually considered dispersing (Casey, 2015).

Table 2.1 Identity of binder additives shown in Figure 2.3.

Group	Additive	Observed zeta potential (-mV)	Valence
Baseline	None	23	N/A

Coagulant	Aluminum sulfate tetradecahydrate	10	+3/-2
Coagulant	Calcium chloride dihydrate	15	+2/-1
Coagulant	Magnesium sulfate heptahydrate	18	+2/-2
pH	50:50 ratio of sodium hydroxide and EDTA by weight	33	+1/-1 and +1/-1 to -4
pH	Sodium carbonate	33	+1/-2
pH	Sodium hydroxide	33	+1/-1
Dispersant	Sodium metasilicate	31	+1/poly
Dispersant	Sodium citrate dihydrate	42	+1/-3
Dispersant	Sodium polyacrylate	49	+1/poly
Dispersant	Sodium polyphosphate	55	+1/poly
Dispersant	Sodium tripolyphosphate	55	+1/-5

sodium hydroxide contains 7.3 moles of sodium hydroxide for each mole of EDTA in its acid form, so it should be able to form the tetrasodium salt which should display the -4 valence interaction. Thus, that it does not appear to display dispersing behavior is a bit inexplicable.

These results would also predict that on their own, the effect of dispersants can only account for a stepwise difference of roughly 2-fold in the pellet strength. This is supported by observations with at least some dispersant/binder combinations, such as sodium metasilicate with sodium bentonite as shown in Figure 2.4, wherein the maximum strength of pellets is not observed to increase past the initial addition of dispersant, but the fraction of pellets which display that maximal strength becomes larger instead. This is something which actually can be explained within the context of Rumpf's equation but is not an intuitive result thereof.

Instead to explain it we need to understand the impact of dispersion on the coordination number. The coordination number is a geometric term which describes how

interconnected the particles within a pellet are. For uniform sphere geometries is bound between 0 (spheres with no contact) and 12 (tightest possible sphere packing) but can vary significantly within that range based on the pellet's packing structure and porosity (Bika et al., 2001). If coordination number is the primary variable altered by dispersion and flocculation, then the strength of pellets made with dispersants will increase sharply at a point which coincides with repulsive behavior between the surfaces but will not increase significantly past that point.

The repulsion between surfaces is governed by the surface charge (σ), which is in turn determined by a combination of the zeta potential (ζ), the permittivity of the fluid (ϵ) and the Debye length within the fluid phase (λ_D) (Sze et al., 2003; Makino and Ohshima, 2010), as shown in Equation 2.9.

$$\sigma = \frac{\epsilon}{\lambda_D}\zeta \tag{2.9}$$

The Debye length in turn is shown in Equation 2.10, and depends on Boltzmann's constant (k_b), the temperature of the fluid (T), the permittivity of the fluid (ϵ), the number count of the i-th ionic species (n_i in molecules), the valence of a single ion of the i-th ionic species (z_i), and the elementary charge (e) (Sze et al., 2003; Makino and Ohshima, 2010).

$$\lambda_D = \sqrt{\frac{k_b T \epsilon}{\sum_i (n_i (z_i e)^2)}} \tag{2.10}$$

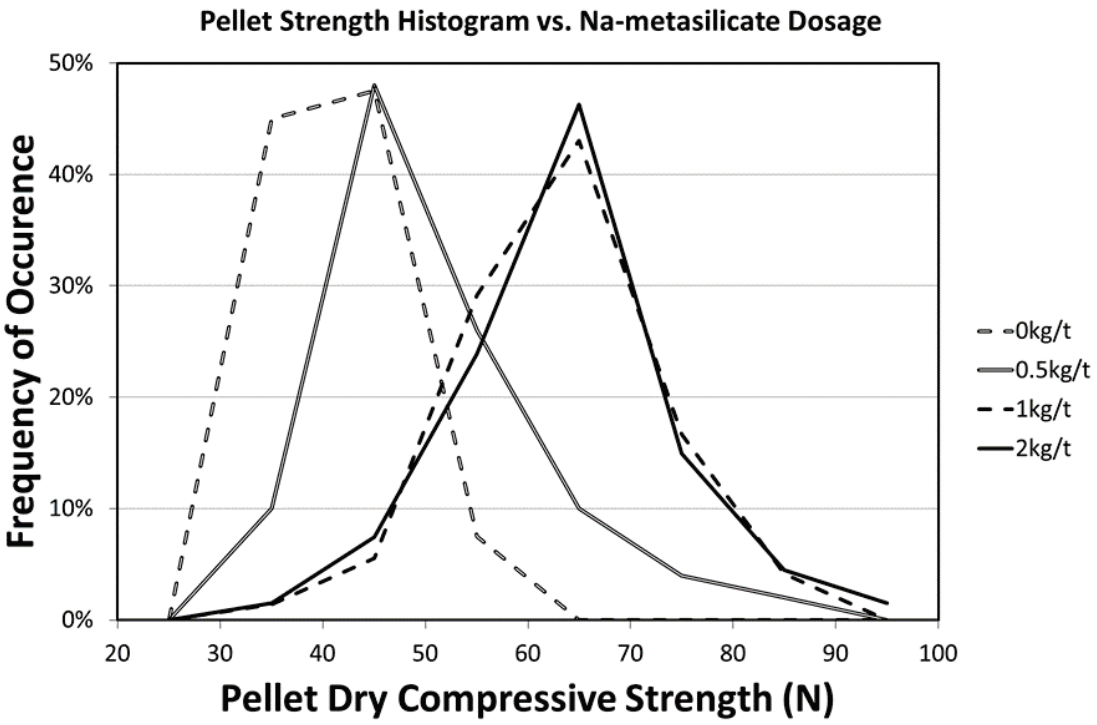

Figure 2.4 Strength histogram of sodium bentonite + sodium metasilicate pellets for varying metasilicate dosages. The frequency of high strength pellets increased, but the maximal strength did not (Claremboux, 2020).

The Debye length depends strongly on the ionic content of the solution and is significantly decreased in the presence of highly polyvalent ions such as those typically used as dispersants. This also means that at sufficiently high concentrations of ions, even relatively non-dispersing and low Zeta potential situations may develop significant surface charges. This surface charge is also inherent to the structure of the surface and can theoretically apply forces onto the pellet even after the liquid layer is forcibly removed, while. Meanwhile Zeta potential is a result of the electric double layer formed by the interaction of the surface and the liquid phase and is only present while the liquid is present.

The repulsive force between the two surfaces will be proportional to product of the surface charges, based on Coulomb's law. Despite some previous works stating that electrostatic forces play relatively little role in pellet strength (Seville et al., 1997, 2000), the results in Figure 2.3 and Figure 2.4 and an analysis of Coulomb's law at short ranges for Equation 2.3 suggest that for fine particles such as the hematite pellet feed used by Halt and Kawatra (2017) are comparable in magnitude to the attractive forces presented by the capillary bridges in the wet pellets (Claremboux, 2020). Thus, they can have a significant impact on the specifics of how the pellets form.

The coordination number is thus decreased further in the dispersion case because the particles are prevented from coming together too tightly too quickly, and instead are given the opportunity to maneuver around each other and settle into an overall tighter fit.

To summarize the current state of understanding pellet strength:

- The effects of traditional binders are not directly explainable by application of traditional pellet strength models. There are not binder specific models to explain their effects either, though there is some work in understanding the impact of the structure of organic materials in binding ability (Qiu et al., 2004).
- It is unclear how to use Rumpf's equation or its direct derivatives to predict the strength of pellets containing arbitrary binders, even as simple as sodium bentonite or starch. There are, again, no particular models to overcome this limitation of Rumpf's equation as of yet.

- It is unclear how to consider combinations of binders using Rumpf's equation, whether that be apparently simple combinations such as partial substitutions of bentonite for starch or for seemingly complex combinations such as starch and dispersants.
- The effects of some of these materials can be explained by significantly expanding on our understanding of the fundamental forces involved in pelletization. In particular, the categorical impact that dispersants appear to have based on zeta potential is something I have discussed thoroughly in the past (Claremboux, 2020).

Therefore, the key points to address in modeling iron ore pellet strength is to focus on a methodology to predict the strength of pellets which contain binders, as that has not been directly considered in as much depth as might be expected.

This will involve the development of a model which accounts for the binding ability provided by each component of the pellet. There are a few major mechanisms by which a pellet can become stronger:

One option is to improve the pellet's packing in the coordination number and porosity terms. The ideal coordination number of perfectly packed uniform spheres is 12, but much lower coordination numbers can be observed in realistic scenarios. Porosities can theoretically vary quite a bit, but in practice even similar porosities can achieve very different levels of coordination. Very high porosities result in forces being concentrated

into very small areas within the pellet, leading to high pressures which can easily cause breakage or deformation.

It is also possible to increase the strongly bound domains of the pellet. Binders improve the pellet locally around where they are physically present and make those specific areas more difficult to break. If the binding domains caused by the local effects of the binder do not span the entire pellet, then the pellet will tend to break along its weakest planes. Binders hinder these general breakage planes, making the pellet more difficult to fracture. This can often be accomplished by increasing the dosages of the binders, but the most extreme example would be induration.

Induration is an example of process to increase the overall size of the strongly bound domain. In induration, the silica is allowed to partially recrystallize and fuse, which can create an overarching “solid fused silica” domain which stretches through the pellet. This hardened silica is responsible for most of the strength of an indurated pellet. A similar effect is achieved when introducing much greater quantities of a binder which can bind to itself, as it can cement around the particles and similarly form a large binding domain which holds the pellets together.

Another option is to increase the strength of the binder’s interaction. This could mean using a cementitious binder like epoxy or molasses in place of a binder which relies mostly on van der Waals interactions or other surface effects. These can form extremely strong pellets because the binding strength of these binders is quite high. They also tend to be dosed sufficiently to form large binding domains through the volume of the pellet.

2.3 Background on pellet abrasion

The abrasion of pellets is discussed throughout literature as a major problem in pelletization (Eisele and Kawatra, 2003; Claremboux and Kawatra, 2022). There are several pieces of research from our group focusing on the measurement and mitigate pellet dustiness (Copeland and Kawatra, 2005; Copeland et al., 2009, 2018; Halt and Kawatra, 2017a; Halt, 2017). A complete theoretical understanding of abrasion is as of yet incomplete, and the development of simplified and usable numerical models remains of considerable interest (Chakravarty et al., 2019). Note that the development of a simplified and practical model of abrasion is also a major goal of this work.

Abrasion and material loss from small impacts are particularly critical as it represents the realistic use case in which most pellet material is lost (Tavares et al., 2018). Very few pellets are lost due to failures in the compression strength overall.

Abrasion refers to specifically the loss of very fine material from the surface of the pellet due to mechanical actions around the pellet. This is a difficult problem to approach from the perspective of pellet binders, as the forces involved in abrasion arise due to extreme concentrations of forces evolving on any particles which are sticking out from the surface of the pellet. If a particle with a radius of around 25 μm is sticking out of a 10mm diameter pellet with a specific gravity of 3.5, then the pressure on the contact area between the particle and the pellet due to the pellet's own mass is 36.5 MPa. For the same pellet, an acceptable dry crush strength value is 22.2 N, which over the cross section of the pellet implies a pressure of about 0.28 MPa. For a fired pellet, the

compressive crush strength over the same cross section is only about 22.4 MPa. Thus, even in fired pellets, it should not be expected that abrasion can be completely prevented without either increasing the cross-section of the attachment or preventing the existence of outlying material.

If pellet binders are only expected to create pellets to withstand compressive forces on the order of a quarter to half a megapascal of pressure, then how can we hope to prevent abrasion where the forces evolved by the pellet on itself are so much stronger?

There are models to describe how pellet breakage and fracture occur, and what the results of such fractures are. Models describing the population balances around attrition or abrasion processes were also developed quite early (Sastry and Fuerstenau, 1977a).

The population balance model is useful for investigating abrasion processes, and essentially consists of a continuum of mass balances over a regime of input variables. The full population balance model as it applies to the pellet growth process consists of several terms, but for abrasion alone only one term is necessary. The earliest, general, pure abrasion population balance is shown in Equation 2.11 below (Sastry and Fuerstenau, 1977a).

$$\frac{\partial n(m,t)}{\partial t} = \frac{\partial}{\partial m}\left(R(m,t)n(m,t)\right) \tag{2.11}$$

Where $n(m,t)$ is the numerical quantity of particles of mass m at time t, and $R(m,t)$ is a function describing the rate of attrition.

If $R(m,t)$ is not allowed to vary with time, reducing it to $R(m)$, then it turns out that there is a general solution to this partial differential equation. First, let us remove the dimensional quantities from the equation by applying $\tau = t/k$ and $\omega = m/\Omega$, where k and Ω are characteristic rates and masses of the system, whatever those may end up being. Then we have, after some rearrangement:

$$\frac{\partial n(\omega,\tau)}{\partial \tau} = \frac{\partial}{\partial \omega}(R(\omega)n(\omega,\tau)) \tag{2.12}$$

We can safely assume that R does not vary with time in a consistent system because R should be dependent only on the physical laws governing the system and the availability of forces within that same system. If we are modeling an abrasion process which is being applied continuously without changing the availability of forces, then the consistency of physical laws means that the elimination of the time dependence should be a non-issue.

If we define a related rate function, $r(\omega)$ such that $r'(\omega) = 1/R(\omega)$, we can rearrange Equation 2.12 into:

$$\frac{\partial n(\omega,\tau)}{\partial \tau} = \frac{\partial}{\partial \omega}\left(\frac{n(\omega,\tau)}{r'(\omega)}\right) \tag{2.13}$$

Utilizing Wolfram *Mathematica* as a computer algebra system, it can be found that this equation has a solution of the following form:

$$n(\omega,\tau) = \Phi\big(\tau + r(\omega)\big)r'(\omega) \tag{2.14}$$

Where $\Phi\big(\tau + r(\omega)\big)$ is an arbitrary 1-dimensional function which is determined by the initial condition. This means that all solutions to the abrasion equation are of the form of stretching or shifting the initial conditions of the equation. We can pin the shifting onto the term $\tau + r(\omega)$, meaning that we can relate an initial condition ω_0 to all future conditions by the same term:

$$r(\omega_0) = \tau + r(\omega) \tag{2.15}$$

Which can be differentiated and rearranged as:

$$r'(\omega_0)d\omega = d\tau + r'(\omega)d\omega \tag{2.16}$$

$$\frac{d\omega}{d\tau} = \frac{-1}{r'(\omega)} = -R(\omega) \tag{2.17}$$

Equation 2.17 is actually quite convenient to have, as it verifies that the population balance model directly connects to the kinetics of a single pellet in an intuitive way.

We will also evaluate one special case of Equation 2.14 for later convenience, assuming that $R(\omega) = \omega$. The general case can be rewritten as a shifting of an initial size distribution:

$$n(\omega, \tau) = n(\omega_0, 0)f(\omega, \tau) \tag{2.18}$$

Where, for the specific case that $R(\omega) = \omega$, it can be verified that the following values result in the appropriate solution:

$$\omega_0 = exp(\tau)\,\omega \tag{2.19}$$

$$f(\omega, \tau) = exp(\tau) \tag{2.20}$$

This solution is pulled out separately because it will be useful later.

Tavares et al. (2012) describes the kinetics of the breakage of fired pellets by considering the probability of fractures occurring. Tavares et al. proposes a model in which when a pellet is dropped, it may either break or be abraded. In the latter case, it accumulates damage (due to for example the formation of small cracks) and becomes weaker. The chance of a particle breaking in any given drop is governed by a probabilistic process. Pellets which do not reach their required fracture energies in a single drop undergo some amount of abrasion and damage until repeated drops eventually causes pellet failure.

Notably, Tavares et al. (2012) suggests that the fracture energies of fired pellets can typically be described by a log-normal distribution, which is a potential useful target for understanding the breakage of dry pellets as well. Tavares et al. also assumes in their analysis that the fracture energies of pellets of a given size are consistent regardless of their origin (whether the pellets were grown to that size or reduced to that size by breakage).

We would naturally expect that the behavior of the particles making up the pellet are governed by how they are positioned relative to their neighboring particles. The abrasion of the pellet cannot inherently depend on purely the position of a particle within the pellet, but instead must depend on the relationship between a particle and its neighbors.

Despite a perception in industry that organic binders lead to the formation of dusty pellets, there is a limited amount of work discussing the mechanisms by which dusty pellets are formed in the context of the behavior of pellet binders. For fired pellets at least, the fact that organic binders are incinerated during the pelletization process would seem to imply that the loss of pellet strength is unavoidable while using organic binders. However, previous work by Halt et al. (2017a) has shown that the structure of the formed pellets is typically more important than the actual physical presence of the binder in the final pellet.

2.4 Background on pellet binders

There are many pellet binders which have been tested and investigated. There has been significant investigation into the specific mechanisms of how the binders work, and considerable effort put into comparing their effectiveness. The point of this all of course is to come up with pellet binders which help the pellet meet their strength and composition goals.

Table 2.2 Commonly used binders in iron ore pelletization (based on Kawatra and Claremboux, 2021b; Claremboux and Kawatra, 2022)

Name	Comments	Typical Dosage (kg/t)	References
Sodium bentonite	Most commonly used in U.S, provides good control of pellet moisture	5.0-6.6	(Ripke and Kawatra, 2002a; Eisele and Kawatra, 2003; Forsmo et al., 2006)
Calcium bentonite	Often outside of U.S. Does not disperse as well in pellet.	10-20	(Eisele and Kawatra, 2003; Fan et al., 2011)
Soluble lime compounds	Cementitious binder and flux. Incompatible with bentonites due to calcium.	2-20	(Pal et al. 2014; Wang et al. 2020)
Corn starch	Readily available, requires some processing to reach maximum effectiveness.	1.0-6.6	(Eisele and Kawatra, 2003; Halt and Kawatra, 2017a; McDonald and Kawatra, 2017)
Carboxymethyl-cellulose	Trade name: Peridur. Commonly used in South America. Often contains tripolyphosphate as a dispersant to control calcium and magnesium.	1.0-4.0	(De Souza et al. 1981; Goetzmann et al. 1988; Quon and Kuriakose, 1990; De Lima and Chaves, 1993; De Moraes et al. 2018; Lu et al. 2018; Li et al., 2019)
Sodium tripolyphosphate	Strong dispersant, used with other binders to control water hardness or as a binder on its own.	1.5	(De Lima and Chaves, 1993; Cassola and Chaves, 1998; Halt and Kawatra, 2017a,b; De Moraes et al. 2013, 2018)
Polyacrylates and polyacrylamides	Several trade names: Dispersol, Floform 1049 V, Alcotac. Strong dispersant used for water softening.	0.2-1.5	(Srivastava et al., 2013; De Moraes et al., 2018)
Modified humic acids	Trade name: Funa. Prepared from coal via causticization and modification of humic/fulvic acid ratio.	1.5	(Qiu et al., 2004; Han et al., 2012; Huang et al., 2013; Zhou et al., 2015, 2016, 2017; Zhou and Kawatra, 2017a,b)
Molasses	Cementitious binder, usually used with some calcium source.	30-80	(Halt and Kawatra, 2014; Halt et al., 2015; Kotta et al., 2019)

The key binders which have at least at one point seen significant use or interest in industry are detailed in Table 2.2.

However, Table 2.2 is in no way to be taken as an exhaustive list of pellet binders. Even the trio of review papers we prepared on different types of pellet binders (Kawatra and Claremboux, 2021a,b; Claremboux and Kawatra, 2022) should not be taken as an exhaustive list of all possible pellet binders, even if restricted to only those which have in any way been tested.

The truth of the matter is that almost anything that can be found in a pellet can be characterized in some way to describe how it will interact with the pellet. Some major and obvious characteristics include those which summarily prevent a material from being an effective binder:

1. A material which does not disperse throughout the pellet will not be effective as a pellet binder. There are numerous examples of materials which have either been attempted to be used as pellet binders and were ineffective at improving dry strength for this reason but particularly non-expanding clays (Eisele and Kawatra, 2003), including colemanite (Sivrikaya et al., 2013). Insoluble organic materials also behave poorly as binders in most cases for this same reason.
2. A material which cannot form bonds with the pellet material is also clearly unsuitable for use as a binder. However, few materials truly fall into this category. The options for binding with the pellet are quite wide: even extremely short range van der Waals interactions can be a non-trivial binding effect, though this is often

only capitalized on by the raw concentrate material itself containing ultra-fine hematite or silica. Most industrially used binders bind via hydroxyl or carboxyl groups, sometimes based on inorganic backbones like Si-OH in bentonites or metasilicates.

Essentially any other material can be used as a binder with some level of success. A notable example of a binder with an interesting mechanism begins with bentonite itself. Bentonite clay is usable as a binder because it is an expanding clay which forms a strong binding network within the iron ore as it expands (Kawatra and Ripke, 2002b, 2003; Eisele and Kawatra, 2003).

Sodium bentonites in particular break away from themselves as they absorb water, greatly dispersing into the pellet during that process (Eisele and Kawatra, 2003). A typical sodium bentonite has a plate water absorption capacity of around 8-11x its mass in water. This results in significant expansion within the pellet and during the wetting phase, and the bentonite does not contract away from the pellet particles during the drying process. Instead, it forms a backbone throughout the pellet, and given the opportunity can form long fibers within the pellet (Kawatra and Ripke, 2002b, 2003).

Sodium bentonite's effective availability can be improved by approximately a factor of two by modifying the mixing technique to ensure the formation of these fibers. Ripke and Kawatra (2002b) demonstrated that by using roll mixing the formation of these fibers could be mechanically induced. They found that by using such mixing the effective dosage of sodium bentonite could be reduced by approximately half without sacrificing

effectiveness. Roll mixing was achieved using a roll mill with a gap separation wide enough such that no material was crushed or ground but narrow enough to allow the falling material to be mixed by the roll.

Calcium bentonite is economically available in more parts of the world, but when used in pelletization its effective availability in the pellet is significantly lower than sodium bentonite's. While calcium bentonites are still water absorbent, it is often on the order of only 3x their weight in water. More importantly, calcium bentonites do not separate from themselves as they absorb water (Eisele and Kawatra, 2003). This greatly limits the dispersion of the calcium bentonite material through the pellet, requiring higher dosages to make up the difference. Correspondingly, the typical dosage of a calcium bentonite is often double or more than the typical dosage of a sodium bentonite (Eisele and Kawatra, 2003; Zhou et al., 2016; Kawatra and Claremboux, 2021b).

Bentonites are primarily composed of phyllosilicate materials, which is advantageous in firing because the silica re-crystallizes and forms the main backbone of the fired pellet's strength. However, it is disadvantageous from the perspective of creating a concentrated iron ore product. What is the point of spending the energy on grinding, the capital on the equipment to reduce the iron ore to its liberation size, the cost of operating the crushers and magnetic separators or flotation cells and hydrocyclones in this process to remove silica if up to 2.0wt% of a silica-bearing clay is just going to be added into the final pellet?

If the minimum possible dosages of bentonite are used, such as the 3.3kg/t that was used successfully by Ripke and Kawatra (2002b) achieved by using a roll mixed sodium bentonite with a material that was naturally somewhat amenable to pelletization to begin with, then it is probably not a huge matter to add that bit of silica back into the pellet.

However, sodium bentonites also readily pick up calcium cations and convert themselves into calcium bentonites (Eisele and Kawatra, 2003). As part of our groups' work on the flotation and filtration processes, we have found in multiple instances that calcium cations are an unavoidable fact of life in process water. The presence of calcium and magnesium for values typical in our laboratory research during this project specifically are reported in Parra-Álvarez et al. (2021) and Kawatra and Claremboux (2021b). These values are reproduced below for completeness:

Table 2.3 Abundance of calcium and magnesium in process water in our laboratory and in the facility the majority of our material used in these projects originated from. Values determined by ICP-MS.

Species	**Concentration in Laboratory Tap Water (Houghton, MI)**	**Concentration in Plant F Laboratory Water**
Calcium	62 mg/L	3.2 mg/L
Magnesium	13 mg/L	1.4 mg/L

It has also been shown that calcium and magnesium can become super concentrated during the filtration process, as calcium and magnesium preferentially bond to hematite or magnetite instead of leaving with the water (Ripke and Kawatra, 2003; Eisele et al., 2005). This can result in calcium and magnesium concentrations in the filtrate moisture of upwards of 5000 mg/L.

So even if efforts are taken to use specifically sodium bentonite, then its potential efficacy in the pellet is naturally limited in the pellet by the fact that it will encounter calcium or magnesium and be converted into less effective calcium or magnesium bentonite in short order within the pellet.

Even if efforts are taken to eliminate all calcium and magnesium in the process water, the ore contains a non-trivial amount of material as well. In a mass balance developed for this same iron ore bearing material (Parra-Álvarez et al., 2021), we determined that even before crushing down to liberation size the ore itself must (at least at the time we collected it) contain around 0.185wt% calcium and 0.335wt% magnesium to begin with. While part of this calcium and magnesium is likely not available to dissolve the pellet moisture, it is likely that at least some of it is available enough to interact with the typical 0.66wt% dosage of sodium bentonite.

In short, sodium bentonite should be an even better binder, for an unrealistic material which is completely devoid of calcium or magnesium. If pellets are formed from material which has been washed several times with distilled water to remove the calcium and magnesium cations, this is indeed observed (Ripke and Kawatra, 2002a, 2003). It is also possible that this is a part of the reason for consistently improved pellet performance observed in mixtures of bentonite and dispersants. However, in realistic materials in the absence of materials to limit the presence of calcium and magnesium, sodium bentonites cannot exhibit similar dosage performance to other binders.

This observation is phrased in that fashion for a reason: there is no fundamental reason why any given binder should, if effectively dispersed, require a significantly higher dosage than another binder to achieve similar performance if it has comparable binding strength. The mechanism by which bentonite binds parts of the iron ore pellet together is actually very similar to organic binders such as starch or carboxymethylcellulose (Claremboux and Kawatra, 2022). In all cases the material forms bridges between separate particles within the pellet via hydrogen bonding-type interactions, thus improving the structure of the pellet. The strength of two different hydrogen bonds need not be the same and do vary quite a bit (Qiu et al., 2003), but it would be very strange if they were to differ by a significant fraction in this sort of scenario where similar types of hydrogen bonds are being observed in similar media.

Then, why does sodium bentonite require a dosage of 5.0 kg/t to 6.6 kg/t to achieve the same kind of pelletization performance as a typical organic binder like corn starch? The density of sodium bentonite varies based on its moisture content but is often between a specific gravity of 2 and 3 when dry. At the highest moisture loadings its density should approach the density of water, which is similar to the dry density of most carbohydrates like starch or carboxymethylcellulose. As such, the difference in required dosage is not merely due to requiring higher mass to achieve the same volume loading within the pellet.

The conclusion of this train of thought then is that the dispersion of bentonite throughout the pellet must be limited somehow. Potentially this is merely due to the bulkiness of individual bentonite platelets limiting the rate at which they expand through the pellet.

Potentially this is due to the rapid conversion of sodium bentonite to calcium bentonite even within the pellet moisture. Potentially both effects occur and are significant contributors to the comparatively high necessary dosage for effective binding.

As mentioned, the binding mechanism of starch is quite similar to the binding mechanism of bentonite. Soluble starches spread throughout the pellet and coat the particles within the pellet bridging them together (Halt and Kawatra, 2017a; McDonald and Kawatra, 2017; Lu et al., 2018; Claremboux and Kawatra, 2022), which is essentially the same idea as the bridging promoted by bentonite fibers (Ripke and Kawatra, 2002b). Carboxymethylcellulose also bonds similarly, though the binding is less all-encompassing than starch (Yuan and Zhang, 2018), but has been noted to have very good synergy with bentonite binders resulting from the formation of compound structures which further enhance the dispersion of the bentonites (Li et al., 2019). Essentially, it has been observed that the carboxymethylcellulose can bind to the outside of the bentonite platelets and peel them away from the bentonite bulk.

While Table 2.2 mentions 6.6 kg/t as a potential typical dosage of starch, the lower bound of 1.0 kg/t is what is typically used to match sodium bentonite pellets for strength. Partial replacement of 6.6 kg/t bentonite by 1.0 kg/t of starches has been attempted and found to be quite successful in maintaining pellet strength (McDonald and Kawatra, 2017).

Like bentonite, starch and carboxymethylcellulose are quite sensitive to calcium and magnesium cations. Most recently, our group has thoroughly established that a small amount of calcium and a very small amount of magnesium can activate starch for

adsorption onto hematite surfaces (Parra-Álvarez et al., 2021). However, the addition of a greater amount of calcium or magnesium immediately inhibits the possibility of selective flotation performance. We believe the mechanism of this to result from:

1. A reduction in the selectivity of the absorption of starch, minimizing the distinction between hematite and silica. Starch is naturally selective towards hematite more-so than silica, which is a property that is exploited to selectively depress hematite during flotation processes (Zhang et al., 2021). However, the addition of excess calcium or magnesium would appear to make the silica and hematite surfaces more similar for the purpose of starch adsorption, and thus decrease the separation possible in flotation. This would have little impact on binder performance, however, as improving the adsorption of starch to silica or hematite would improve the structure of the pellet either way.
2. A general reduction in the availability of starch, by causing the starch to flocculate with itself. This removes active starch from the solution, as it is either precipitating out of solution or at least has all its active bonding sites in use sequestering calcium or magnesium. This would significantly affect the performance of pelletization because starch which is not available to bond with the pellet materials is useless for the formation of a strong pellet, even before firing.

Looking only at the effects of calcium and magnesium in flotation, we were not able to determine which of these two mechanisms were occurring. However, the materials involved in the flotation of iron ore and the pelletization of iron ore are not different. As

such, this work can tangentially comment on this: calcium and magnesium do not improve pellet strength in the presence of starch, so mechanism 1 does not contribute positively enough to the strength of pellets to be of interest in pelletization. However, the presence of calcium and magnesium also appear to make pellets worse on their own, and the amount of strength decrease due to calcium and magnesium vs. calcium and magnesium in the presence of starch is not particularly different. Thus, mechanism 2 is not particularly supported either. Of these it is more likely that an excess of calcium and magnesium simply causes starch to be less selective in binding to hematite over silica, and the detrimental effects to pellet strength in starch pellets are not due to sequestering starch but instead due to the coagulant properties of calcium and magnesium.

Calcium and magnesium are also certainly incompatible with dispersant additives. Most dispersants are very effective chelating agents which are particularly selective towards polyvalent cations such as calcium and magnesium. Dispersants have also been reported to be extremely beneficial to the strength of starch-containing pellets (Halt and Kawatra, 2017a), to carboxymethylcellulose containing pellets (De Lima and Chaves, 1993; Cassola and Chaves, 1998; Halt and Kawatra, 2014), and to bentonite containing pellets (Claremboux, 2020). This work will also show that even those which exhibit no special performance as binders by themselves are still effective for improving the strength of pellets on their own. There are a few mechanisms proposed for why dispersants improve binder strength:

1. They improve the fundamental structure of the pellet by allowing it to compact better during pelletization (Halt and Kawatra, 2017a; Claremboux, 2020). This is

because it prevents the material within the pellet from becoming caught on itself and locked up in otherwise loose and porous configurations, as flocculants would tend to cause. Instead, particles are allowed to move and rotate somewhat freely, since the repulsive force between the individual particles is a relatively "squishy" electrokinetic potential instead of a hard rigid-body interaction of a solid. This is an effect that we have previously suggested is a step-change between flocculating and dispersing conditions (Claremboux, 2020). Such a step change is observed in both historical and continuing experimental data.

2. They improve the dispersion of other binders within the pellet (Claremboux, 2020). In other words, the separation they induce between particles within the pellet during the pelletization process allows for binders to more cleanly and more rapidly move through the pellet. This should correspondingly improve the mixing of the binders with the pellet and improve bonding in that way.

Note that in the second option the other binders need not be materials intentionally added to the pellet. Ultra-fine materials in the iron ore, such as colloidal hematite, can also serve as a very good binder if they can be mobilized. This effect has been suggested as a binding mechanism for some particularly potent dispersants, including tripolyphosphates (de Moraes et al., 2013).

Cementitious binders are often explored for cold bonding purposes, which avoids the induration step entirely. This is an important alternative, as induration is one of the largest usages of energy in a pelletization plant, on par with comminution (Halt and Kawatra, 2014). However, a major downside of cold-bonding is that binders for cold-

bonding usually require much higher binder dosages, such as the 30-80 kg/t dosages shown for molasses in Table 2.2. Cold bonding was not directly investigated in this project, but the trends found in this research are expected to extend to or at least inform of the behavior of cold-bonded pellets.

2.5 Other options for modelling pellets

There are a couple of big categories of pellet features which have received significant attention in modeling, and which have resulted in about four separate approaches. This section will review them in detail, but the primary takeaway of this part of the literature review is that there are essentially no existing methods for accounting for binders directly and in a generic fashion.

2.5.1 Population balance models

Firstly, the growth and failure behavior of large swarms of pellets have been investigated via population balance models. Population balances are mass balances over populations of similar but distinct species, such as pellets of a given size. Key literature for the development and early application of population balances to pelletization kinetics are the works of Kapur and Fuerstenau (1964, 1969), Sastry and Fuerstenau (1970, 1971, 1972, 1975, 1977a,b), and Sastry and Gaschignard (1981), wherein the basic interactions available to pellets are be examined and understood. These works primarily focus on the development of a quantitative understanding of the kinetics of pellet growth, and these are occasionally used for the investigation and understanding of plant scale kinetic behaviors (Cross et al., 1970; Kapur et al., 1981; Abouzeid and Fuerstenau, 1982). By

1985, the application of population balances as a method of modeling granulation processes was well established (Ramkrishna, 1985).

A simple population balance for the abrasion case was presented in section 2.3, but similar models exist for four other mechanisms within pelletization as well. All five mechanisms of pellet evolution together are:

1. Abrasion – the loss of very fine particles from the surface of the pellet due to mechanical damage occurring while the pellet moves.
2. Breakage – the loss of macroscopic chunks of the pellet due to mechanical damage resulting from impacts or other mechanical failure within the pellet.
3. Layering – the acquisition of very fine particles due to the presence of capillary interactions at the surface of the pellet.
4. Coalescence – the acquisition of macroscopic particles or other pellets due to the presence of capillary interactions between them.
5. Nucleation – the spontaneous generation of macroscopic particles by the engulfment of fine particles by a large water droplet.

Layering and abrasion have the same form, which was given in Equation 2.11. The difference is that the rate function in the abrasion term has a sign which causes the pellets to become smaller over time, while the rate function in the layering term has a sign which causes the pellets to become bigger over time.

Like with the abrasion equation, the rate function (also referred to as the kernel in other works) in the layering equation is at least partially determined by how exactly the

material required to grow the pellets is made available to the pellets. An example of a common assumption is that the material is always available via a constant supply and the rate at which it is picked up by any given pellet is proportional to that pellet's surface area. Unlike the abrasion equation, the layering equation needs to account for the impact of water content implicitly or explicitly, as layering does not occur at all in dried pellets.

Like the abrasion equation, the layering equation predicts that any given size distribution of seed pellets is only shifted and stretched or squished by the layering process. There are no pellet-pellet interactions which cause the fundamental shape of the distribution to be changed in any way.

Coalescence is a generalized case of layering. The coalescence equation determines the rate at which pellets of size $x + y$ are created based on the availability of pellets of size x and of size y individually. It has a form as follows, from Sastry and Gaschignard (1981):

$$\frac{\partial n(m,t)}{\partial t} = \frac{-1}{N(t)^{2-\kappa}} F_d(m,t) + \frac{1}{2N(t)^{2-\kappa}} F_c(m,t) \tag{2.21}$$

Where F_d describes the rate at which pellets of size m disappear at time t (due to being consumed to form larger pellets) and F_c describes the rate at which pellets of size m appear at time t (due to being formed from smaller pellets). κ is a parameter which is 1 for locked systems (like pelletization) and is 2 for free systems (such as aerosols). The forms of these terms are:

$$F_d(m,t) = \int_0^{\infty} \lambda(m,m')n(m,t)n(m',t)dm' \tag{2.22}$$

$$F_c(m,t) = \int_0^{m} \lambda(m',m-m')n(m',t)n(m-m',t)dm \tag{2.23}$$

Where $\lambda(m,m')$ is the rate at which pellets of mass m and m' combine. This equation does not readily admit an analytical solution, but robust problem formulations and numerical solution methods have been devised (e.g. Sastry and Gaschignard, 1981; Verkoijen et al., 2003; Immanuel and Doyle III, 2005). The limiting form of the coalescence equation for a large quantity of fine material behaves similarly to the layering equation, especially if interactions between particularly massive pellets are taken to be unlikely.

The coalescence equation allows the fundamental shape of the pellet size distribution to change, based on the interactions of pellets of differing sizes with each other. The coalescence equation generates wider size distributions over time than its input. This is because if a size distribution contains pellets of size m_1 and size m_2, then coalescence can create pellets of sizes $2m_1$, $2m_2$, and $m_1 + m_2$. Additionally, not all the material will be instantly converted. In this way, 2 possible sizes of pellets become 5 possible sizes of pellets. This argument also applies to continuous size distributions since the results for any size distribution can always be broken up into a linear combination of the point-by-point distributions, at least on an instant-to-instant basis.

The coalescence equation also provides very little insight on its own into the strength of pellets. While it can be useful for understanding how pellets grow statistically, like all

population balance equations it is simply a mass balance over the possible varieties of pellets. There is no fundamental insight into whether pellets of a given category are strong or not.

The breakage equation is the opposite of the coalescence equation, simply reverse the meaning of F_c and F_d. This equation is actually far more problematic than the coalescence equation, however. Whereas in the coalescence equation, if only two species of pellet masses are present, there are only five possible species available in the immediate next instant. However, with the breakage equation starting from a single mass species it is immediately possible to acquire any species with less mass. For example, a pellet of mass 10 can break into a pellet of mass 2 and 8, or 3 and 7, or 5 and 5, or 6.7 and 3.3. All these possibilities are equally valid from a statistical perspective.

However, only one breakage option out of all possibilities can happen at a time. If a pellet of mass 10 breaks into two pellets with mass 5, then this precludes the possibility that a pellet of mass 6 exists. In this way, the breakage equation as a population balance is statistically meaningful but divergent when trying to inspect a specific instance of breakage. The statistical approach would insist that no matter how much time passes, a pellet of mass 8 could potentially exist, but in this scenario where a mass 10 pellet undergoes breakage, the instant more than 2.0 mass worth of broken pellets appear then there can no longer be such a pellet.

Note that while the breakage equation necessarily has an interpretation that lends itself to understanding pellet strength, the statistical nature of the breakage equation means that it

is somewhat hard to tie pellet size distributions directly to strength values using it. Furthermore, there is a full dimensional component of free variables in the likelihood that a pellet of arbitrary mass m breaks into a pellet of m_1 and $m - m_1$. Thus, there is a distinct difficulty in being assured of the connection between a predicted size distribution and an individual instance of a size distribution from an experiment which could be tied back into a measurement of the pellet strength.

Nucleation is a simple equation again, $F_N(m)$, which gives the rate at which new pellets are formed at a given mass. This function would be chosen to match the appearance of new pellet nuclei almost entirely due to water droplets coming into contact with the fine material.

These models can all be combined as linear combinations of each other, forming a partial differential equation involving integral terms. The solution of such an equation is complicated analytically, but by understanding that the meaning of the equation is to represent the mass balances of all possible types of pellets makes approaching the numerical solutions much more reasonable. There are numerous limitations to the 1-dimensional approach where pellet mass is the only variable accounted for: among other things, it cannot account for the effects of changing water content (Iveson, 2002). This is particularly important, as pellets tend to lose water as they roll in the drum, and the growth of pellets is very dependent on maintaining a consistent water content on their surfaces.

By adding additional dimensions to capture the variables of interest, the ability of the population balance equation to capture more of the real phenomena increases significantly (Iveson, 2002; Poon et al., 2008). A carefully chosen approach, perhaps based on the volume of each material in the pellet including the void space, as proposed by Verkoeijen et al. (2002) could easily be adapted to include information about the effects of binders in the rate kernels.

However, their ability to predict the effects of binders is limited. The meaning of the coalescence kernel is slightly ambiguous, and the interpretation of the breakage kernel is muddied by the holistic statistical approach of the breakage equation. The only population balance equation which has a clear physical interpretation that can be related directly to effects involving the pellet's strength is the abrasion equation.

In summary, these equations are useful for modelling the kinetics of pellet growth and breakage on a large scale but are not very helpful for understanding the impacts of pellet binders. They can be used as a basis for quantifying some of the effects of pellet binders in wet pellets, but their predictive ability in this regard is low. However, the quantification of these effects is still very useful, as population balances can be used to summarize and isolate the key statistical quantities of a large number of pellets at once.

2.5.2 Discrete element method

Discrete element method is a direct physical simulation approach for systems with finite numbers of particles. Each particle is assigned a location and momentum in space, and the equations of motion are solved over a series of timesteps for the particles with all

possible interactions with each other. Whenever particles collide or otherwise exert forces on each other, their momentums are correspondingly updated, and the simulation continues. By stepping through this process systematically and rigorously, the hope is that the true physical characteristics of a complicated system can resolved using only information about the basic material properties of the system.

There have been some very successful applications of discrete element method to simulating pellet flows throughout industrial processes (e.g. Wang et al., 2015; Silva et al., 2018) and some dedicated efforts to determining appropriate parameters and necessities for simulating iron ore pellet motion (Barrios et al, 2013; Coetzee, 2016, 2017).

These results have shown that with an accurate estimation of the material properties of green or dried pellets and an appropriate choice of model parameters, it is certainly possible to accurate predict the flow of pellets through a process. Naturally, since the input parameters to these models can be directly related to the mechanical forces acting on the pellets, it would be quite tempting to try to use these numerical methods for the simulation of the interior of pellet.

That is, why not use discrete element method to simulate the behavior of a pellet based on the individual constituent grains instead? From there, the behavior of the particles should be described by first principles and it should be possible to determine the pellet behavior from only fundamental interactions, shouldn't it?

With present technology, it is probably technically possible to simulate the life of the particles in a singular pellet for a meaningful amount of time. It simply is not worth it. There are several challenges posed by the application of discrete element method to the ab initio prediction of pellet properties which do not apply to the issue of predicting pellet motion or behavior in general.

Firstly, one particularly glaring difference between pellets and the particles that make up the pellets is the size distribution of particles of importance. With full sized pellets, where discrete element method has been successfully applied, the difference in size between the largest pellet and the smallest pellet is, after pellet growth, ideally around a factor of 1.5 to 2. Even accounting for realistic deviations from this ideal, the smallest pellet tracked as a pellet is likely only 10% of the radius of the largest pellet tracked as a pellet.

If examining the components that make up a pellet fundamentally, however, size distributions are readily available in the literature showing that these particles have sizes covering two orders of magnitude or more (e.g. Kawatra and Halt, 2014). That is to say that particles smaller than 1 micron and larger than 25 microns coexisting is completely expected in the simulation of the particles within an iron ore pellet. This is an important aspect of the properties of a pellet, but is computationally troublesome to work with due to the wide size differences to be modeled.

This poses an issue which is perhaps not intuitive outside of highly detailed numerical simulations. Let us detail the process a bit further: when simulating two particles, a general outline of a single timestep proceeds as follows:

1. Check if any pair of particles are touching.
2. Apply forces to any intersecting particles to accelerate them away from each other based on their overlap and transfer momentum/torque between the two particles.
3. Based on the accelerations calculated from the forces in step 2, calculate the new velocities and positions of every particle for the given timestep.

The important part to notice here is that while collisions are only checked at each time step, if the particles end up moving too quickly relative to each other they may end up moving through each other without registering as a collision. This can be partially mitigated by using far more complicated methods of checking for particle path intersections, which even assuming perfect uniform spheres greatly increases the complexity of the problem. However, there is still a limit to how effective this can be:

The larger particles can be expected to be more than fifteen thousand times more massive than the smaller ones, even if a relatively narrow size distribution is assumed. A contact force between a large particle and a small particle will result in an acceleration of over 15,000 times more on the smaller particle than the larger particle. Or, correspondingly, any numerical error accumulated on the smaller particle's position is 15,000 times greater than the numerical error accumulated on the larger particle's position. Since computers have finite precision available to them, both particles will encounter some degree of numerical error, and as such neither of them has a completely inconsequential amount of error. 15,000 times the minimal possible error is actually very significant in single precision floating point arithmetic, but this can be avoided by using more precise forms

of math readily available in computing. However, it is still a concern evolved from these very large differences in particle sizes and must be accounted for in these simulations.

However, this vast size disparity also has strong implications about the choice of timestep to be used. Again, we must ensure that particles move little enough in each time step that they do not pass through each other, at least if we want to ensure that our system is converged as it should be physically. Or, equivalently, we want to ensure that the results of integration do not wildly diverge when the timestep changes slightly, and a bare minimum requirement of that is that particle collisions that the integrator does not believe happens at one step size do not suddenly begin to happen at some slightly smaller step size. This problem is mostly exacerbated by the number of particles involved.

So let us assume for a moment that we are interested in modeling just a pellet sitting on a surface in this fashion. The particles are stacked on top of each other, subjected to short range binding forces of some variety which hold the pellet together, and every particle in the pellet is simultaneously subjected to a uniform downward acceleration due to gravity.

If the pellet begins at rest, then after one time step only the bottom particles immediately touching the bottom surface are subjected to any change in acceleration. The next time step another layer of particles above that may begin to feel the change in acceleration. And again for each subsequent timestep, until the particles in the pellet are all back in equilibrium and the movement of the pellet re-stabilizes to zero. For physical accuracy, which should be taken as a base requirement of system stability, there is a minimum

speed at which this force information should be transmitted through the pellet: this is the speed of sound of a pellet. The speed of sound represents the speed at which mechanical forces can be transmitted through a material, and the speed of sound for most crystalline materials which could compose a pellet is on the order of kilometers per second.

Let us assume generously that this simulation only needs to be able to accurately transmit wave information at one kilometer per second, for a pellet which is 12.7mm in diameter, and for particles which are, say, 25 microns in diameter. If we assume that a central tower of particles exists directly in the center of this pellet, that means that there are 508 of these 25 micron particles on top of each other, and that the maximum timestep which could be allowed for this to be physically accurate is determined as follows:

1. It takes 12.7mm / (1km/s) = 12.7μs for the pressure wave to transmit across the diameter of the pellet.
2. It transmits one-by-one through 508 particles to do so, requiring at least 508 time steps, meaning that each time step is at most 25ns long.

Since the interesting pellet properties are those which are observable on millisecond to second to minute scales, this means that there are at the very least 40,000 time steps to be taken between the beginning of a simulation and seeing anything of interest. Note that each halving of the minimum particle size halves the minimum acceptable timestep for this problem.

Note that because this problem is due to the transmission of information rather than numerical accuracy, this is also not a timestep issue that can be readily overcome by

simply using a more sophisticated timestep based integrator. While higher order integrators can certainly help still, getting the accurate wave propagation velocity will require the use of very small time steps. However, again this is a surmountable problem on its own. As an example, André et al. (2012) approached the mechanical wave propagation problem in a solid medium via discrete element method and found that these properties were well predicted with good input information.

However, the time scales of interest for any interesting information about a pellet are vastly longer than the time scales involved in accurate modelling of mechanical wave propagation in a pellet. However, without the latter, it is impossible to even begin to trust the former. After all, for pellet strength especially, it is clearly observable that:

1. Pellet breakage is clearly a phenomenon resulting from mechanical wave propagation, as it is clearly a result of pressure build-ups within the pellet due to mechanical actions.
2. Pellet breakage can take a very long time, on the order of multiple milliseconds if the crack grows slowly enough. This is occasionally observed experimentally when performing compressive strength tests on dried pellets and is the default mode of operation for wet compressive strengths.
3. Abrasion occurs in significant quantities over several minutes, and so is even more difficult to directly address via these methods.

Not allowing force to propagate entirely through the smallest particles in the system also means that the smallest particles may end up in extremely improbably configurations,

such as entirely embedded inside of larger particles. This results in more excessive restitution forces which amplifies the problem caused by the high acceleration rates on the smaller particles even further.

However, each time step also allows numerical error due to rounding errors to propagate one step further, which in turn means that having too many time steps means that the results become less trustworthy as well. On its own, the effect of time steps would be proportional to the number of timesteps taken and the scale of the rounding error being applied. Unfortunately, this is a many-body problem in a very tightly packed situation, so the result is undoubtedly going to express some chaotic tendencies. Chaotic is used here to refer to an extremely high dependence on the initial conditions such that error propagation will inevitably become exponentially different from an arbitrarily close alternative initial condition.

On the bright side, chaotic does not necessarily imply locally divergent. It is likely that, for an appropriately small time step, the results of such an integration would at least be physically meaningful over time. They would be different based on extraordinarily minute differences in the input condition. This is only mildly troubling because there is an associated experimental difficulty in producing two identical pellets – namely, that for iron ore doing so is essentially impossible. Without the ability to produce and compare identical pellets, it is also pretty much impossible to experimentally identify and confirm issues posed by the chaotic nature of the problem. This is perhaps the most surmountable issue yet on the theoretical side. The numerical error itself is concerning though, as it is

most likely to manifest in the finest particles being somewhere they probably should not be.

We should also note that uniform spheres are a terrible approximation for the particles within a pellet. If the particles are to exhibit realistic physical properties, then most of the properties they would acquire by being perfect spheres are as far from that as possible. The most immediately obvious issue is that a pile of perfect spheres cannot stack – there is no angle of repose such that a shallower stack of uniform spheres will successfully hold themselves up indefinitely. Since pouring a sample of hematite pellet feed onto a flat surface will form a cone of material, this immediately shows that the perfect spheres assumption is not ideal. The angle of repose is determined in part by the frictional and elastic properties of the material, but also in large part by the geometry of the particles.

So, what shape are the particles in an iron ore pellet feed? Abazarpoor and Halali (2017) and Abazarpoor et al. (2017) clearly show that it depends on, among other things, the grinding mechanism. HPGR and ball mills present very obviously different shape characteristics with the iron ore alone. This has been observed to have a considerable impact on pellet properties, some of which are relevant to pellet strength (van der Meer, 2015). The shape distribution of iron ore pellet feed is, however, only vaguely studied. Abazarpoor and Halali (2017) report less than a dozen particle shapes and only in 2-dimensional form based on SEM imagery. It is unclear how transferrable such information is, or how accurately a 3-dimensional version of those shapes could be reconstructed.

Additionally, the handling of binders in this scenario also requires detailed information about how the shape of the binders influences their motion within the pellet. While several binders are fairly well characterized in this regard (e.g. starch would dissolve and could be treated as a long molecular chain following molecular dynamics simulations), the characterization of some of the most common binders is lacking in ways that would be satisfactory for this form of modeling. For instance, despite a fairly extensive literature search, there is relatively little concrete quantitative information on how much bentonite swells during the hydration process and the shapes it goes through as it does so. Such information would be invaluable for truly understanding its motion through the pellet feed but is practically very difficult to acquire.

Water also poses a considerable challenge to this process, as there is not a clear appropriate approach to bring the fluid behaviors brought out by the water into harmony with the mathematical approach for the solid materials. A basic approach may be to construct a fluid mesh at each time step and apply computational fluid dynamic methods to the mesh to determine the water's contribution to the pellet's motion but ensuring convergence of CFD methods is tricky enough when the mesh is constant. Combined with the difficulty of determining measurable, useful, consistent statistical parameters for wet pellets, making it at present very difficult to ensure that there is a good correlation between physical reality and the mathematical procedure, the computational effort is difficult to justify.

Another common issue with discrete element method is that it is often too precise – or rather, too focused on minute details to make the whole picture clear. In some ways, this

can be helpful in challenging our assumptions about what we are measuring, but it can also be quite misleading. As an example, consider how to calculate the porosity of a pellet. In reality the typical procedure is to measure the density of the pellet via some method and compare it to the expected density of the materials composing it, via a variety of methods. But to determine the bulk density in discrete element method, a choice must be made regarding a volume of interest.

A representative volume within the interior will give reasonably consistent results, but "representative" can be tricky to define. It needs to be significantly larger than a single particle, so that a single particle cannot completely occlude the entire volume and give an apparent porosity of exactly 0. It cannot contain too much space which is clearly exterior to the pellet, otherwise the apparent porosity will tend to 1. Moving the representative volume within the sample ideally does not significantly change the measured porosity, no matter which way it is moved. Measuring the porosity with an expanding sphere originating at the pellet's center of mass seems to give consistent results, but do not necessarily correlate well to observed behavior when assuming perfect spheres. It does highlight that the variation of porosity through the pellet may be several percentage points from the average porosity. There is also the question of how much extra space at the surface is counted or not counted by experimental tests and in theoretical considerations.

Of course, for a question about pellet breakage, another very interesting question is "given a random plane through the pellet, what is the porosity along that plane?" This is a question that is well suited for discrete element method, but the interesting parts of the

question particularly apply to anisotropic pellets. Anisotropic in this case meaning pellets where the properties of the pellet strongly depends on the orientation of the pellet. An example of a highly anisotropic pellet-like object would be a stack of coins, which can easily slide past each other on two axes but not at all on the third. However, discovering anisotropic behavior through discrete element method would again require a strong focus on determining the shape distributions of the particles forming the pellets.

To summarize, the reasons why discrete element method is difficult to apply to iron ore pelletization are as follows:

1. The iron ore pellet contains a very wide range of particle sizes, necessitating special measures to decrease error propagation including very small timesteps and careful choice of numerical methods. Thus, the computational effort of even a simple simulation is considerable.
2. The iron ore pellet contains an unknown distribution of shapes of particles, even assuming pure materials, necessitating guesswork on the geometry involved. Uniform spheres are a usable assumption for a small number of pellet properties, but fail to capture the mechanical behavior of the real material even in the simplest of cases. Determining the shape distributions present in iron ore would be a tremendous undertaking in and of itself, and if alternative methods provide reasonable estimates of the properties of interest to begin with it may not be an easily justified endeavor.
3. The presence of water adds a tremendous amount of computational complexity, meaning that the simulation of wet pellets (and correspondingly pellet growth) is

extremely complicated, and it is unclear how such simulations, even if successfully computed, would be correlated with reality.

4. Particular care must be taken when extracting statistics from discrete element method work, and particular care must be taken when examining empirical statistics meant to correlate with those theoretical ones. In particular, determining when a pellet breaks is also a difficult endeavor in discrete element method, since it is not always entirely clear that bonds are broken from the information which is easily visualized from the discrete element method results.

Practically speaking, my own experience with discrete element method is that the complexity of the pelletization system is high enough and there are enough free parameters which cannot readily be nailed down that discrete element method is simply not yet prepared to answer questions about complicated microstructural effects, especially binders.

Probably the most major point which could help make discrete element method attractive would be the formalization of the concept of shape distributions for microscopic discrete element methodologies. Unfortunately, this is a very in-depth project on its own, and not one I identified in full early in this work. Ideally, this would include the measurement of shapes found in the iron ore particles, a formalization of a method of retaining and sharing this information, and the development of a framework to utilize this information. Preferably, this could be done for at least a few iron ores under a few grinding conditions and perhaps a few binders as well. This would allow a great deal more confidence to be

had in the application of discrete element methodologies to the prediction of iron ore pellet behaviors.

However, considering that most of the time iron ore pelletizers are interested in general results that apply broadly to their pellet feed, which can rapidly respond to changes in the ore feed or other such empirical difficulties, the extreme detail of discrete element method is not as attractive in general.

2.5.3 Machine learning methods

As applies to iron ore, machine learning methods primarily refers to artificial neural networks and such. Machine learning is essentially highly sophisticated, highly responsive model fitting techniques, which have great applications in many, many fields. The use of these techniques has generally been successful in developing usable models for predicting and controlling specific facilities. Some such successes include Dwarapudi et al. (2006), Dwarapudi and Rao (2007), Fan et al. (2012), and Miriyala and Mitra (2020).

The nature of an artificial neural network model is to take a vector of data X as an input and apply a series of linear and non-linear transformations to it with adjustable parameters w until a vector output Y is well fit. In essence, it is the automatic construction of an $f(X, w) \approx Y$ where w can be varied so that for a set of input X values a corresponding set of Y values are well fit.

A typical linear transformation is matrix multiplication, where the values within the matrix are members of w. Ideally, this allows the mixing of the input data in various amounts, emphasizing or de-emphasizing certain linear features or trends in the data. A typical non-linear transformation is the sigmoid function, which transforms any input number into a number between 0 and 1 with an S-shaped curve. Even just these two transformations, when combined across several layers, are capable of fitting essentially any data set.

However, the introduction of large numbers of parameters (such as all of the w values previously mention, along with potential bias values at each layer) means that being able to fit anything is the expectation, not in the most general case a meaningful result. The meaningful value of artificial neural networks comes from generating fits with good fitting parameters even with parameter sets that are far smaller than the data set being trained to, and which results in a good fit even on test data which the model was not specifically fitted to.

There are numerous methods by which to construct these functions and find their fitting parameters. Artificial intelligence and machine learning are very fast paced fields, with a tremendous amount of supporting infrastructure and computer programs which allow for the rapid handling of very large datasets and very complex models very efficiently. Furthermore, the most remarkable applications of these models have shown them to be incredibly powerful in many domains, and the results shown in iron ore processing also seem to agree with that.

However, these models do have some significant limitations which make them ill-suited for the goal of this work. One, they require a very large amount of data to verify that the fit is actually fit to the trends being modeled rather than just an arbitrary exact fitting of the data using the degrees of freedom provided in the parameters. Two, they provide very little physical insight into anything beyond "parameter X influences result Y".

A natural thought with artificial neural networks is that each transformation contains some natural meaning where the proper weights clearly help identify meaningful components of the original data set. For the vast majority of models, it has been found that this is generally not what occurs. Weight parameters are typically chosen randomly or semi-randomly and then refined using algorithms such as gradient descent with backpropagation, which results in often random looking parameters in w all throughout. Dissecting any individual layer is made more ambiguous by the fact that often the outputs of an individual layer (which are also vectors like the inputs and outputs of the overall network are) are typically exactly re-orderable, so long as the weights of the following layer are appropriately modified to make use of the re-ordering. Mix in two or three of these hidden layers which allow any such re-orderings and can re-mix any such re-orderings however, and it becomes clear that having a simple and straightforward explanation of what a neural network is doing is an exceptional case.

Thus, despite having exceptionally good fitting ability for large data sets, their use in fundamental work is somewhat limited. They are useful for identifying if a data set contains enough information to make a fit work at all, which is particularly useful with

many-dimensional data being fit to many-dimensional outputs, but they cannot necessarily provide insight into what the appropriate fit would be.

It is for this reason that this work does not focus heavily on machine learning approaches. However, it is certainly highly recommendable for industrial applications, where having a highly effective model is often just as useful for practical matters as having a highly explanatory one.

3 Goals and Hypotheses

From here on out, we work to develop a novel method of understanding the strength of dried iron ore pellets. We seek to clarify the behavior of dried iron ore pellets specifically, with the following reasoning:

1. The drying stage is one of the weakest stages of the iron ore pellet's life. Although they are physically less resilient in the green ball phase, they are readily capable of reforming due to the availability of water. While they are also weaker during the induration stage, it has already been shown that binders which promote good iron ore pellet structure will lead to strong fired pellets (Halt and Kawatra, 2017a). Furthermore, fired pellets can be made stronger as necessary by altering the firing temperature (McDonald, 2017), and the heat load implications of the addition of surface-active binders are minimal compared to the heat load implications of ore variations (Kawatra and Claremboux, 2021b). Even more so, the vast majority of interesting alternative binders do not survive the induration process, so everything interesting that they do to the pellet simply must occur before the induration step to begin with.
2. The dry pellet stage is also the stage where binders have the greatest impact on the performance of the pellet, and thus the stage where the greatest gains in optimizing binder performance can be had. Starch clearly has no special role in the induration of pellets and yet can make perfectly acceptable fired pellets, but the potential to replace silica-containing bentonite with corn starch can be a

> significant economic opportunity for a pellet plant where high quality bentonite is unavailable or for whom a slight decrease in silica could allow them to sell their pellets at a higher price. In either case, so long as pellets which are strong enough to survive induration can be made, the choice of binder is often quite open.

Thus, this project seeks to clarify the behavior of dried iron ore pellets so that the factors which go into making good pellets at this critical stage can be clearly identified and subsequently quantitatively analyzed and predicted.

In doing so, this project hopes to clarify:

1. That the necessary traits of a pellet binder, as laid out in the background section, are appropriate for the estimation of the binder's performance, both individually and in some varieties of binder mixtures.
2. The breakage parameters of iron ore pellets are well correlated with each other and can be sensibly predicted using each other or information regarding the structure and mechanisms of the binders and pellet materials together.
3. That the behavior of pellets during various types of breakage can be treated in a predictable fashion given only information about the pellet feed material and the binders in use.

In other words, this project seeks to show that an effective pellet binder can be chosen, and that a known pellet binder contributes a known amount of strength to the dried pellet. To the best of our knowledge, a quantitative undertaking of this process has not previously been performed. In particular, during our literature review of iron ore pellet

binders (Kawatra and Claremboux, 2021a,b; Claremboux and Kawatra, 2022), there has been no particular explanation forthcoming for the quantitative behavior of the pellet binders reviewed.

Other reviews of iron ore pellet binders also did not provide insight into a mathematical methodology for understanding the strength of iron ore pellet binders (Eisele and Kawatra, 2003; Halt and Kawatra, 2014). A review of major pellet strength models (Rumpf, 1972; Bika et al., 2001; Iveson et al., 2001) clarified how to approach pellet strength but provided no mechanism for modeling the effects of binders on pellet strengths.

Even previous work in this group focused on quantifying the impact of binders on iron ore pellet strength relied only on empirical models (Halt, 2017). Speaking personally, this author notes that essentially the only available model to build an understanding from is their own prior work (Claremboux, 2020), which identifies primarily that dispersion and flocculation are two major and distinct regions in pelletization behavior.

There has been meaningful work in quantifying the impact of specific functional groups in the development of organic binders (Qiu et al., 2003), but while it provides significant insight into the design of the binders themselves it does not directly connect this quantification all the way back to measurable pellet properties.

From these points, the author believes that the novelty and practicality of this project are clearly identified:

1. Despite extensive literature review, the mathematical handling of how to understand pellet binders seems to be sorely lacking, at least in the context of iron ore pellets. This is especially true of composite binders, referring specifically to binders composed of two or more separate materials.
2. The value of understanding how to minimize binder usage should be immediately evident, as this allows for both better product grades and lower operating costs. The value of understanding how to choose pellet binders to make strong dry pellets should also be immediately obvious. Even in the worst-case scenario that the pellet binder turns out to be active during induration in an undesirable fashion, a solid baseline understanding still allows us to avoid selecting binders which had no chance of success to begin with.

Coincidentally, this project will also help to establish a framework for understanding how to approach pellet breakdown, and that existing tests for these properties have strong theoretical backing that allow their values to be linked together. This is also novel, while providing a strong theoretical framework to justify a simple but effective test of pellet abrasion. It also allows the connection of abrasion resistance to pellet strength by treating the pellet breakdown as an irreversible energetic breakdown.

There are also some open questions which arise from related physics in other parts of the iron ore concentration process which the behavior of iron ore pellets may be able to

clarify. Where possible, these will be highlighted, and we will take advantage of the fact that these materials are handled in so many distinct ways while undergoing the same overall physics to clarify what potential mechanisms may be at play.

3.1 The strength of an iron ore pellet is consistent

Let us begin with a bold claim that applies to iron ore pellets in general. We want to say that the strength which holds the iron ore pellet together is a consistent property which applies to many types of breakage, not just the one that it is measured against.

Now, to back off on the strength of this claim just a little bit: real iron ore pellets have a tremendous amount of internal structure and variation. This is not to say that a real iron ore pellet has a singular, uniform, evenly distributed strength. Nothing could be further from the reality when investigating an individual pellet: each pellet has its own unique defects, cracks, or instances of catastrophically poor mixing.

However, we can assume that any decently formed pellet has a somewhat decent amount of mixing, and that pellet breakage will almost certainly occur somewhere along the pellet's weakest planes.

We can also assume, following the footsteps of even the earliest analyses such as Rumpf (1972), that the fundamental informative action about pellet breakage is the energy required to pull two parts of the same object away from each other. The tensile strength of an object is cleanly predictable for a basic model of an iron ore pellet and represents the minimal amount of energy required to pull two parts of it apart. While Rumpf's

derivation is often considered to be an inaccurate model of compressive strength, speaking quantitatively (Iveson et al., 2001), it is typically because it omits necessary frictional terms that appear during compression testing.

Fundamentally, the most general form of a strength model based on this energy formulation is something like:

$$F = \sigma A \tag{3.1}$$

Where F is the force required to overcome the binding, σ is the binding pressure, and A is the area over which the binding is being broken. This is directly reminiscent of the measurements taken during compression testing of iron ore pellets. In such a case, σ can be approximated by taking the peak force at the breakage point and dividing it by the effective cross section of the pellet ($A \times (1 - \varepsilon)$) to acquire an indication of the binding pressure.

The differential form of this model also provides insight into how to expand this model to handle binders:

$$dF = A(d\sigma) + \sigma(dA) \tag{3.2}$$

The assumption we are making here is that $d\sigma$ is essentially constant so long as the materials are not physically changing. Thus, we can acquire a total force by instead integrating the strength at each point along the new surfaces (S) to be formed from the break. Note that technically the strength should probably be halved and the surface should correspondingly be double counted, but this cancels out perfectly.

$$F = \int_S \sigma dA \tag{3.3}$$

The main use of Equation 3.3 as shown here is to predict the compressive strength of pellets when crushed. The value however is that σ is a function which we know varies only with the binders and other materials present at the location of interest.

It would not be good to forget that force is a vector quantity, however. The binding force along a potential surface is of half the magnitude shown above but contains a directional component due to the surface normal vector $\hat{n}$:

$$\vec{F} = \int_S \frac{\sigma}{2} \hat{n} dA \tag{3.4}$$

Thus, pellet breakage occurs if there exists an external force F_c which can be redirected such that along some surface S it contributes an acceleration which moves one side of the potential surface away from the other faster than the other can keep up.

This also means that unusually shaped breaks average out to only require the area of their cross section, from a tensile strength perspective. Note however that particularly unusual breakages are unlikely because there is a significant frictional component not included in Equation 3.4 which opposes shear movement along the surface S. Furthermore, if a breakage surface becomes too complicated, then it eventually reaches a point where there is guaranteed to be a simpler breakage surface which will fail first.

Again, this sort of treatment is the same as is used in Rumpf's equation and in subsequent pellet strength modeling work (Rumpf, 1972; Bika et al., 2001; Iveson et al., 2001). All

pellet strengths end up being at least this predicted tensile strength, with excess strengths occurring because of frictional effects or energy dissipation due to excess breakage. Previous research has shown that it is reasonable to assume that pellets are essentially spherical (Gustafsson, 2017; Cavalcanti and Tavares, 2018).

The novelty of this assumption will be the simultaneous application of this strength formulation to both compressive and abrasion resistance, later.

3.2 The strength of an iron ore pellet is determined by its structure and composition

Now that we have established that we can connect the geometry of the pellet to its strength, let us establish that we can connect the composition of the pellet to its strength.

One of the more intriguing aspects of Rumpf's work (1972) is that during the derivation, the size distribution of particles was assumed to be uniform. The explanation for this included a few parts:

1. The break would never occur through a solid particle, given the option, as the tensile strengths of the crystalline materials which form the particles are incomparably higher than the tensile strengths evolved by the close proximity of the particles within the pellet.
2. Even if a non-uniform particle distribution were present, the larger particles would contribute less bonds overall to the pellet because there are numerically fewer of them. This, combined with the idea that individual bonds between

particles were of constant strength regardless of the size of the interacting particles leads to the idea that the binding is overwhelmingly dominated by the finest particles present.

For as much as it would be preferable to approach this problem from a first principles standpoint, there are some significant unknown variables which are difficult or impossible to measure, or which even if they are measured are unlikely to remain constant enough to be of any actual value. Most notably, this includes specific characteristics of bentonite including particle size, particle surface area, and so on. This imposes a great amount of difficulty in utilizing pre-existing models such as those proposed by Rumpf (1972) or Chan et al. (1983) as proposed.

However, there are some consistent trendlines shown in mixtures of pellets and binders which can be used to form a basis of a practical model. Fundamentally, the strength of a binder depends on its presence within the pellet and what it contacts. For a perfectly mixed binder, the chance of its presence in any given location in a perfectly uniform pellet is equal to its volume fraction. The chance of two different phases being in contact at the same point, considering this hypothetically perfectly mixed pellet, is equal to the volume fractions of each phase multiplied together.

This provides a mixing rule for binder strengths evolved from perfectly compatible binders, which is not something which appears to be available in the literature. This provides a novel way of determining whether or not binders display synergistic effects, largely do not interact, or interfere with each other.

The natural binding potential of a perfectly and uniformly mixed pellet would therefore be something like:

$$\sigma_{mix} = \sum_{i,j} V_i V_j \sigma_{i,j} \tag{3.5}$$

Where i and j are the species present in the pellet, V_i and V_j are the volume fractions of said species, and $\sigma_{i,j}$ is the binding potential between i and j.

However, a point on a plane can only actually neighbor a finite number of materials at once. Formally, almost everywhere along the plane the plane can only be in direct contact with zero, one, or two materials, with each probability decreasing tremendously. If a plane directly intersects the perimeter of a 3-phase border, then an effectively zero measure set of 3-way intersections is also possible.

The zero-material case is thankfully relatively simple: the presence of no material leads to no pellet strength from that point. The major questions arise from handling the one and two material cases.

First, if a point is represented only by a single material, then it is likely inside of particle within the pellet. These particles are, on the energy scales involved in pellet breakage, effectively indestructible. We can shift along the normal of the plane to reach the nearest surface and handle it as a two-material interaction instead.

The two-material interaction is then a matter of trying to consider all possible material interactions without double counting any point. This gives a range of potential strength

values with their own relative frequency, which in turn should denote the overall possible strengths of the pellet.

The probability that a pellet breaks from a given interaction then should be based on the probability that the pellet's breakage strength turns out to be less than the energy available to cause the break.

The probability of a material being on either side of the planar interaction in a perfectly uniform and perfectly mixed pellet can be readily approximated by the volume fraction of the material, as mentioned in Equation 3.5, but instead of totaling all possible interactions at the point we must choose only one interaction per point. This provides a distribution of possible pellet strengths for any given plane.

If we generalize this to something less intrinsically dependent on the volume fraction, instead focusing on the surfaces in contact between each species, then the distribution is simply that the relative likelihood of the strength being exhibited by the interaction of species i and j is simply the likelihood of a contact existing between i and j. Thus, a pellet where the interactions caused by the binder are stronger than the interactions between the bare particles would expect to increase in strength as the dosage of binder increases, and approximately linearly at low surface concentrations of binders.

At higher concentrations, the proportion of binder-binder interactions increases, which may or may not improve pellet strength depending on the binder in question. For binders like starch, molasses, or epoxy, the binder binding to itself can form very strong bonds and make very strong pellets. For a material like sodium acetate, there is no value to

allowing acetate-acetate interactions, as such bonds contribute essentially nothing to the strength of the pellet.

This immediately highlights an idea that there should be at least three distinct categories of materials:

1. Materials which do not interface with themselves at all, or only interface with the pellet materials very poorly. The overall binding interaction of such materials is limited either by very low binding potential or very low potential binding surface area. The former is demonstrated by a material like sodium acetate while the latter is shown by a material like colemanite. Sodium acetate is soluble in water and spreads through the pellet well but does not have a high binding potential for reasons that will be addressed later. Colemanite is not water soluble nor does it absorb water. It simply does not spread well into the pellet because it has no mechanism by which to do so.
2. Materials which interface with the hematite or magnetite well, but which have a limited interaction with themselves. This includes materials like sodium metasilicate or other dispersants. Since they disperse themselves, they cannot typically be expected to contribute strongly to the strength of the pellet by their own binding. However, they can improve the strength of the pellet considerably because the surface interactions they promote allow the formation of stronger pellets in general. This may be a more general effect, however, that should be handled separately. However, no matter how strong of pellets these binders make initially, continued addition will quickly level off in performance.

3. Materials which bind strongly with themselves as well as the hematite or magnetite. They can form bridges between individual particles within the pellet or completely encase the pellet in a binding matrix. These pellets can grow tremendously strong since the binder dosage can often be increased almost without limit until the desired strength is achieved. This includes materials like starch or carboxymethylcellulose. Sodium bentonite should also behave in such a way, but its interaction with the water content of the pellet precludes using very high dosages.

To form strong pellets adding a material from the second or third category would be essentially a requirement. Most binders identified in earlier reviews (e.g. Eisele and Kawatra, 2003) fall squarely into the third category, but more recent work has focused materials and mechanism which fall into the second category (e.g. Halt and Kawatra, 2017a).

The strength of bonds formed between two materials, excluding chemical reactions, should be approximately the same for any particular pelletization environment. Thus, if bentonite is found to have a specific level of interaction with hematite in pellet A made from feed material A, then bentonite should exhibit that same level of interaction with hematite even in pellet B made from feed material B, no matter what the feed material is – again, excluding chemical reactions. For example, extreme differences in soluble calcium could trivially explain significantly different bentonite behaviors between pellets.

In summary, we expect that each binder contributes a measure due to its ability to spread through along the surfaces of the particles within the pellet, and a related measure based on its ability to form overall bridging between particles within the pellet. Furthermore, since any position along a breakage plane can only neighbor two separate materials at once, there is a statistical distribution of potential pellet strengths for any given breakage plane.

Furthermore, both porosity and particle size have subtle influences on these effects. Porosity influences the number of surfaces which are exposed to empty space instead of bordering two separate materials. Porosity also has a very important effect of decreasing the effective cross-sectional area of the breakage plane, increasing the effective pressure available for causing the break.

Particle size influences how strongly the material at a given point influences the material at a nearby point. With very large particle sizes, nearby points are almost certainly the same material as any given point, while with very small particle sizes the primary material at any two points may be completely uncorrelated. However, this would primarily seem to suggest that in pellets with small particle sizes better mixing is easier to achieve. There is not a clear indication that pellet strength should be improved by a decrease in particle size, in contrast to derivations such as Rumpf's (1972) equation.

As mentioned in the background section, this peculiar result of not directly relating particle size to pellet strength has been shown in the literature prior for at least magnetite materials. This is shown in Figure 3.1.

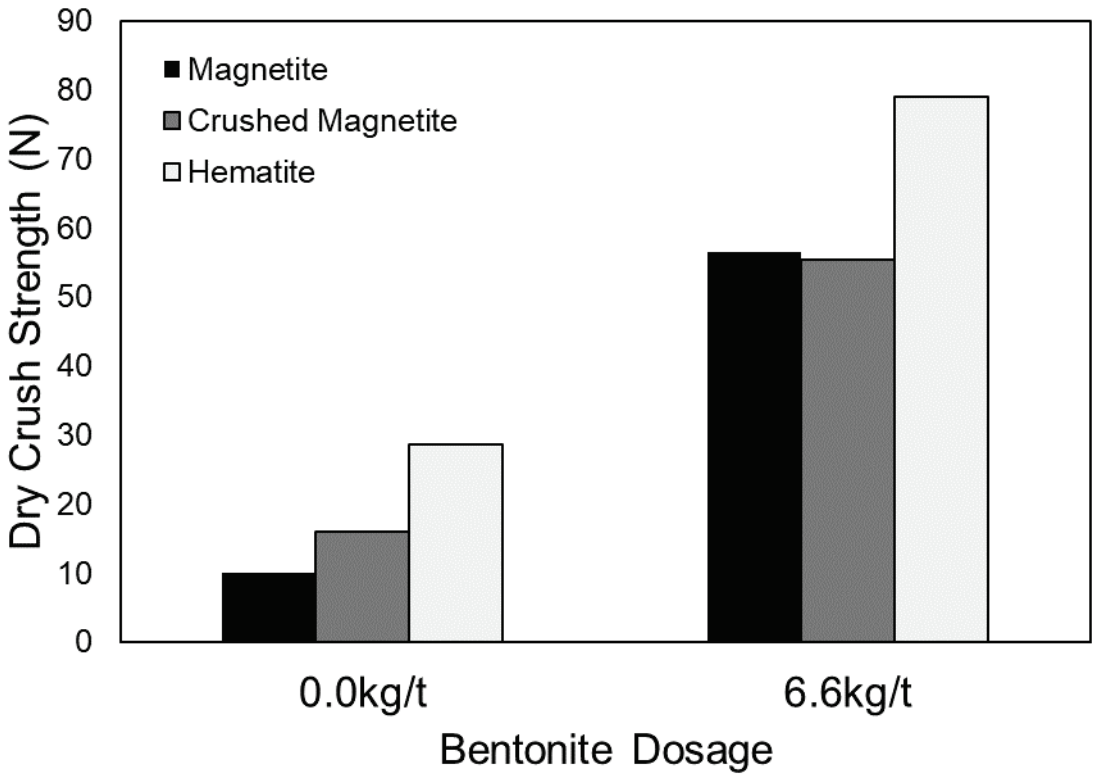

Figure 3.1: Strength of pellets formed from a hematite (80% passing 30 μm), magnetite (80% passing 40 μm), and ground magnetite (80% passing 31 μm) with sodium bentonite. The ground magnetite was prepared by grinding the coarser magnetite sample. Observe that pellet strength only marginally improves without bentonite and not at all with bentonite. (Based on Kawatra and Halt, 2011)

In Figure 3.1 the strength of the magnetite pellets was only marginally improved by decreasing its particle size when bentonite was absence, and once bentonite was added there was little discernible difference in strengths between the coarse and crushed magnetites. Rumpf's equation and other pellet strength models do not provide an explanation for this lack of change, but this system of focusing on the contact surface area rather than the number of contacts does.

Firstly, crushed iron ore is not composed of uniform spheres where maximizing the number of contact points clearly improves interparticle bonding. Rather, it is likely that the geometry of the crushed material presents wider contact areas than simply pointwise contacts presumed in Rumpf's analysis. This is especially true in the presence of bentonite, as it was the same bentonite used for each material. Bentonite's binding mechanism is spreading through the pellet as it absorbs water, achieving a high degree of surface contact between the particles. While the surface area of the particles within the pellet has increased, the surface area of the breakage cross section has largely remained the same. Furthermore, the relative probabilities of any particular interaction existing also remained the same.

It is also worth noting that the dosage of bentonite used in Figure 3.1 is likely in excess for use as a surface-active binder. Thus, even though the amount of surface area displayed by the magnetite is increased, there is not necessarily a deficit in the bentonite dosing. In particular, even though the surface area of the magnetite increased from a Blaine value of 2250 cm^2/g to 3262 cm^2/g, the hematite used in the same figure already had a Blaine value of 4255 cm^2/g (Kawatra and Halt, 2011). As such, the dosage of 6.6 kg/t of bentonite was clearly enough to achieve as much binding as it was able to for the fine hematite, and the comparatively smaller surface areas of the magnetites are unlikely to be a concern here.

3.3 Pellet strength for traditional binders is predictable

Traditional binders here will refer to binders which bind to themselves as well as to the ore. This refers to the third category of binder expected from the previous section, and certainly includes bentonites, starches, and celluloses. This section will go into showing that these binders have a predictable behavior stemming from the hypothesis that the major contribution of binder dosage is to the interfacial areas which are coated by the binder.

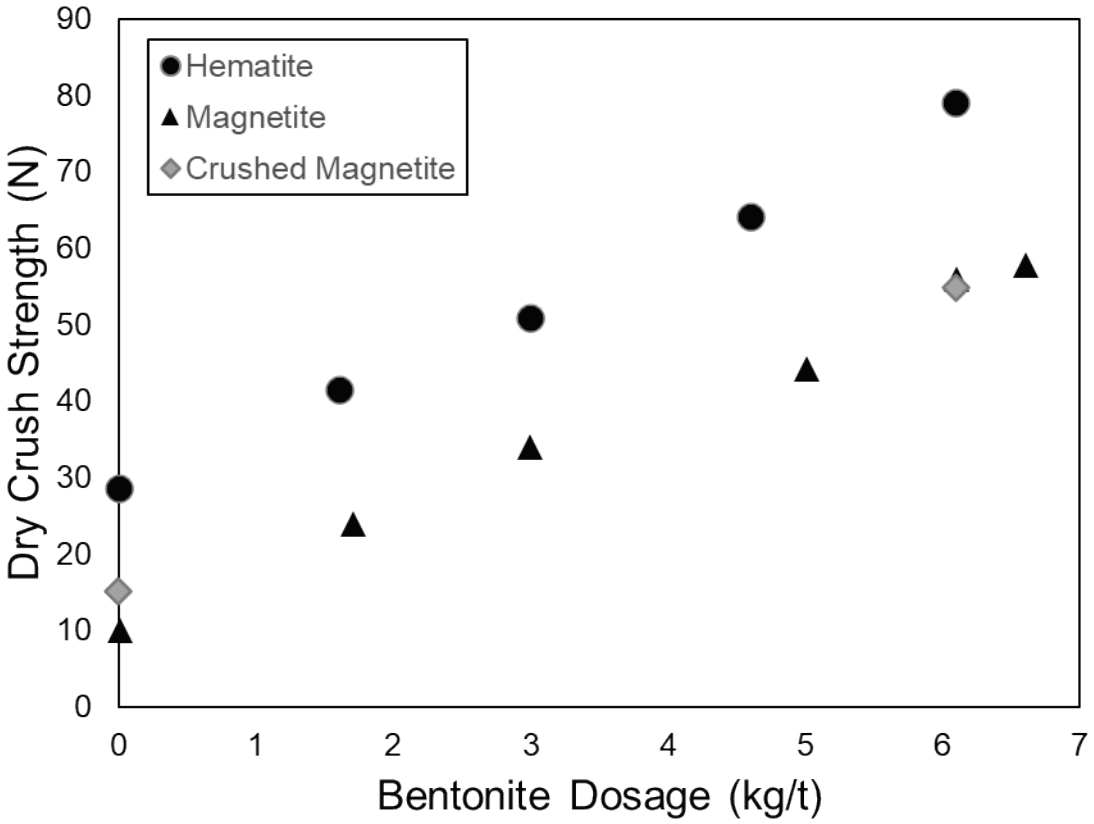

Figure 3.2: The addition of bentonite to magnetite or hematite results in a linear increase in pellet strength, at least at typical bentonite dosages. This partially supports the claim that the primary contribution of a binder is based on its contact area with the particles. (Based on Kawatra and Halt, 2011).

Figure 3.3: Dry crush strength for varying starch and bentonite dosages with a hematite pellet feed. Total binder dosage is 6.6 kg/t, with an increasing fraction represented by a 60% soluble corn starch. (Based on data from McDonald, 2017).

Also from the same work, we see a linear relation between the addition of bentonite and the increase of pellet strength for both hematite and magnetite pellets. This is shown in Figure 3.2 (based on data from Kawatra and Halt, 2011), which was collected for an unrelated inquiry. This result is in agreement with the expectations set forth by the claim that the particle strength evolves from the interparticle contact areas.

This is because the amount of bentonite found in the binding plane is expected to be linearly proportional to the amount of bentonite added, and as such the amount of binding it contributes is expected to be linearly proportional to the amount of bentonite added.

This is also true for a binder such as corn starch. McDonald (2017) reported a dry strength data set involving mixtures of bentonite and starch binders for a hematite pellet feed which is reproduced in Figure 3.3.

Assuming that the starch and the bentonite do not have strong effects on each other's mechanisms, then knowing that bentonite behaves roughly linearly allows us to remove its linear effect from consideration in this graph and realize that starch must also linearly increase pellet strength. The reasoning is the same: the chance of finding starch in the binding plane is essentially directly proportional to the amount of starch in the pellet.

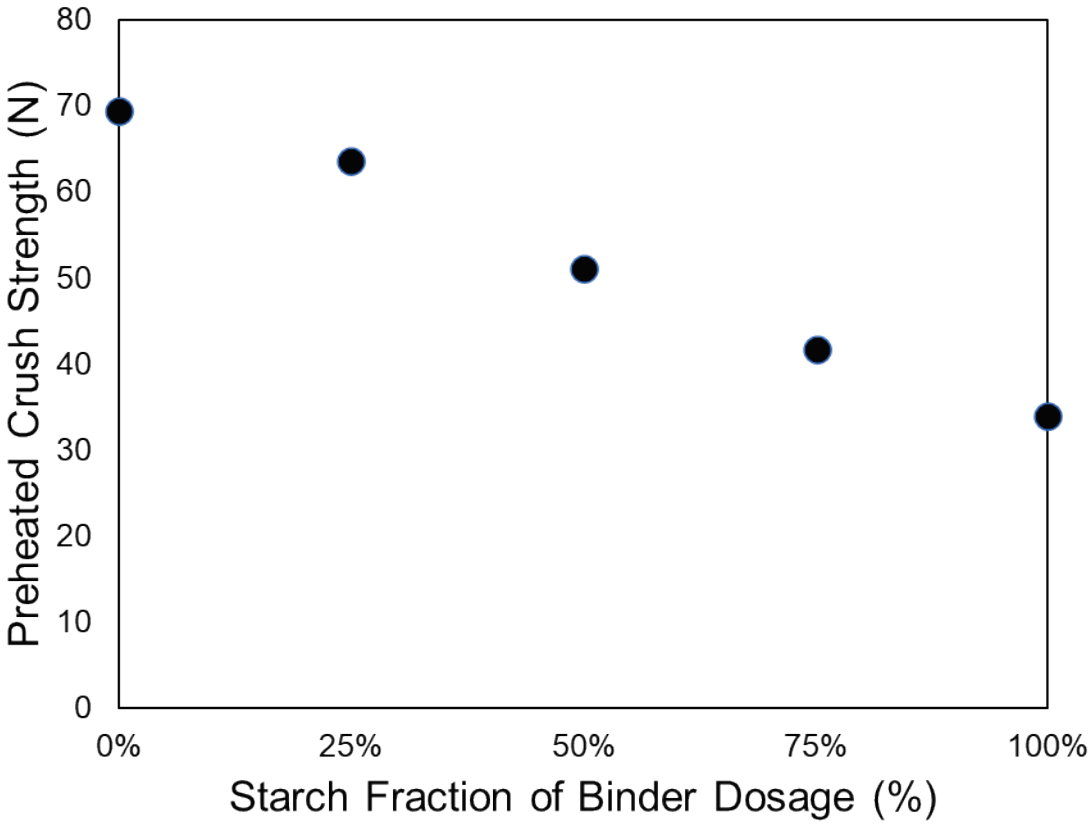

Figure 3.4: The strength of the pellets shown in Figure 3.3 after firing at 500 °C to remove the starch via combustion. (Based on data from McDonald, 2017).

There is an accompanying data set from McDonald (2017) which shows the strength of these pellets after being roasted at 500 °C to remove the starch by combustion. This should exactly remove the interfacial bonds provided by the starch. The results are shown in Figure 3.4.

The bentonite is not removed from the pellet during this firing process, so in essence these pellets should correspond to the hematite pellets made for Figure 3.2. Plotting these values on the same graph with the same axis clarifies this point. Again, these data sets have not previously been compared in this fashion, but the correlation is rather striking.

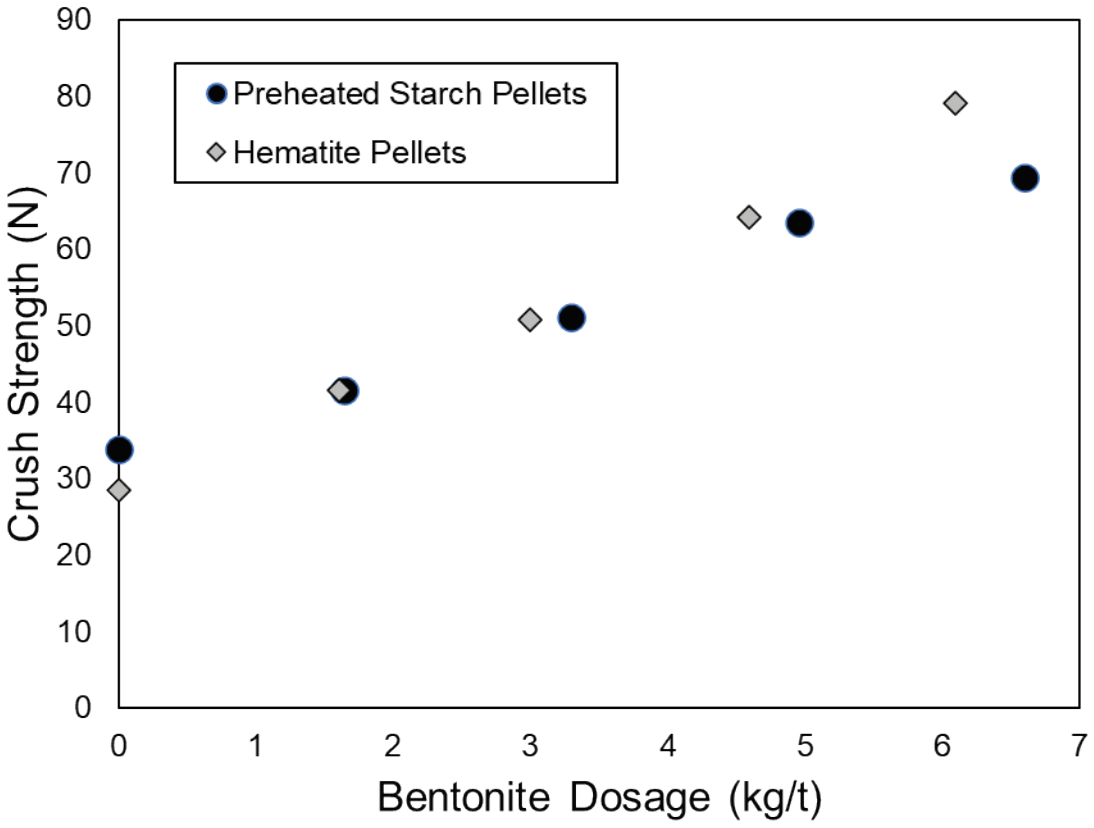

Figure 3.5: Crush strengths of pellets from Figure 3.2 and Figure 3.4, made from similar hematite materials using sodium bentonite. The pre-heated starch pellets previously contained starch, which was burned away at 500 °C.

Yet, the results shown in Figure 3.5 should not be a surprise at all. The preheated starch pellets turn out to be slightly weaker overall than the pellets directly made with bentonite after the 500 °C heat treatment. The differences observed are small and the feed material in these two cases is not identical, but overall it appears that these pellets have similar strengths because they have similar binding structures and similar overall compositions. The heat treatment also positively impacted the strength of the 6.6 kg/t (by about 15 N, or +27%) bentonite pellet, which contained no starch.

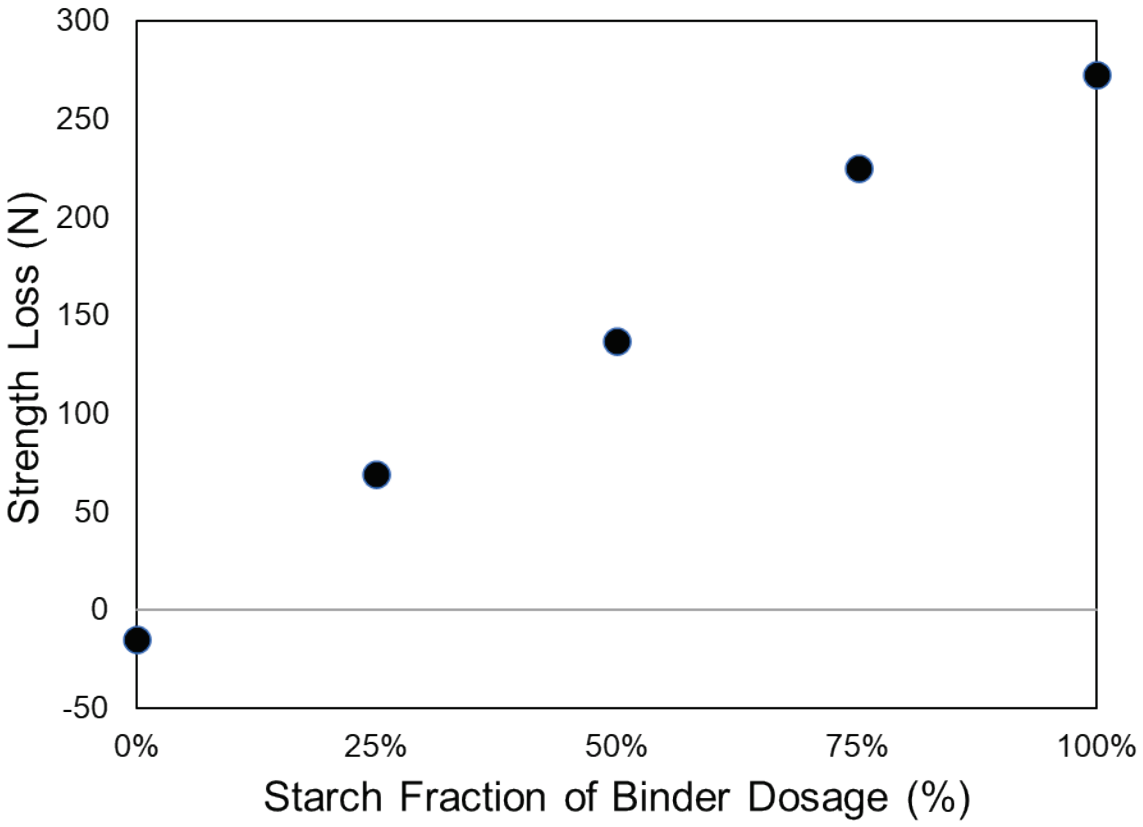

Figure 3.6: Strength loss (or gain) of pellets made with 6.6 kg/t of binder made from a mixture of starch and sodium bentonite after heat treatment at 500°C, based on the differences between Figure 3.3 and Figure 3.4.

This also demonstrates that the impact of starch on the pellet should be linear based on the addition of starch, as the removal of increasing amounts of starch results in a linear decrease in pellet strength, although the effect of bentonite is still not specifically accounted for in Figure 3.6.

Quon and Kuriakose (1990) show that similar trends exist for 3 other types of organic binders, showing that the linear trends continue for hydroxyethylcellulose, at least some carboxymethylcelluloses, and guar gum. They do find that at least one carboxymethylcellulose eventually stops contributing to the pellet strength at high enough dosage, but the details of the compound in question are not provided so the reasoning for that result is unclear.

While the data used in this section is from previous works, this analysis of these effects depends on the approaches developed in sections 3.1 and 3.2. It is worth emphasizing that while these works noted these trends, there has been little to no discussion in pelletization literature as to why this trend should exist in the first place for different binder dosages. Focusing on the interfacial surface area helps to clarify this effect.

3.4 Upper limit on the effect of surfactants

Not all materials which improve (or harm) pellets behave via the same kind of mechanisms as the traditional binders. The most ubiquitous and notable of these is certainly calcium and magnesium. Here is a proposed mechanism for the behavior of soluble calcium and magnesium during the pelletization process:

1. Calcium and magnesium are specifically adsorbed cations on hematite, magnetite, or others. This means that calcium and magnesium form strong bonds with hematite and magnetite surfaces, lowering their effective surface charge and in turn promoting both the adsorption of other negatively charged species and the potential flocculation of the iron ore material.
2. These flocs, when formed, would be expected to point their more neutral surfaces towards each other. That is, the sides with the calcium or magnesium are expected to form small, heavily interlocked flocs within the pellet. These flocs may also capture some significant quantity of any other binding materials within the feed. This state makes it harder to grow pellets and can interfere with the activity of other binders.
3. Eventually there is enough calcium and magnesium that some level of dispersion can be achieved again because the surface charges are beginning to become more positive, and thus the similarly charged surfaces begin to repel each other once more. This state allows pellets to recover some potential strength but can still interfere with the activity of other binders.

Calcium and magnesium interact with essentially every binder that could be put in a pellet in one way or another. Starch is already known to significantly interact with calcium and magnesium (Zhang et al., 2021; Parra et al., 2021; Parra, 2021). Bentonite is readily converted to calcium or magnesium bentonite, reducing its effectiveness dramatically (Eisele and Kawatra, 2003; Ripke and Kawatra, 2003; Kawatra and

Claremboux, 2021b). Carboxymethylcellulose is often shipped with an included dispersant to help minimize the presence of calcium (Claremboux and Kawatra, 2022).

Not all of these interactions are negative, however. Fly ash-based binders require calcium to produce strong pellets (Ripke and Kawatra, 2000). Molasses and some other sugars can be cemented in the presence of starch (Halt and Kawatra, 2014; Halt et al., 2015; Kotta et al., 2019). Additionally, lime and quicklime can be used directly as a binder for cold-bonding applications, since interaction with added CO_2 can form calcium carbonates within the pellet (Pal et al., 2014).

Furthermore, Halt (2017) reported that the addition of calcium chloride decreased the amount of pellet material lost into the finest size fraction during abrasion. However, the total amount of material lost during the abrasion test did not decrease compared to the other coagulated pellets. This is, when combined with the abrasion model which will be presented later, clear evidence in favor of the idea that these flocculants can create small, strongly bound domains within the pellet. After all, the only way for fine material to decrease while maintaining the same total mass loss from the pellets in the abrasion equation, is if the particles coming off during abrasion become physically larger – and thus do not pass the screen used as the cutoff for the “fine” fraction measurement.

The impact of dispersants is due to exactly the opposite phenomenon but leads into a somewhat different mechanism.

1. Dispersants cause strong surface charges to occur on the surface of the particles in the pellet. This causes the pellet material to become dispersed within the pellet

water, rather than clumping up and forming flocs. The strongest dispersants are suggested to be capable of liberating additional colloidal material within the pellet, providing more fine material for additional binding (De Moraes et al., 2018).

2. This dispersion means that particles are only minimally in contact with each other, and during pelletization have more ability to rotate and maneuver within the pellet to find dense packings. This effect has a strongly positive impact on pellet quality (Halt and Kawatra, 2017a; Claremboux, 2020). However, this should be a stepwise effect. There is a lower limit to the zeta potential which will allow the particles to maintain a capillary separation distance (Claremboux, 2020), and there is an upper limit to how densely any given distribution of particles can be packed without the ability to change the shapes of those particles.

The dispersion and flocculation effects in a pellet have already been shown to have a clear impact on the structure of the pellet and subsequent strength. However, there is no existing model to quantify and take advantage of this knowledge.

The effect of dispersion is believed to occur due to changes in the structure of the pellet. It is known that having a high degree of dispersion increases the strength of starch-bound pellets by about 80-100% from baseline (Halt and Kawatra, 2017a). Similarly, the addition of sodium metasilicate increases the strength of bentonite bound pellets by about 80% but no further (Claremboux, 2020). The increase in pellet strength from a scenario where no special measures are taken to disperse the pellet to a scenario where the pellet is completely dispersed is about that 80-100%. This may be because of more effective

forming of salt bridges during the drying process, the more effective packing of the pellet during the rolling process, or a general increase in binding strength between dispersed pellet surfaces compared to non-dispersed ones.

The strength of bentonite-bound pellets can also be decreased by the addition of calcium or magnesium, by up to about 60% (Claremboux, 2020), but this could as easily be explained by the conversion of sodium bentonite to calcium or magnesium bentonite. However, similar differences were observed for similar amounts of additions of coagulants including calcium and magnesium to starch pellets (Halt and Kawatra, 2017a). In this case, it is particularly peculiar because our work in flotation has identified calcium and magnesium as good activating agents to promote starch adsorption onto hematite or silica (Parra-Álvarez et al., 2021).

Note that there is also a competing explanation for why dispersants help improve pellet strength: since the dispersants spread the material out some, it should be easier in a dispersed pellet for binders to spread within the pellets. We will argue against this possibility in a later section.

To summarize, the most important prediction to be made here is that there is an upper limit on how much strength can be acquired from dispersion alone, and that mixtures of dispersants with traditional binders should yield increases from the traditional binder and from the dispersion effect.

3.5 Crushing strength and abrasion strength are related

Equation 3.1 provides an expression for understanding the crush strength of pellets, but it can also be rearranged to describe the abrasion case. Instead of trying to determine the pressure at which the pellet can be crushed, what if instead we determine the amount of energy required to deconstruct the pellet in its entirety? This treatment of the abrasion test is novel and provides a distinct path towards predicting the behavior of the pellet strength using both compressive and abrasion testing. In particular, connecting the pellet's strength to the rate of energy applied during an abrasion test provides a novel insight into the rate at which pellets should abrade which has not previously been explored in the context of the testwork which will be performed to verify this result.

This rearrangement is achieved by integrating the force over the surface of pellet from its exterior to its core. The energy required for complete abrasion E_a depends on the same statistical strength parameter as in Equation 3.1 and the radius of the pellet R.

$$E_a = \int_R^0 \sigma(4\pi r^2)\, dr \tag{3.6}$$

As written, it is assumed that all structural information is being encoded into σ in the same way that it would be encoded in the compression strength test.

$$E_a = \frac{-4}{3}\pi\sigma R^3 \tag{3.7}$$

This expression is useful because if the strength of the pellets is known and the rate at which energy is input into breaking the pellets is known, then the rate at which the pellets

become smaller can also be determined. Obviously, it is known that the efficiency of comminution processes is often quite low. In mineral processing often comminution is no more than 3 or 4% energy efficient.

However, we will insist that the energy available is, for at least softer materials such as dry pellets, well correlated with the energy that goes into breaking the pellets. This assumption probably gets worse for stronger pellets which are more able to resist smaller quantities of energy.

Rearranging Equation 3.7 to isolate the rate of change of the pellet radius, we acquire:

$$\frac{dE}{dt} = -4\pi\sigma R^2 \frac{dR}{dt} \tag{3.8}$$

$$\frac{dR}{dt} = \left(\frac{-1}{4\pi\sigma R^2}\right)\hat{E} \tag{3.9}$$

Where $\hat{E}$ is the amount of kinetic power available to abrade the pellet.

For the test that we will be using to measure abrasion strength, the energy available is kinetic energy derived from a roughly constant velocity distribution available to the pellets, multiplied by a constant term which includes the efficiency of energy transfer from kinetic energy into pellet breakage and the size information required to determine the rate at which these impacts occur (Cv). Although the average velocity is held constant throughout these tests, as the rotap machine was not adjusted, it is expected to appear as a cubic term due to its presence in both the kinetic energy and collision frequency terms.

$$\hat{E} = \frac{1}{2} m v^2 \times C v \tag{3.10}$$

Where m is the mass of a given particle and v is the velocity at which it is moving. Plugging this into the expression we already have for the radius:

$$\frac{dR}{dt} = \left(\frac{-1}{4\pi\sigma R^2}\right)\left(\frac{1}{2} m v^3 C\right) \tag{3.11}$$

We can expand m because we know the volume and are assuming that pellets are roughly uniform spheres:

$$m = \frac{4}{3}\pi R^3 \tag{3.12}$$

$$\frac{dR}{dt} = \left(\frac{-R\rho v^3 C}{6\sigma}\right) \tag{3.13}$$

$$R = C\, exp\left(\frac{-t v^3 \rho}{6\sigma}\right) \tag{3.14}$$

Which we can rewrite in terms of mass so that we can start to connect it to the population balance equation we derived in Equation 2.18.

$$m = \frac{4}{3}\pi\, C\, exp\left(\frac{-t v^3 \rho}{2\sigma}\right) \tag{3.15}$$

We connect this through Equation 2.17 which allows us to relate the mass rate of change to the rate function we use in the population balance:

$$\frac{dm}{dt} = \frac{-v^3\rho}{2\sigma}\left(\frac{4}{3}\pi C\, exp\left(\frac{-tv^3\rho}{2\sigma}\right)\right) = \frac{-v^3\rho}{2\sigma}m(t) \tag{3.16}$$

This is a linear rearrangement of the population balance we assumed in Equation 2.18, so we move the constant term into the t term and call it the rate constant: $\tau = kt = t/\left(\frac{v^3\rho}{2\sigma}\right)$. The de-dimensionalized mass term is typically picked simply so that the largest pellet of interest has mass equal to one.

In any case, we can now use the de-dimensionalizing factors we determined from Equation 3.16 to relate the abrasion equation we derived in Equation 2.18 to the size distribution of particles throughout the abrasion test. This equation is re-written and re-shown here below:

$$n(\omega, \tau) = n(exp(\tau)\,\omega, 0)\, exp(\tau) \tag{3.17}$$

This equation simply shifts the input distribution as the time factor increases, and eventually reaching 0 because there's a certain point at which enough energy has certainly been added to reduce the pellet to its constituent particles.

Assuming a constant and uniform pellet density and that pellets are grown to a 7/16" x 1/2" size distribution, then all pellets will have a reduced size distribution fitting into the range of approximately 0.669922 to 1. The former number is 343/512 and is derived by converting the radius in the size distribution into a mass and then forcing the largest mass to be 1. Any pellets used to initialize an abrasion test should be in this sort of range.

For a given reduced mass ω_0, the total mass fraction of the pellets larger than that fraction are given by:

$$M = \int_{\omega_0}^{1} \omega n(\omega, \tau) d\omega \tag{3.18}$$

This will be useful again in connecting real, measurable data to this idea.

Thus, if we know the crushing strength, we should reasonably be able to predict the abrasion strength. Conversely, if we know the abrasion strength, we should reasonably be able to predict the crushing strength. There is an efficiency of energy transfer term here which is likely close to unknowable, but overall this expression gives us reason to believe that we can predict the movement of the distribution for various abrasion conditions.

If we are particularly careful about how we correlate the cross-sectional breakage area with the volume of the pellet we can acquire another relationship between the pellet strengths:

$$\sigma = \frac{\sigma_T}{S} = \frac{\sigma_A}{V} \tag{3.19}$$

Where σ is the strength factor as shown in 3.16, σ_T is the measured tensile strength of the pellet, S is the cross section of the break in tensile failure, σ_A is the energy required to abrade the pellet to only fines, and V is the volume of the pellet. Again, there is a relationship between these values for perfect spheres along the strongest breakage plane:

$$\sigma = \frac{\sigma_T}{\pi R^2} = \frac{\sigma_A}{(4/3)\pi R^3} \tag{3.20}$$

Which can be further rearranged to:

$$\sigma_T = \left(\frac{3}{4R}\right)\sigma_A \tag{3.21}$$

Deviations from sphericity can be measured based on how much cross-sectional area is actually found versus the amount expected, as a ratio ω which may be more or less than 1. More than 1 means that the cross-sectional area is larger than would be allowed for a sphere of equivalent volume, while less than 1 means that the cross sectional area is less than would be expected for a sphere of equivalent volume.

With this term, we can include that fact that pellets are not usually perfect spheres into the equation:

$$\sigma_T = \left(\frac{3\omega}{4R}\right)\sigma_A \tag{3.22}$$

Note that for non-spherical pellets, the geometry of the compression strength test will tend to cause ω to be less than 1, meaning that less spherical pellets should have progressively lower measured compressive strengths than perfectly spherical pellets. This is because pellets tend to not stand on end even if so placed. Since the pellet is laying down, the cross section is typically chosen from its shorter two axes.

We can also rearrange this equation to be in terms of σ instead of σ_A, since we are not measuring σ_A for individual pellets but instead the average overall σ for an entire batch of pellets simultaneously.

$$\sigma_T = \pi R^2 \left(\frac{\omega}{\omega_0}\right)\sigma \tag{3.23}$$

Thus we would expect that pellets which exhibit greater dispersion and better compacting during rolling will in turn demonstrate higher proportions of compressive strength to abrasive strength.

We would also expect that the tensile strength of pellets will vary based on the size distribution of pellets formed. Since the size distribution formed in the laboratory pelletization procedure is 7/16" to ½", the minimum possible range of pellet strengths which should be observed, assuming maximal strength breaks on all pellets, is between 76.6% to 100.0% of the maximum strength observed. Any compressive strength distribution narrower than that would be of considerable interest. Skipping ahead to the data section, no distributions of pellet strengths are observed to be even close to being that narrow, with the narrowest being 68.1% to 100.0% of the maximum strength observed experimentally. Wider distributions are expected due to imperfections in the breakage planes which occur during compression and less than perfectly spherical pellets.

Again, it is also worth noting that this analysis allows for a novel direct comparison of compression strength and abrasion strength, and also for a way to isolate the effect of binders from the highly variable geometric effects which impact compression strength.

3.6 Input size distribution to abrasion does not matter

One advantage of testing pellets via abrasion is that in a theoretically ideal abrasion test each pellet is abraded only by its own properties and not be interaction with other pellets. As such, the input size distribution should have minimal effects on the results.

Let us consider two plausible size distributions, one informed by the expected results from the coalescence equation that governs pellet growth and one informed by the nature of sieves being a size classification.

These two size distributions are the size distribution where mass is uniformly distributed among all possible pellet sizes and the distribution where particles have uniformly distributed particle radius. The distribution of particles at each mass, in that case, can be normalized to the curves in Figure 3.7. These two size distributions are reasonably dissimilar, as can be observed.

Now, let us consider the mass fraction above +3 mesh for these two size distributions. This is given by utilizing Equation 3.18 to find the mass fraction above a reduced mass of 0.148811 (derived from a mesh passing size of 6.73mm and a top size of 12.7mm, cubed). The results are shown in Figure 3.8, which highlights that there is only a very small area where the size distribution affects the measurement of the mass of the +3 fraction. As such, for the top size, the input distribution cannot have much of an impact on the measurement of the abrasion properties.

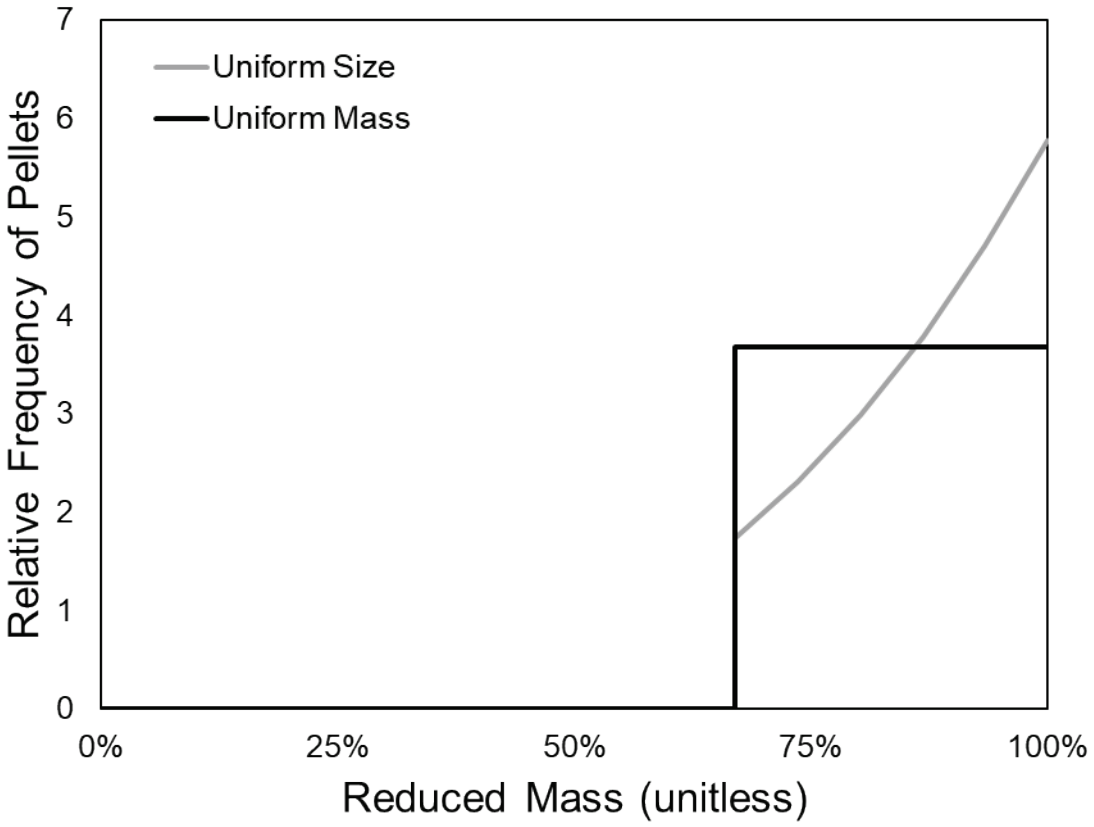

Figure 3.7: Two theoretical, plausible size distributions for pellets screened to 7/16" x 1/2".

We can also consider a mass fraction such as 3mesh x 35mesh, which contains all of the material which is larger than the 35 mesh opening but smaller than the 3 mesh opening. In the reduced mass, the 35 mesh opening is at 7.62797×10^{-6}, derived from cubing 0.25mm divided by 12.7mm. Plotting out everything +35 mesh and then subtracting off everything +3 mesh gives us an intermediate curve shown in Figure 3.9.

These values can be changed for any other mesh sizes of interest, but these mesh sizes are chosen based on the meshes that will be used in the testwork later and because of the use of these mesh sizes in some previous works.

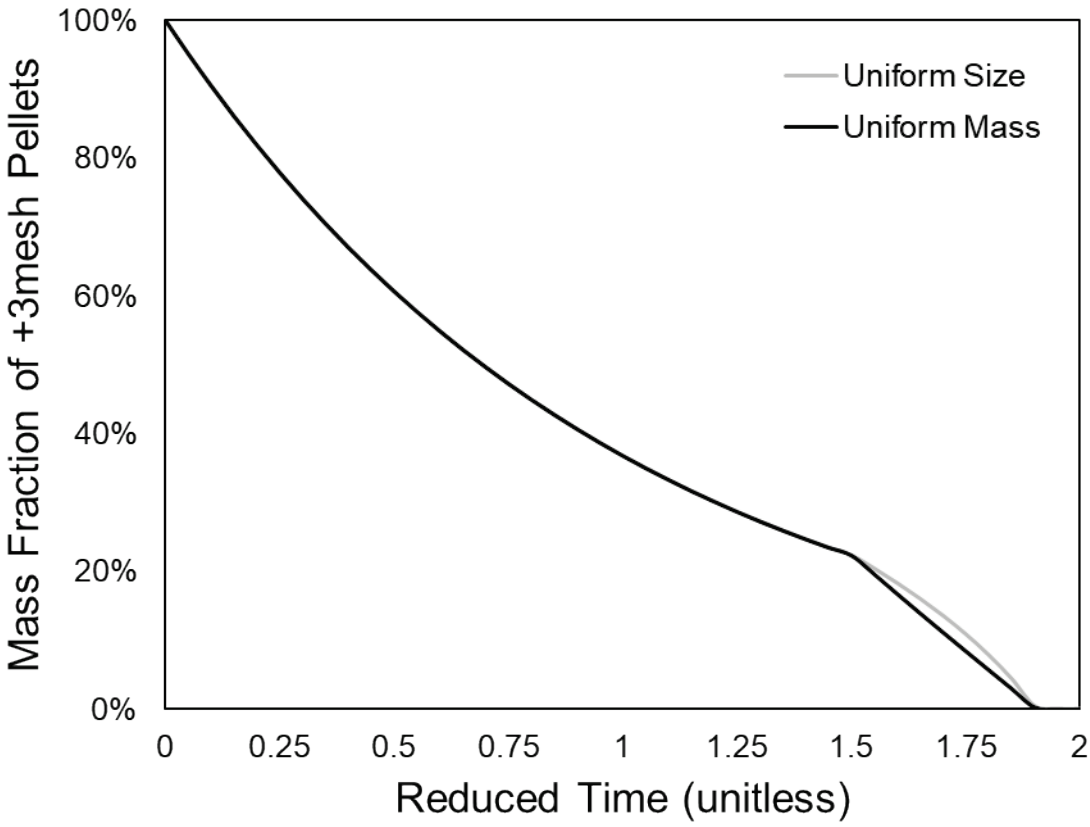

Figure 3.8: Difference between uniform mass and uniform size distributions in the fraction of +3 mesh pellets, predicted, over an abrasion test.

Again we see in Figure 3.9 that the mass fraction of pellets in the 3x35mesh range only depends on the size distribution in a very narrow interval of reduced times. In this curve we see that there is an expectation that there will be a small amount of +35 mesh fraction even quite far into the abrasion test.

It is also worthwhile to determine the -35 mesh fraction. In this case, we apply a mass balance and simply subtract the +35 mesh fraction from everything. This is shown in Figure 3.10. As shown, the size distribution has no apparent effect on this fraction at all.

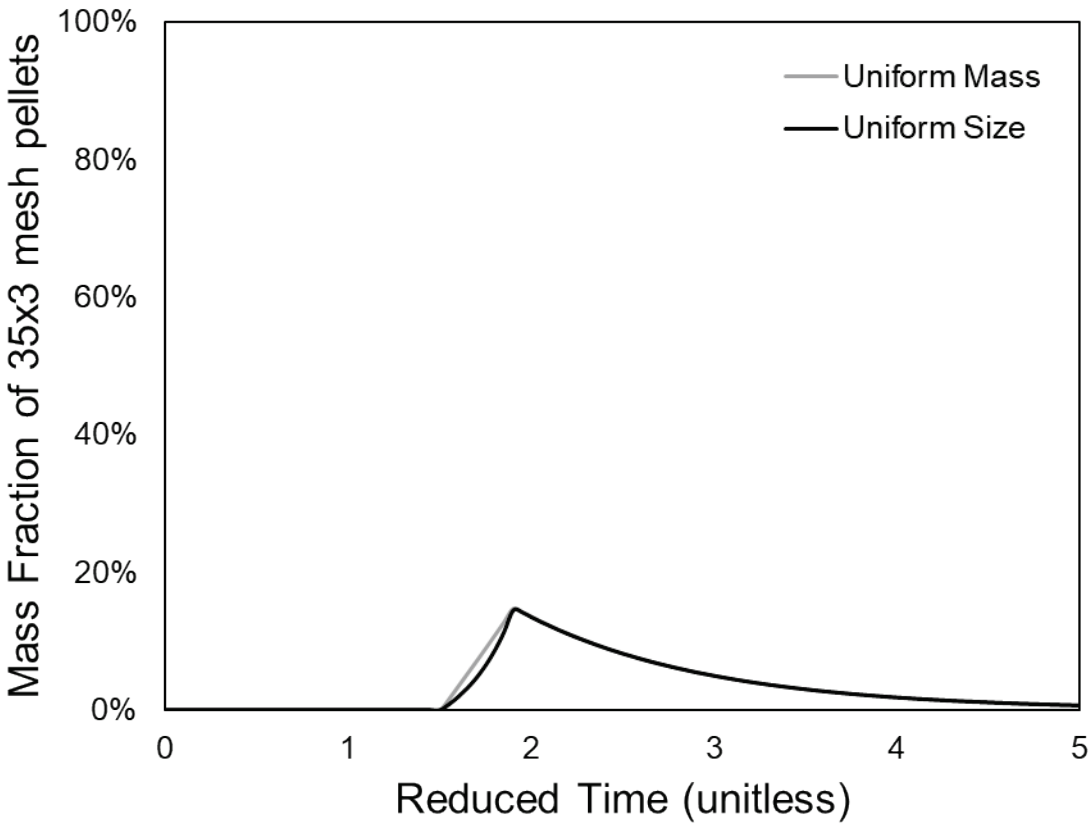

Figure 3.9: Difference between uniform mass and uniform size distributions in the fraction 3x35 mesh pellets, predicted, over an abrasion test. Note that the x-axis is necessarily wider here than in Figure 3.8.

Thus, we do not need to concern ourselves too much with ensuring a proper size distribution for the input into an abrasion test, only that there is enough material to measure each size fraction as necessary and that the sample is representative.

Furthermore, if abrasion is the only mechanism encountered during the abrasion test and if the prediction regarding the addition of kinetic energy is correct, then these results should be the only possible results, after reducing the dimensional variables, for any pellet we test.

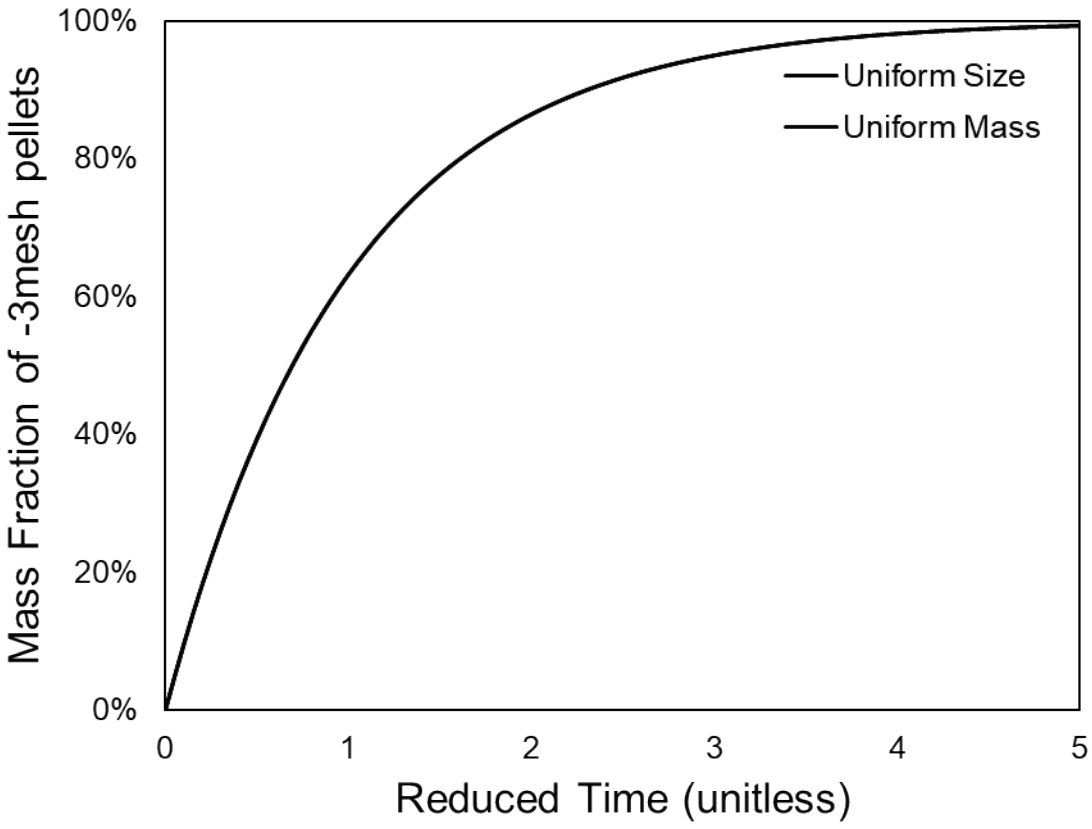

Figure 3.10: Mass fraction of -3 mesh pellets and pellet material, predicted, in an abrasion test. That the curves are assigned the same color is not a mistake – they are indistinguishable for this fraction.

Importantly, the singular variable we are able to use for fitting is the rate constant, which has a clear and obvious interpretation. Rate constants which move the pellet farther ahead into time represent weak pellets which abrade rapidly, while rate constants which move the pellet nearer to the origin in time represent strong pellets with good resistance to abrasion.

And, again, as posited in Equation 3.16, this same rate constant should also be inversely correlated to the pellet strength, allowing us to identify the strength of a pellet in abrasion and in compression simultaneously.

This would have a few advantages:

1. The abrasion test, as it will turn out, is very reproducible and leaves very little room for user error or misinterpretation. Furthermore, relatively large batches of pellets can be tested at once, making it easier to ensure that the sample size is representative.
2. This will allow the abrasion and dustiness of dry pellets to be understood directly in terms of strength, which can potentially provide insight into reducing the dust formed during pre-heating or after firing.
3. Unlike the compression strength test, there is not a hidden and often unrecorded dependency on the size distribution of the pellets.
4. Additionally, there is not a highly variable dependence on the geometry of the pellets as there is in the compression test due to the random selection of a fracture plane. By focusing on the energetic analysis of destroying the whole pellet via abrasion, we are able to force the contributions from all possible fracture planes to appear simultaneously.

Furthermore, this theoretical work provides a very strong foundation for this abrasion test. As such, we hope that this work helps provide significant confidence that the test proposed here for abrasion is truly measuring abrasion with only very small deviations from the expected results even for relatively weak pellets.

Finally, if it is observed that the premise that abrasion strength and dry strength are correlated turns out to be false, we will have identified some binder property or

characteristic which supports abrasion resistance or compression strength over the other. The materials chosen for this test are unique enough that this should allow a specific property to be highlighted as the primary point of difference that leads to higher strengths in one area over another.

3.7 The reaction of binders to each other can be predicted

Previously in section 3.2 a couple of possible categories of binder interactions were declared:

1. Binders which can interface with themselves and the pellet materials to form extensible binder networks.
2. Binders which interface with the pellet materials but not themselves, or themselves but not the pellet materials, but otherwise contribute something useful to the pelletization process.
3. Materials which do not interface with themselves or other common materials.

In essence, this requires predicting the sign of the strength interaction between two materials: $\sigma_{i,j}$ for species i and j. This however can be done with only fairly limited information regarding the compounds in question, so long as sufficient information is available about the types of interactions to investigate.

For inorganic compounds, like hematite, silica, or bentonite, these materials can be modeled as a series of planes through the crystal which capture the average charges

presented at each point. At long ranges or for very small contact areas these planes can be considered as a line of point particles instead, but at normal contact ranges treating them as infinite planes is also likely valid.

Crystallographic data is available for many compounds, but even a loose approximation of the behavior of these materials should suffice to help explain some of the oddities observed in the empirical data. We can choose to model hematite as a series of 2 planes, exposing a -1 charge per HO-Fe unit followed by a +1 charge for the same unit, separated by a distance of approximately 1.26Å. More precise calculations could be made by examining the crystallographic location data and accounting for the partial charges present in the H-O- grouping. As is, H-O is assumed to be completely covalent and as such the hydrogen is electrically neutral. However, this assumption is sufficient to tell that there is no large scale electrostatic attraction between hematite surfaces.

This can be determined by considering the Coulomb force between two point particles:

$$F = k\frac{q_1 q_2}{d^2} \tag{3.24}$$

Where k is a constant term based on the medium, q_1 is the charge on particle 1, q_2 is the charge on particle 2, and d is the distance between the two particles. The potential energy of this can be obtained by integrating it, resulting in an equation which looks very similar except the k value acquires a negative sign and d is not squared. The force between two planes also looks similar to the potential energy between two points, except k is not

negated and the q values refer to charges per unit area instead of charges, and the final force is also per unit area.

By summing these terms over each charge plane of interest, the minimum potential energy can be either at 0 distance (always attractive), finite distance (attractive but a separation distance is implied in the electrostatic term), or a very large or unbounded distance (repulsive). The interaction between two hematite surfaces based on the model suggested above is always repulsive.

If we assume some degree of dispersion, the model can instead become a layer of $-q$, $1 + q$, -2, +1 starting from the outermost layer and moving inwards, each separated by about the same 1.26Å. This is based on the idea that a dispersant is an effective dispersant if it presents a negative charge (in this case, q) facing the bulk of the solution. For charge balance reasons, it is assumed that the positive charges the dispersant brings are held internally near the hematite surface. For varying degrees of dispersion, a wide range of potential behaviors are observed:

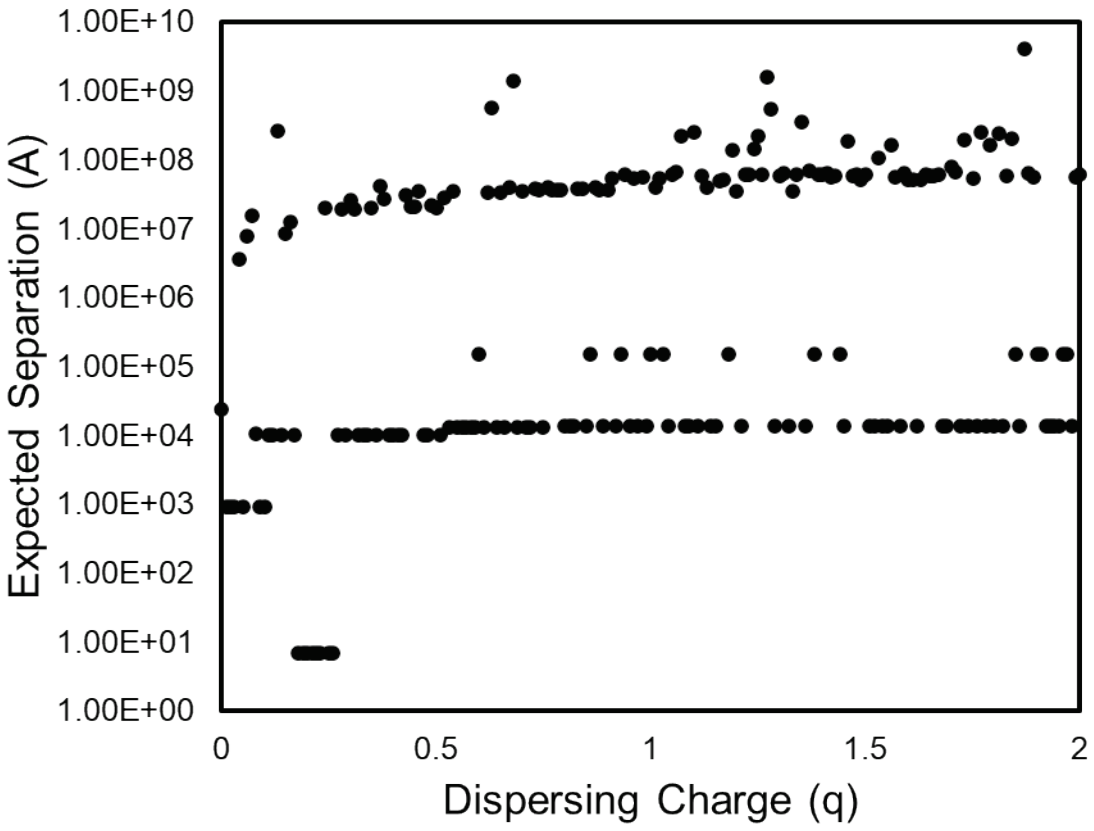

Figure 3.11: Expected separation of hematite surfaces under varying dispersing conditions. This assumes that the dispersant expresses an attached charge of q on the hematite surface, and the result is found to be extremely chaotic.

As shown in Figure 3.11, the location of the minimum separation distance varies apparently chaotically depending on the magnitude of charge assumed for dispersion. Each of these various charges is potentially possible, depending on the efficacy of charge separation on the dispersant in question and the relative density with which the dispersant can attach to the hematite surface. Thus, we would expect that pellet strength may increase by a small or large amount somewhat chaotically based on the exact activity of the dispersant, at least if no other binders are present.

Silica can be represented with a fairly simple model as well, with charge separation of -1, +4, -3 from the outside in on its surface, at 0Å, 1.6Å, and 2.1Å approximately. This is based on the $^{-}$O-Si-O_3- structure of a tetrahedral silicon with one outward facing Si-O bond. The area of this unit can be approximated as the cross-sectional area of a hexagon with edge length of approximately 1.38Å. Again, more precise predictions could be made by assuming far more about the specific crystallographic arrangement of the silica, but the silica present in iron ore may vary and need not be ideal quartz. The properties this simple model is based on are usually fairly consistent, and thus it is assumed to be a workable model of the silica surface.

This surface also shows repulsion when evaluated against itself but shows very slight potential attraction between hematite and silica surfaces. At dispersing conditions, including $q = 0$ (which refers to a -2 charge on the oxygen layer with a counterbalancing ion instead of an O-H group on the hematite surface), silica is slightly attracted to hematite. However, eventually the addition of more dispersant should result in silica being repelled a significant distance from the hematite surface, around $q = 0.22$. Thus, the addition of dispersant to materials containing some silica may improve binding. This was not tested as silica is essentially always present but could be viewed opposingly in that the addition of dispersant to pure hematite should show less of an improvement in pellet strength. These effects are shown graphically in Figure 3.12.

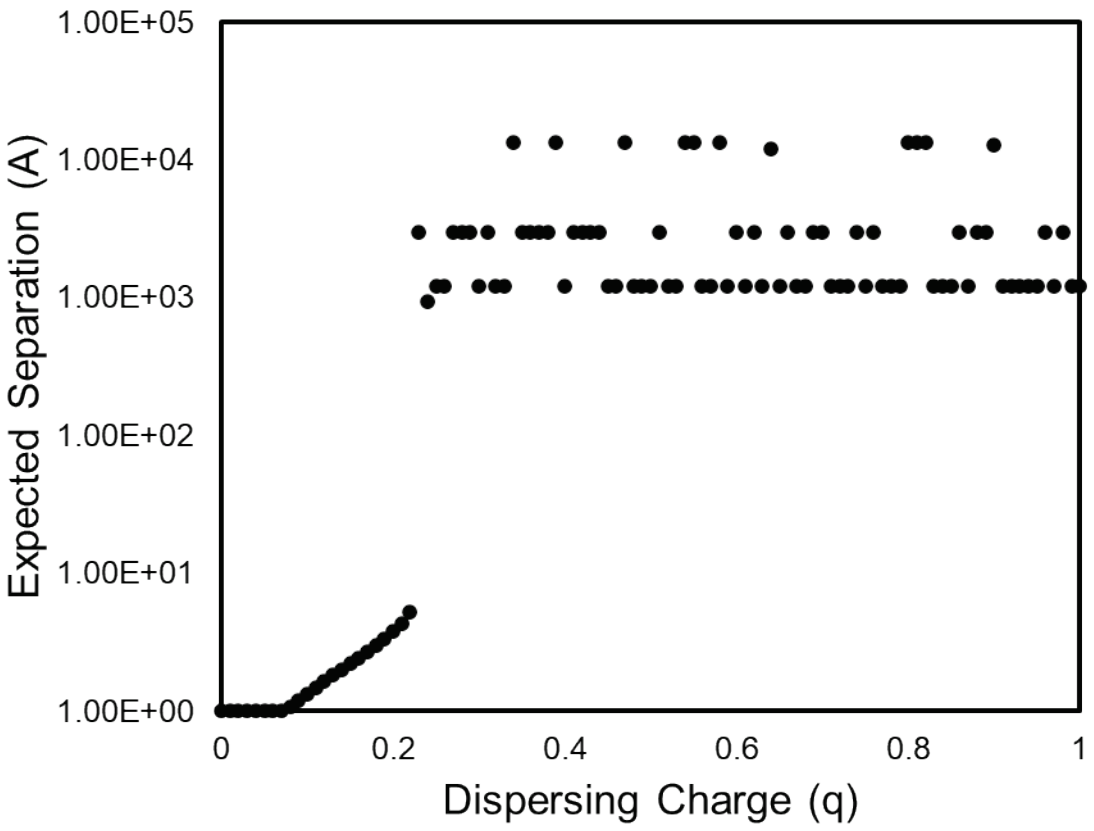

Figure 3.12: The expected separation distance between a dispersed hematite surface and a silica surface. The separation distance grows until separation is completely achieved at around $q = 0.22$.

Bentonite is primarily composed of montmorillonite minerals, which have a fascinatingly appropriate structure for the binding of pellets. The layers of montmorillonite were extracted from crystallographic data and can be summed up as an outer layer of positive cations (sodium or calcium), a layer of oxygen, silicon, oxygen, alkali or alkaline cations, oxygen, silicon, oxygen, and then an outer layer of cations again. In short, the material is symmetric with roughly +3, -9, +13, -11.5, +12, -11.5, +13, -9, +3 as its charge planes at 0Å, 3.75 Å, 4.22 Å, 5.63 Å, 6.56 Å, 7.50 Å, 8.91 Å, 9.38 Å, and 15.00 Å respectively. This peculiar arrangement of charge planes provides a compelling reason for why bentonite is so useful for binding oxide minerals which are typically negatively charged

on their exteriors. Bentonite provides strong positive charges near its surface which can overcome the negative repulsion between its oxide layers and the oxide minerals its binding with. Plugged into the model, bentonite displays strong attractive properties with every other material inspected, besides itself. Bentonite's repulsive interaction with itself is also supported from the perspective of empirical data, as it does disperse well in water and easily spreads even when dry.

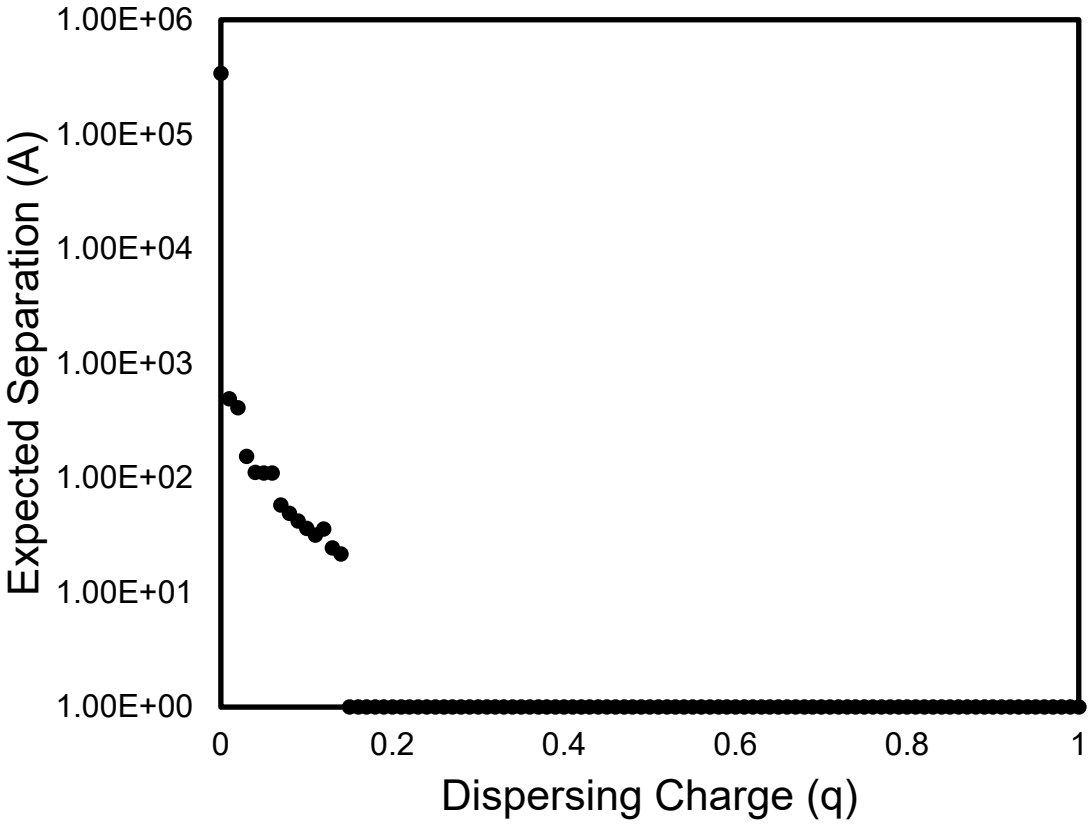

Figure 3.13: Expected separation distance between a dispersed hematite surface and bentonite. Complete attraction is achieved at dispersion above around $q = 0.17$ or so.

As shown in Figure 3.13, bentonite is strongly attracted to highly dispersed hematite, but somewhat repelled by only slightly dispersed hematite. The positive layer of counterions present with only slight dispersing conditions is apparently expected to decrease the

binding ability of bentonite to hematite. This prediction is slightly surprising, as sodium hydroxide is known to improve bentonite performance at least somewhat when added to bentonite pellets – though this is often attributed rather to the isolation of calcium from calcium bentonite instead.

As an alternative example, this model also can predict that kaolinite would likely be an ineffective clay to bind pellets with. Kaolinite consists of an oxide, silicon, oxide, aluminum, oxide layer, and from crystallographic data its layers are -7, +6, -7, +14, -6 at 0 Å, 0.77 Å, 2.04 Å, 3.08 Å, and 4.09 Å respectively. Note that either side can be an exterior, so the reverse arrangement of 4.09 Å, 3.32 Å, 2.04 Å, 1.01 Å, and 0 Å should also be observed. Kaolinite's obvious shear plane provides a very unsymmetric surface behavior. Only the reverse arrangement of these layers is attracted to hematite or silica. Furthermore, the forward and reverse arrangements of kaolinite only attract each other in that order – the front can only attach to the back side of another plane of kaolinite (with a predicted separation of 5.27 – 7.07 Å, which is similar to the empirical crystallographic data). Thus, kaolinite can attach itself to hematite in only one orientation and can thus not form bridges between two hematite particles on both sides.

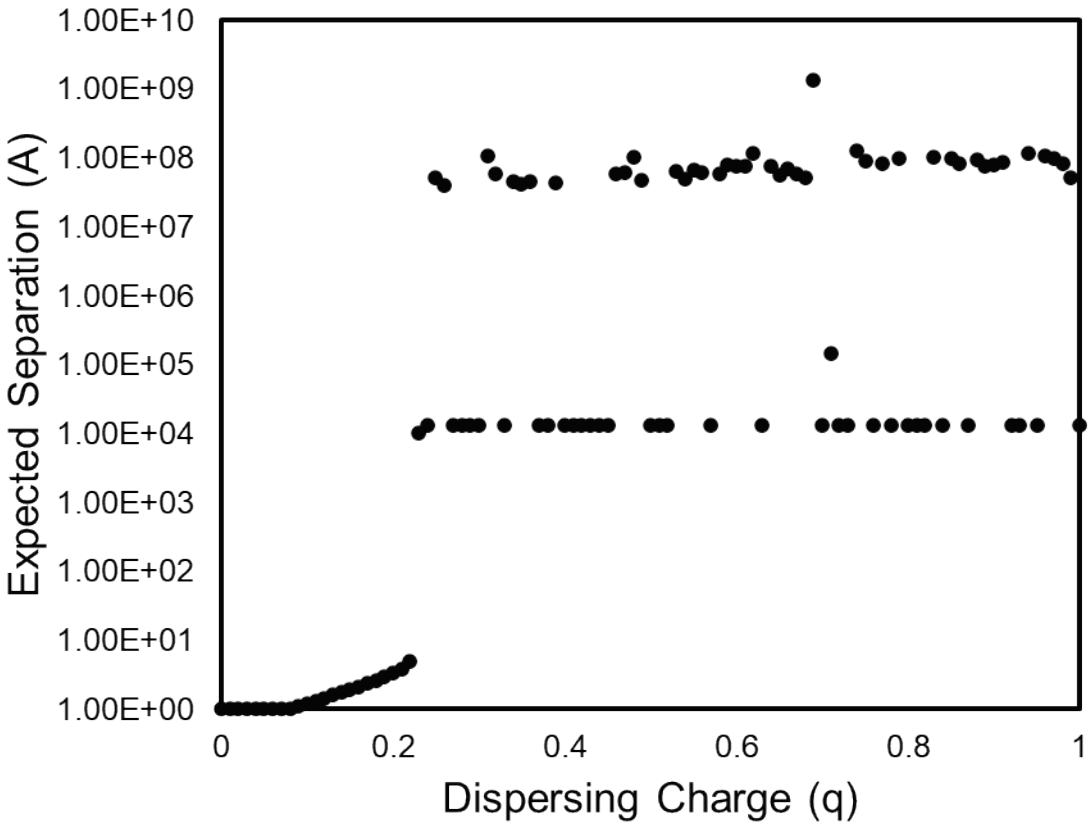

Figure 3.14: Expected separation between the forward arrangement of kaolinite and dispersed hematite. At slight dispersion conditions, some bonding might be possible with the forward arrangement.

The ineffectualness of kaolinite as a binding clay has typically been ascribed to its failure to disperse within the pellet (Eisele and Kawatra, 2003; Kawatra and Claremboux, 2021a,b), but in actuality it appears that the material within the iron ore pellets is likely more mobile than we often give it credit for during balling. This is especially obvious with colemanite, which is often described as a non-expanding clay with no potential for binding the iron ore pellet as a result of its non-expanding nature. But, obviously colemanite does disperse through the pellet, otherwise it would not be effective in increasing the strength of fired pellets – it simply cannot actually bind the hematite or silica to each other on its own because its structure is more like kaolinite than bentonite's.

In Eisele and Kawatra (2003) nontronite is mentioned as an alternative clay, which has a similar smectite structure to bentonite. It is for this reason that this model would expect it to be successful as a pellet binder. However, nontronite was also not tested in the experimental work. However, theory suggests that it should be viable.

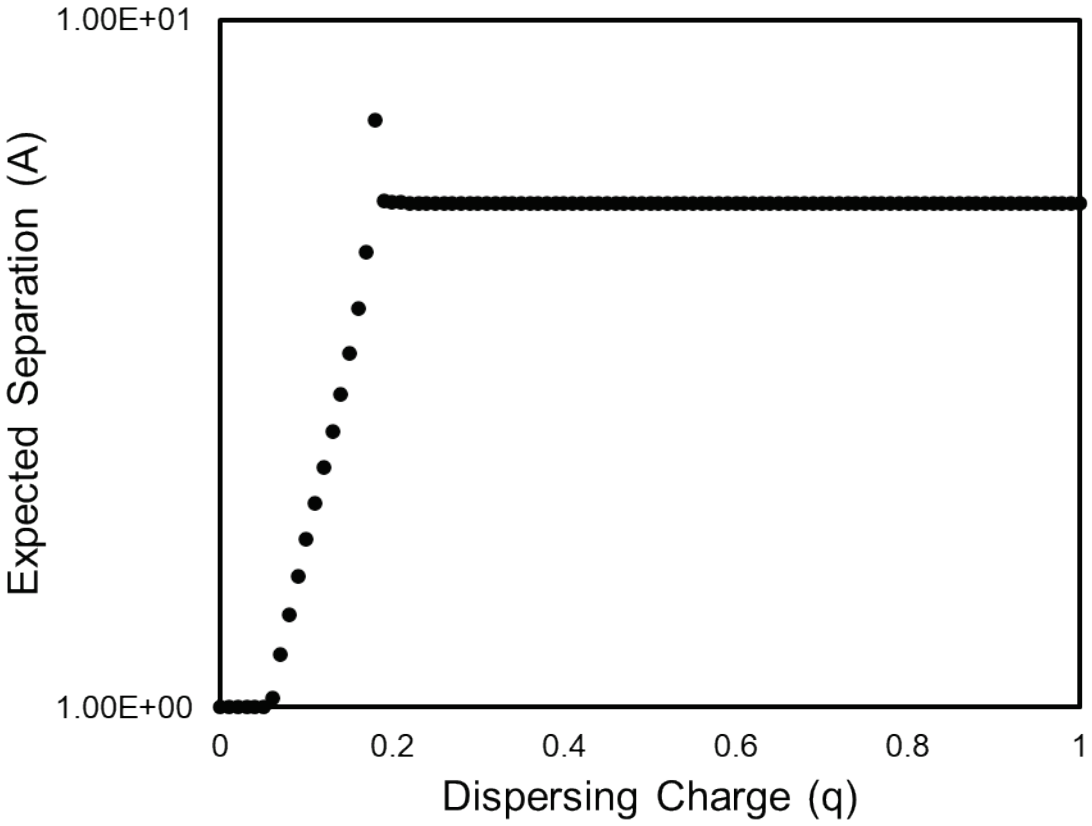

Figure 3.15: The expected separation distance between the reverse arrangement of kaolinite and dispersed hematite. This is always attractive, but more so at slightly dispersed conditions.

Note in particular that Figure 3.14 and Figure 3.15 provide a testable prediction of this model. If a slightly dispersed hematite (e.g. perhaps with sodium hydroxide as an additive) can be effectively mixed with kaolinite, some increase in pellet strength should be observed. This would not be expected to be extremely useful, as the kaolinite will

need to be carefully mechanically mixed because it does not disperse easily with the water, but it should be able to form bonds between separated hematite surfaces on both sides under these conditions. A brief overview of related literature suggests that this prediction is supported by the idea of alkali-activated binders in the context of cements cements, including those based on kaolinite (Ababneh et al., 2022; Ponomar et al., 2022), but it does not appear to have been applied to the preparation of iron ore pellets.

This methodology can be stretched a little bit further to understand the behavior of organic binders. The strength of the interactions between any organic binder and the hematite surface is going to be fairly consistent even between different organic binders, because organic compounds do not evolve particularly extreme charge distributions and as such do not show particularly inconsistent behavior between similar bonds in different compounds.

The question becomes “is the surface formed by the organic binder on the hematite or silica better or worse at binding than it was before?” For instance, if sodium acetate is added as a binder, the acetate anion will attach to the hematite surface via the carboxylic acid group. The remainder of the acetate is essentially neutrally charged, so in essence the acetate anion serves to shield the hematite surface from interaction with other charged surfaces. As such, acetate pellets would be expected to be quite weak, and experimentally this is found to be the case.

However, sodium tripolyphosphate performs almost exactly the opposite role, attaching the pentavalent anion tripolyphosphate to the hematite surface. This presents an

extremely negative charge to the surroundings, which can strongly interact with other materials in the system.

Sodium metasilicate should behave similarly to the silica model presented prior, with a limited charge density compared to tripolyphosphate. Its lower charge density means that it may help or hurt depending on exactly what materials are present. In particular, it likely competes with tripolyphosphate for attachment sites on the hematite surface and is also likely introduces repulsive behavior between most of the surfaces present and any tripolyphosphate surfaces available. This is a case where we would expect poor interaction between the two binders, despite being of a similar type. It is also worth noting that it is likely not the case that metasilicate is particularly selective towards any one type of surface in the pellet. As such, its effects on pellet strength should be expected to be somewhat limited as it does not contribute a strict binding mode.

Sodium polyacrylate is a less intense dispersant than tripolyphosphate but does include a clear binding mode that metasilicate does not. The carboxylate bonds in polyacrylate are known to be able to firmly attach to hematite surfaces, and the backbone of the polyacrylate polymer should allow it to behave similarly to starch and form bridges between different hematite particles. It should similarly compete with tripolyphosphate, but unlike metasilicate its efficacy as a binder is a bit more straightforward. As such, the interaction is likely to be less adversarial. However, it is probably not synergistic either, as the negative charges presented by both tripolyphosphate and metasilicate are likely to hinder the formation of strong bonds between the inorganic surfaces.

4 Methods and Materials

The most important novel analysis to be tested is the correlation of abrasion and compression strengths for various binders and establishing that mixtures of binders should have linearly additive pellet strengths. Experimental work was undertaken to explore both of these points by creating pellets and utilizing compression and abrasion testing to evaluate their performance once dried.

The primary experimental methods used for this work are similar to those used by Halt (2017) and my own previous work (Claremboux, 2020). Emphasis was placed on understanding how pellets break in especially dry compressive strength.

In all cases, pellets were formed in a laboratory balling drum and then subjected to a variety of tests. The pellet feed material has previously been characterized in a variety of conditions which were performed as part of earlier work and in my Master's thesis.

Pellets were formed in a laboratory balling drum utilizing a fine hematite pellet feed, collected from an operating plant facility. This material has an 80% passing size of less than 35 μm. The material was balled at a variety of moisture contents, targeted primarily at 8.5wt% to 9wt%, but always recorded fact. Some feed mixtures were found to require far more or far less water to make an acceptable pellet.

The additives were chosen based on differing impressions of their binding characteristics. Binder dosages were taken uniformly based on typical dosages for organic binders in

general, or 6.6 kg/t as a typical bentonite dosage. Data from previous work is also correlated into this work where necessary to enhance understanding.

The additives used for this work specifically are less varied than they were in my M.S. work, focused instead on understanding differences in pelletizing behavior that were likely to expose interesting behavior and insights. They were investigated as pure binders and in many cases as mixtures of similar or dissimilar binders.

Sodium bentonite was chosen as a reference additive, as the most commonly used pellet binder for both industrial use and for comparison. The sodium bentonite used for this study is similar to other sodium bentonites used in previous work at Michigan Tech, and was received from Plant F.

Sodium tripolyphosphate (technical grade, 85%, from Sigma-Aldrich) was chosen as a dispersant additive, as a dispersant with different character than other dispersants which were tried in my M.S. thesis. Unlike the other primary dispersants chosen for this work, sodium tripolyphosphate is small molecule which is soluble in water and has an extremely high valence anionic component ($P_3O_{10}^{5-}$). As such, it is not expected to show any polymeric effects like sodium polyacrylate or sodium metasilicate might.

Sodium metasilicate (Alfa-Aesar, technical grade) was chosen as a dispersant additive, as a dispersant which has a polymeric character which also appears to have potential as a binder but was not observed to result in unlimited binding in my M.S. work. Sodium metasilicate was chosen as a representative dispersant which appeared to have little binding properties of its own merit, and thus as a reference.

Sodium polyacrylate (as poly(acrylic acid sodium salt) from Sigma-Aldrich, average molecular weight of 5100 by GPC) was chosen as a dispersant additive which was also expected to have binding properties due to its relatively high molecular weight.

Sodium acetate (>99%, from Sigma-Aldrich) was used once as a dispersant additive as a reference for the activity of a low valence salt.

Sodium polystyrenesulfonate (molecular weight around 70000, from Sigma-Aldrich) was also tested once to see if the sulfonate bond would perform particularly well or poorly in the work.

Pellets were produced following procedures reported in my M.S. thesis and in my reviews (Kawatra and Claremboux, 2021a). The pelletization procedure proceeds as follows:

1. Feed material de-lumped and weighed.
2. Solid binder materials measured out and added to feed, mixed in an orbital kneader-mixer for 5 minutes.
3. Water added to adjust moisture content of the feed as necessary, mixed in an orbital kneader-mixer for 5 minutes.
4. Feed material de-lumped and brought to laboratory pelletizing drum.
5. A small amount of material added to the drum, allowed to roll for a few minutes, and then discarded to ensure that the drum's surface is prepared for balling.

6. A small amount of material is added to the drum and sprayed with water to form seeds. These seeds are grown and occasionally removed from the drum and sieved to ensure a narrow size distribution in the drum.
7. Material and water is added as necessary until the pellets have grown to 7/16”x1/2” in diameter.

Water was added during the pelletizing process as necessary to ensure the capillary interactions described in Chapter 2.

Some pellets were made by layering different types of materials on top of each other. In such a case, the pellets were grown to a specific size using one material, and then grown to their final size using another. The typical cutoff point is at the 3/8” mesh, allowing pellets to be grown up to 3/8”x7/16” using one material and then from 7/16”x1/2” using the other.

The procedures for typical tests were followed as shown in Table 1.1. Compression strengths were determined using a Mark-10 M5-50 force sensor, crushed at a constant linear velocity of 40mm/s. Wet compressive strength and wet drop number were tested immediately after pelletization if recorded, while dry compressive strength was tested after drying in an oven at 105 °C overnight.

The last remaining experimental technique is the abrasion test. As opposed to the test outlined in Table 1.1, the following test is proposed:

1. A portion of pellets (>50g and <1kg) is placed onto a sieve stack consisting of a 3 mesh, 35 mesh, and bottoms pan. The material which naturally ends up on each layer is recorded as the +3 mesh, +35 mesh, and total masses.
2. The material is placed in a Ro-tap machine for a specified amount of time. The material is allowed to abrade against the sieve for the specified duration, and the +3, +35, and total masses are recorded afterwards.
3. As necessary for additional data points, the test can be repeated with the already abraded material.

Breaking the test into multiple segments is a novel modification which allows for the direct verification of the form of the kinetic model described in section 3.6. This is also helpful as it provides a significant theoretical backing for both the model and the use of the one timestep test which sees some significant use in industry.

Each individual test condition and their corresponding results are reported in Chapter 5.

5 Results and Discussion

Again, there a few goals which this test work aimed to address:

1. We wished to verify the prediction that the abrasion test using the Rotap machine would provide repeatable and consistent results in line with the predicted abrasion curves given in section 3.6.
2. We wished to verify the prediction of a correlation existing between the abrasion rates and the compressive strengths of the pellet materials in question.
3. We wished to verify that mixed binders resulted in mixed strengths, as predicted in section 3.1 and 3.2. It is hoped that the relation will be clearer in abrasion strength than in the compression strength as the abrasion test is expected to help eliminate the impact of the pellet geometry on the strength results.

The following test work was performed in Michigan Tech laboratories to address these points, and the results reported below are novel to this dissertation. These results are intended to make the cases for each of these three goals directly and are analyzed in that context.

The tests included pure binders for comparison as baselines, binary mixtures of binders to verify binder interactions as discussed in Section 3.7, layered pellets in an attempt to create pellets which would require multiple rate constants to model with the kinetics derived in Section 3.6, and utilizing roll press mixing on bentonite to determine if the dispersing affects previously acknowledged for that process would aid abrasion strength.

5.1 Pure binder baselines

The main binders investigated were sodium bentonite, sodium metasilicate, sodium tripolyphosphate, and sodium polyacrylate. As a baseline to compare further results to, these materials were tested on their own. The dosages of the organic binders were held constant at 1.0kg/t, while bentonite as added at 6.6kg/t.

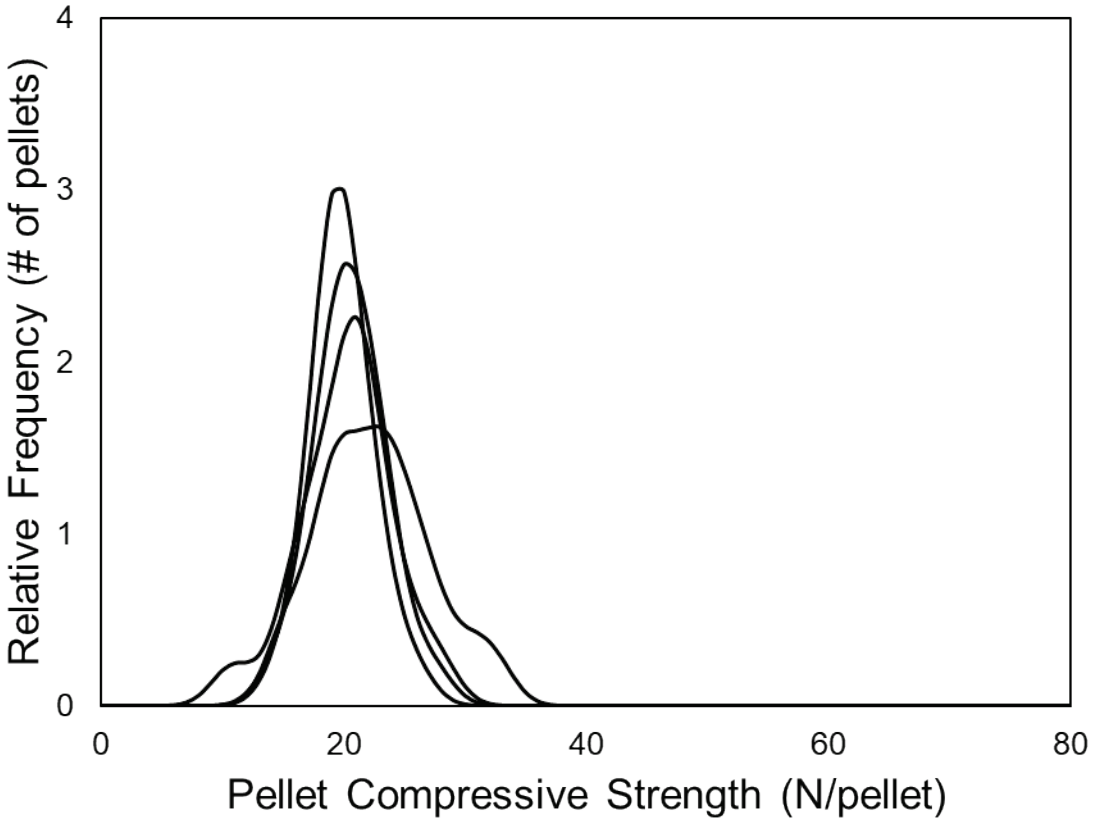

Figure 5.1: Histogram of pellet compressive strengths for hematite pellets formed with 6.6 kg/t of sodium bentonite as binder. Each line represents a sample set.

Starting with the sodium bentonite pellets, smoothed histograms of the pellet strengths are shown in Figure 5.1. These were quite consistent, with the histograms looking quite similar for each sample. On average for this material bentonite did not exceed the

suggested minimum industrial dry compression strength. The moisture contents of these bentonite pellets varied quite a bit but centered on 8.0wt%. Whether created with too much water or too little, the performance was surprisingly bad, at least compared to many of the other materials used with this material successfully.

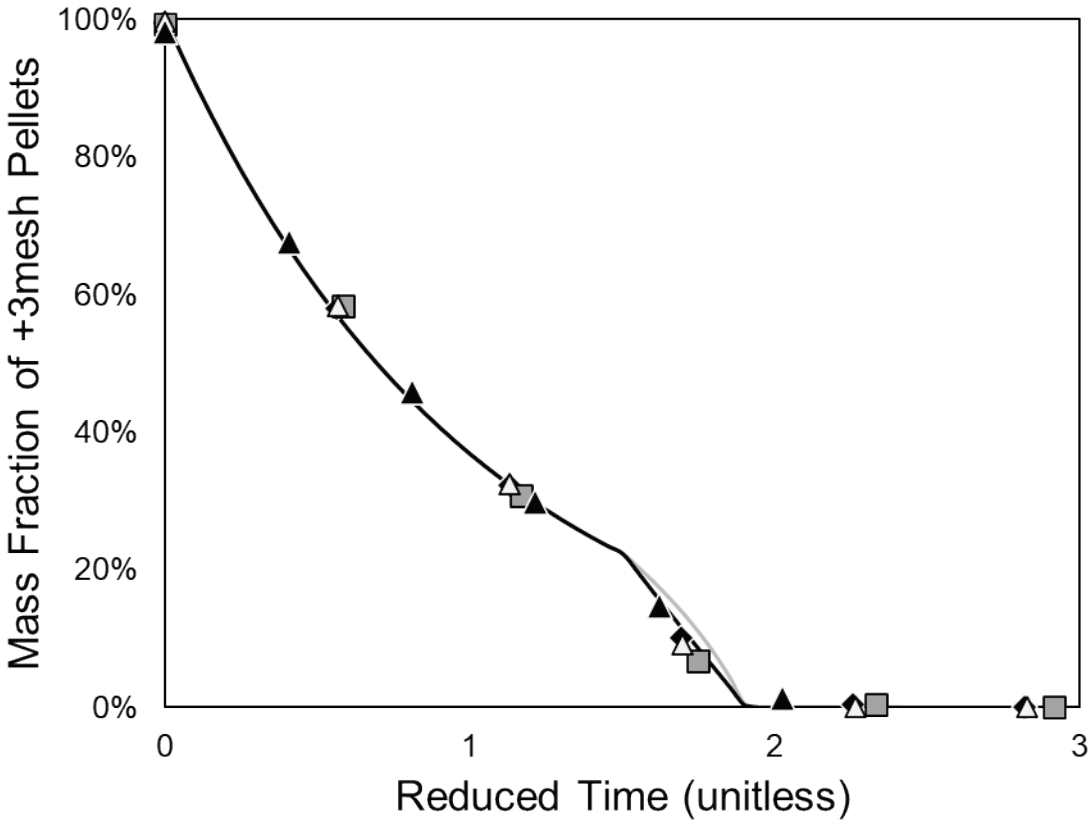

Figure 5.2: Results from the upper mass fraction of the abrasion test, using a reduced time which minimizes the difference between the measured data and all three mass fraction curves.

The reduced time used in Figure 5.2 is based on a rate constant determined entirely systematically via numerical minimization. As should be clear from even just this first data set, the theoretical basis seems to have done an excellent job at describing the behavior of the material during the abrasion test.

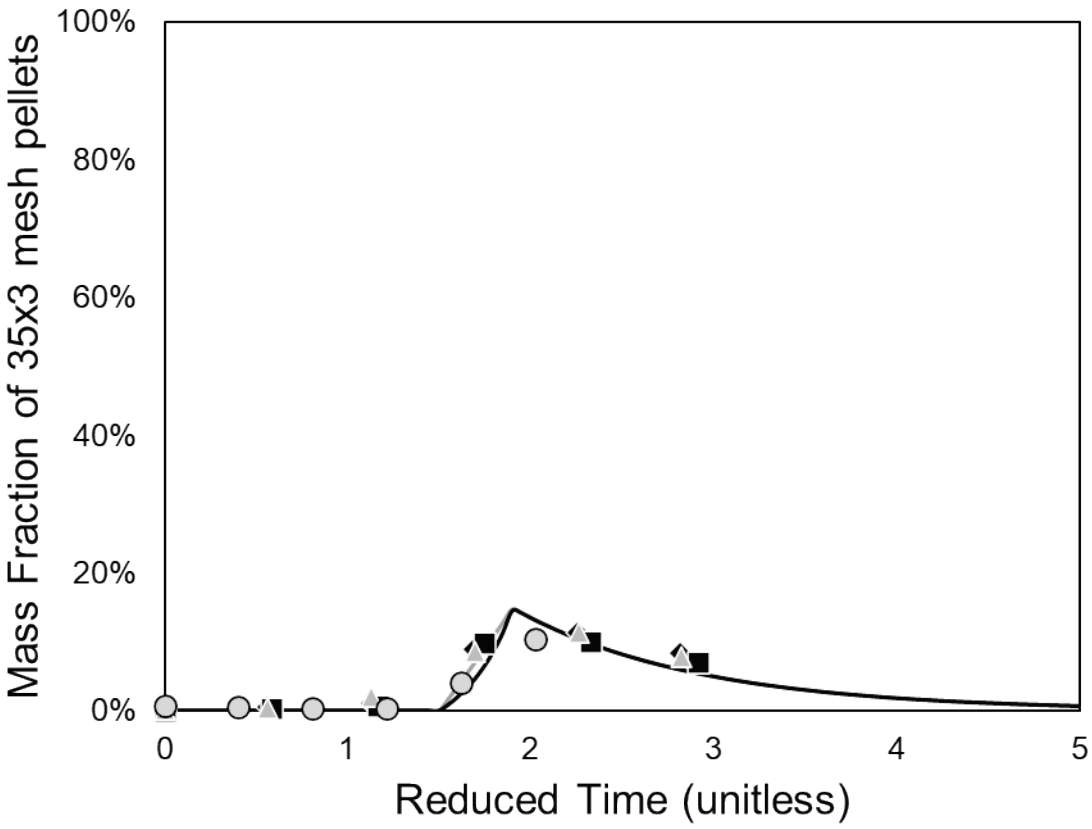

Figure 5.3: Results from the middle mass fraction for pellets bound with 6.6kg/t bentonite. The first odd point is present at reduced time 2 here, as it falls under the curve. This would suggest that a complete pellet break has potentially occurred.

Figure 5.3 shows that the middle mass fraction is also well predicted by the theoretical lines. However, there are a few small deviations. The points which are a little bit above the line are easily explained by a small quantity of finer materials being present from the very beginning of the test, but the one point which is below the line requires breakage or material loss to be explained.

Breakage is certainly a possibility, as the material is being beaten against a sieve using a Ro-tap as a method of determining its abrasion resistance. However, Figure 5.3 and every

subsequent test is going to show that it is very likely that only a very small fraction of pellets undergo complete breakage during the abrasion test.

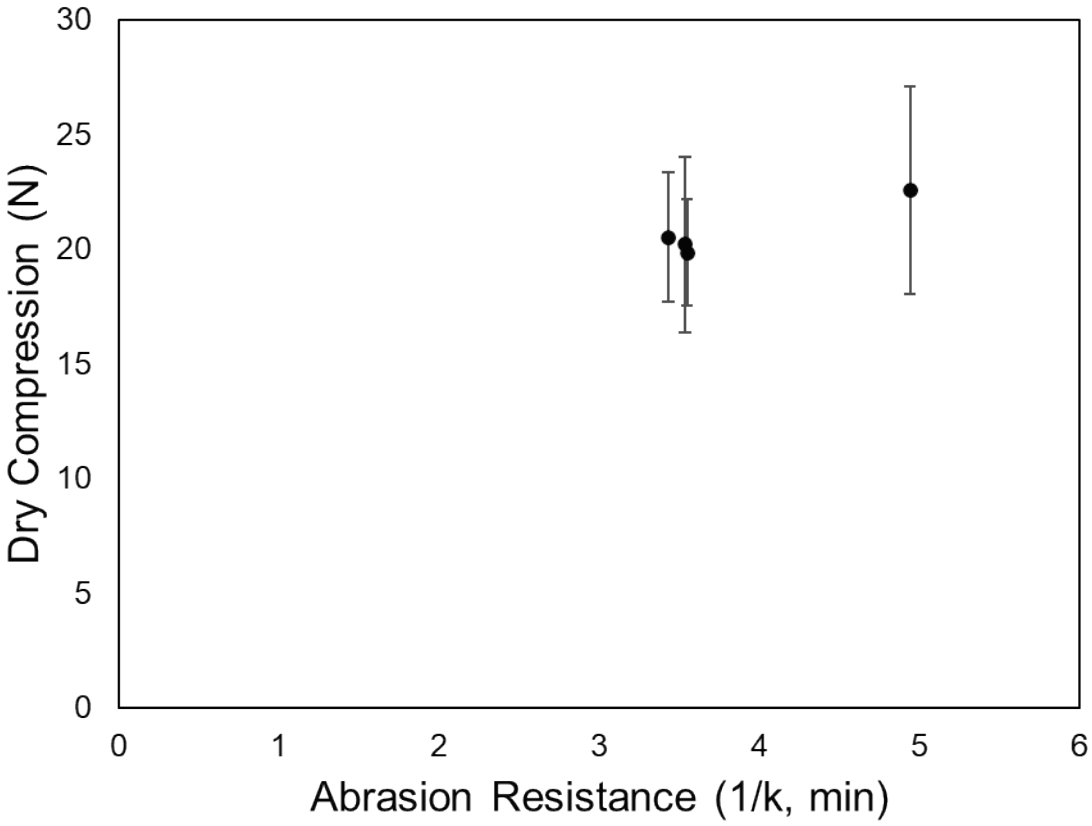

Figure 5.4: Comparison of abrasion resistance to the dry compression for sodium bentonite containing pellets. While error bars are not shown for abrasion resistance here, they are relatively small.

Figure 5.4 is shown to report the dry strength and rate constants for the pure bentonite pellet samples made here for which abrasion data is available. As of yet, there is nowhere near enough data to say if there is a consistent trendline connecting these data points as plotted.

Next up, 1.0kg/t sodium metasilicate. When used with sodium bentonite, it had previously been found that even slight additions of sodium silicate greatly improved the

maximum observed pellet strength (Claremboux, 2020). This occurs again in a few samples this time as well, with a couple of high strength peaks scattered throughout as shown in Figure 5.5. However, overall metasilicate by itself is consistently around the minimum required dry strength as well.

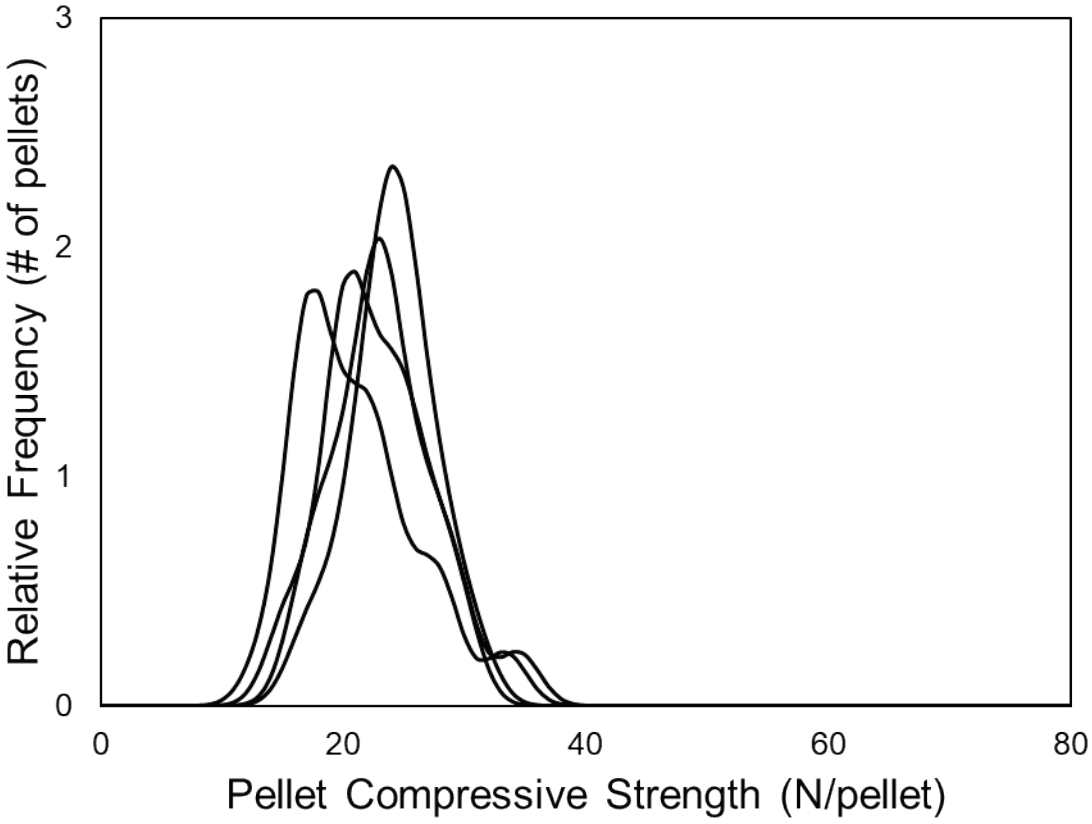

Figure 5.5: Strength histogram of pellets formed with 1.0kg/t of sodium metasilicate as an additional binder. Each line represents a unique sample.

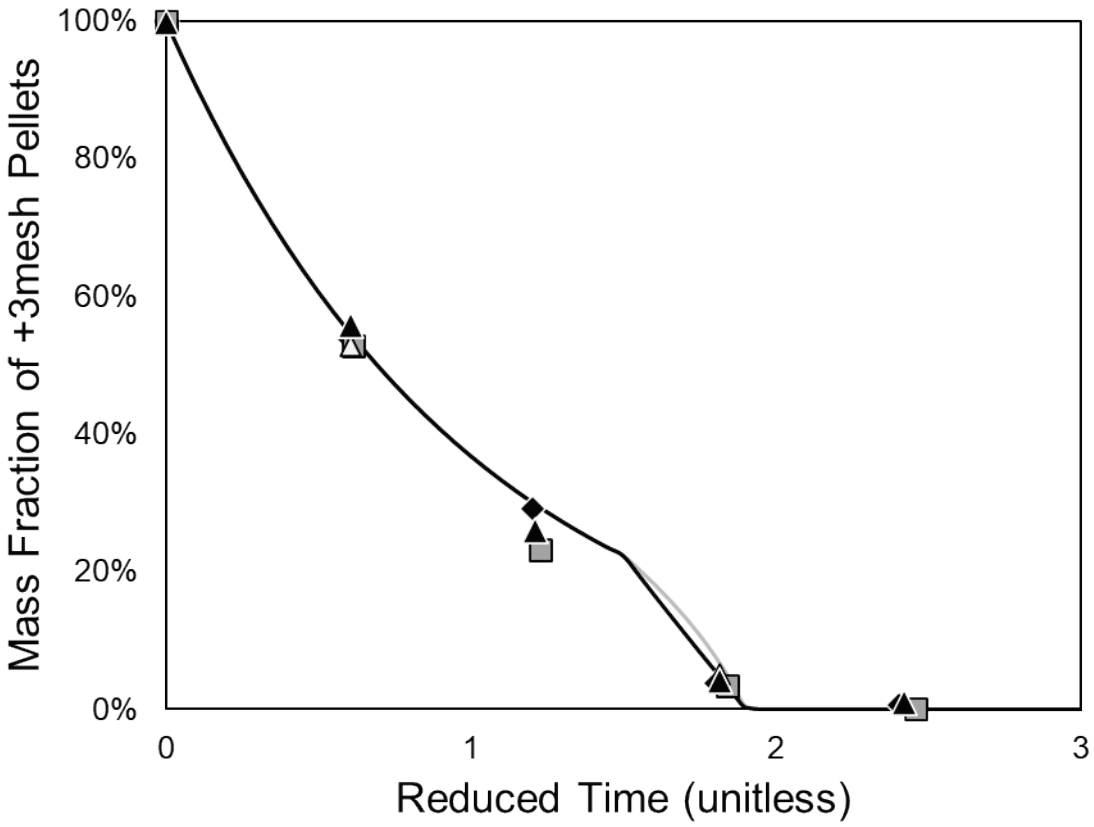

Figure 5.6: Upper mass fraction from the abrasion test of 1.0kg/t sodium metasilicate test. Again, very good correlation is seen between theory and data. However, the points around time 1.2 seem to have reliably experienced breakage or some other phenomenon to be consistently below the trendline.

Figure 5.6 shows that again the abrasion theory is followed very closely. Unlike with the sodium bentonite, however, it seems that the metasilicate pellets are breaking a little bit more quickly than expected near reduced time 1.2 or so. This may be a sign that metasilicate pellets are somewhat more prone to chipping than bentonite pellets are.

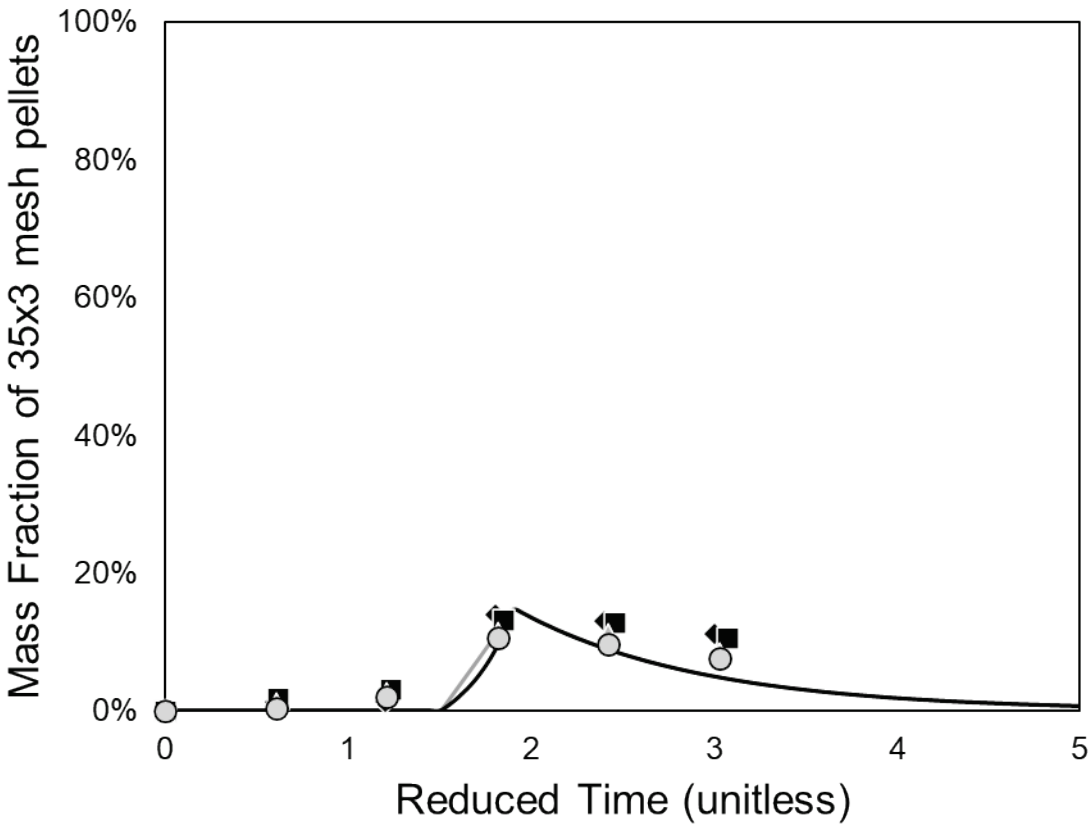

Figure 5.7: Middle mass fraction for abrasion of 1.0kg/t sodium metasilicate pellets. None of these results are below the expected values, meaning that nothing in this size range appears to have broken unexpectedly. However, each sample does seem to have picked up a little more mass than expected.

Figure 5.7 is not as cleanly fitting the theory as Figure 5.3 did for bentonite pellets. However, the explanation is still that a small amount of pellet breakage likely occurred to the sodium metasilicate pellets. Even still for metasilicate the majority of mass changes are still accounted for by the abrasion theory.

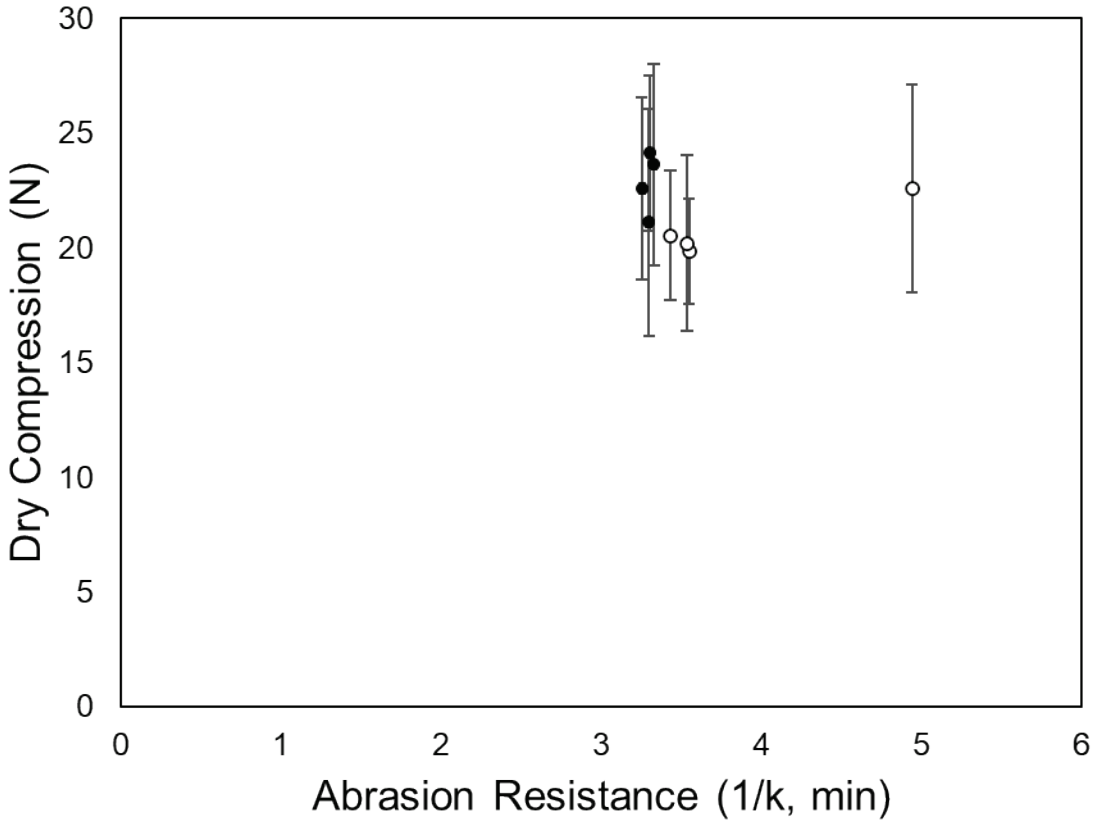

Figure 5.8: Adding 1.0kg/t sodium metasilicate points to Figure 5.4. Old points (bentonite) are shown with white dots, while new points are shown with black dots.

Figure 5.8 does a better job of showing that both the abrasion resistance and mean dry strength results can be relatively stable for a given material. Metasilicate and bentonite have similar performance, but the overall trends would seem to imply that metasilicate is a somewhat worse binder for abrasion resistance than bentonite at the same pellet strength. This is somewhat curious, as metasilicate's behavior as a dispersant would be expected to help pellet compaction, which is believed to be strongly related to the abrasion resistance (Halt and Kawatra, 2017a; Claremboux, 2020). However, on its own it does not seem to accomplish that goal.

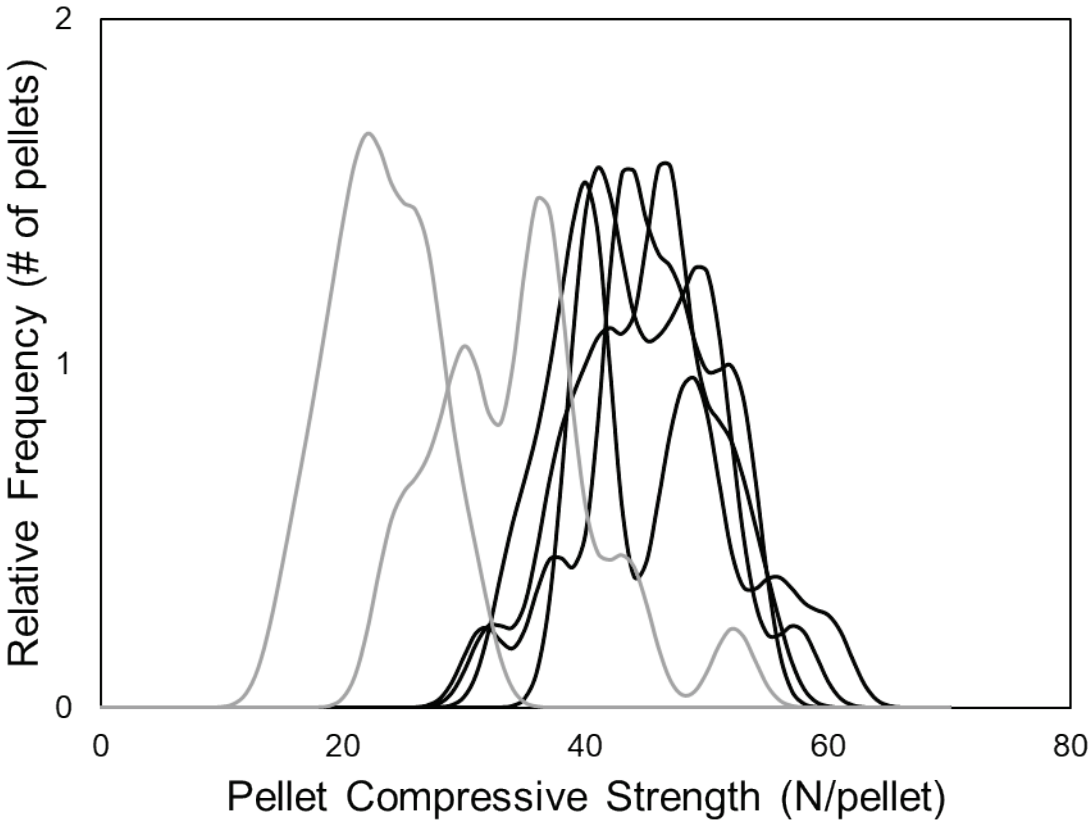

Figure 5.9: Strength histogram of pellets formed with 1.0kg/t of sodium tripolyphosphate as an additional binder. Each line represents a unique sample. Grey lines were considered outliers. The reason for their low performance is somewhat unclear, however.

Figure 5.9 shows the first major improvement in pellet strength. Sodium tripolyphosphate is capable of increasing pellet strength considerably with similar mass addition to any of the other organic binders. However, some of the tests did not result in as much strength improvement. It may be as simple as varying calcium contents in the pellet feed, or it may be a case that the tripolyphosphate dosage is very close to the limit at which dispersion is achieved. It could also be evidence that dispersion alone results in chaotically inconsistent binding between adjacent hematite material. The observed strength difference from the sodium metasilicate is approximately a 100% increase, as

would be expected between a non-dispersing and dispersing condition, so that is a possibility. However, sodium tripolyphosphate has a very intense effect on the zeta potential along with a very small critical zeta potential for dispersion effects (Claremboux, 2020).

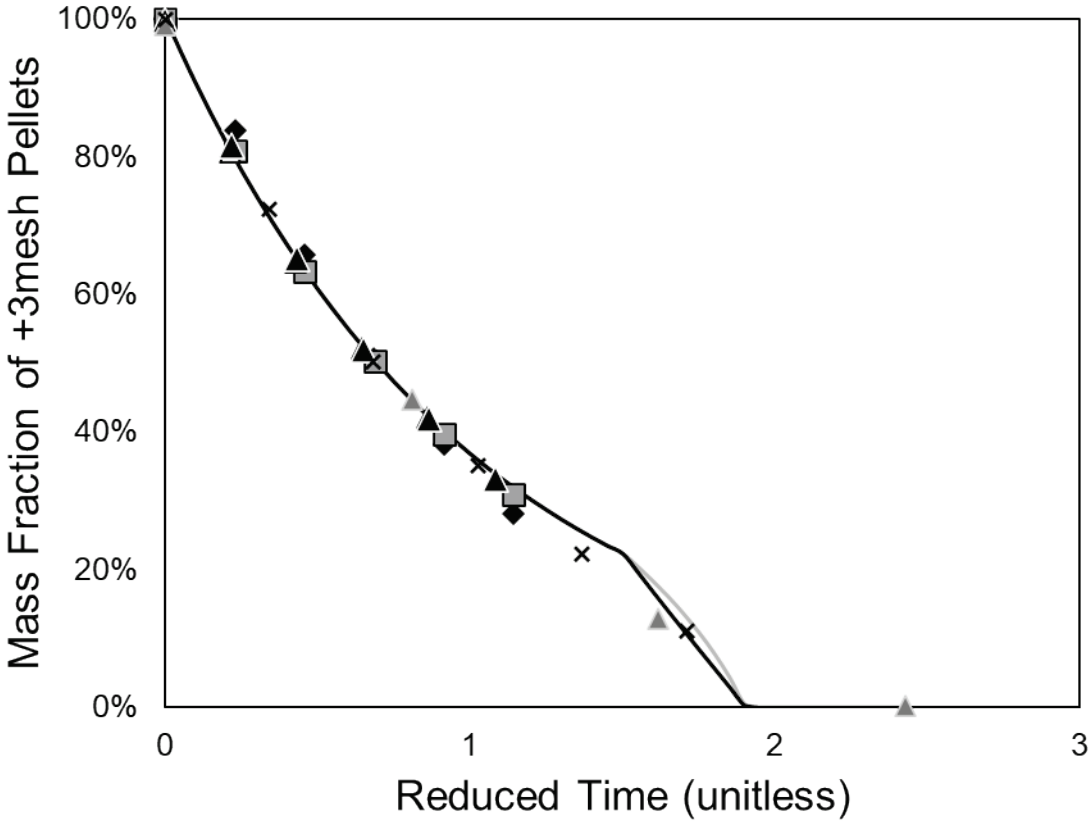

Figure 5.10: Upper size fraction for abrasion test of 1.0kg/t sodium tripolyphosphate. Again near 1.1-1.5 there are a few points which are a bit lower than the line, suggesting that some breakage may have occurred.

Figure 5.10 continues to show that the theory matches reality quite well. Again a small handful of points have likely undergone breakage, but it is a very small fraction of the material overall.

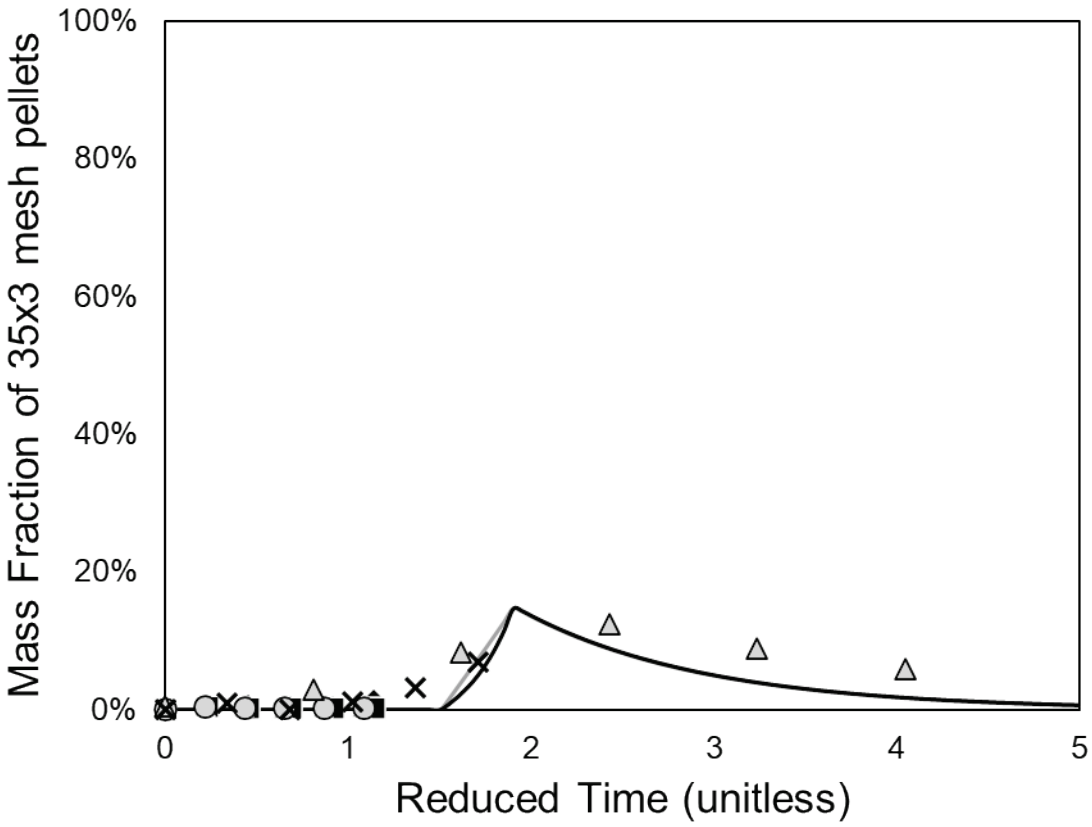

Figure 5.11: Middle size fraction for pellets bound with 1.0kg/t sodium tripolyphosphate. The weakest batch of pellets shown in Figure 5.9 are the ones which extend past the hump in the graph, and apparently also underwent breakage to maintain large particles for as long as they do after time 2.0.

Figure 5.11 finds that all abrasion tests result in at least as much material as predicted by the theory ending up in the middle mass fraction again.

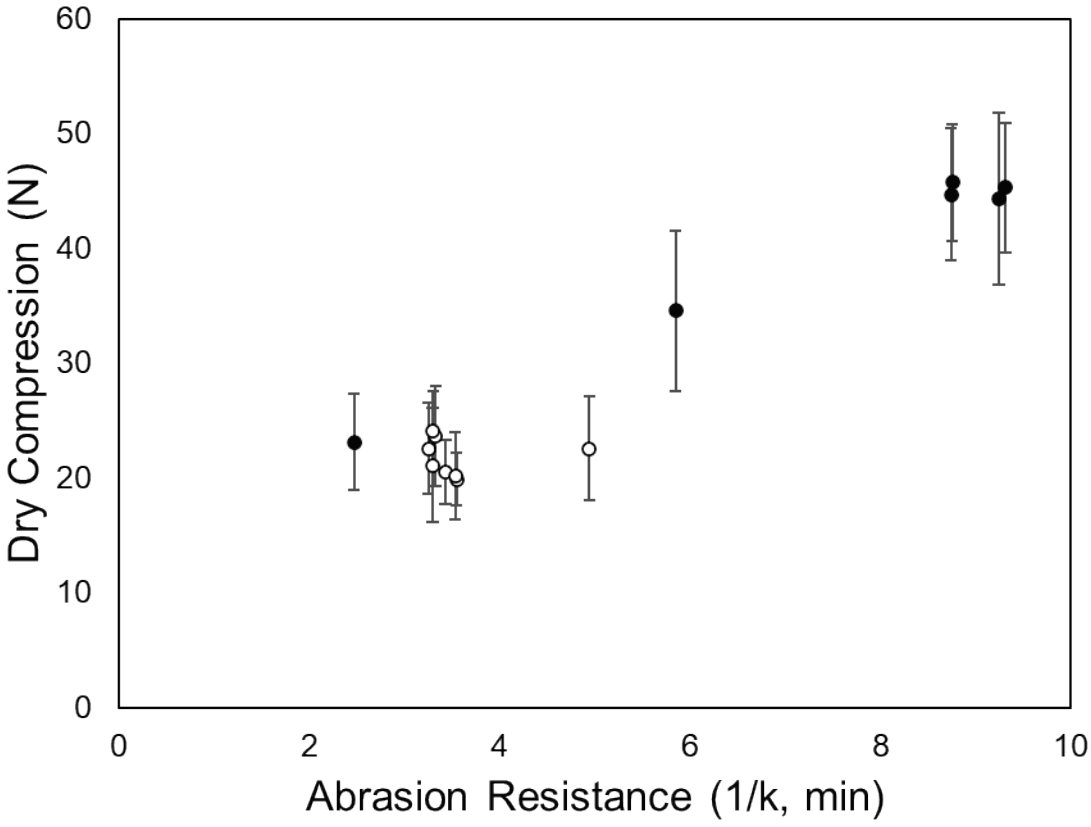

Figure 5.12: Adding sodium tripolyphosphate pellets to Figure 5.8. A wider trendline is proposed for the tripolyphosphate material. It may be that direct correlation with the mean dry strength may be difficult due to the wide variation inherent in the dry strength test.

Figure 5.12 shows a roughly increasing trendline for abrasion resistance versus dry compression, as would be expected from the math laid out in the previous chapter. However, the variation of the dry strength means that it is not a clean correlation yet.

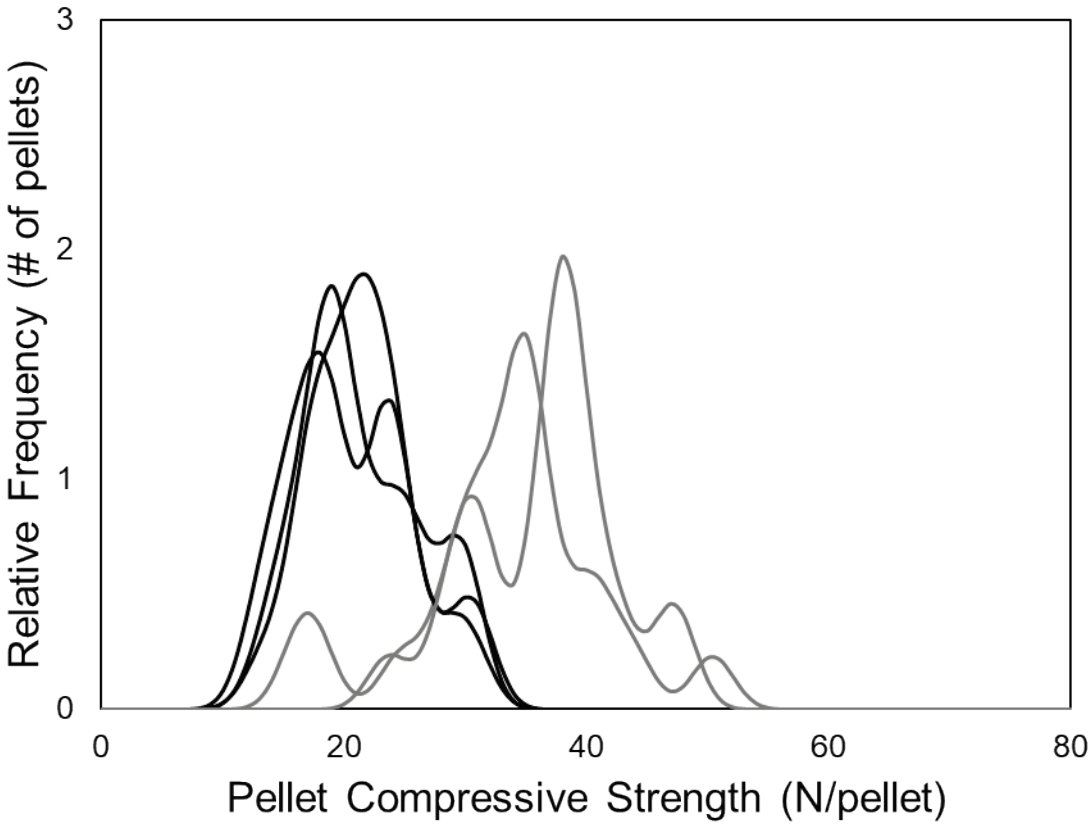

Figure 5.13: Strength histogram of pellets made with 1.0kg/t of sodium polyacrylate. Similarly to the tripolyphosphate results, there are a couple of samples where a strength increase is achieved, but typically on its own its performance is comparable to bentonite.

Figure 5.13 shows that a similar split of what is likely dispersing or non-dispersing conditions occurs with sodium acrylate as with sodium tripolyphosphate. If normalized based on charge added, the normal dosages of both are fairly similar: 0.0136 mol valence per kilogram of ore for tripolyphosphate, 0.0106 mol valence per kilogram of ore for polyacrylate. However, the normal dosage of metasilicate was around 0.0164 mol valence per kilogram of ore, and it should also have a very low critical zeta potential due to its polymeric anionic nature, so it should have also displayed dispersing effects at these dosages. However, since the valence available in metasilicate or tripolyphosphate is more concentrated, it may be one unit of calcium or magnesium has a greater effect on them

than it does for polyacrylate. Again, this could also be taken as evidence that dispersants used on their own appear to result in inconsistent binding between adjacent hematite surfaces.

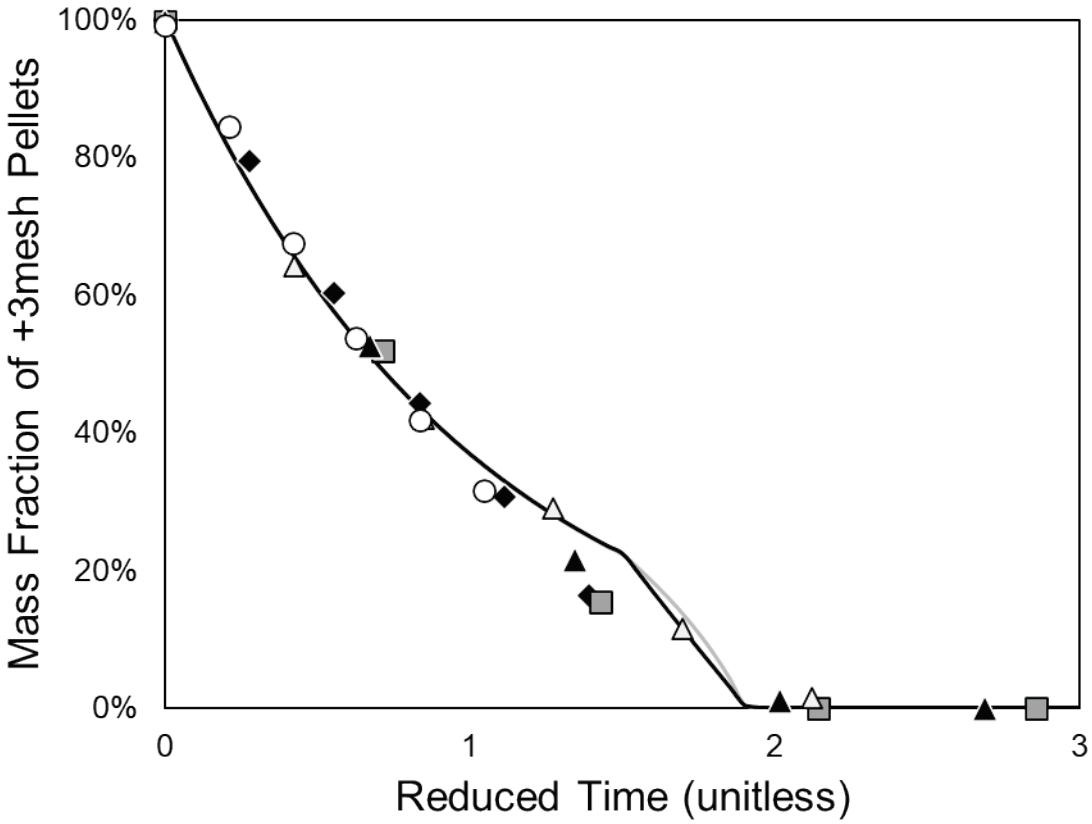

Figure 5.14: Top mass fraction of reduced abrasion test results for 1.0kg/t sodium polyacrylate. These are the first set of points which do not appear to line up as nicely as the rest, but this is still within the realm of being explainable by pellet breakage.

Figure 5.14 suggests that sodium polyacrylate either promotes an alternative abrasion rate correlation with the kinetic energy, or more likely that sodium polyacrylate also forms pellets which chip or break more readily than bentonite pellets do at these dosages.

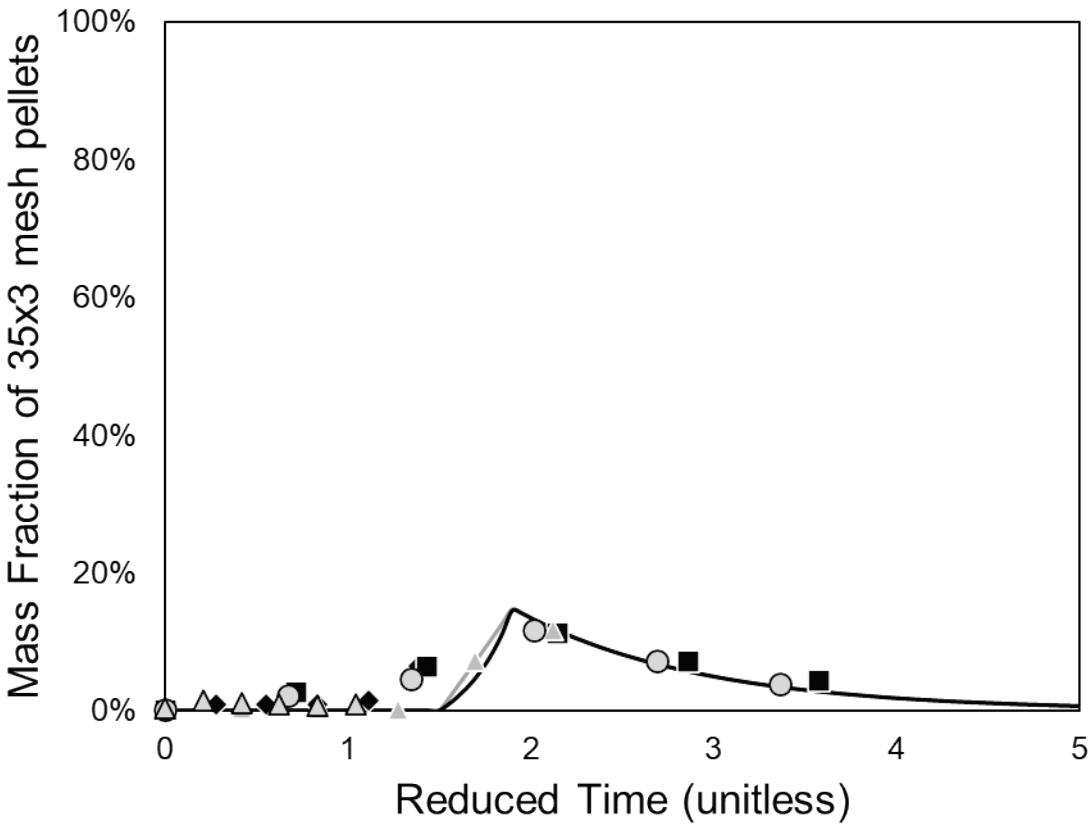

Figure 5.15: Middle mass fraction for pellets made with 1.0kg/t sodium polyacrylate binder. Again, it appears that pellet breakage may be occurring in small quantities in some of these pellets.

In any case, it seems apparent from the metasilicate and polyacrylate results that relying primarily on a dispersant alone is not ideal for consistent pellet formation, as the outlying strength results shown in Figure 5.9 and Figure 5.13 were performed at very similar conditions utilizing the same materials. The difference in results despite consistent methods would suggest that relatively small changes in some part of the pellet mixture can negatively impact the efficacy of these binders on their own.

However, the observed differences in strength performance did not seem to negatively impact the consistency of the abrasion results. To finish off the pure binder results, we also present pellet strength versus abrasion resistance with this last set of data added:

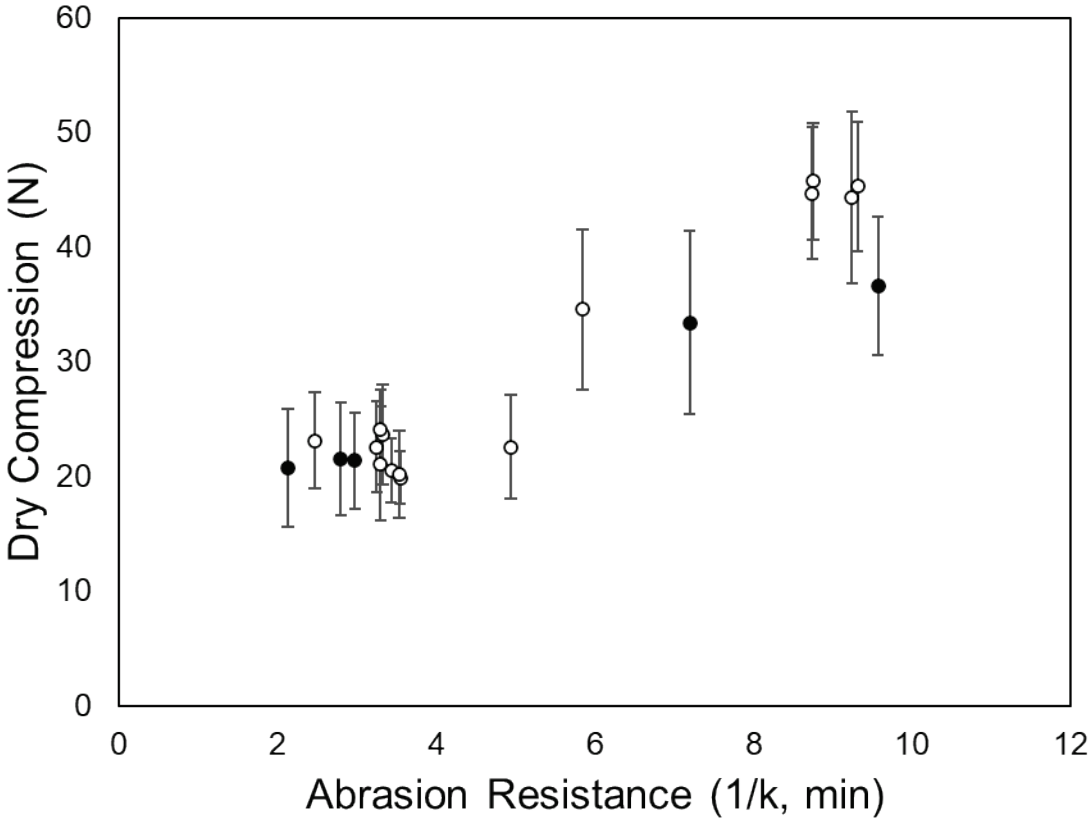

Figure 5.16: Adding the 1.0kg/t polyacrylate material to Figure 5.12. The lower strength regions shows reliable correlation still, while it looks like at higher strengths the contribution of polyacrylate is more focused on abrasion resistance than pellet strength.

The results in Figure 5.16 are interesting, because it appears that polyacrylate has a stronger contribution to abrasion resistance than pure pellet strength, at least compared to the other pure binders tested. Polyacrylate seemed to be the material that seems most like a traditional organic binder, when compared to starch, having relatively long chain polymers as a part of its structure and clearly being able to successfully form bonds with

the hematite and silica surfaces. Thus, it was expected that it would be, if anything, more firmly involved in improving crush strength than abrasion resistance. However, it still has the key feature of being primarily a dispersant, which also likely means that unlike starch it is strongly disinclined to stay bundled up when dissolved in water. The high ratio of compressive strength to abrasion strength may simply be taken as a tendency to form less spherical pellets as well.

Perhaps this abrasion resistance is a sign of being well dispersed through the pellet – although, sodium tripolyphosphate also certainly achieves that by being monomeric. However, tripolyphosphate is forming relatively slightly stronger pellets at the same abrasion resistances as the stronger polyacrylate samples.

The same sort of relationship is also seen between bentonite and metasilicate, though it is subtle enough that it is probably safe to suggest that it not be taken too seriously. However, it looks like abrasion resistance favors binders with larger binding domains (e.g. long chain polymers), with bentonite (being a large, expanding clay) forming slightly more abrasion resistant pellets than metasilicate (of relatively low molecular weight) at the same compression strength and polyacrylate forming more abrasion resistant pellets than tripolyphosphate at the same compression strength. However, all binders are chosen because they can evolve large binding volumes within the pellet to begin with, and even monomeric compounds like tripolyphosphate can pressure their surroundings enough to significantly impact pellet strength – in this case, far more so than bentonite or metasilicate.

Despite the differences between these binders, it seems clear already that the dominant factor influencing the abrasion resistance of a dry pellet is simply the overall strength of the pellet as predicted in section 3. Furthermore, the observed variation in the abrasion resilience is very small compared to the variation observed in pellet strengths.

Another subtler thing to note is that metasilicate and bentonite did not show as many outlier pellets in their strength histograms. As the mixing procedure for each of these materials was the same, and the bentonite is expected to be the most difficult to mix because it is not water soluble, the reasoning for outlier pellets in the strength histograms is not readily satisfied by issues occurring during mixing. Since the outliers in the tripolyphosphate and polyacrylate pellets also persisted between different iterations of the same procedure, it would seem to highlight a more fundamental trait of these two binders in how they differ from bentonite and metasilicate.

5.2 Mixed dispersants

Binary mixtures of several of the binders were tested to understand perceived differences in materials which behave more like traditional binders and materials which behave primarily like dispersants. In this case, the expectation would be that dispersants cannot significantly improve upon an already dispersed material. Thus, the focus was on mixtures of dispersants with each other, metasilicate/polyacrylate, polyacrylate/tripolyphosphate, and tripolyphosphate/metasilicate. Some tests were also run with bentonite and the dispersants for materials for which data was not already available.

However, based on the results of the previous section, it should already be obvious that combinations of these binders should be different from each other.

In this case, the total binder dosage is increased because the binders are mixed together. For mixtures of compatible binders this has previously been shown to result in roughly linear increases of strength. This assertion is supported both by tests varying binder dosages such as Figure 3.2 and for tests replacing one binder with another such as Figure 3.3 and Figure 3.5. Incompatible or highly synergistic binders may display other behaviors, however.

As such, we tested these binary combinations hoping to identify which of four possibilities each of these combinations are:

1. Compatible – based on some hematite strength baseline, the strength of the combined binders is the baseline plus the individual effects of both binders added together. Binders coexist but do not directly support each other.
2. Dispersion limited – pellet strength may improve slightly due to adding more dispersant, but the binding contributed by the addition of the materials is limited. Results would be similar to either binder added individually in the same amount.
3. Synergistic – pellet strength improves beyond what would be expected for or could be explained by the compatible case.
4. Incompatible – pellet strength decreases below the minimum suggested by the dispersion limited case. None of these binders are expected to be incompatible.

We already know that the dispersion limited case occurs for sodium bentonite plus sodium metasilicate at higher dosages, as it was encountered in a previous work of mine (Claremboux, 2020), but since bentonite does not exhibit strong dispersing properties on its own it was still clearly improved. Furthermore, we predict in section 3.7 that metasilicate and tripolyphosphate likely interfere with each other, but there is no clear reason to believe that polyacrylate should perform poorly with either of the others.

First, let us examine pellets made with 1.0kg/t sodium metasilicate and 1.0kg/t sodium polyacrylate.

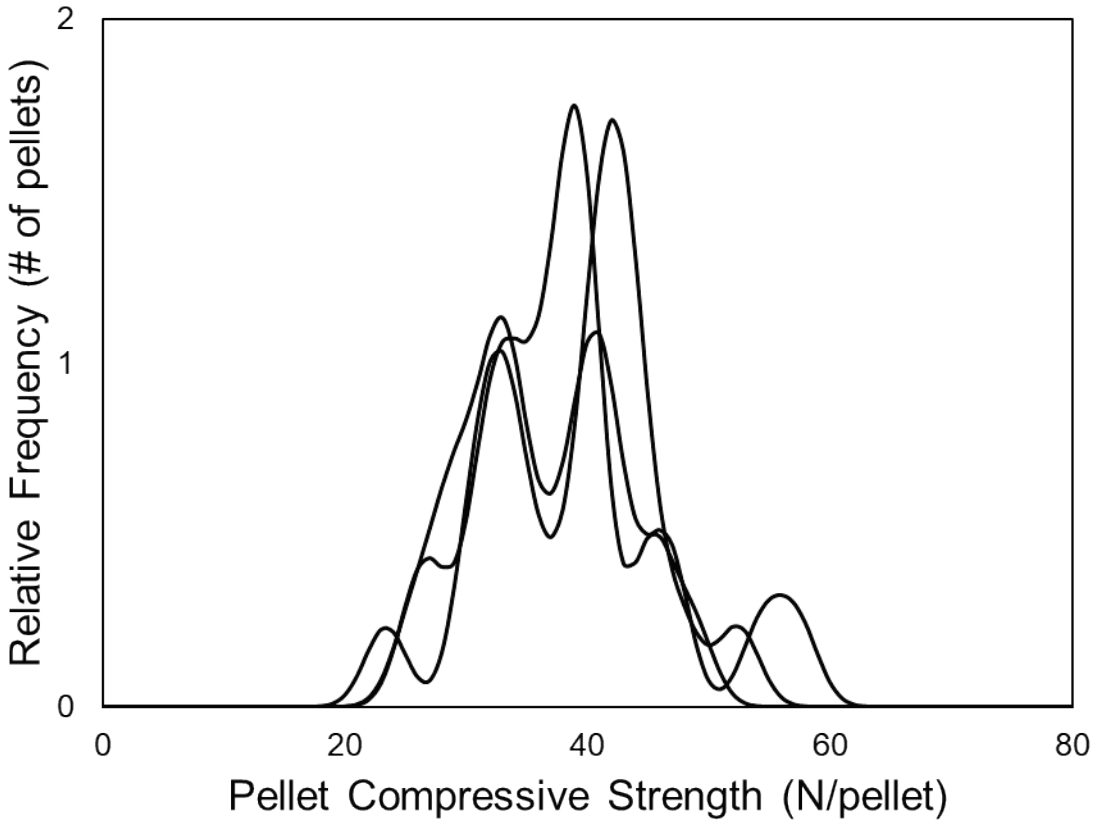

Figure 5.17: Compressive strength of pellets made from 1.0kg/t sodium metasilicate + 1.0kg/t sodium polyacrylate. Average strength is similar to the stronger batches of pellets observed from the 1.0kg/t sodium polyacrylate tests.

As shown in Figure 5.17, the compressive strength of the mixed metasilicate and polyacrylate binders were superior to metasilicate alone, but only on par with the stronger results observed for polyacrylate. It does not appear that the compressive strength improved much, but the quality of the pellets became a bit more consistent.

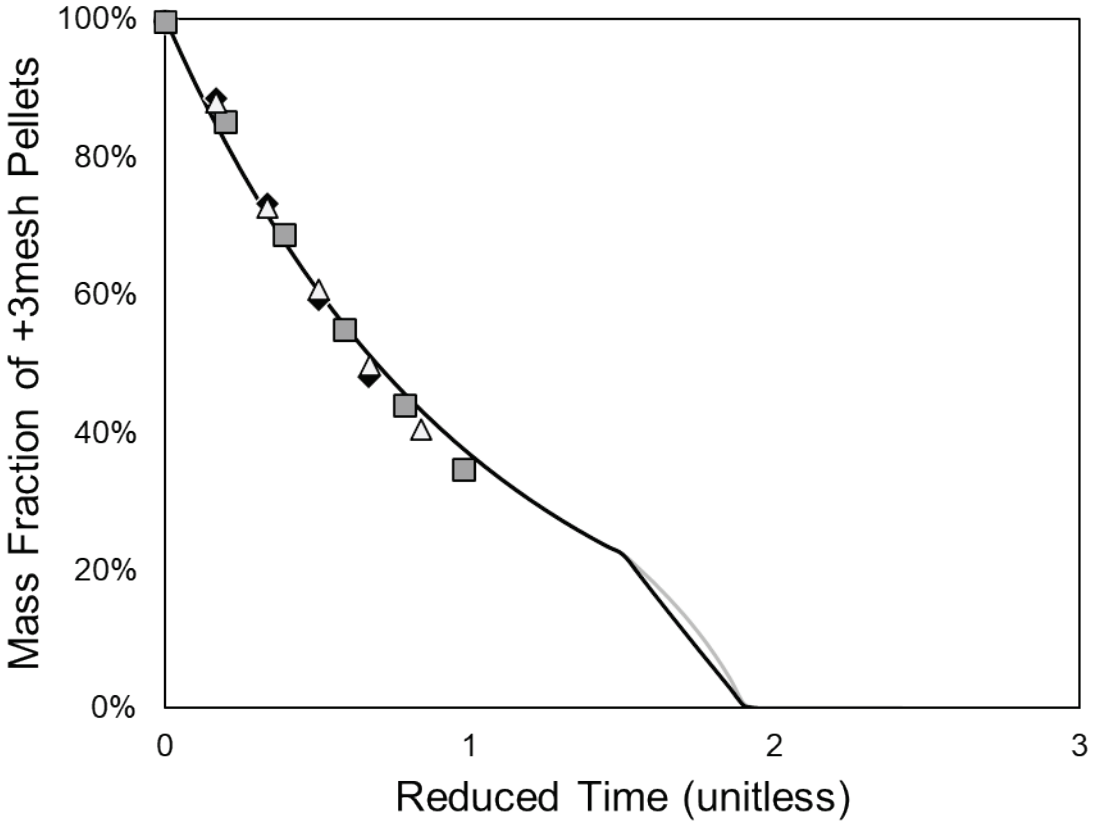

Figure 5.18: Upper mass fraction from abrasion tests of 1.0kg/t metasilicate + 1.0kg/t polyacrylate pellets. These pellets only make it to reduced time 1 due to their relative resistance to abrasion. These results are comparable to the strongest pellets observed from polyacrylate alone again.

In the abrasion results shown in Figure 5.18 and Figure 5.19. The performance demonstrated is slightly better than any abrasion resistance with polyacrylate or

metasilicate alone. Again, the consistency of these pellets is much higher than with either alone – which suggests that either the sodium metasilicate helps the sodium polyacrylate behave consistently, or that the increased dosage is important to ensuring that there is enough binder to connect all individual binding domains.

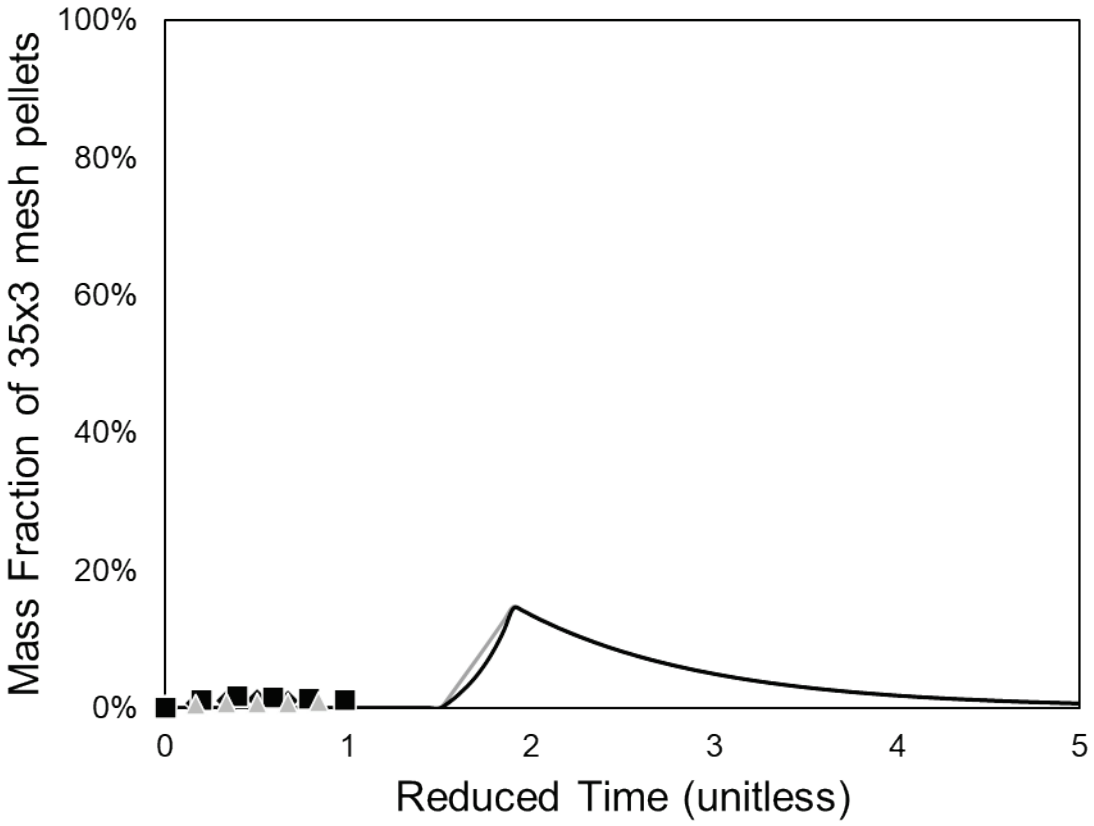

Figure 5.19: The middle abrasion test mass fraction for pellets produced with 1.0kg/t metasilicate and 1.0kg/t polyacrylate. These results are exactly what would be expected from Figure 5.18.

It appears that adding metasilicate to polyacrylate improves consistency of pellet formation and potentially improves abrasion resistance. This is further supported by Figure 5.20, which shows that these pellets have the best abrasion resistance of anything tested so far.

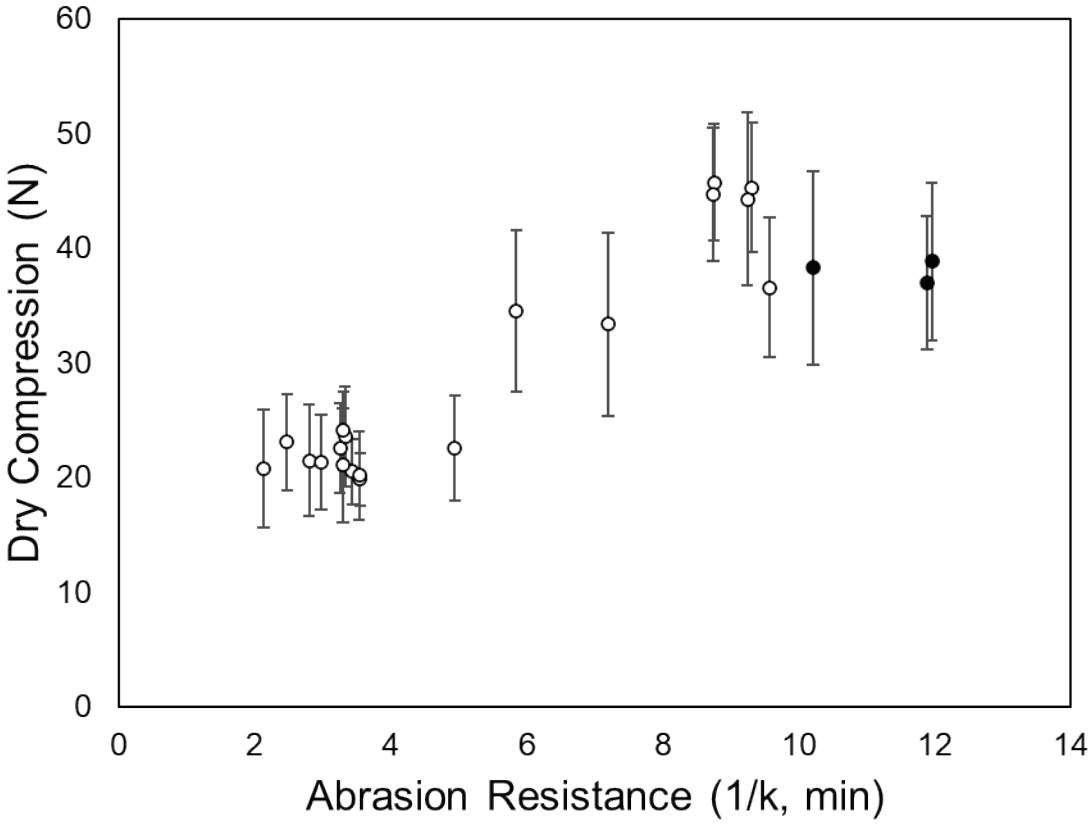

Figure 5.20: Adding the 1.0kg/t metasilicate + 1.0kg/t polyacrylate pellets to Figure 5.16. This shows improved abrasion resistance for and compressive strengths equivalent to the only polyacrylate pellets.

If we apply the 4 categories of binder compatibility suggested earlier to these results, then we find that the compressive strength and the abrasion resistance seem to imply different results. Note that the abrasion resistance of mixed pellets is a little less than the abrasion resistance of metasilicate and polyacrylate added together, but the compressive strength seems to be dispersion limited to only as strong as the best result polyacrylate achieved on its own, and on average performed slightly worse.

The next batch of results are from pellets made with 1.0kg/t sodium metasilicate and 1.0kg/t sodium tripolyphosphate. Of particular interest here is if the addition of metasilicate to tripolyphosphate also seems to improve consistency.

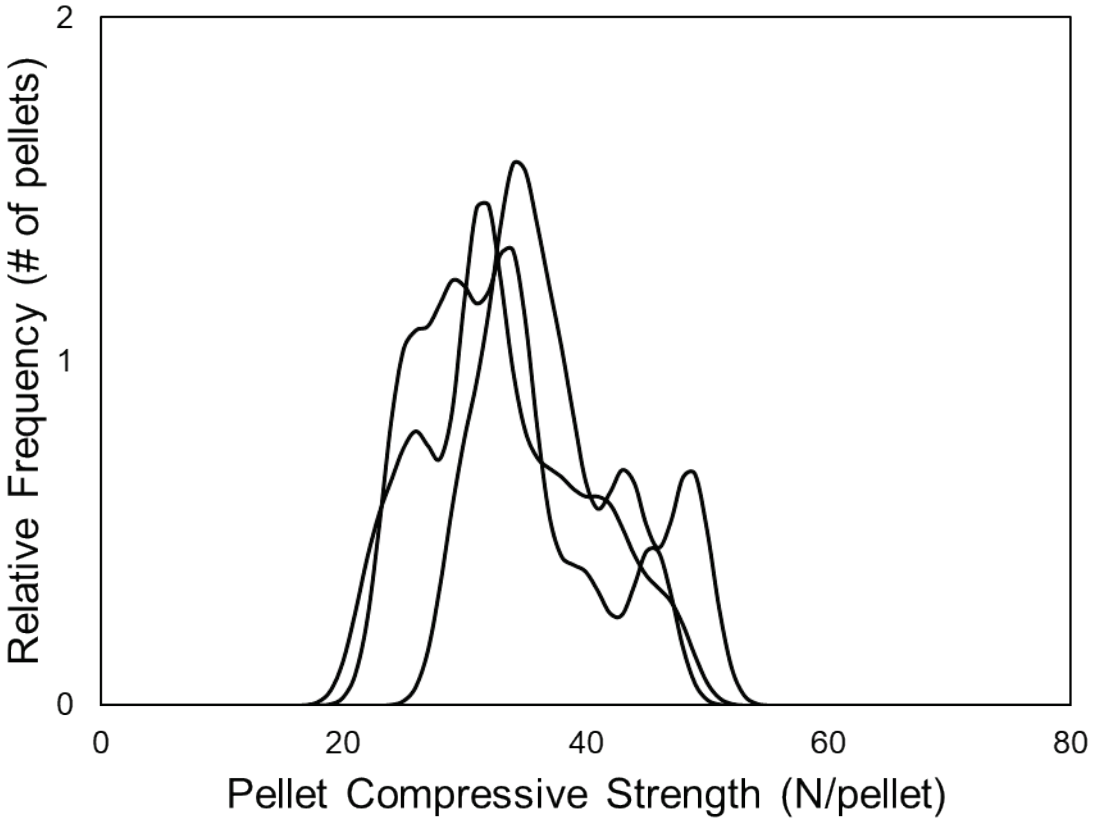

Figure 5.21: Compressive strengths of pellets made with 1.0kg/t sodium metasilicate and 1.0kg/t sodium tripolyphosphate added. Pellet strength and consistency is improved compared to metasilicate alone but somewhat worse than if made with tripolyphosphate alone.

Figure 5.21 shows something unexpected, however. It appears that tripolyphosphate may not be entirely compatible with metasilicate as a binder, as the performance on average appears to have dropped compared to tripolyphosphate alone. Is this something which also appears in the abrasion data?

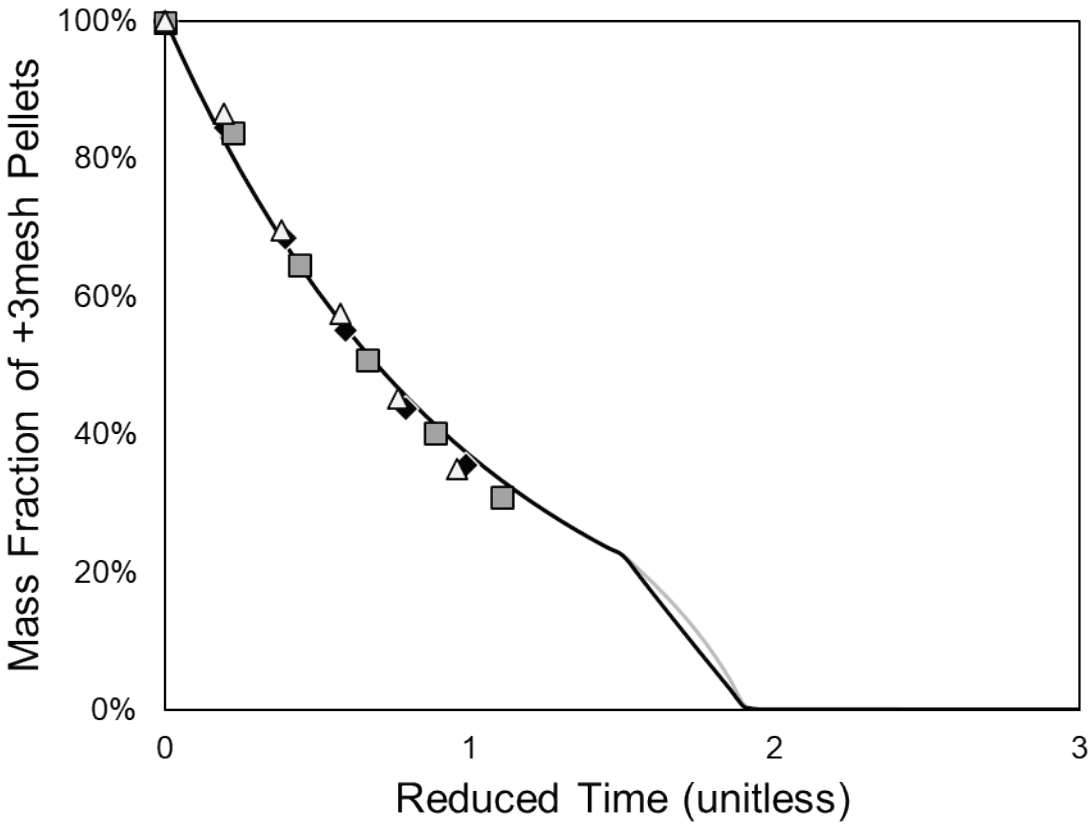

Figure 5.22: Abrasion upper mass fraction for pellets made with 1.0kg/t sodium metasilicate and 1.0kg/t sodium tripolyphosphate. Similar abrasion resistance to the mixed metasilicate/polyacrylate pellets.

Figure 5.22 would suggest that the abrasion resistance of these pellets is similar, however, to the mixed metasilicate and polyacrylate pellets, which were more abrasion resistant than any previous pellet. Thus, adding metasilicate to tripolyphosphate slightly improved abrasion resistance but hurt compressive strength some compared to tripolyphosphate alone. This would imply that the pellets are deviating further from being spherical.

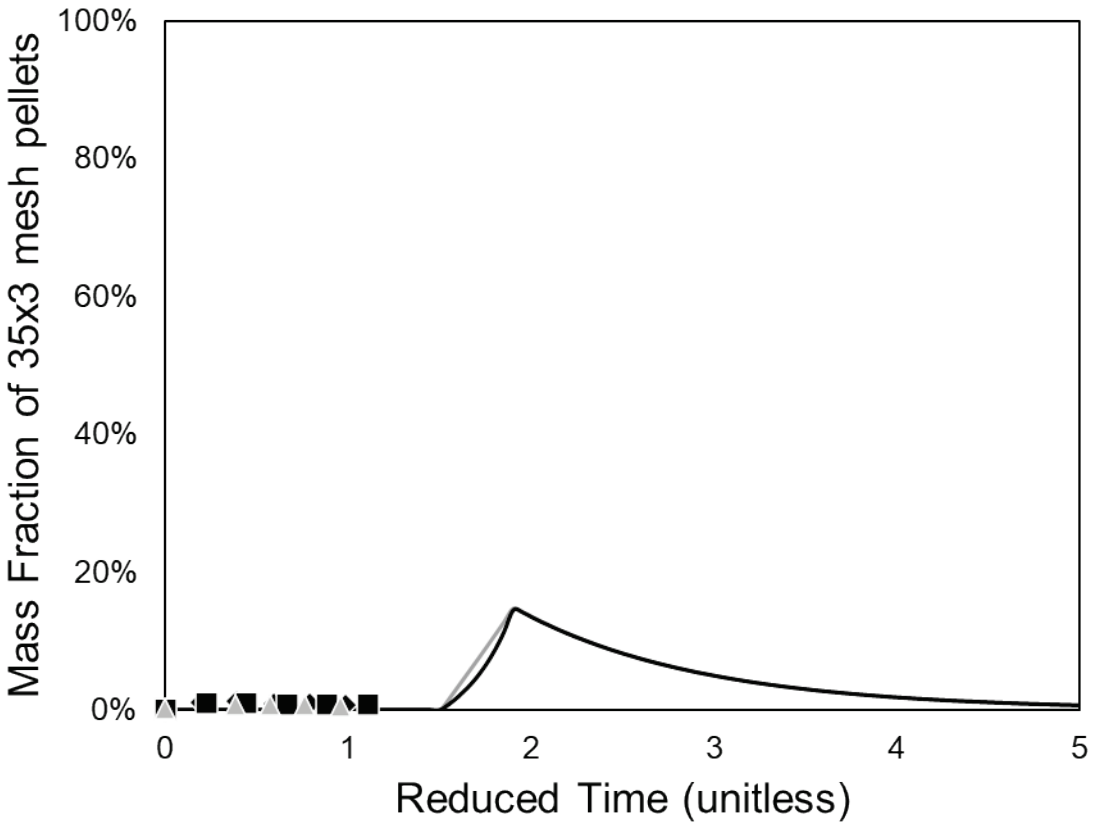

Figure 5.23: Middle abrasion result for pellets made with 1.0kg/t sodium metasilicate and 1.0kg/t sodium polyacrylate. Exactly as would be expected given Figure 5.22, showing that no early breakage occurs throughout the test.

Figure 5.23 is again not particularly exciting other than to verify that the abrasion theory matches very well with the behavior observed.

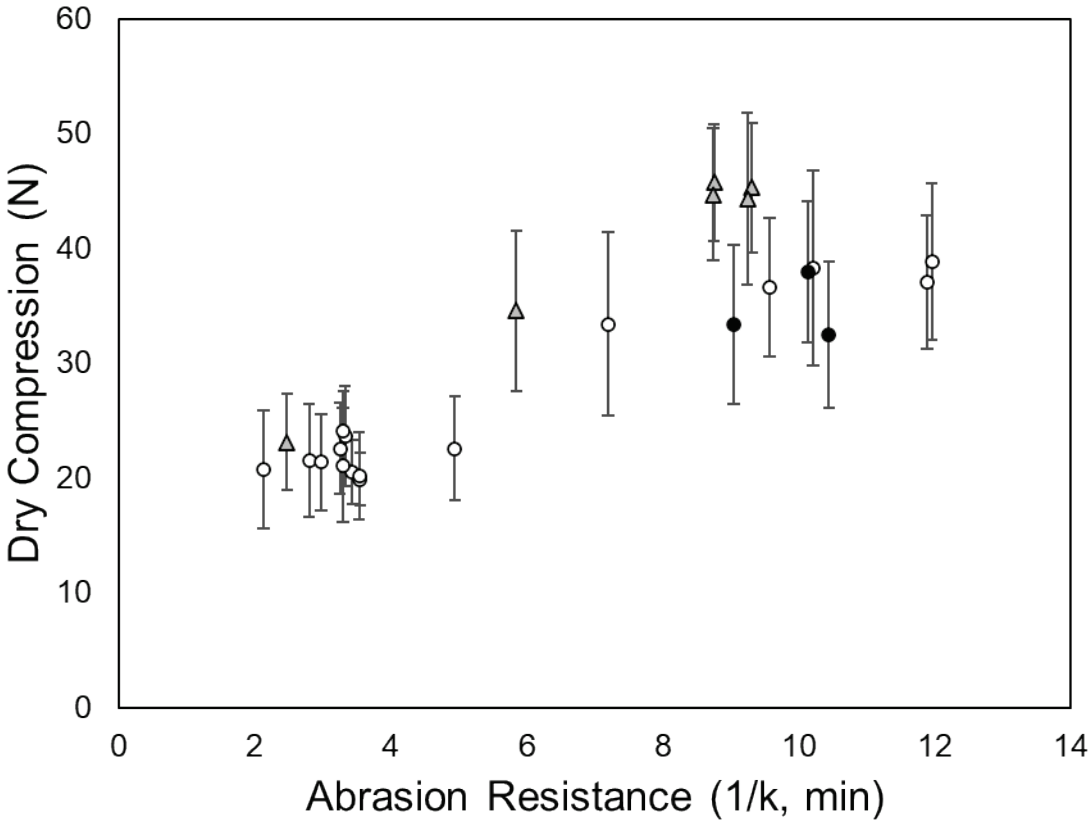

Figure 5.24: Including 1.0kg/t metasilicate + 1.0kg/t tripolyphosphate materials in Figure 5.20. For this specific graph, the 1.0kg/t tripolyphosphate pellets are noted with a triangle marker, while the new mixed material is marked with filled circles. These materials have a slightly higher abrasion resistance than the tripolyphosphate materials, but lower average strengths. The compatibility of these two dispersants is thus called into question.

Figure 5.24 shows that compressive strength and abrasion resistance can have opposing trends, which distinctly disproves the simplest theories to connect the two. This is particularly interesting because it also suggests that two dispersants could potentially be incompatible with each other, which goes against previously established thoughts for binder compatibility (that is, that binders with similar binding mechanisms will generally be compatible). A possibility is that a significant portion of tripolyphosphate's binding ability likely stems from being a strong enough dispersant to start mobilizing ultrafine colloidal hematite particles, which the sodium metasilicate may be interfering with.

The last binary mixture of dispersants tested was 1.0kg/t sodium tripolyphosphate with 1.0kg/t sodium polyacrylate. Since metasilicate and polyacrylate were compatible but potentially dispersion limited with each other, it would be expected that sodium tripolyphosphate interacts with both in roughly the same way.

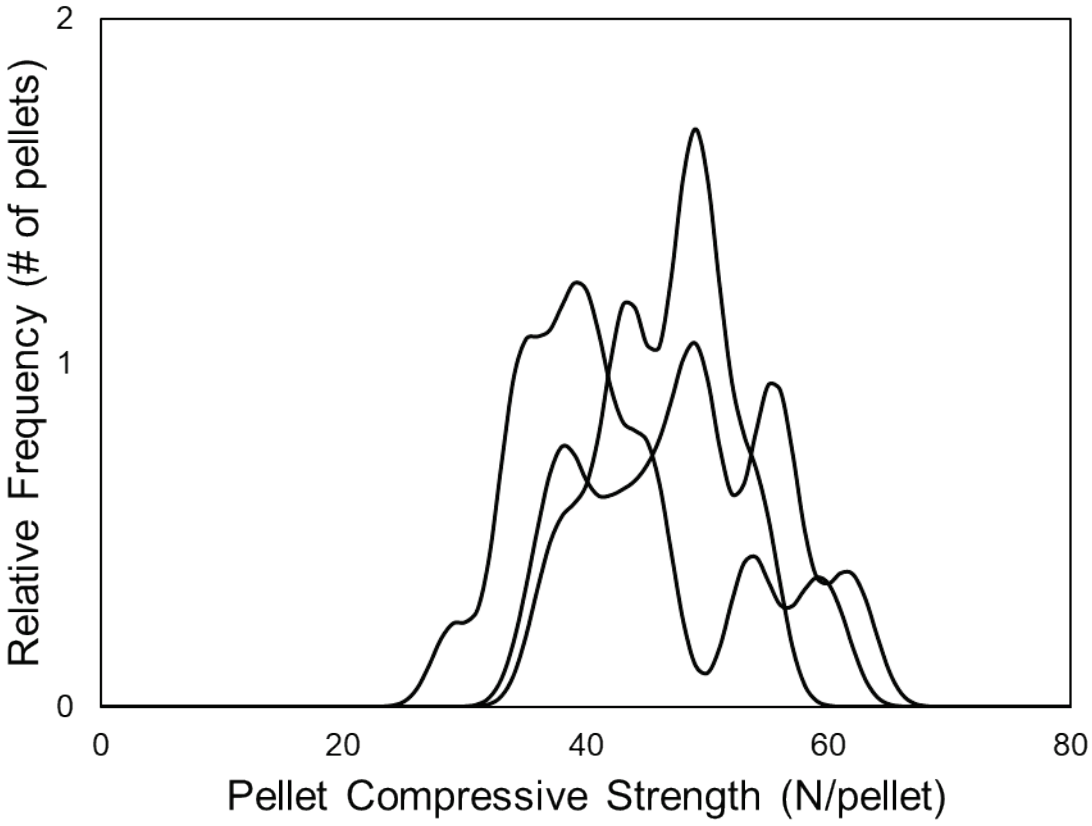

Figure 5.25: Compressive strength of pellets created with 1.0kg/t sodium polyacrylate and 1.0kg/t sodium tripolyphosphate. Strength is improved from polyacrylate alone, polyacrylate plus metasilicate, or metasilicate plus tripolyphosphate.

However, Figure 5.25 shows that instead tripolyphosphate and polyacrylate are likely compatible binders, as strength was improved by mixing the two.

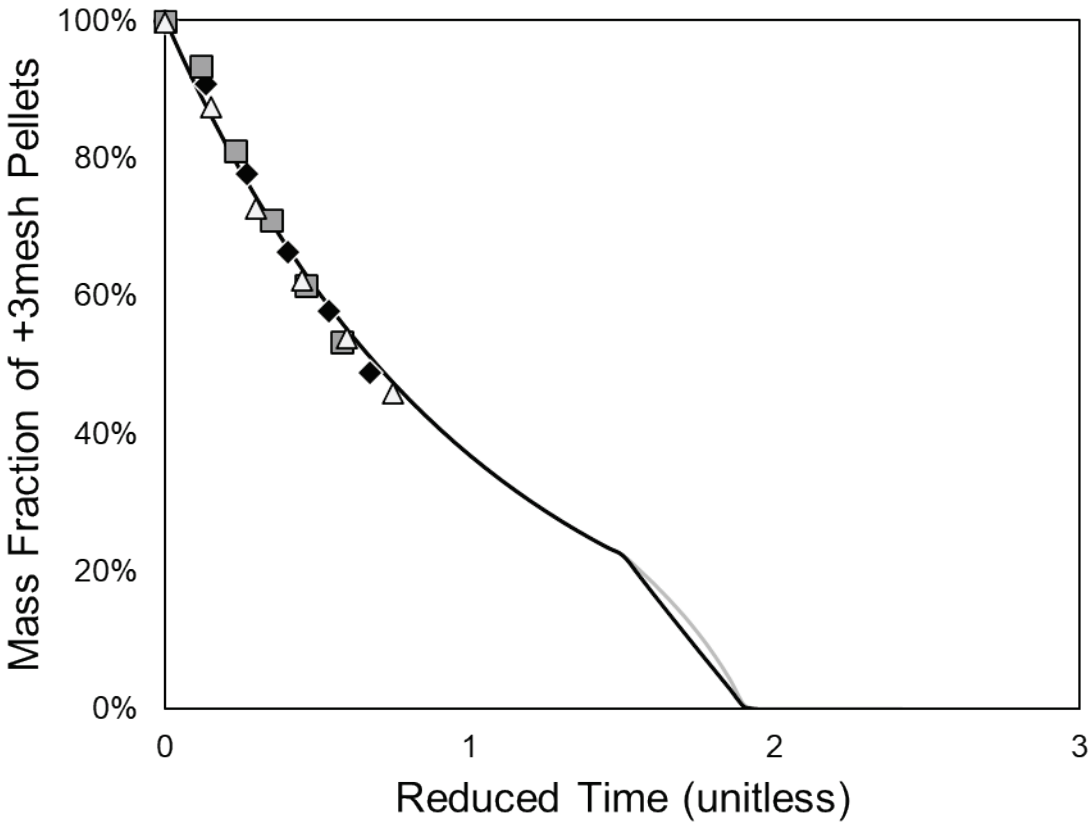

Figure 5.26: Upper abrasion fraction for 1.0kg/t sodium tripolyphosphate + 1.0kg/t sodium polyacrylate pellets. These pellets demonstrate very high abrasion resistance, noted by the very small reduced time values observed over the 10-minute test.

Figure 5.26 also suggests that the combination of sodium tripolyphosphate and sodium polyacrylate is a compatible binder mixture which overall improves upon the abrasion resistance. Figure 5.27 shows that a small amount of breakage occurred in one sample, probably during handling. The overall results are not particularly affected by this, however.

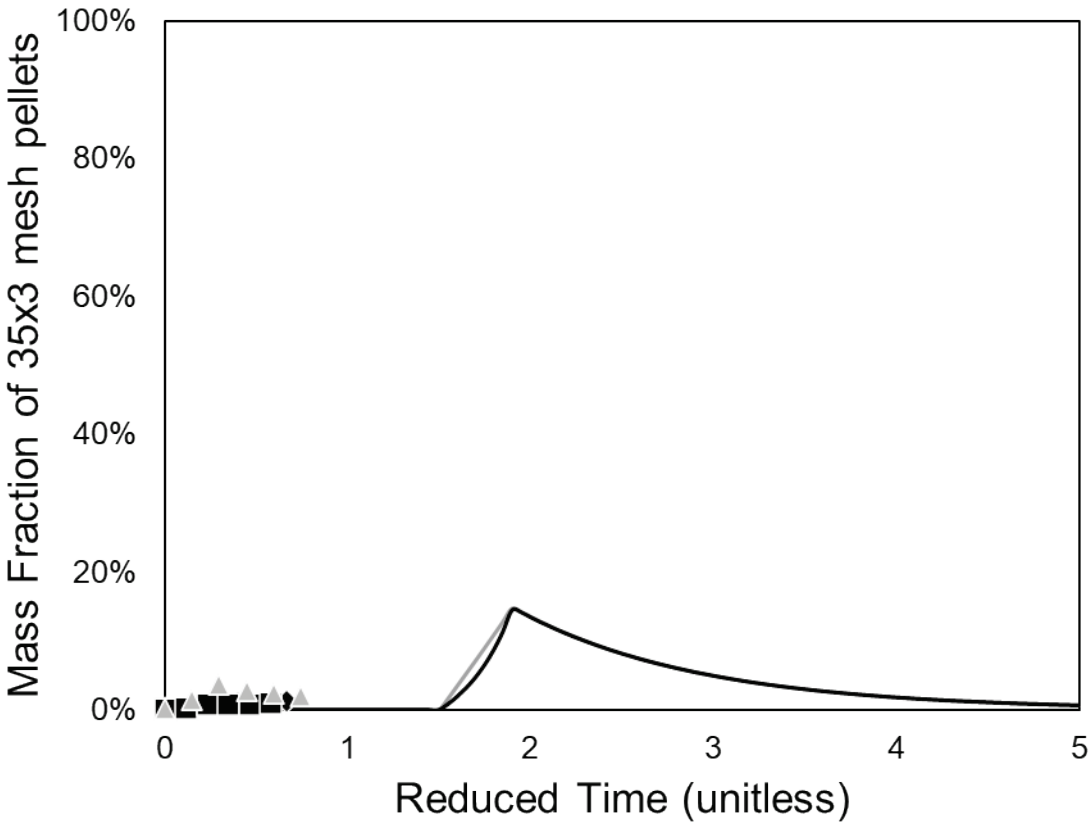

Figure 5.27: Middle abrasion fraction for 1.0kg/t sodium polyacrylate + 1.0kg/t sodium tripolyphosphate pellets. Some breakage is observed in one sample, but otherwise the data fits the expected curve as usual.

Figure 5.28 shows clearly that the abrasion resistance of the mixed polyacrylate and tripolyphosphate pellets has improved considerably, though the compressive strength is about the same as for the tripolyphosphate pellets. The average abrasion resistance of the properly dispersed tripolyphosphate pellets is around 9 minutes, the average abrasion resistance of the properly dispersed polyacrylate pellets is around 8 minutes, and the abrasion resistance of these mixed pellets is around 15 minutes. If this is direct binder compatibility, then this would suggest that without any additives, the abrasion resistance of a binderless hematite pellet dispersed to the same extent should be around 1-2 minutes, which seems reasonable but is impossible to test due to the dispersion requirement.

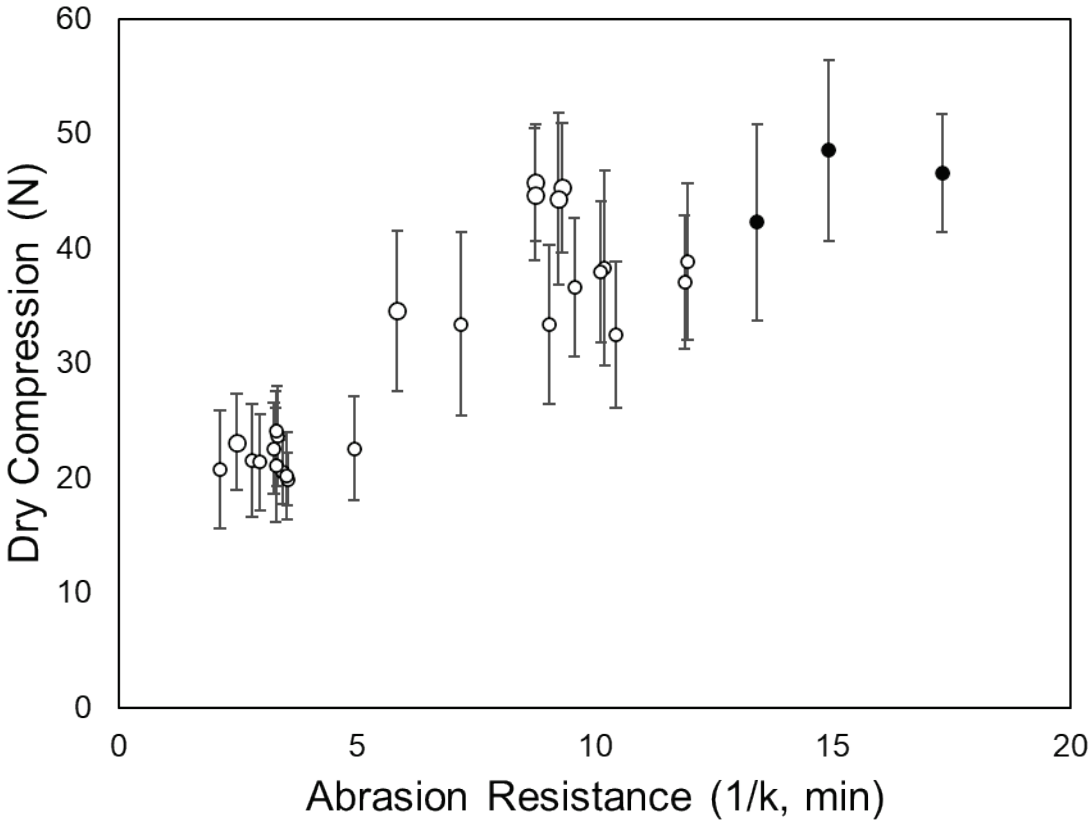

Figure 5.28: Adding 1.0kg/t sodium tripolyphosphate + 1.0kg/t sodium polyacrylate pellets to Figure 5.24. These pellets exhibit much higher abrasion resistance than any pellets tested thus far and have strengths comparable to the strongest tripolyphosphate pellets tested.

One last set of pellets is provided for reference, which contained 2.0kg/t of sodium tripolyphosphate. This essentially is to provide a reference for adding other binders to tripolyphosphate.

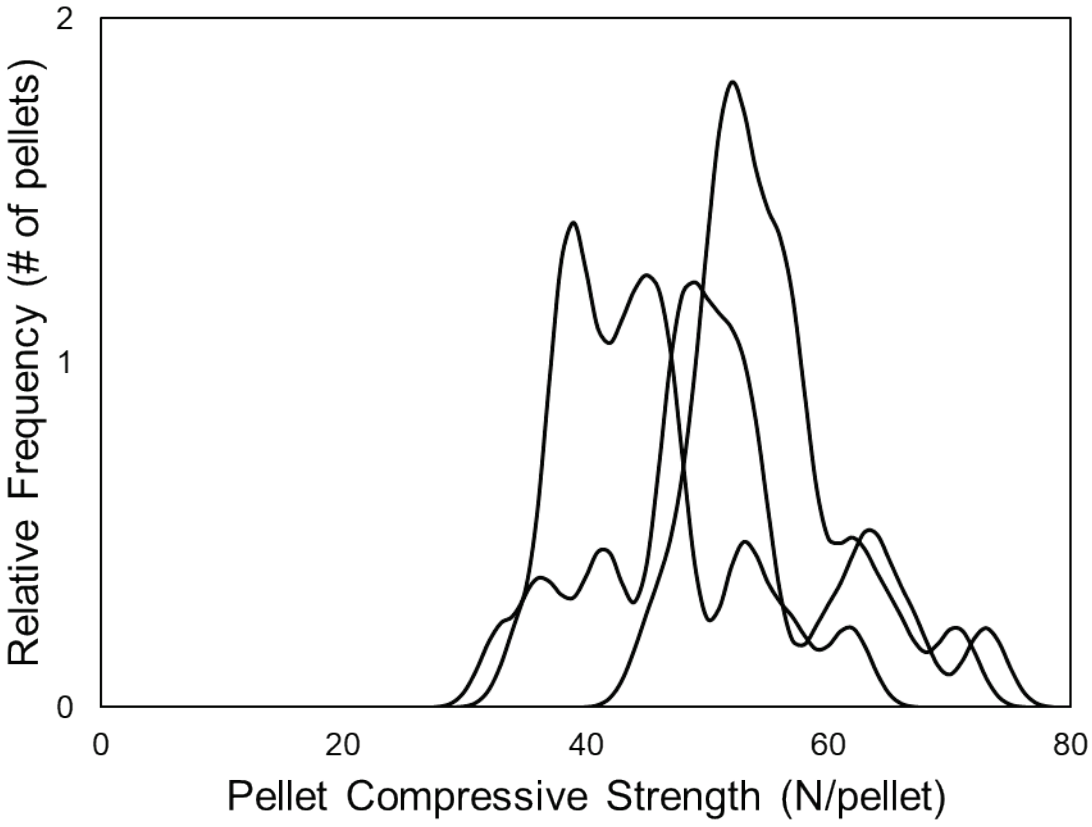

Figure 5.29: Compressive strength of pellets created with 2.0kg/t of sodium tripolyphosphate as binder. These pellets are stronger than those created by mixing tripolyphosphate with either of the other dispersants, suggesting that it benefits more from its own mechanisms than from the mechanisms of other dispersants.

Figure 5.29 shows that the compressive strength of pure 2.0kg/t sodium tripolyphosphate pellets exceeds the compressive strength gained by adding the other binders. In short, tripolyphosphate is more effective as a binder alone than it is in the presence of metasilicate or polyacrylate.

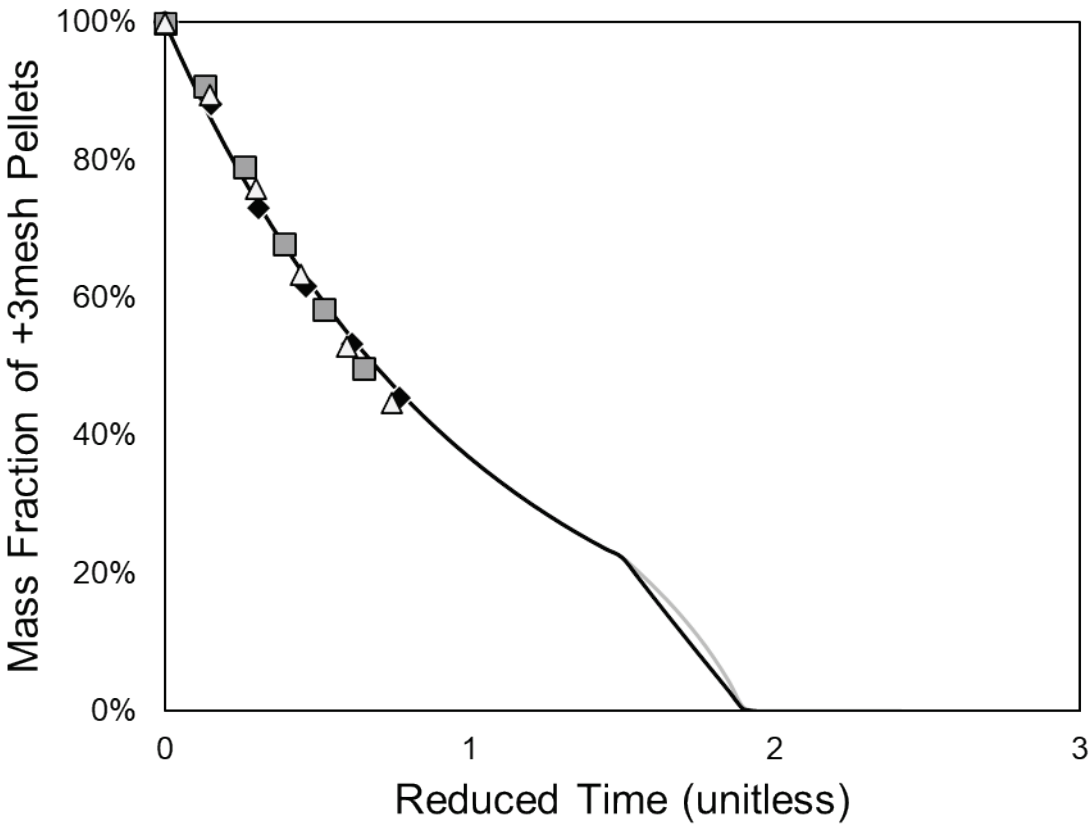

Figure 5.30: Upper abrasion mass fraction for pellets created with 2.0kg/t sodium tripolyphosphate binder. Similar to the other mixed binders, but not particularly good or bad.

Figure 5.30 and Figure 5.31 show that these pellets have abrasion resistance comparable to the other mixed binders, despite the clearly higher compressive strengths. This also supports the idea that tripolyphosphate is evolving higher pellet strengths simply by mobilizing the ultrafine colloidal particles in the hematite ore.

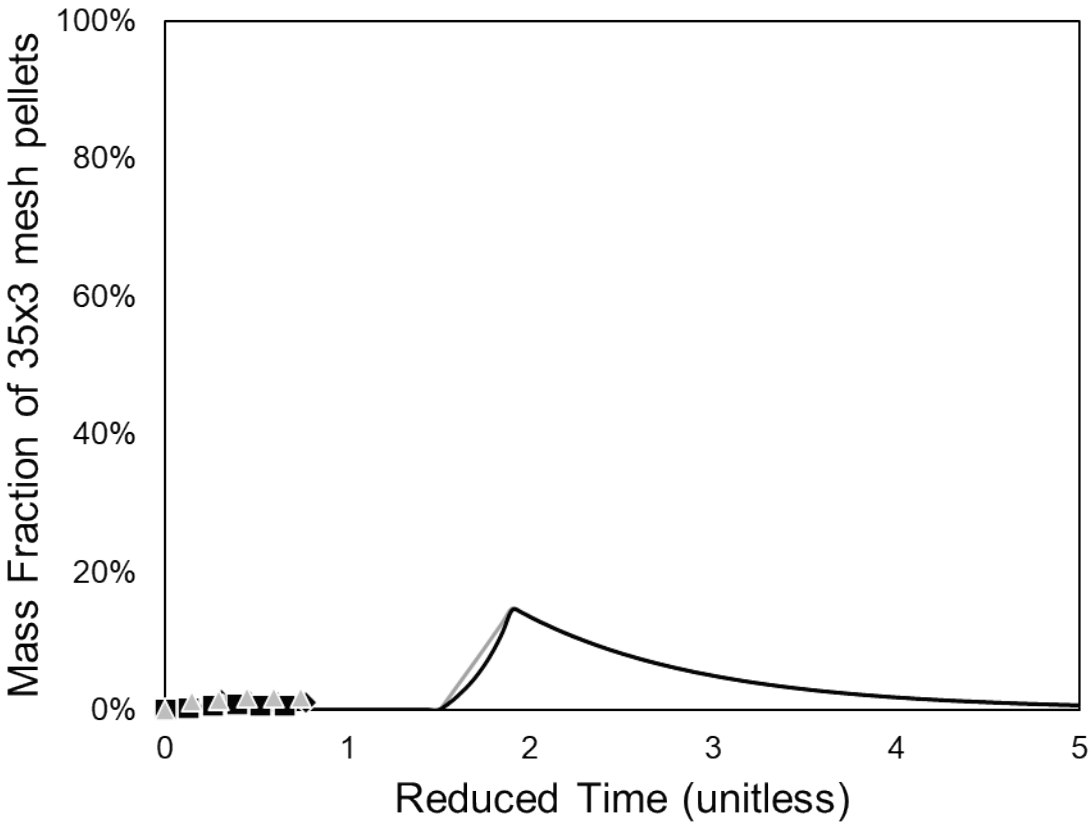

Figure 5.31: Middle abrasion mass fraction for 2.0kg/t sodium tripolyphosphate pellets. Again, there is nothing particularly unusual about this curve.

Figure 5.32 shows that these pellets have properties very similar to the tripolyphosphate + polyacrylate mixed pellets shown in Figure 5.28. However, somewhat similar to what happened with the tripolyphosphate + metasilicate mixed pellets, the change of adding 1.0kg/t extra tripolyphosphate instead of 1.0kg/t polyacrylate appears to have traded a little bit of abrasion resistance for a little bit extra compression strength.

The dynamic of this effect would almost certainly have to stem from the impact of the ultrafine colloidal material which tripolyphosphate has been shown to have a strong effect on. The additional mobility of the colloidal material allows for tighter overall

packing in the pellet, but perhaps a bit of that strength comes at the cost of excess rigidity that is not as resilient to abrasive conditions?

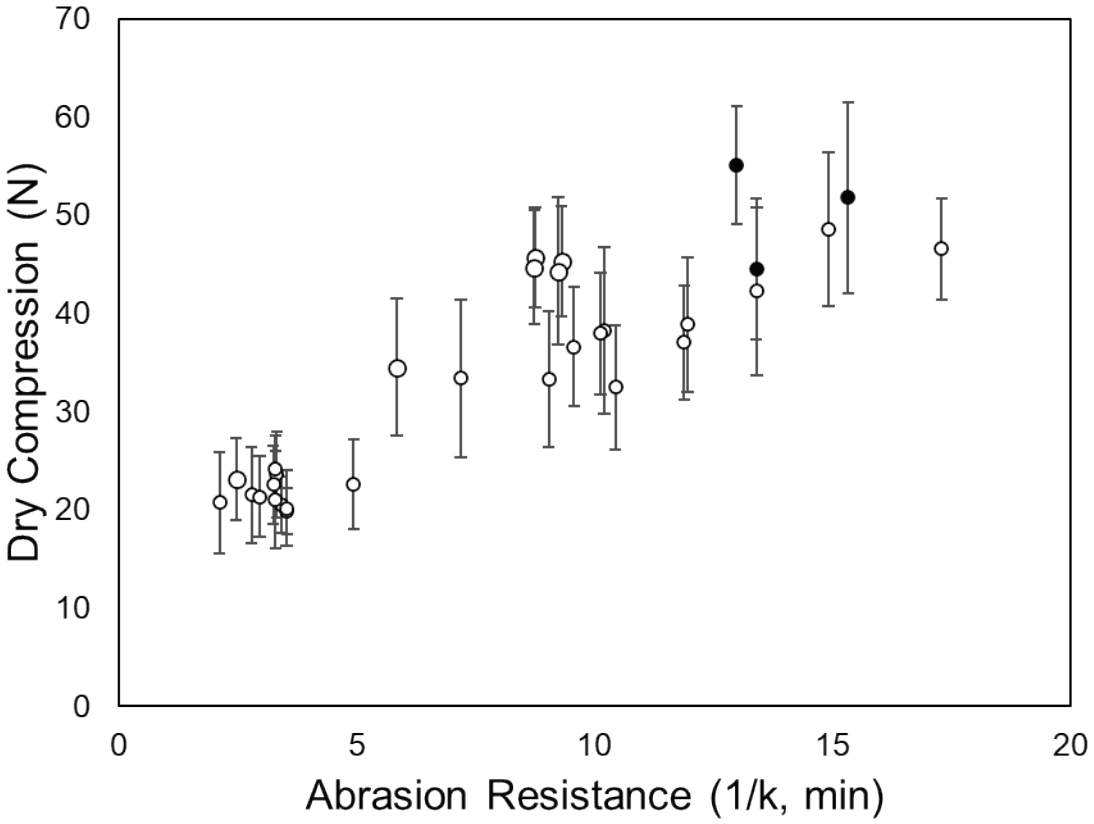

Figure 5.32: Adding 2.0kg/t sodium tripolyphosphate pellets to Figure 5.28. These pellets have abrasion resistance slightly less than tripolyphosphate + polyacrylate pellets, but slightly higher compressive strength on average.

Table 5.1: Abrasion resistance and compression strength of well dispersed samples hematite pellets made with 1.0kg/t of pure and/or 1.0kg/t+1.0kg/t of mixed dispersants.

Binder	**Compressive Strength (N)**	**Abrasion Resistance (min)**	**Binder Compatibility?**
Metasilicate	23	3.3	N/A
Polyacrylate	35	8.4	N/A
Tripolyphosphate	45	9.0	N/A
Metasilicate + Tripolyphosphate	35	9.8	Incompatible
Metasilicate + Polyacrylate	38	11.4	Compatible, dispersion limited
Tripolyphosphate + Polyacrylate	46	15.2	Compatible, dispersion limited
Tripolyphosphate + Tripolyphosphate	50	13.9	Dispersion limited

The results for the dispersant mixtures are summarized in Table 5.1. Adding more dispersant always increased abrasion resistance, but only rarely increased the measured pellet strength. It did however increase the tendency for the pellets to behave well-dispersed judging by the pellet strengths observed. If the compression strengths for pure binders were expanded to include all compression strengths, then the mixed binders would clearly show an improvement based on the improved consistency of dispersion.

However, when only the dispersed pellets are observed, then every binder appears to be dispersion limited in the pellet strengths which can be achieved via dispersion alone. However, each binder hits a different maximum for that same result – with metasilicate being the weakest binder of the bunch, polyacrylate performing better, and tripolyphosphate performing the best.

Yet, tripolyphosphate's performance is actually decreased by the addition of metasilicate. These two binders display an incompatibility in binding mechanisms, which would

presumably be due to an interaction of sodium metasilicate with the colloidal ultrafine hematite which tripolyphosphate can mobilize as an additional binding agent. Considering the strongly negative charges present on the dispersants themselves, it seems unlikely that they would be interacting with each other.

However, no such incompatibility is detected between tripolyphosphate and polyacrylate. The reasoning for this difference in behavior is not immediately obvious. Some possibilities are:

1. The tripolyphosphate anion is particularly compatible with silica surfaces, and thus can be collected by the metasilicate even despite the difference in charges. This would likely not be observed on the polyacrylate. This seems unlikely because of the strength of those electrical charges, but tripolyphosphate does appear to strongly attach to hematite surfaces in solution as well.
2. The metasilicate chain is capable of attaching to even negatively charged hematite surfaces, which allows it to capture the colloidal materials made available by the sodium tripolyphosphate. This hypothesis depends on the Si-OH bonding available to metasilicate being particularly aggressive, but this is somewhat contraindicated by the fact that metasilicate is an ineffective binder compared to other dispersants.
3. The metasilicate is attaching to the colloidal materials and protecting them from the tripolyphosphate, while polyacrylate may or may not attach to them but cannot successfully protect them from being mobilized by the tripolyphosphate.

Of these, option 3 seems the most likely, but proving the effect would be more involved than the tests so far allow for.

5.3 Layering binders

Another proposed method of mixing binder properties, particularly between binders which perform well in different aspects, is to layer binders on top of each other. This has the advantage of being relatively simple to implement on an industrial scale and using less of each individual binder. However, it is not entirely clear that the properties of each binder will be improved by such. The primary binder for each of these tests is bentonite, as bentonite is considered to create appropriately abrasion resistant pellet surfaces compared to other organic binders. Though it is worth noting that so far the binders tested for this project have all performed better than bentonite in measures of abrasion resistance, bentonite is likely one of the most interesting binders to compare to.

For these tests, the pellets were made with a material containing one binder or the other, grown to the penultimate size fraction, and then finalized with the material containing the other binder exclusively. The expectation is that the abrasion resistance of the outer binder will be represented early on during the abrasion test, while the compressive strength of the inner binder will be represented as well.

For these tests the main emphasis was on dispersants layered with bentonite externally, as the dispersants were expected to have better overall pellet strength and the bentonite was expected to improve abrasion resistance. Only a limited number of the reversed trials were run, just to get a sense of how the reversed pellets were likely to work.

Firstly, the following pellets were made with a core of 1.0kg/t metasilicate bound material surrounded by 6.6kg/t bentonite.

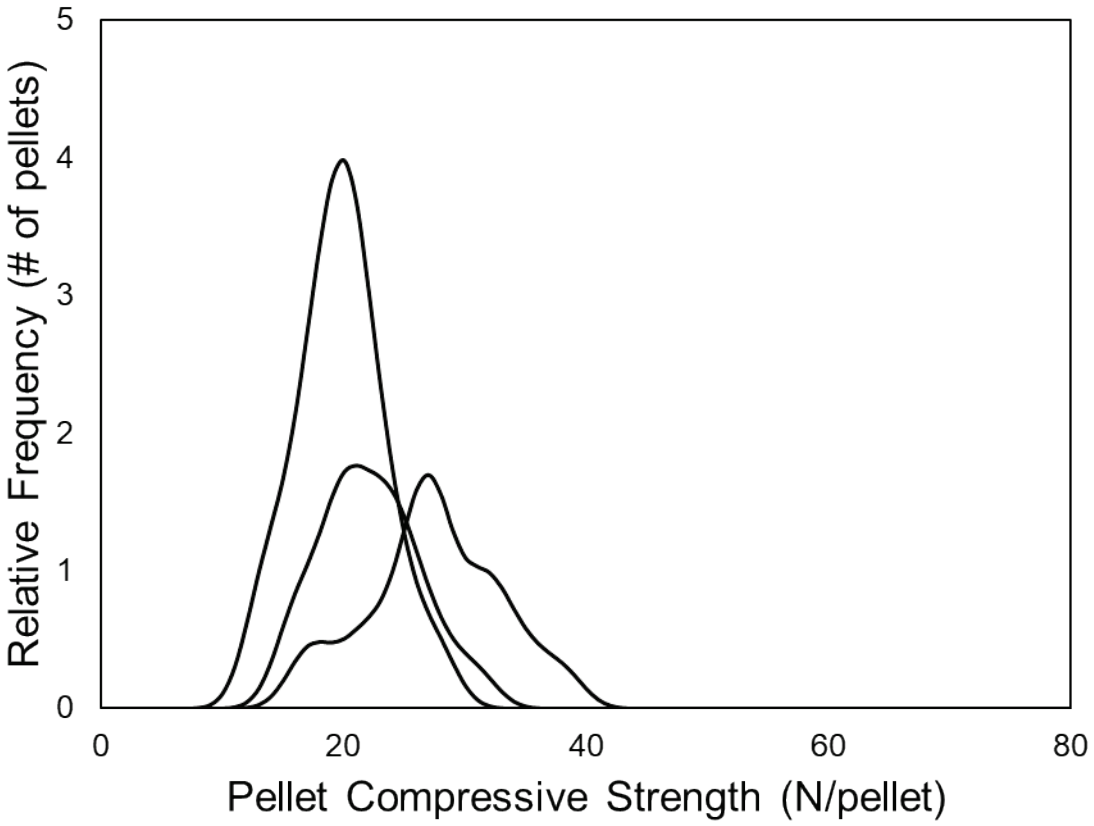

Figure 5.33: Compressive strength of 1.0kg/t metasilicate pellets layered with 6.6kg/t bentonite material. These pellets were not consistently much better than pure bentonite pellets, however a fraction of the pellets in at least one test appears to have higher than expected strength.

Recalling that metasilicate and bentonite tended to produce fairly similar pellets (see Figure 5.8 for bentonite + metasilicate), Figure 5.33 is a little surprising, as at least one of these tests performed better than either individually. Clearly, layering the pellet materials does allow for some intermingling of the binder materials, so this is likely due to compatibility between the metasilicate and bentonite binders.

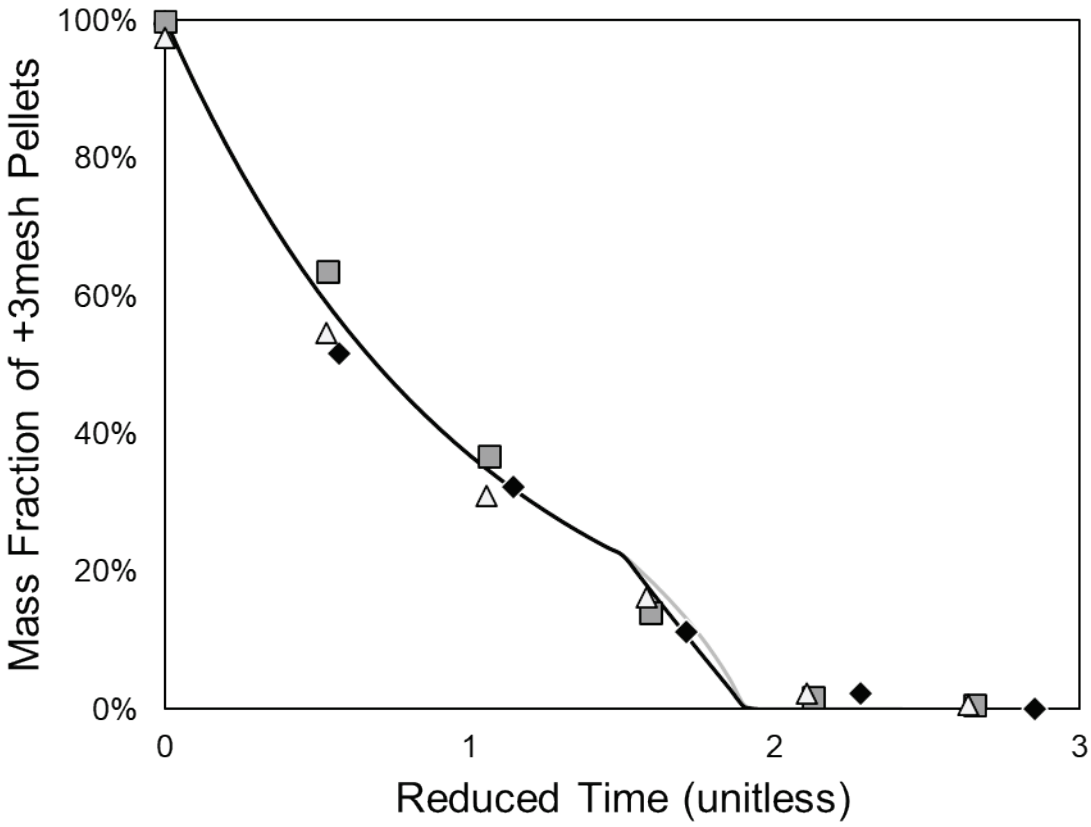

Figure 5.34: Upper abrasion mass fraction for 1.0kg/t metasilicate pellets layered with 6.6kg/t bentonite. Since the time constant is being determined without considering the layering effect here, it should be remarked that the fit is still fairly good. There is not a clear deviation from the previously observed trends shown at this sampling resolution.

Figure 5.34 should also be somewhat surprising, in that the impact of layering is not very readily apparent on the fitting graph. The deviation from the predicted curve is perhaps not as large as would be expected for a change of rate constant midway through. Figure 5.35 shows that one sample appears to have early breakage so there is a large piece in the middle range for most of the test, but otherwise the model is followed well.

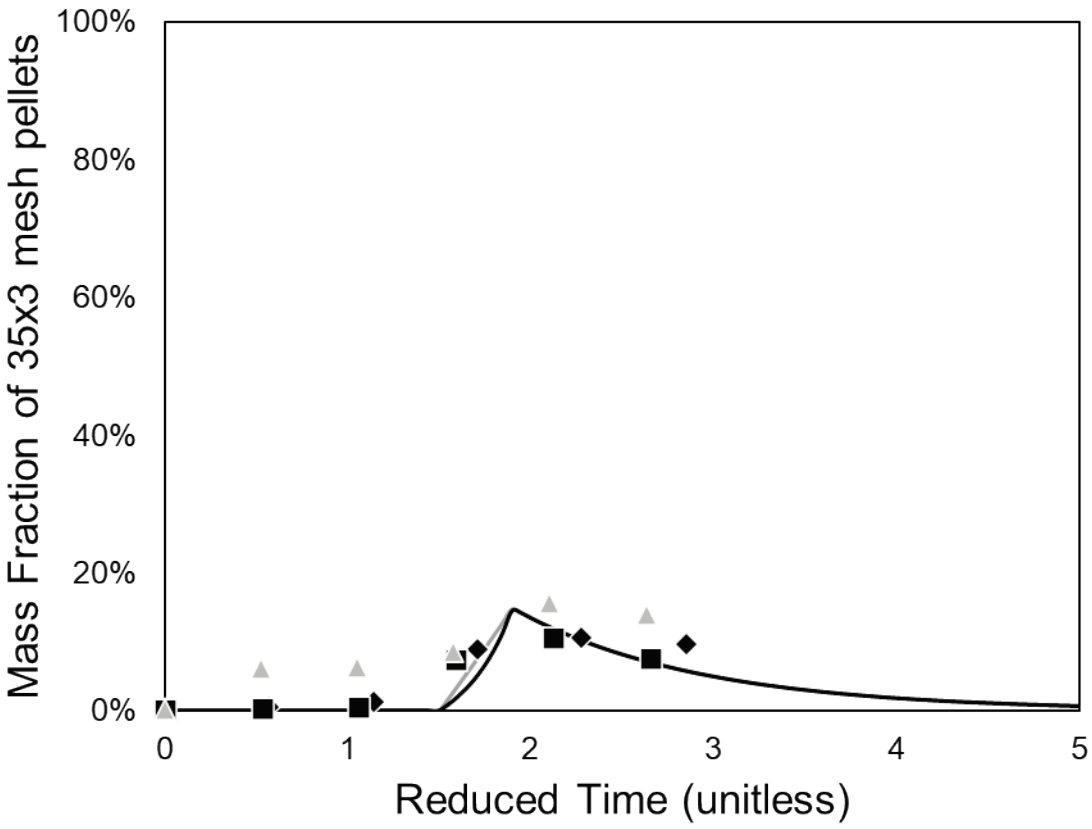

Figure 5.35: Middle abrasion fraction for pellets made with 1.0kg/t sodium metasilicate layered with 6.6kg/t sodium bentonite. One of the samples appears to have undergone early breakage, but otherwise very little unexplained deviation is shown here.

Figure 5.36 shows that these pellets perhaps perform slightly better than unlayered pellets of the same material for abrasion resistance, which could potentially occur due to synergistic binder effects at the boundary between the inner core and the outer shell. However, the effect is, at best, slight. In compression, these pellets are not noticeably better or worse than their individual components would suggest.

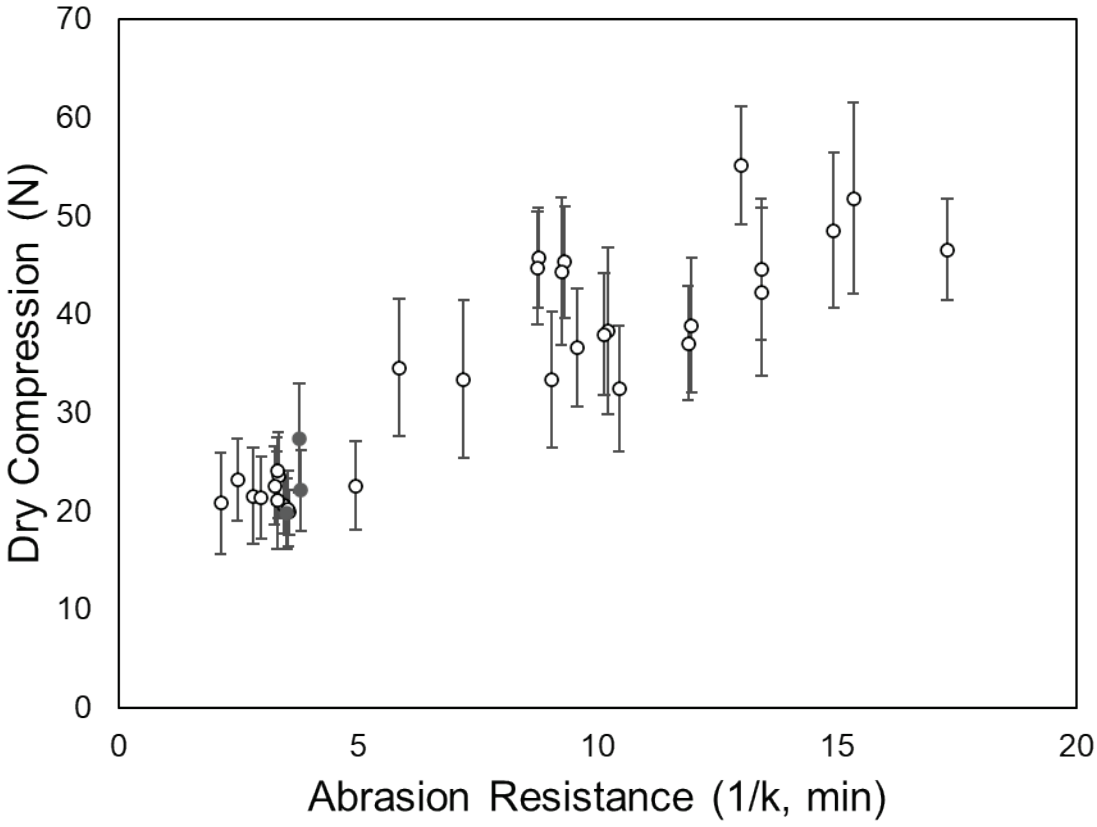

Figure 5.36: Adding pellets made with 1.0kg/t metasilicate and layered with 6.6kg/t bentonite material to Figure 5.32. These pellets are a little more abrasion resistant than average for bentonite or metasilicate pellets, but otherwise their performance is unremarkable.

However, metasilicate and bentonite have had similar performance in all of the tests performed so far. Let us consider binders which have had slightly different impacts next. The next material is 1.0kg/t sodium tripolyphosphate layered with 6.6kg/t sodium bentonite binder. Since tripolyphosphate shows a significant improvement over bentonite, the impact of the two separate binders should be much clearer.

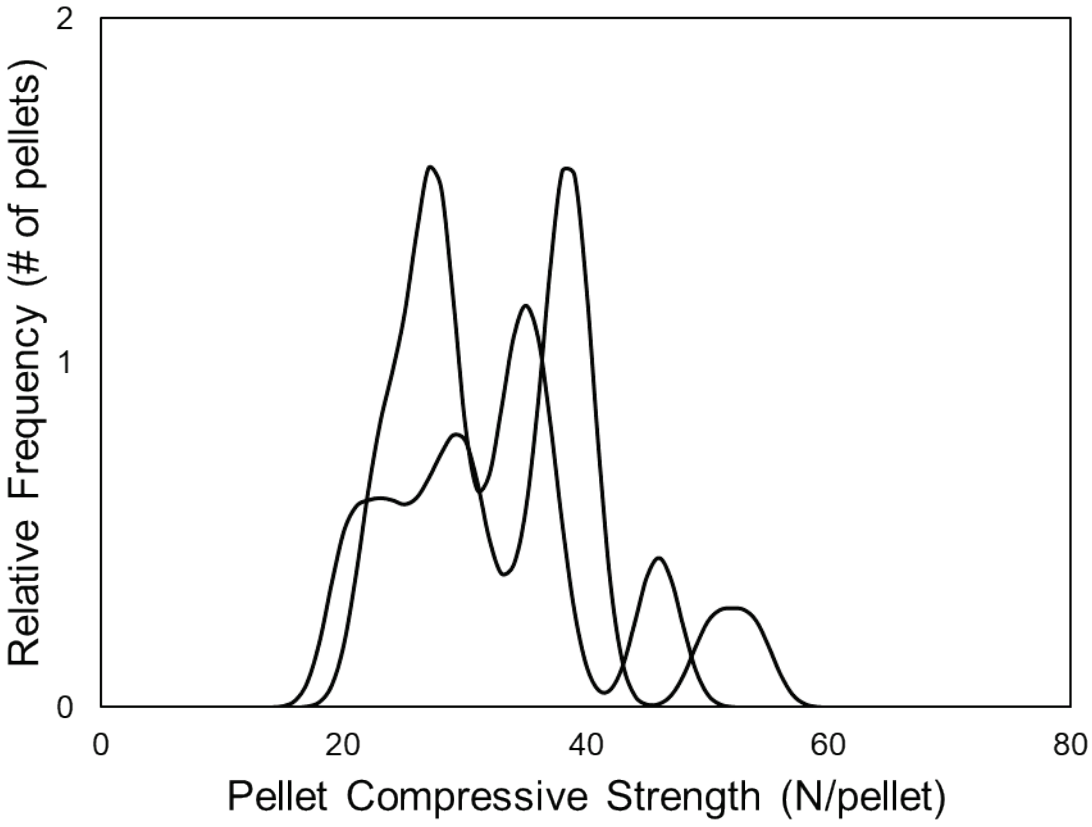

Figure 5.37: Compressive strength of 1.0kg/t sodium tripolyphosphate pellets layered with 6.6kg/t sodium bentonite. The partial replacement of tripolyphosphate with bentonite is unfavorable for the pellet strength overall, but a significant strength improvement is seen over bentonite alone.

The pellets in Figure 5.37 are weaker than the 1.0kg/t tripolyphosphate pellets in Figure 5.9, almost certainly due to the loss of some of the tripolyphosphate binder due to replacement by bentonite. This loss outweighs any compressive strength benefits that may have been gained by mixing effects at the boundary layer.

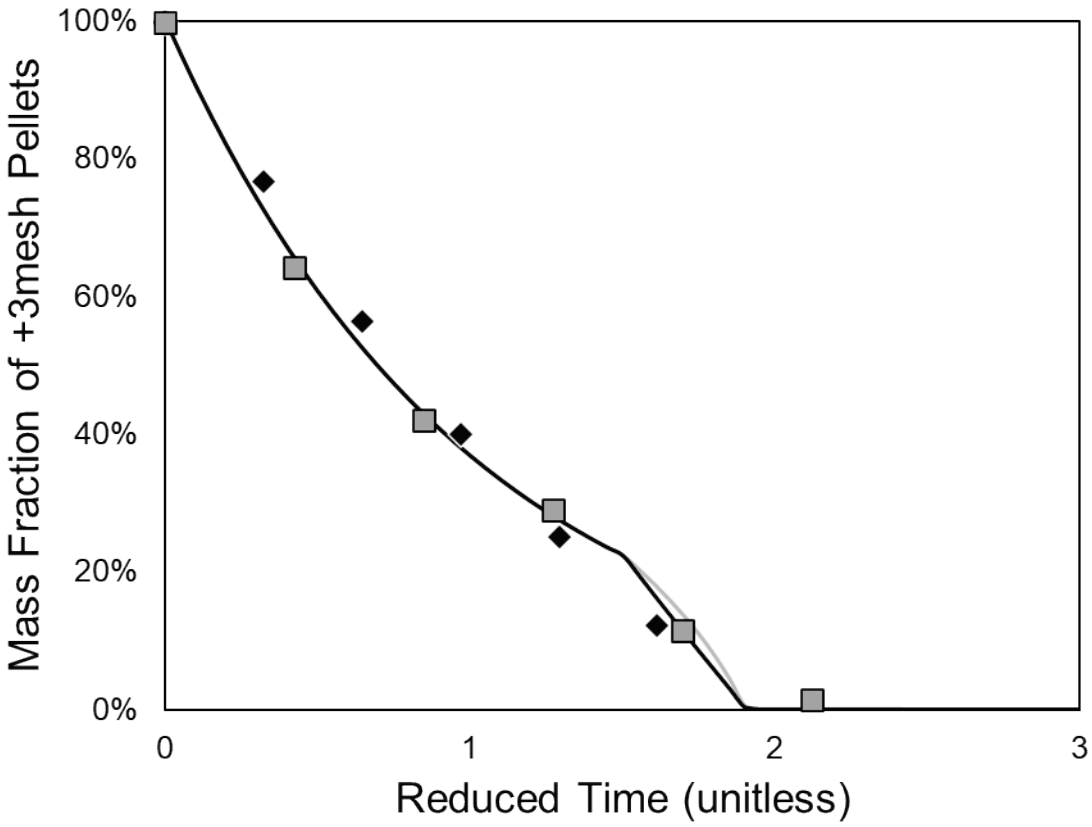

Figure 5.38: Upper abrasion fraction for 1.0kg/t sodium tripolyphosphate material layered with 6.6kg/t sodium bentonite material. The fit still shows no signs of the boundary that should be occurring due to the layering, and the choice of rate constant did not account for it in any way.

Figure 5.38 also does not show any change in pellet abrasion rate due to the material layering. It was expected that the rate constant would show a clear change between a strongly abrasion resistant binder and a weakly abrasion resistant one, but the lack of such a distinction suggests that perhaps the pellets are more homogeneous than initially thought. Figure 5.39 is also very close to the theoretical prediction for a homogeneous pellet.

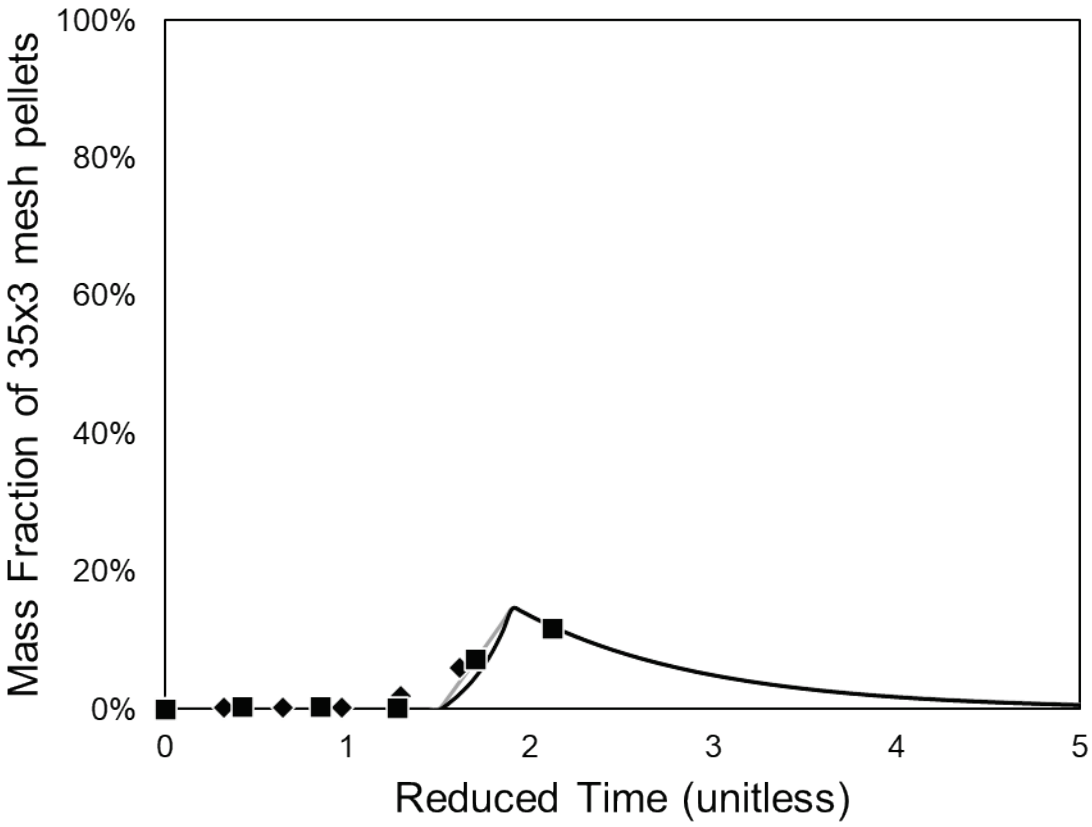

Figure 5.39: Abrasion middle fraction for 1.0kg/t sodium metasilicate material layered with 6.6kg/t sodium bentonite. These results also fall directly onto the uniform mass-distribution line specifically, which is neat but not strongly indicative of that being generally true.

These pellets are also very middle of the road for pellets containing tripolyphosphate, but as shown in Figure 5.40 they do appear to also have the higher compressive strength vs. abrasion resistance ratio that, at this point, seems to be a trend of the sodium tripolyphosphate containing pellets.

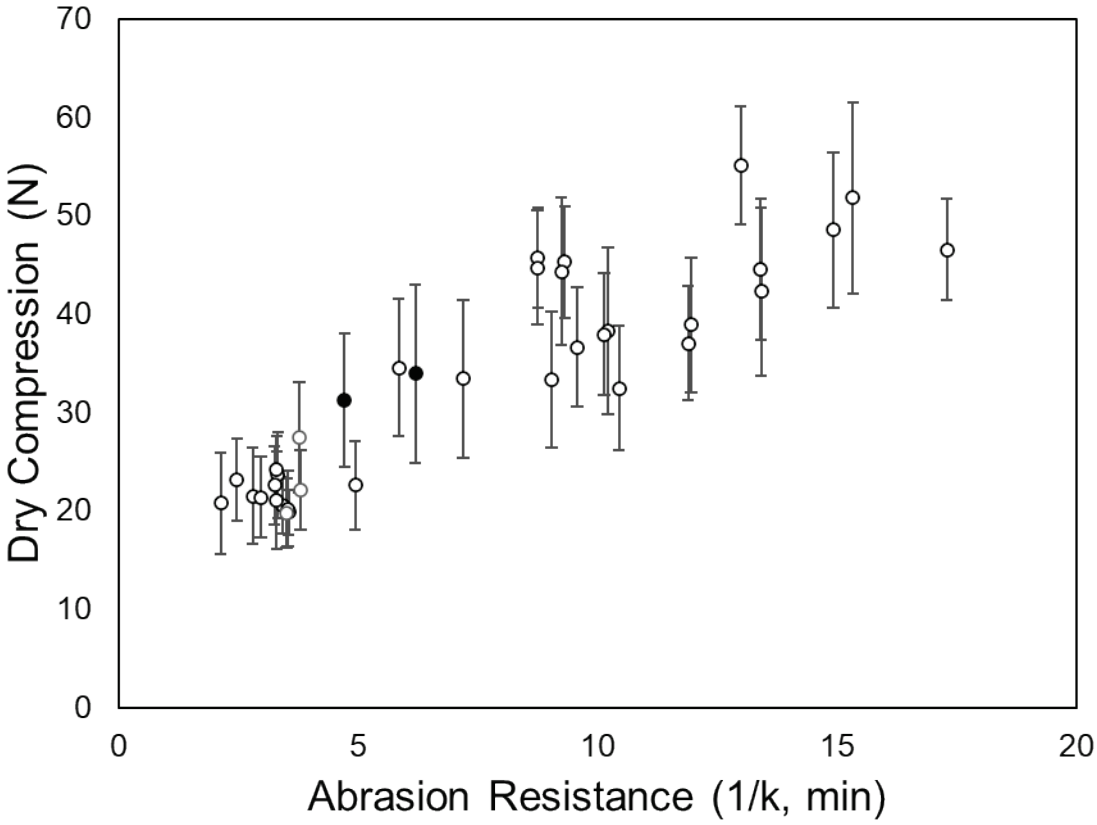

Figure 5.40: Adding 1.0kg/t sodium tripolyphosphate layered with 6.6kg/t sodium bentonite materials to Figure 5.36. These samples are in the middle of the pack but appear to be along the upper line which has so far been associated with the presence of sodium tripolyphosphate in general.

The next set of pellets was created using 1.0kg/t of sodium polyacrylate layered with 6.6kg/t of sodium bentonite. The tests shown in Figure 5.41 are sufficient to show that layering bentonite onto polyacrylate does not necessarily improve the pellets, but in this case the resulting strength distributions are reminiscent of the multiple types of distributions seen with pure sodium polyacrylate as well. Perhaps sodium polyacrylate is generally ill-suited to form the core binding volume of a hematite pellet.

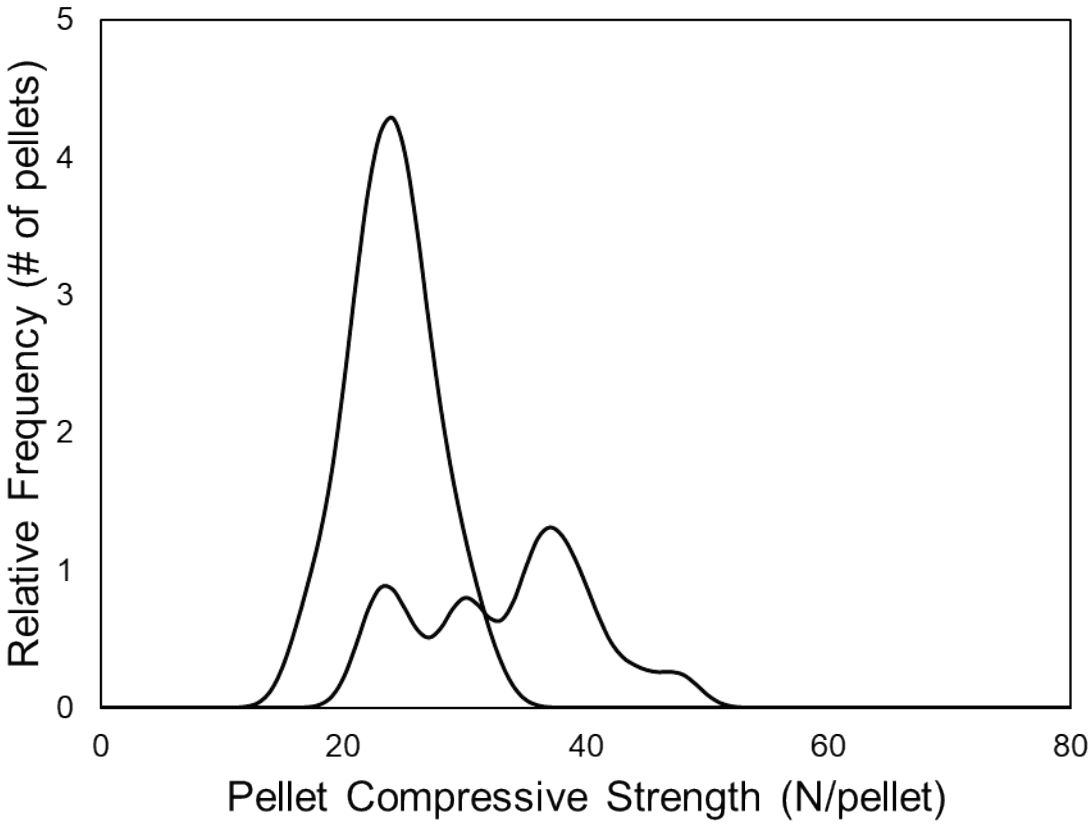

Figure 5.41: Compressive strength of pellets made from 1.0kg/t sodium polyacrylate layered with 6.6kg/t sodium bentonite. These differing distributions are reminiscent of the differing distributions observed for 1.0kg/t sodium polyacrylate pellets without layering.

Again Figure 5.42 does not appear to necessitate treating these layered pellets with multiple rate constants. The fit is still very reasonable and the resulting fit constant is in line with other pellets of these strengths and displaying these mass losses. Figure 5.43 could be interpreted as suggesting that a secondary rate constant is warranted, but it is the first of these layered pellet abrasion results to do so, and it could also be interpreted as breakage as well.

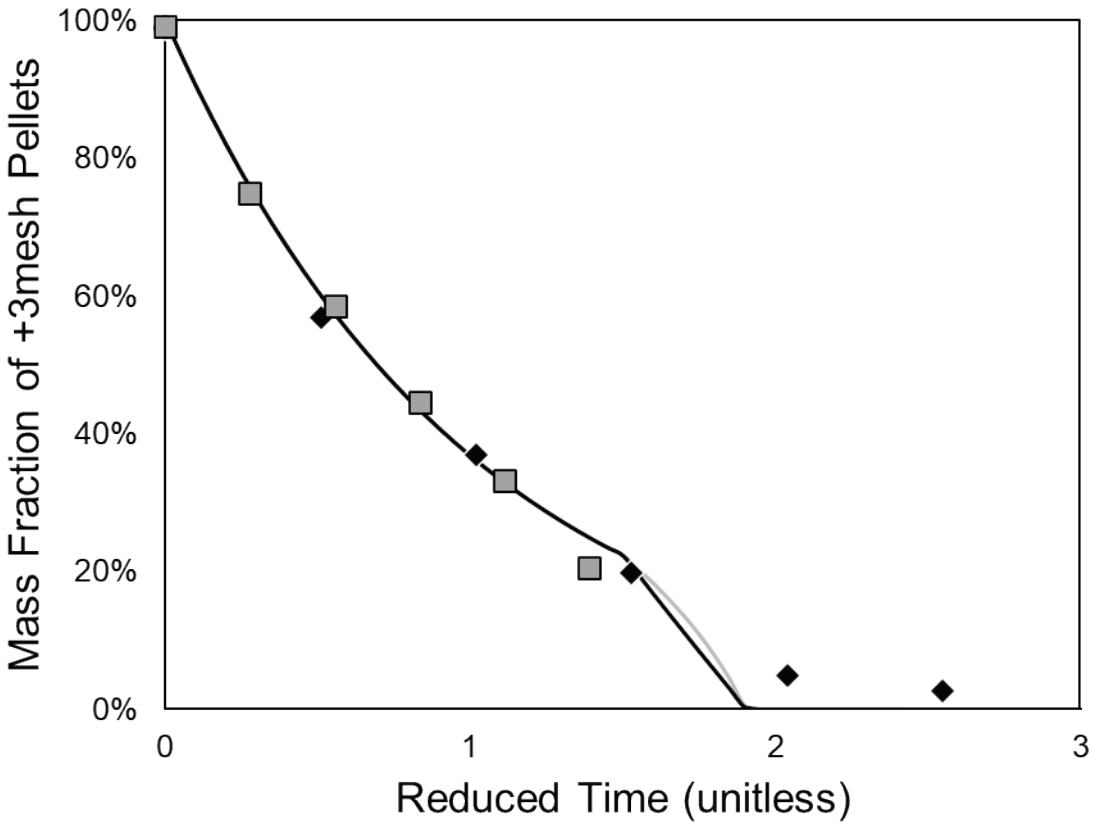

Figure 5.42: Upper abrasion fraction for 1.0kg/t sodium polyacrylate layered with 6.6kg/t sodium bentonite pellets. Again, no significant change in rate constant is immediately apparent in this data, though some breakage may have occurred in the weaker set of pellets here.

Thus, even considering how strange it is for it do so, it appears that the abrasion equation appropriately models layered pellets without any adjustment. In short, so far layering seems to be ineffective at creating a pellet with two separate categories of abrasion behavior. This would suggest that either the binders are contributing less directly than anticipated to the final abrasion strength, or that the pellet's internal structure is far more homogeneous that anticipated. The latter may be due to the activity of dispersants in the pellet, which may become clear from the reversed layering trials where bentonite is the core.

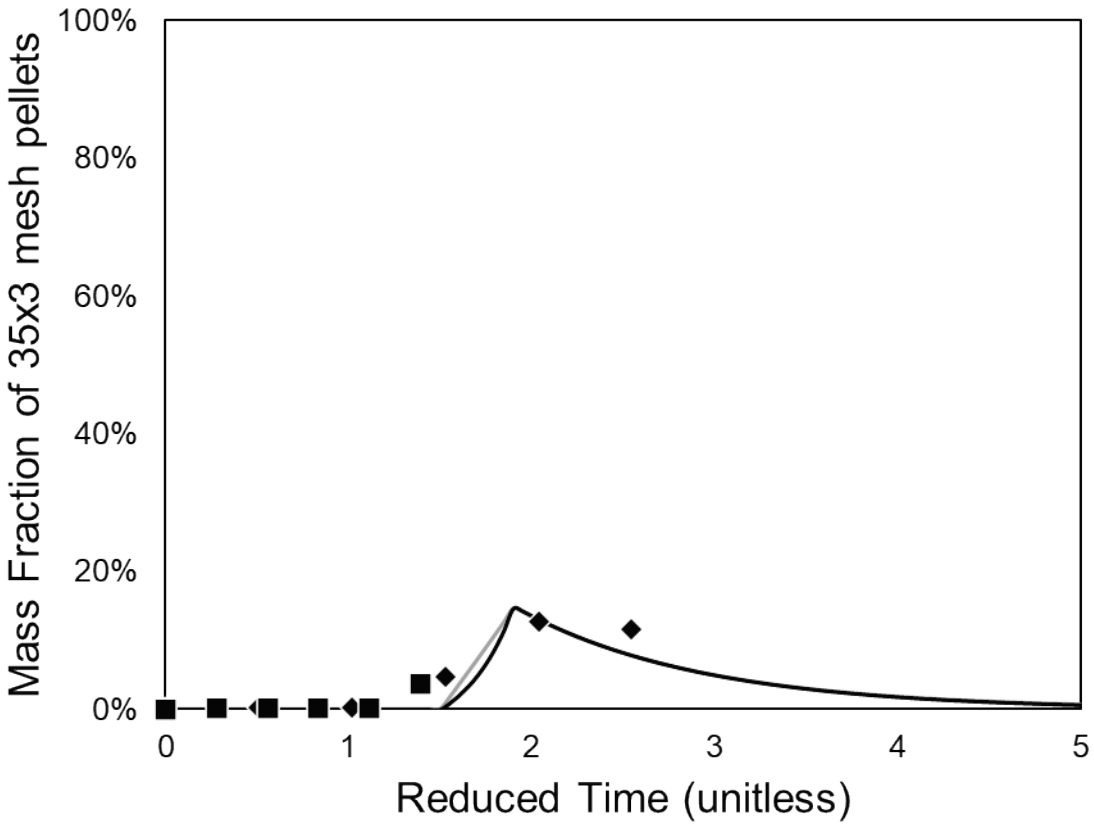

Figure 5.43: Middle abrasion fraction for pellets made with 1.0kg/t sodium polyacrylate and layered with 6.6kg/t sodium bentonite. It is possible to attribute the early rise around reduced time 1.5 as a sign of a potential rate constant shift, but it could also be understood as a sign that a small amount of pellet breakage has occurred.

The strength of these 1.0kg/t sodium polyacrylate layered with 6.6kg/t sodium bentonite pellets is shown in Figure 5.44, and follow the already established trends along the same line as the pellets which do not contain tripolyphosphate.

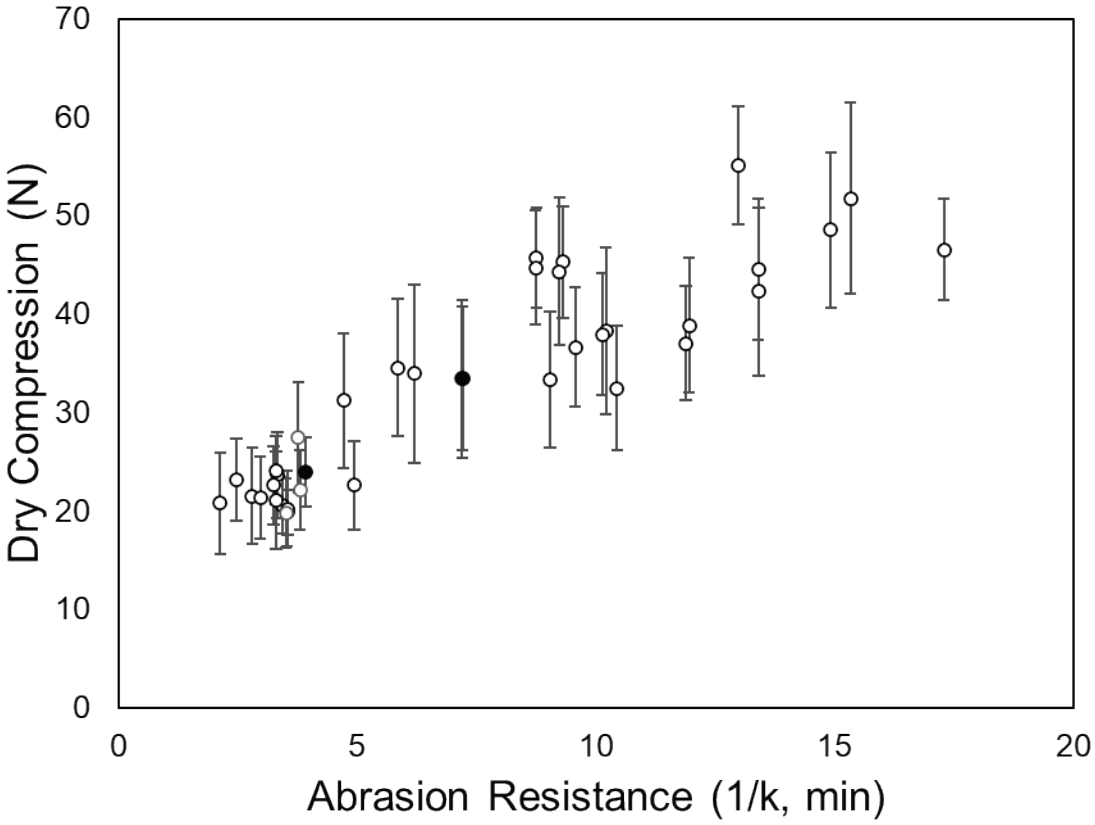

Figure 5.44: Adding 1.0kg/t sodium polyacrylate layered with 6.6kg/t sodium bentonite pellets to Figure 5.40. These pellets fall into pre-established trends as would be expected of their strength values and are similar to polyacrylate pellets in both cases.

Next up are some reverse layered pellets, where bentonite-bound pellets are layered with a small amount of dispersant containing material instead. Again, these tests were considered less representative of a realistic use case, and thus only limited data were collected. Furthermore, considering that the forward layered tests showed only at best middling results and only provided a limited insight into the nature of the different pellet binders, experimental efforts ended up focused elsewhere.

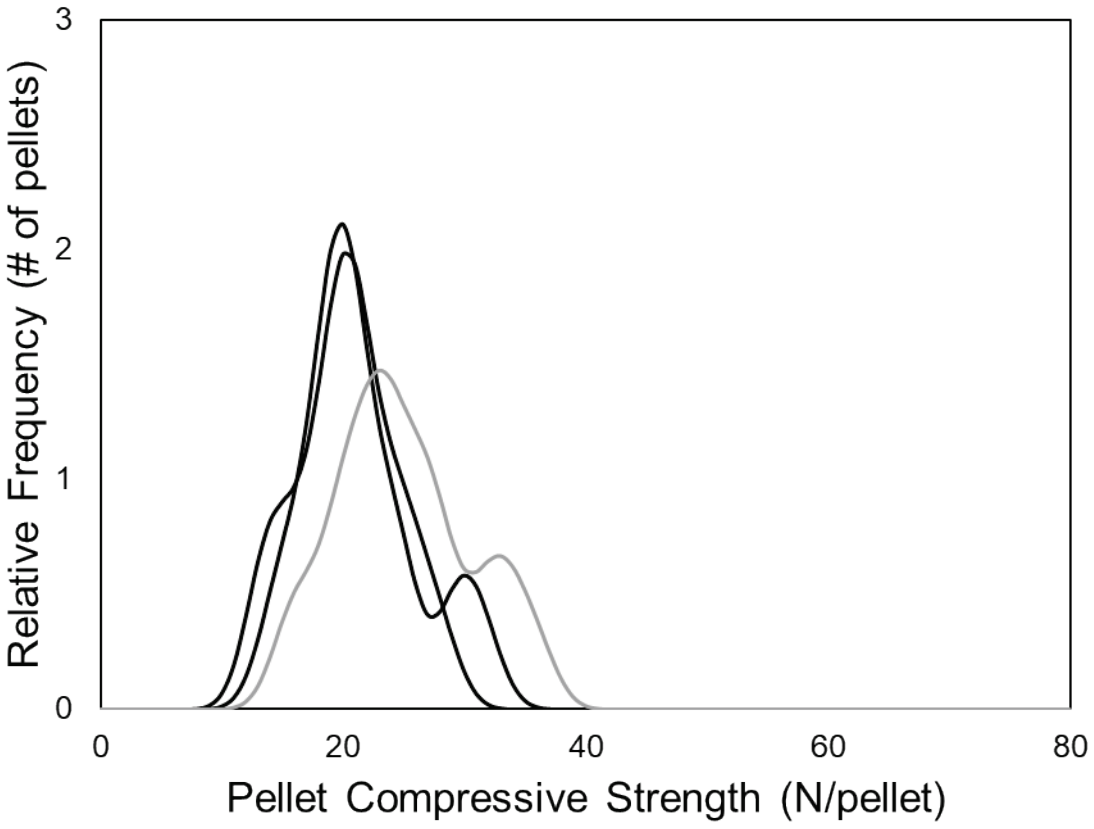

Figure 5.45: Strength of pellets made with 6.6kg/t sodium bentonite layered with 1.0kg/t sodium metasilicate (black lines) and 1.0kg/t sodium polyacrylate (grey line). These results are not strongly distinguishable from the bentonite-exterior layering tests.

Figure 5.45 reports the pellet strength results for the reverse pellet tests, which are essentially the same as were expected for the forward tests for the same material combinations.

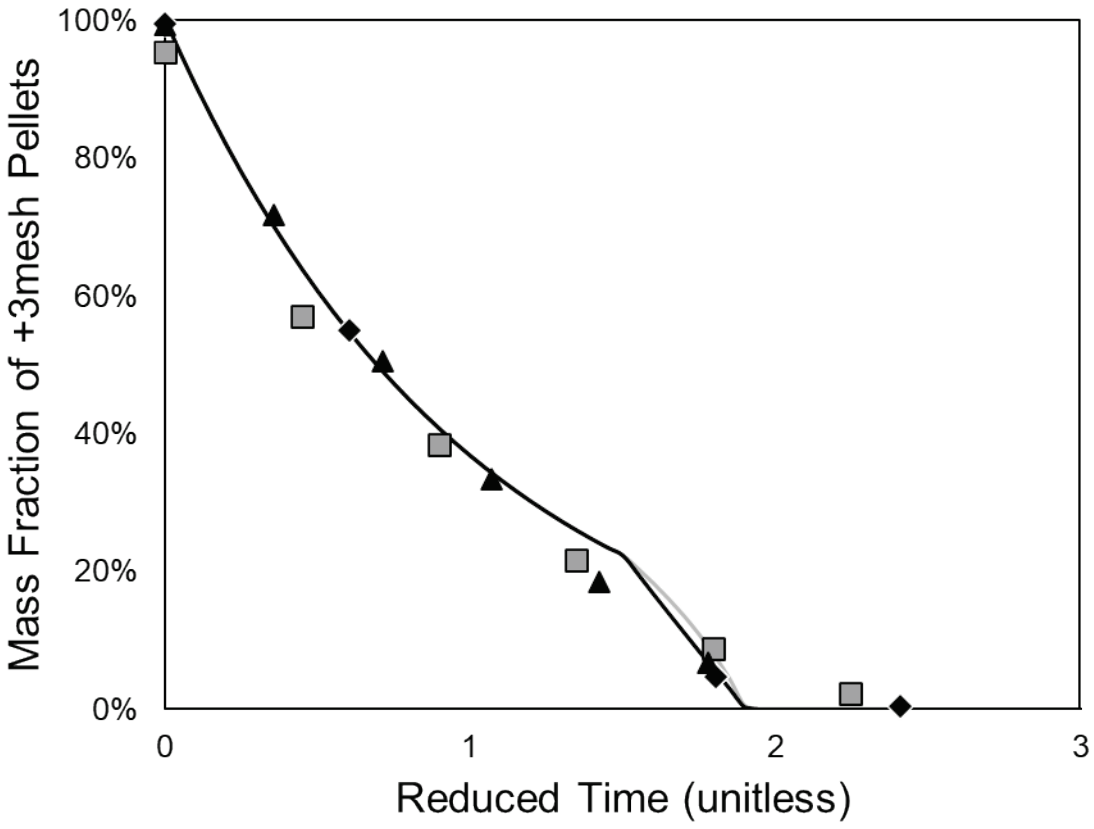

Figure 5.46: Upper abrasion fraction of pellets made with 6.6kg/t bentonite layered with 1.0kg/t sodium polyacrylate (black triangles) or 1.0kg/t sodium metasilicate (others). Again, no consistent evidence that multiple rate constants are necessary, though the fit is not as good as normal for these pellets.

Figure 5.46 shows that the abrasion test fit is a little bit looser than normal for these pellets, but it is unclear if the deviation should be considered to be caused by breakage or the effect of layering. In the case of layering, it is potentially the case that the bentonite-cored pellets are less mobile than the dispersant-cored ones, so it is more difficult for the compounds added to the exterior of the pellet to become incorporated into the core of the pellet. However, the effect could still be hidden away in pellet breakage even here, especially as these pellets are not unusually durable to begin with. Figure 5.47 is also difficult to consider decisive as is.

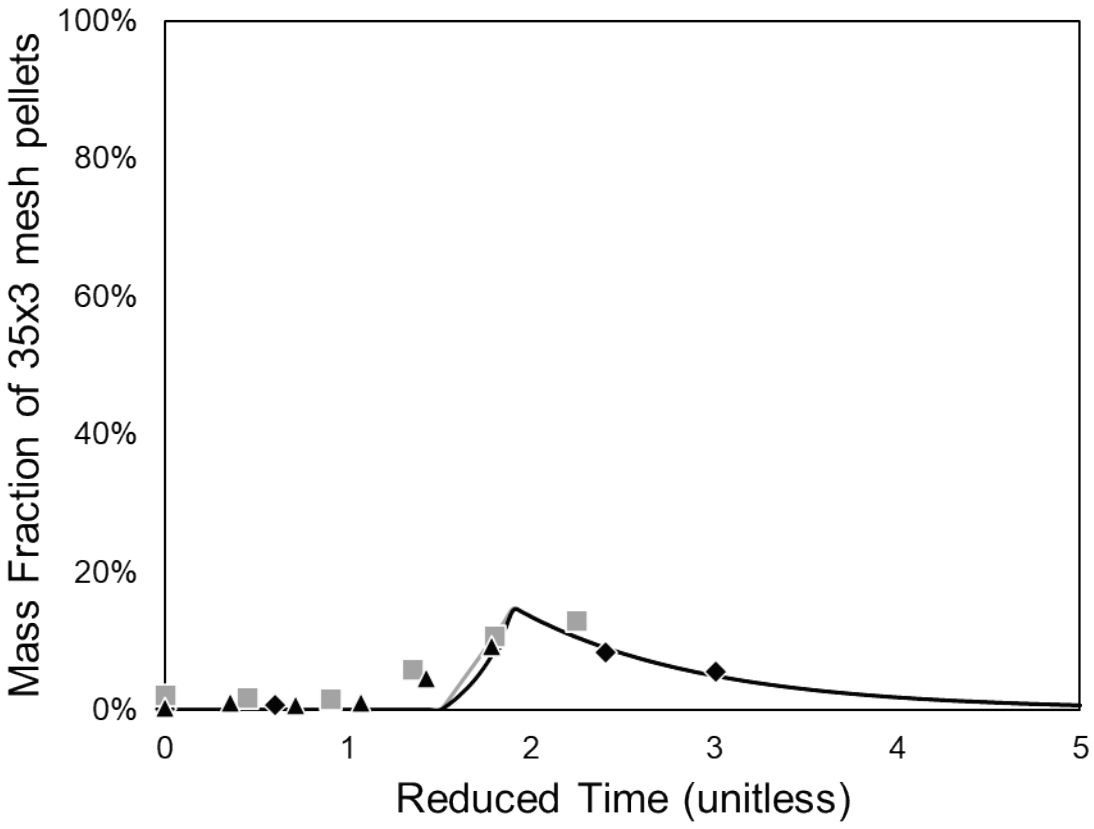

Figure 5.47: Upper abrasion fraction of pellets made with 6.6kg/t bentonite layered with 1.0kg/t sodium polyacrylate (black triangles) or 1.0kg/t sodium metasilicate (others). The grey squares trendline might seem to suggest a change in rate constant but does not appear to increase steeply enough for that.

The final strengths of these materials are also very much in the middle of established trends, as shown in Figure 5.48.

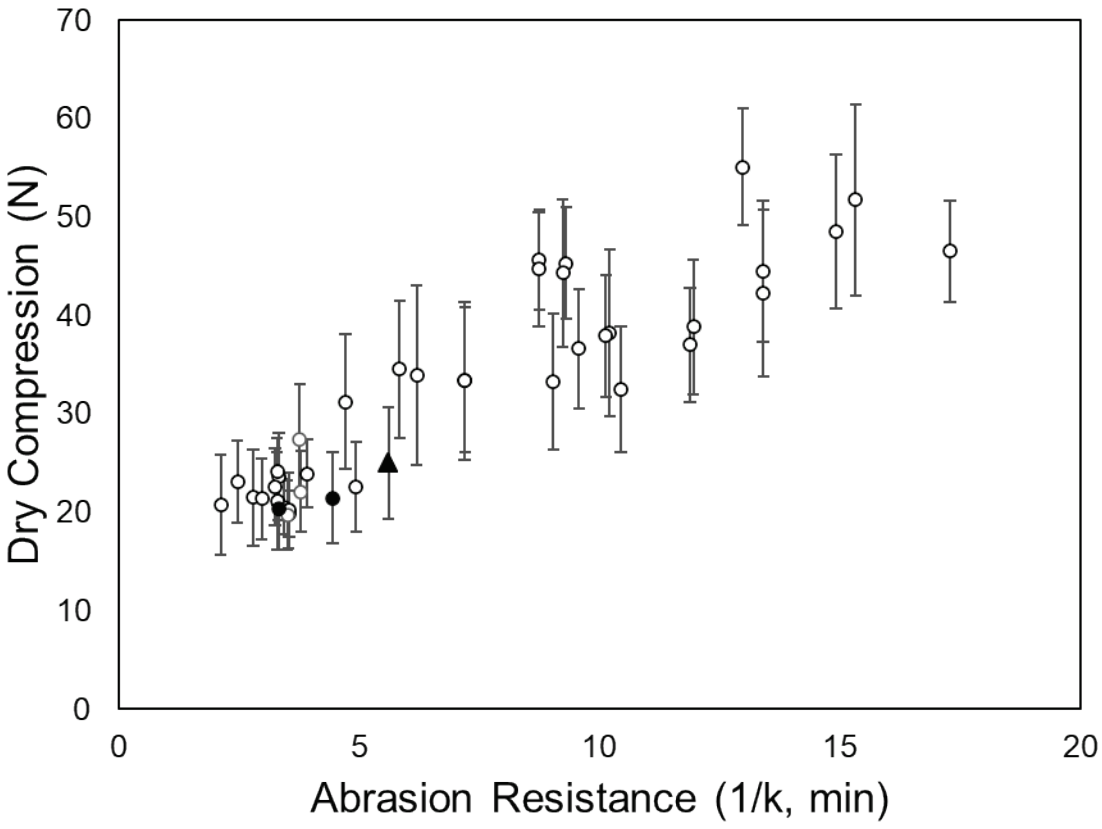

Figure 5.48: Adding 6.6kg/t sodium bentonite pellets layered with 1.0kg/t sodium metasilicate (black circles) or 1.0kg/t sodium polyacrylate (black triangle) to Figure 5.44. These pellets are in the lower trendline group, as would be expected of pellets not containing tripolyphosphate at this point.

The results of all of these layering experiments highlight some major points. These pellets were surprisingly homogeneous, even though they were specifically designed not to be. The abrasion test could accurately fit them with only a single rate constant. Potential explanations for this are:

1. The presence of dispersants enables a high mobility within the core of the pellet, allowing material added at the end of the pellet's growth to migrate into even the core of the pellet and influence the pellet strength as a result.
2. Alternatively, all pellets are more capable of wet restructuring than originally anticipated, and this phenomenon occurs even without requiring the core to be dispersed, which appears to be the case here with the reverse layered pellets.
3. Somewhat more extremely, perhaps the emphasis on the potential behavior of the binder is missing the forest for the trees here: the majority of bonds within the pellet may be determined more by the pellet's structure and adjacency than the presence of these binders. Thus, the material structures provided by the inner and outer layer homogenize due to their mechanical interactions with each other resulting in a relatively homogeneous set of pellet bonds after drying all throughout the pellet.

Considering that the whole idea of wet pellets is that they can have new material added readily and be compacted readily by rolling in the drum, the most likely hypothesis here is option #2. However, Halt (2017) showed that the addition of a layer of bentonite onto starch pellets was effective for reducing the dustiness of those starch pellets, but perhaps the effect had more in common with a direct mixing of the binders than had been originally anticipated. Halt (2017) did relatively limited testing to verify the abrasion resistance of the pellets in question and did not investigate the kinetics deeply enough for us to retroactively make strong conclusions about the nature of the pellet's structure.

It may also be that starch's layering behavior significantly differs, although given that polyacrylate and metasilicate are also long polymers which interact with hematite, it seems likely that if starch could truly immobilize the core so as to prevent this sort of mixing, so would one of these two dispersants.

5.4 Roll press mixing

Roll press mixing is a technique for mixing bentonite into pellet feed more effectively. This was originally described by Ripke and Kawatra (2002b). A roll press is used at a separation distance wide enough to allow material to pass through without being crushed, but where the rolls can come into contact with the bentonite material and shear it into long fibers of material. This has been shown to greatly increase the availability of the bentonite within the pellet, which can greatly increase its effectiveness at the same dosages.

A later test was performed by McDonald (2017) which seemed to be based on the same principle of trying to improve how the bentonite could spread out within the pellet. Dispersants were mixed with the bentonite before addition to the pellet feed (no improvement) or alongside the bentonite in the pellet feed (Claremboux, 2020; improvement observed). The idea in both cases seemed to be that the addition of a dispersant would help improve the mobility of the bentonite as it expanded through the pellet.

However, an investigation of the relative mobility of particles in a dispersed crystal grid versus a tightly packed crystal grid suggested that even infinite dispersion could not increase the mobility far enough to demonstrate the improvements observed.

This was determined by comparison to the geometry of the tightest possible packing of uniform spheres. This closest possible packing is well described in literature, the one chosen for this is an infinite hexagonal close packing which achieves a porosity of 0.25952, which is comfortably below the porosities typically expected of iron ore pellets.

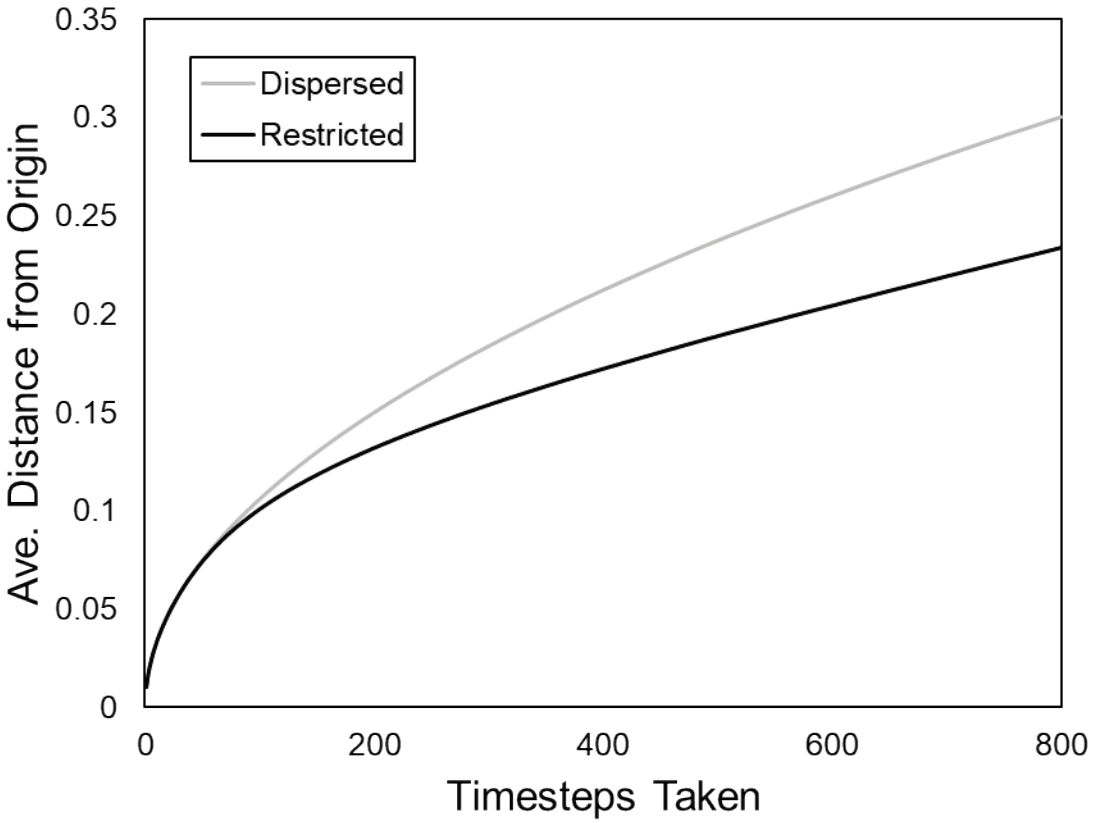

Figure 5.49: Relative rate of diffusion between free space and the hexagonal close packing of spheres for two identical particles. The unit distance is the distance between the centers of two adjacent spheres.

Brownian motion was simulated within this close packed lattice, where a particle's motion was assumed to be a random walk with instantaneous velocity normally distributed. Collisions were assumed to be perfectly elastic with the larger particle unmoving. For an ensemble of particles, this behavior averages out to the kinetic behavior of the diffusion equation of transport phenomena. Figure 5.49 shows the extent to which a particle is restricted in diffusion due to the presence of the tightly packed spheres.

In short, a particle in the completely restricted space still achieves 77.8% of the diffusion that a particle in free space does. This means that if a particle could not diffuse beforehand, adding any amount of dispersant to separate the particles in the pellet has essentially no effect on the dispersibility of the particle. If a particle could already be dispersed effectively in the timespan of preparing pellet feed, increasing the speed by which it does so by about 25% is also irrelevant.

Clearly, this is not the mechanism by which dispersants make pellets stronger. Yet, this mechanical dispersion of the material is the mechanism by which roll-mixing makes bentonite a more effective binder. As such, we would predict that mixing these two mechanisms should have a synergistic effect that exceeds the effect of either material on its own.

Thus, roll-mixed bentonite pellets and roll-mixed bentonite plus dispersant pellets were tested. The roll-mixed bentonite was prepared by passing the pellet feed with bentonite mixed in through a roll press 20 times at a spacing of 1mm. As in the original work by

Ripke and Kawatra (2002b), it must be emphasized that no size reduction occurred during this process. The goal of this mechanical process was to disperse the bentonite more evenly and more thoroughly into the pellet feed. Afterwards, the moisture was adjusted consistent with the other pellets and pellets were formed. In the case of the mixed binder, the dispersant was added after the roll mixing step.

In both cases, 6.6kg/t of rolled bentonite were used. The dispersant for these tests was 1.0kg/t of sodium metasilicate, which is well characterized by other available data both in the absence and presence of bentonite.

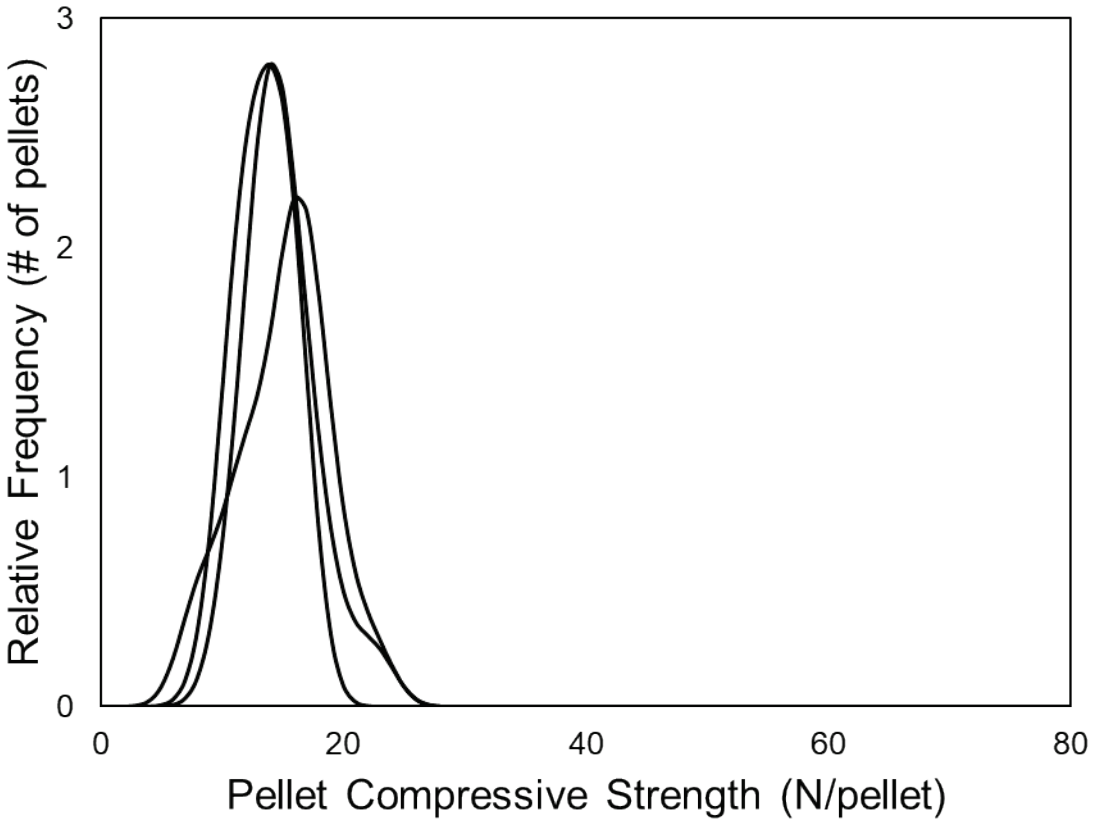

Figure 5.50: Pellet strength of pellets formed with 6.6kg/t of roll mixed bentonite.

Figure 5.50 shows that the roll-mixed bentonite pellets were actually surprisingly weak. Despite the addition of a significant amount of moisture, with final moisture contents of 9.7-10.1wt%, these pellets seemed to be consistently too dry. Observationally, the results seemed consistent with having too much available bentonite, and the resulting pellet strengths seemed to suffer as a result.

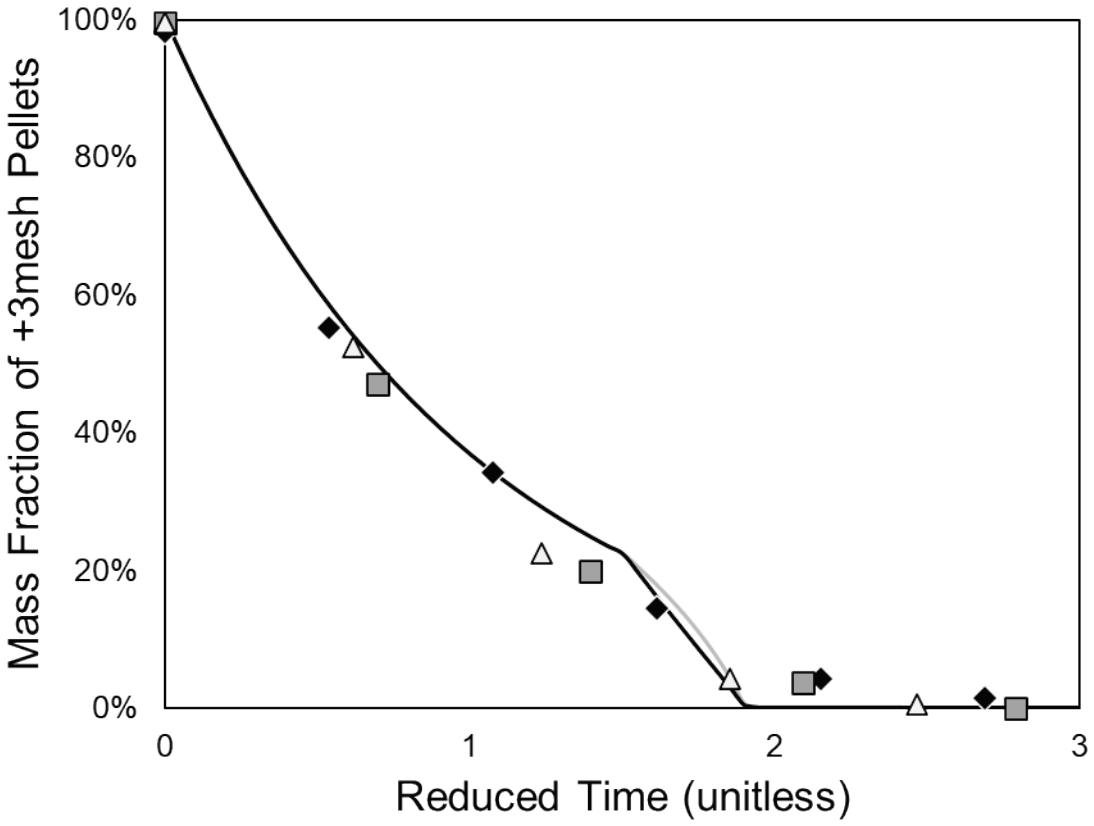

Figure 5.51: Upper abrasion mass fraction for pellets formed with 6.6kg/t of roll-mixed bentonite. Some breakage seems to have occurred, which is unsurprising given the low compressive strengths of these pellets.

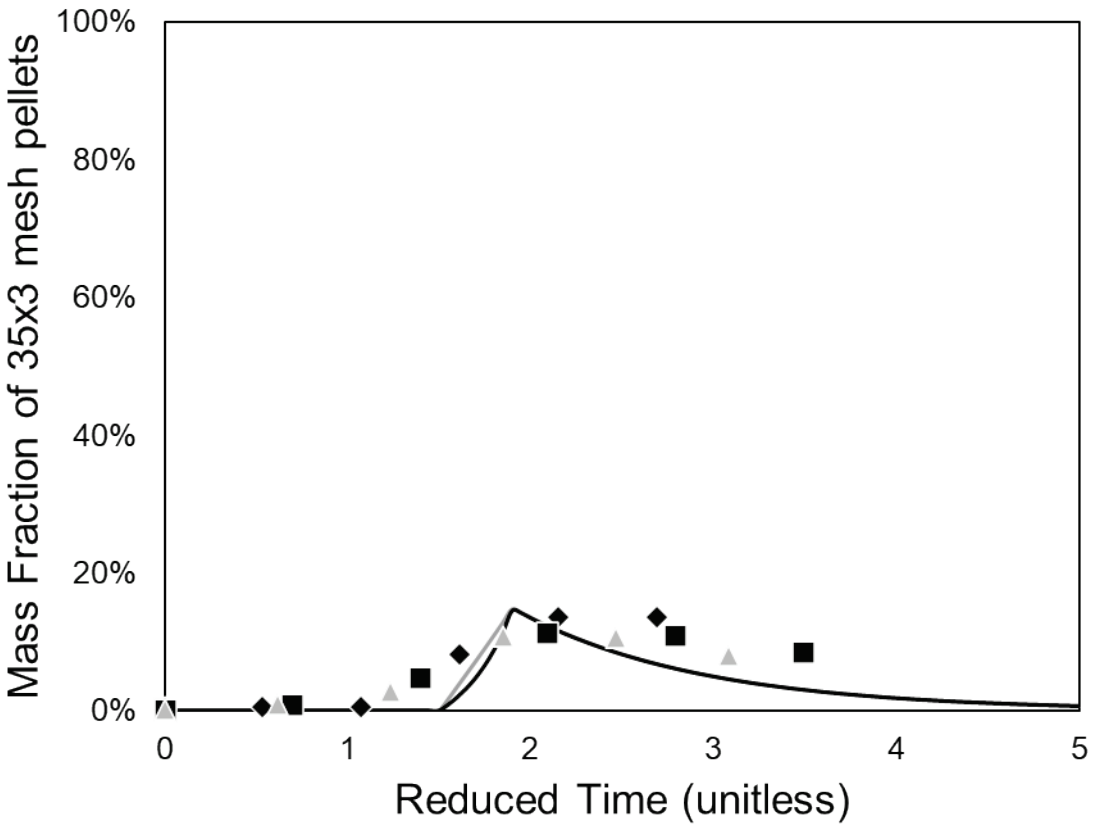

Figure 5.52: Middle abrasion fraction for pellets created with 6.6kg/t of rolled bentonite. These pellets exhibited fairly poor correlation with the expected fit lines, likely due to their very low compressive strength resulting in excess breakage.

Figure 5.51 and Figure 5.52 both show relatively loose correlations with the expected fit lines, but both can be explained by relatively low strengths of these pellets. While these pellets were surprisingly weak, it makes sense that having too much of an excess of bentonite can significantly interfere with pellet strength and growth. In this case, the 6.6kg/t of roll-pressed bentonite seemed to have been a significant overdosing of this material.

So, what happens when we add 1.0kg/t of sodium metasilicate onto that?

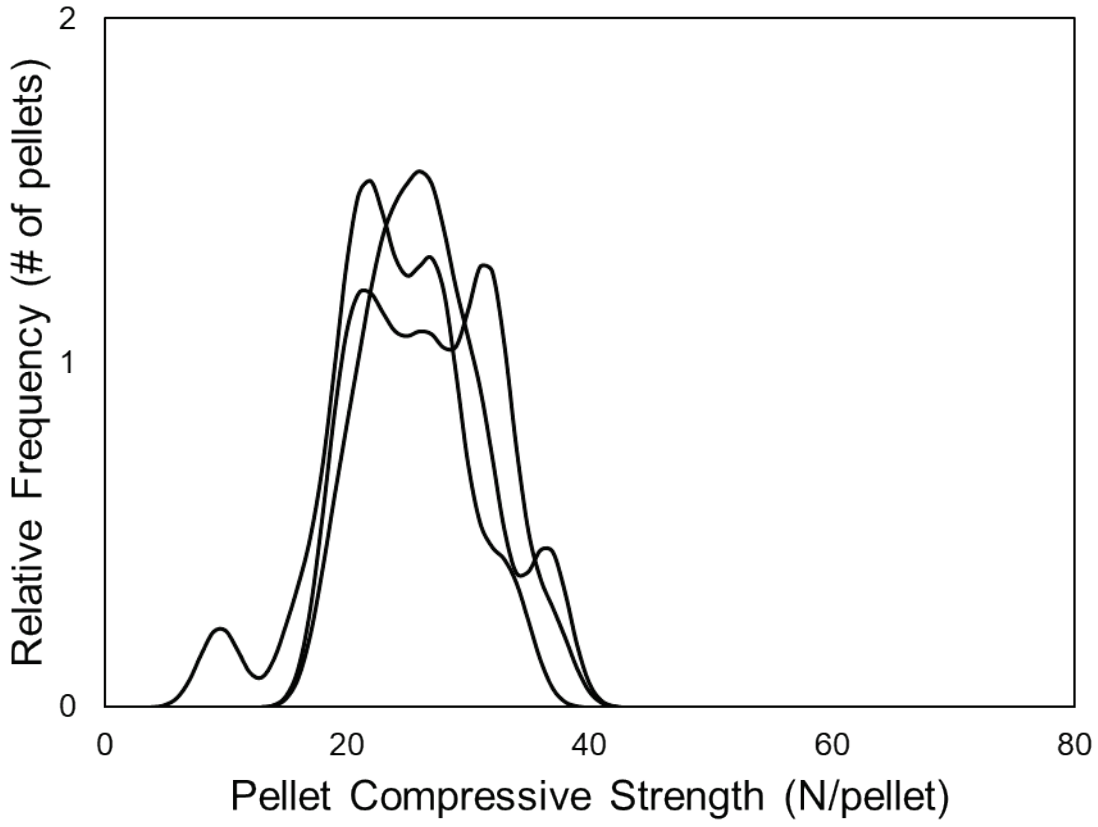

Figure 5.53: Pellet strength of pellets created with 6.6kg/t of roll-pressed bentonite and 1.0kg/t of sodium metasilicate. A considerable improvement in pellet strength is shown versus the rolled bentonite alone.

Figure 5.53 shows that the pellet strength of roll-pressed bentonite with metasilicate improves by approximately a factor of 2, which is very much in line with what has previously been seen with sodium bentonite and sodium metasilicate mixtures (e.g. in Claremboux, 2020).

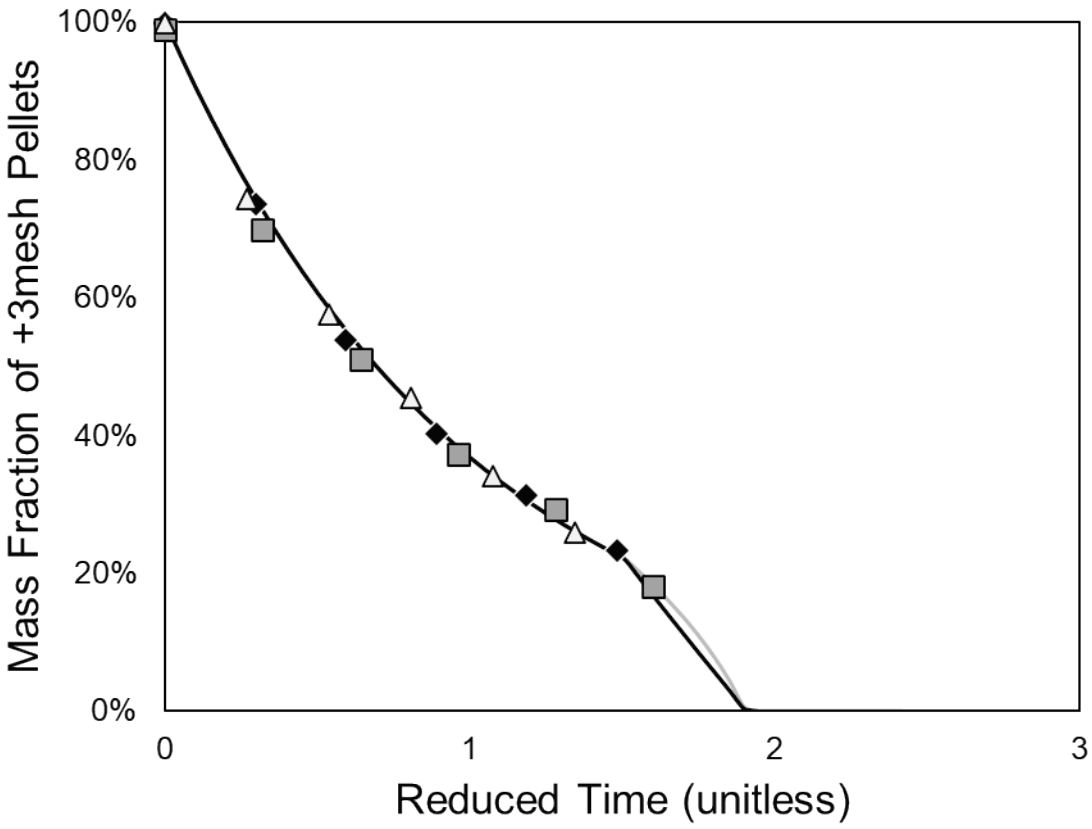

Figure 5.54: Upper abrasion fraction for pellets composed of 6.6kg/t of roll-mixed sodium bentonite and 1.0kg/t of sodium metasilicate. These pellets undergo abrasion without any ambiguity.

Figure 5.54 shows that these pellets containing both roll-mixed bentonite and metasilicate behave exactly according to theory in abrasion. In short, increasing the pellet strength some helped to avoid too much early breakage which made fitting more difficult with the roll-mixed bentonite alone. Figure 5.55 also fits the theory quite well.

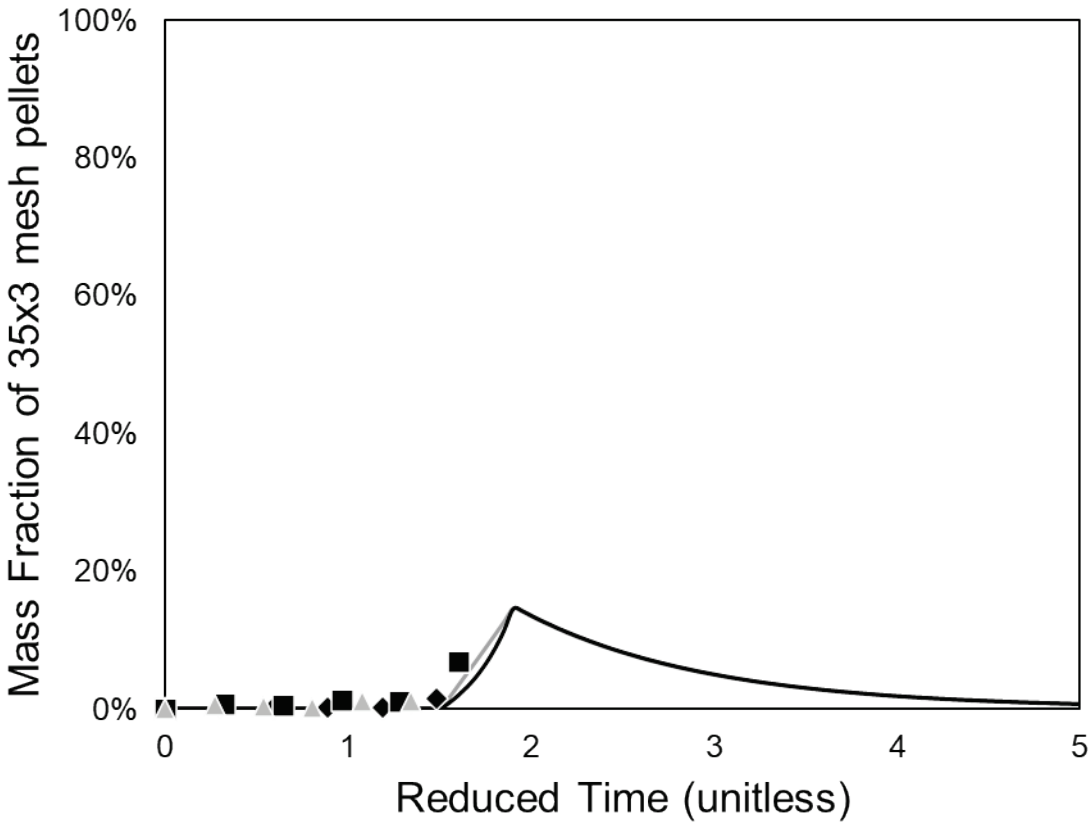

Figure 5.55: Middle abrasion fraction for pellets made with 6.6kg/t of roll-pressed bentonite mixed with 1.0kg/t of sodium metasilicate.

Figure 5.56 shows that the increase in abrasion resistance observed between the samples with and without metasilicate is almost doubled as well. The average abrasion resistance of a 1.0kg/t metasilicate pellet was previously found to be approximately 3.3 minutes, the average resistance of a rolled bentonite pellet is approximately 3.3 minutes, and the average abrasion resistance of a rolled bentonite pellet with metasilicate is 6.8 minutes. If anything, this effect appears to be slightly synergistic, developing a bonding interaction that exceeds the individual components, and that is assume that the material would have no inherent abrasion resistance without these binders.

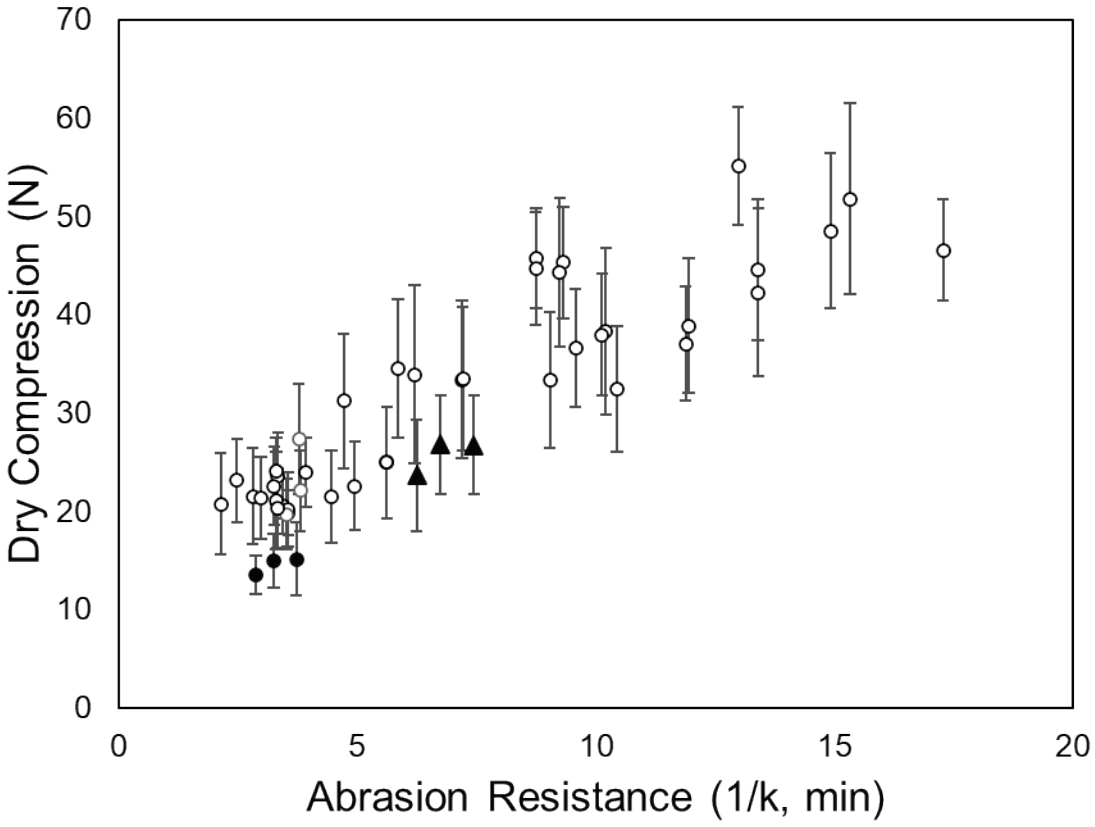

Figure 5.56: Adding pellets made with 6.6kg/t roll-mixed bentonite both without (black circles) and with 1.0kg/t sodium metasilicate (black triangles) to Figure 5.48.

6 Conclusions

We established as one of our hypotheses in Chapter 3 that the abrasion test can be combined with established mathematics around abrasion to form a strong theoretical basis for understanding it. Most of the graphs shown in Chapter 5 show again and again that the abrasion test generates data which fits incredibly well with the single-parameter model devised in Chapter 3.

This model, which requires only the determination of a rate constant was in turn also connected to the strength of the pellets. As has been shown, these data sets can be fit very consistently, and the reproducibility on repeated abrasion tests is very high whenever the pellets are themselves consistent. While accuracy could potentially be improved for very weak pellets by improving our understanding of pellet breakage within the Rotap itself, the introduction of breakage terms would allow for significantly more room for error in the interpretation of the model's results.

Thus, we would like to propose that the single-parameter model is an appropriate theoretical framework for using a Rotap machine to test the abrasion of a low to moderate strength material like iron ore pellets. There is a strong theoretical basis that differs from reality by at most a constant factor, as evidenced by the numerous different types of materials, including intentionally nonhomogeneous layered pellets, which were very precisely explained by the proposed model.

As evidence of the general applicability of the final fits, the following graphs combine all kinetic data recorded in this work, including for pellets which were stronger and weaker

than those reported in Chapter 5. The labels of the materials are intentionally omitted in this graph to emphasize the generality of the approach – since the approach is meant to apply to the abrasion of all pellets in this sort of process, the ability to identify a single type of material from a data point on this graph would prove that the approach is incomplete.

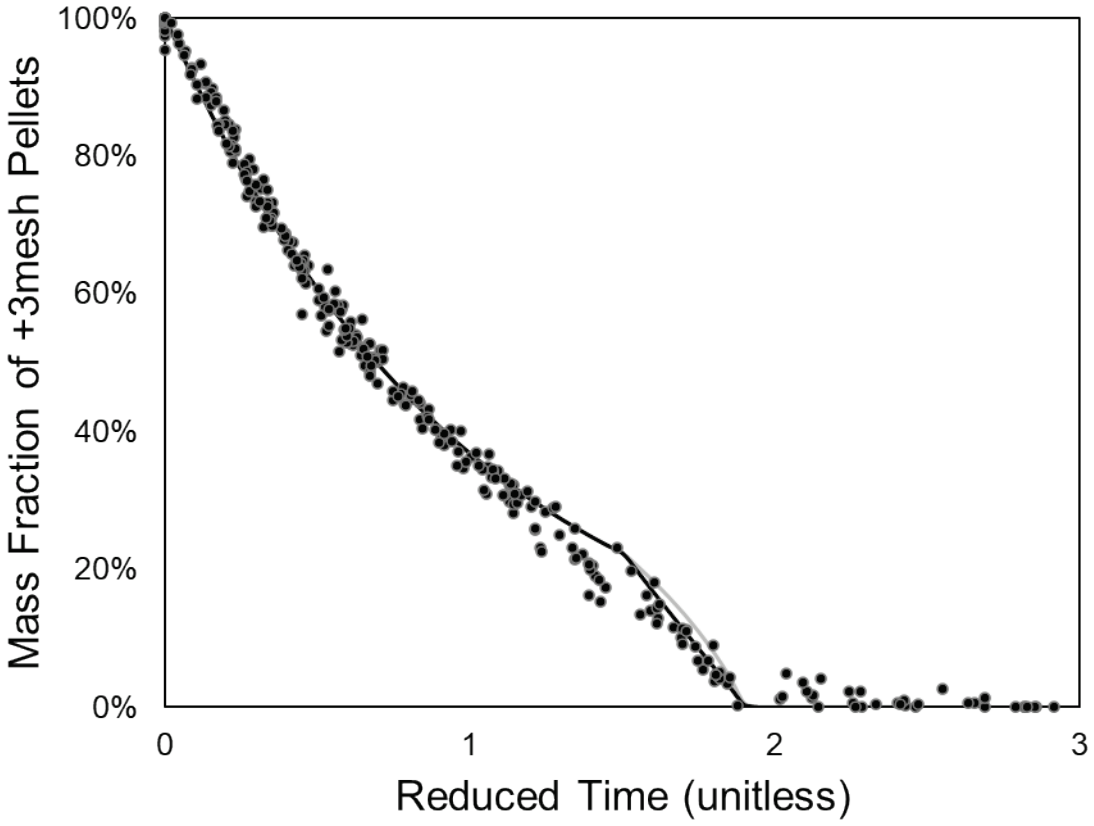

Figure 6.1: All upper mass fractions from all abrasion test data collected, in reduced time basis. While most sample points deviate from the line slightly, there is a very strong trend especially before the first inflection point.

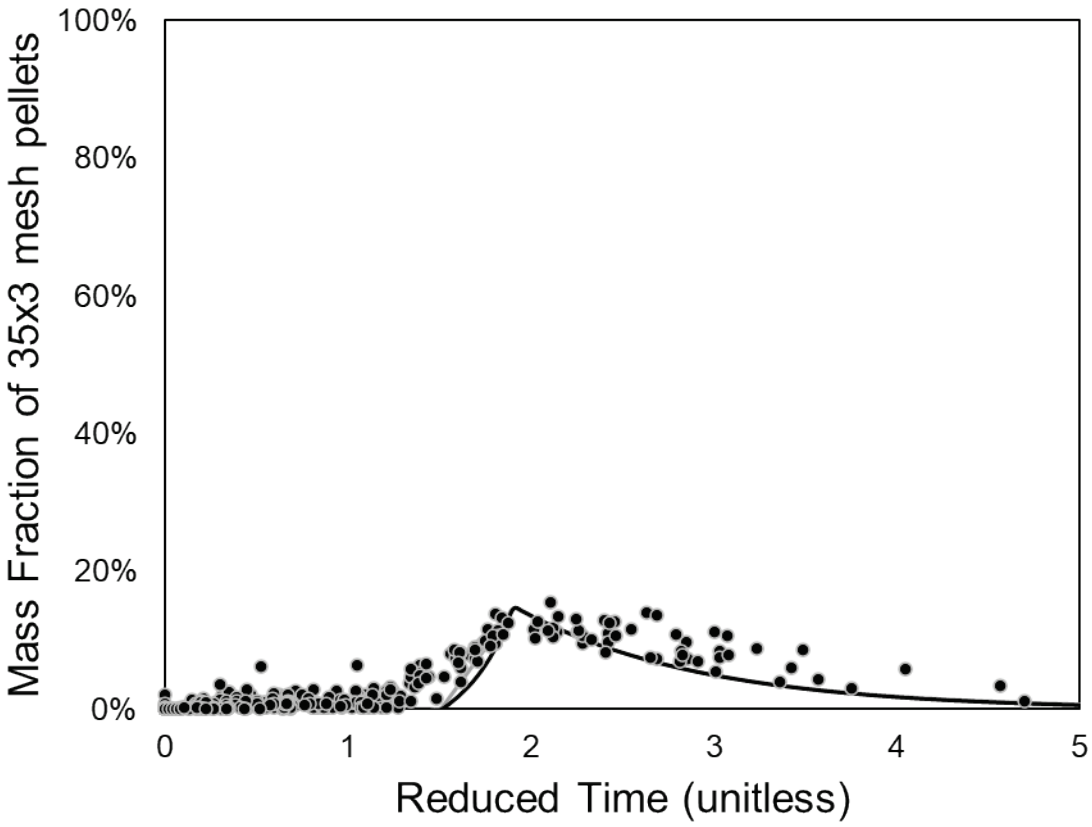

Figure 6.2: All middle mass fractions from all abrasion test data collected, in reduced time basis. While the deviation on this graph is far more obvious than on Figure 6.1, the explanation for it is the occasional occurrence of breakage. Note the very small number of samples recorded even slightly under the predicted curve.

Figure 6.1 and Figure 6.2 make a strong argument that this approach is valid for predicting the mass loss which occurs during an abrasion test, and directly connects it to a single parameter which serves as a rate constant. This rate constant exists for all pellet types tested and provides a convincing though not always perfect fit for every one of these abrasion tests.

The abrasion resistance was also found to seem to follow linear combination trends when multiple binders were combined. This was most strongly observed between binders that appeared to have good compatibility in compression strength but occurred slightly even

between binders which did not have good compatibility in compression strength. In all tests performed, the addition of a dispersant which was expected to have a positive contribution to abrasion strength never decreased the resulting abrasion resistance.

This is likely somewhat more consistent than it appears to be in compression strength primarily because the extent to which the pellet is broken differs so dramatically between the two tests. In the abrasion test, if the binder is present within the pellet, at some point its strength will have to contribute to the strength of the pellet simply because the area it is binding will become subjected to the abrasion.

Meanwhile, compressive strength testing tests the weakest planes that can be readily found within the pellet. Thus, the addition of a small amount of binder should generally accomplish nothing unless the binder disperses very well and forms very large binding domains for its size.

However, aside from frictional components, the fundamental strength of the bonds being tested should remain the same in each test. And we indeed find that there is a loose correlation between the pellet strengths measured and the abrasion resistances measured. This correlation is muddled due to the imperfect fracture planes observed during compression testing, the imperfect sphericity of real pellets, and the variance of the pellet's radius directly influencing the variation observed in the compression strength results. However, the variation observed in pellet strengths was found to never be less than predicted for the size distributions tested.

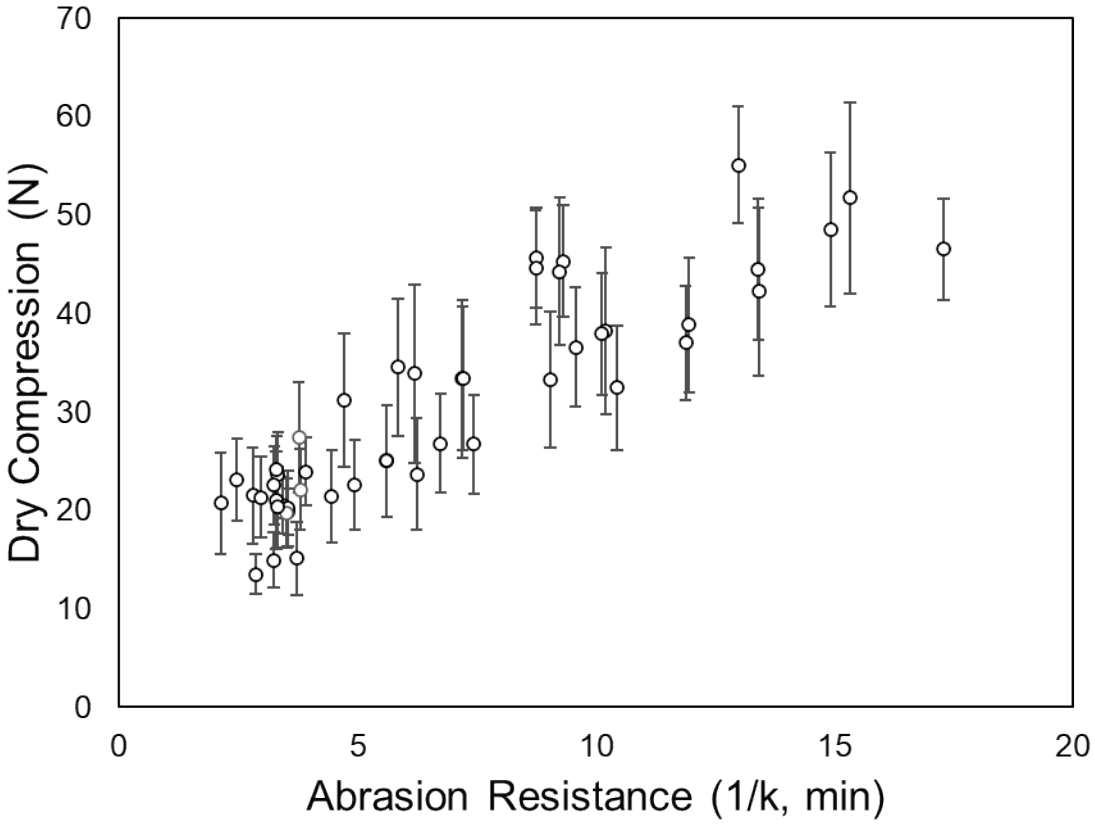

Figure 6.3: Dry compression versus abrasion resistance for all pellets reported in Chapter 5.

Figure 6.3 shows that there are two or more different trendlines occurring here, but overwhelmingly an increase in abrasion resistance or mean pellet strength is expected to coincide with an increase in the other, all other things being equal. However, the rate of increase seems to depend on the pellet's composition, with pellets containing tripolyphosphate usually ending up on the higher end of this curve, while other pellets end up on the lower trendlines.

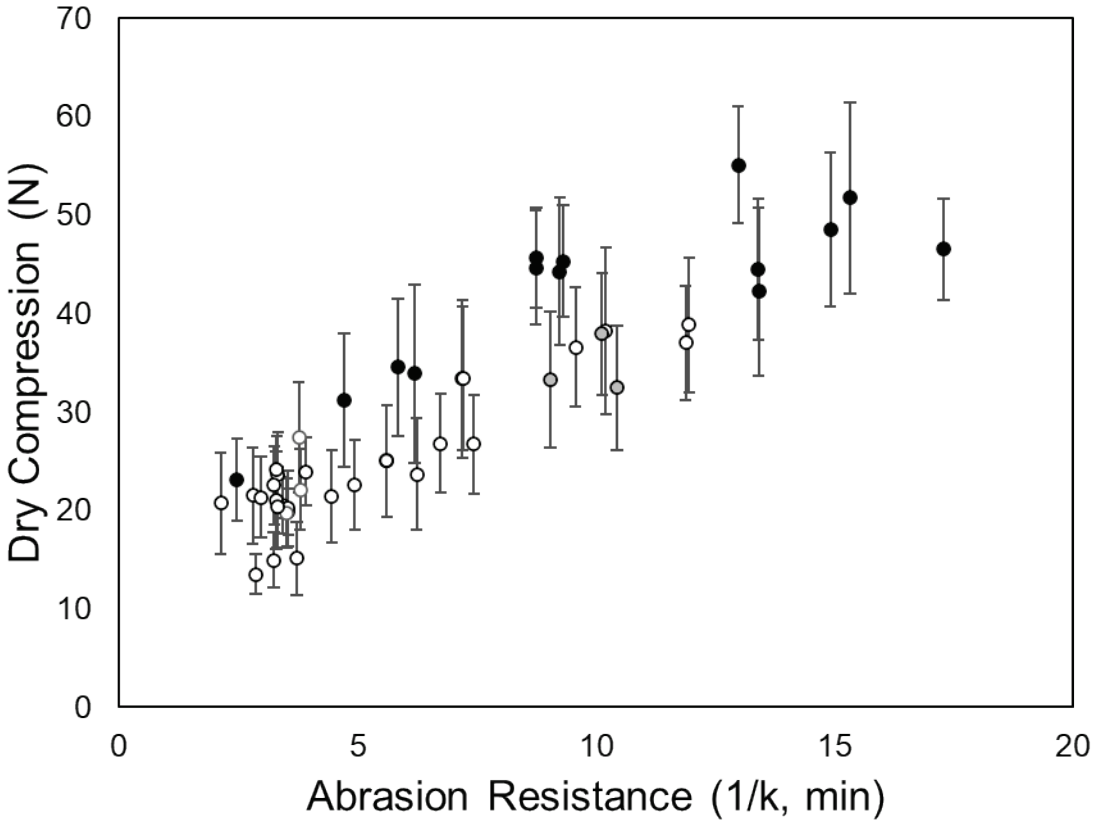

Figure 6.4: Figure 6.3, but pellets containing tripolyphosphate but not metasilicate are marked black, and pellets containing tripolyphosphate and metasilicate are marked grey.

Figure 6.4 highlights this trend as well. While the trend is not perfect, pellets containing more tripolyphosphate tend to have high compression strengths at otherwise similar abrasion resistances. The most likely explanation for that is that tripolyphosphate is promoting the formation of more spherical pellets, as it does not impose any particular structure on the pellet as it rolls. The narrowest distributions of pellet strengths are observed primarily in the tripolyphosphate pellets, but only very loose correlations are demonstrated between the variance of the pellet strengths and the ratio of average compression strength to abrasion resistance.

Another explanation is that tripolyphosphate is capable of mobilizing the colloidal material in the iron ore, which produces a wider available size distribution among the ultra-fine particles. In short, the material being bound is slightly changed, and the amount of fine material available is increased. This is traditionally correlated with a direct increase in binding strength in e.g. Rumpf's equation.

However, in terms of the model put forth here, it is more important that the material is physically present to form bridges to allow high coordination numbers than the actual presence of additional bonding due to ultrafine materials. Additionally, the strength increase exhibited by sodium tripolyphosphate alone is not so remarkable as to meet the expectations of Rumpf's equation. After all, the colloidal particles being made available should bring the average size of an interacting particle down by far more than a factor of 2 or 3, but that is the extent of the strength increase observed even with 2.0kg/t of sodium tripolyphosphate available.

One might expect that the role of a strong binder is actually to minimize the presence of weak planes along which compressive fractures can evolve. However, in general the dispersants do not seem to be able to do that consistently, nor were they expected to from the theory. The observed compressive strength distributions tend to be more scattered for stronger pellets than for ones made with weaker overall pellet strengths, and to an extent that is not entirely consistent with simply being weaker overall. While part of the lumpiness of the reported distributions is due to the choice of width parameters on the smoothed histograms, a large part of it is that there almost always were outlier pellets in any individual sample made with only dispersants. This was even observed for mixtures

of dispersants and traditional binders when full pellet strength distributions were reported (e.g. Claremboux, 2020; for metasilicate and bentonite mixtures). Only with very large dispersant dosages did the entire pellet distribution narrow again.

This continues to support the proposed mechanism of dispersants for pellet strength which was proposed previously (Claremboux, 2020), in that dispersion is a property of the entire pellet, and a pellet either is successfully dispersed or not successfully dispersed. Depending on the effectiveness of mixing the materials, a certain fraction of pellets will probabilistically happen to be dispersed and display the characteristic strength of a dispersed pellet, or they will not be dispersed and be correspondingly weaker.

The other major source of consternation in compressive strength is the fact that the same pellet can hypothetically report a tremendous number of different compressive strengths based on its orientation and which fracture plane is stressed first. Even for a single pellet a wide range of possible fractures can occur and there is a corresponding variation that makes it difficult between two pellets to determine if there was even a chance that they were actually similar in composition.

The inherent minimum strength plane in the compressive strength testing explains a lot of why Table 5.1 shows such dispersion-limited strength effects but compatible abrasion resistance. However, it turns out that abrasion resistance has relatively simple behavior, at least as observed in these tests: In the absence of highly limited or incompatible or highly synergistic binders, the contribution of each binder or material to the abrasion resistance add together to determine the total abrasion resistance of the pellet.

Thus, the conclusions of this work are as follows:

- The Rotap abrasion test is effective, reliable, and highly consistent with the theory of the abrasion of pellets, based on a novel analysis based on the energy input during the test. It is thus recommended as an option for understanding the abrasion of materials such as pellets.
- The theory of abrasion and pellet strength combine to allow predictions using abrasion resistance both for modifications of total amount of binder and for the trends of pellet compressive strength. This is particularly because the abrasion strength test allows the isolation of the binder's contribution to the pellet strength while excluding the impact of the pellet population's macroscopic geometry on the test results.
- A theory of material interaction is developed to predict the impact of dispersants on materials and to predict the compatibility of different dispersants with each other qualitatively, and which was subsequently supported by experimental evidence.
- A consistent correlation is shown between abrasion resistance and compressive pellet strength, the former of which is useful for controlling the dustiness of dried pellets and the latter of which is a primary control variable for pellet quality within a pelletizing plant. The deviations are likely explainable by the varying geometries of pellets versus highly dispersed pellets.
- A linear relation is both expected and observed for mixtures of binders with respect to abrasion resistance. Major exceptions include binders which have self-

limiting properties, such as those which rely only on dispersive effects to improve pellet strength. Deviations from this prediction are readily identifiable and meaningful for designing mixed binders. Most binders with similar mechanisms can be assumed to be compatible, but binders with less explored mechanisms may be tricky (such as tripolyphosphate's apparent incompatibility with metasilicate).

- This linear relation in abrasion strengths combined with the trendline connecting abrasion strength to compression strength provides a foundation for the prediction of the strength of mixed binders without relying on unknowable process or material conditions. Instead, only information about the strengths from pure binders and the character of the binders themselves are necessary to make predictions about the strengths of mixed binders.

In short, a framework now exists, utilizing abrasion resistance as a useful measure, for predicting the impact of mixing binders in an iron ore pellet, without requiring information which is essentially impossible to acquire in the context of iron ore processing due to ever changing process conditions or simply being too time or labor intensive to be economically worthwhile.

7 Reference List

Ababneh, A., Matalkah, F., and Matalkeh, B., 2022. “Effects of kaolin characteristics on the mechanical properties of alkali-activated binders,” *Construction and Building Materials*, Vol. 318, pg. 126020.

Abouzeid, A.-Z.M., 1982. “Performance of an industrial balling circuit,” *Mining Engineering*, Vol. 34, No. 6, pp. 677-684.

Ammasi, A., 2019. “Effect of heating rate on decomposition temperature of goethite ore,” *Trans. Indian Inst. Met.*, Vol. 73, No. 1, pp. 93-98.

André, D., Iordanoff, I., Charles, J.-L., and Néauport, J., 2012. “Discrete element method to simulate continuous material by using the cohesive beam model,” *Comput. Methods Appl. Mech. Engrg.*, Vol. 213-216, pp. 113-125.

Athayde, M., Nunes, S.F., and Bagatini, M.C., 2018a. “A case study on the pellet size fraction influence of pelletizing operation,” *Mineral Processing and Extractive Metallurgy Review*, Vol. 39, No. 4, pp. 276-283.

Bandeira de Mello, L.A.B., Mourao J.M., Cunha, J.M, Piccolo, A.L., and Klein, M.S., 1996. “25 years of pelletizing at CVRD,” United States.

Barrios, G.K.P., de Carvalho, R.M., Kwade, A., and Tavares, L.M., 2013. “Contact parameter estimation for DEM simulation of iron ore pellet handling,” *Powder Technology*, Vol. 248, pp. 84-93.

Besra, L., Singh, B.P., Reddy, P.S.R., and Sengupta, D.K., 1998. “Influence of surfactants on filter cake parameters during vacuum filtration of flocculated iron ore sludge,” *Powder Technology*, Vol. 96, pp. 240-247.

Bika, D.F., Gentzler, M., and Michaels, J.N., 2001. “Mechanical properties of agglomerates,” *Powder Technology*, Vol. 117, pp. 98-112.

Casagrande, C., Alvarenga, T., and Pessanha, S., 2017. “Study of iron ore mixtures behavior in the grinding pelletizing process,” *Mineral Processing and Extractive Metallurgy Review*, Vol. 38, No. 1, pp. 30-35.

Casey, L., 2015. “Organic binders for iron ore pelletization,” Aalto University School of Chemical Technology, Master’s Thesis, pg. 5.

Cassola, M.S., and Chaves, A.P., 1998. “Effect of the Addition of Organic Binders on the Behavior of Iron Ore Pellets,” *KONA Powder and Particle Journal*, Vol. 16, pp. 136-142.

Cavalcanti, P.P. and Tavares, L.M., 2018. “Statistical analysis of fracture characteristics of industrial iron ore pellets,” *Powder Technology*, Vol. 325, pp. 659-668.

Chakravarty, S., Fischer, M., Bihan, O.L., and Morgeneyer, M., 2019. “Towards a theoretical understanding of dustiness,” *Granular Matter*, Vol. 21, No. 4, pp. 1-22.

Chan, S.Y., Pilpel, N., and Cheng, D.C.-H., 1983. “The Tensile Strengths of Single Powders and Binary Mixtures,” *Powder Technology*, Vol. 34, pp. 173-189.

Chen, T., Liang, L., Tang, S., Luo, Y., Zhao, Y., and Song, S., 2018. "A case study on large-scale grate-kiln production of fluxed iron oxide pellets: Zhanjiang pelletizing plant of BaoSteel," *Mineral Processing and Extractive Metallurgy Review*, Vol. 40, No. 2, pp. 123-128.

Claremboux, V., 2020. "Role of Flocculation and Dispersion in Pelletization of Iron Ore," Michigan Technological University, Master's Thesis, pp. 1-63.

Claremboux, V. and Kawatra, S.K., 2022. "Iron Ore Pelletization: Part III. Organic Binders," *Mineral Processing and Extractive Metallurgy Review*, pp. 1-17.

Coetzee, C.J., 2016. "Calibration of the discrete element method and the effect of particle shape," *Powder Technology*, Vol. 297, pp. 50-70.

Coetzee, C.J., 2017. "Calibration of the discrete element method," *Powder Technology*, Vol. 310, pp. 104-142.

Copeland, C.R., and Kawatra, S.K., 2005. "Dust suppression in iron ore processing plants," *Minerals and Metallurgical Processing*, Vol. 22, No. 4, pp. 177-191.

Copeland, C.R., Eisele, T.C., and Kawatra, S.K., 2009. "Suppression of airborne particulates in iron ore processing facilities," *International Journal of Mineral Processing*, Vol. 93, No. 3-4, pp. 232-238.

Copeland, C.R., Claremboux, V., and Kawatra, S.K., 2018. “A comparison of pellet quality from straight-grate and grate-kiln furnaces,” *Mineral Processing and Extractive Metallurgy Review*.

Delenne, J.-Y., Soulié, F., Youssoufi, M.S.E., and Radjai, F., 2011. “Compressive strength of an unsaturated granular material during cementation,” *Powder Technology*, Vol. 208, No. 2, pp. 308-311.

De Lima, J.R.B., and Chaves, A.P., 1993. “Study of Surface Properties in Agglomeration Processes,” *XVIII International Mineral Processing Congress*, Sydney, Australia, May 1993, pp. 1395-1402.

De Moraes, S.L., de Lima, J.R.B., and Neto, J.B.F., 2013. “Influence of dispersants on the rheological and colloidal properties of iron ore ultrafine particles and their effect on the pelletizing process – A review,” *Journal of Materials Research and Technology*, Vol. 2, No. 4, pp. 386-391.

De Moraes, S.L., de Lima, J.R.B. and Neto, J.B.F., 2018. “Effect of colloidal agents in iron ore processing,” *Mineral Processing and Extractive Metallurgy Review*, Vol. 39, No. 65, pp. 414-419.

De Moraes, S.L., Ribeiro, T.R., 2019. “Brazilian iron ore and production of pellets,” *Mineral Processing and Extractive Metallurgy Review*, Vol. 41, No. 4, pp. 247-254.

De Moraes, S.L., de Lima, J.R.B., Neto, J.B.F, Fredericci, C., and Saccocio, E.M., 2020. "Binding mechanisms in green iron ore pellets with an organic binder," *Mineral Processing and Extractive Metallurgy Review*, Vol. 41, No. 4, pp. 247-254.

De Souza, R.P., de Mendonca, C.F., and Kater, T., 1981. "Production of acid iron ore pellet for direct reduction using an organic binder," Society of Mining Engineers of AIME, Preprint Number 81-359.

Devasahayam, S., 2018. "A novel iron ore pelletization for increased strength under ambient conditions," *Sustainable Materials and Technologies*. https://doi.org/10.1016/j.susmat.2018.e00069

Dwarapudi, S., Gupta, P.K., and Gupta, S.S., 2006. "Application of artificial neural network model to predict reduction degradation index of iron oxide pellets," *Ironmaking & Steelmaking*, Vol. 33, No. 6, pp. 500-506.

Dwarapudi, S. and Rao, S.M., 2007. "Prediction of iron ore pellet strength using artificial neural network model," *ISIJ International*, Vol. 47, No. 1, pp. 67-72.

Eisele, T.C. and Kawatra, S.K., 2003. "A review of binders in iron ore pelletization," *Mineral Processing and Extractive Metallurgy Review*, Vol. 24, pp. 1-90.

Eisele, T.C., Kawatra, S.K., and Ripke, S.J., 2005. "Water chemistry effects in iron ore concentrate agglomeration feed," *Mineral Processing and Extractive Metallurgy Review*, Vol. 26, No. 3-4, pp. 295-305.

E Silva, B.B., da Cunha, E.R., de Carvalho, R.M., and Tavares, L.M., 2018. “Modeling and simulation of green iron ore pellet classification in a single deck roller screen using the discrete element method,” *Powder Technology*, Vol. 332, pp. 359-370.

Erdemli, H., 1982. “CVRD and the Brazilian iron ore industry,” *Minerals and Energy*, Vol. 1, No. 2, pp. 36-47.

Fan, X.-H., Gan, M., Jiang, T., Chen, X.-L., and Yuan, L.-S., 2011. “Decreasing bentonite dosage during iron ore pelletising,” *Ironmaking & Steelmaking*, Vol. 38, No. 8, pp. 597-601.

Fan, X.-H., Ying, L., and Chen, X.-L., 2012. “Prediction of iron ore sintering characters on the basis of regression analysis and artificial neural network,” *Energy Procedia*, Vol. 16, pp. 769-776.

Forsmo, S.P.E., 2006, Apelqvist, A.J., Björkman, B.M.T., and Samskog, P.-O., 2006. “Binding mechanisms in wet iron ore green pellets with a bentonite binder,” *Powder Technology*, Vol. 169, pp. 147-158.

Goetzman, H.E., Bleifuss, R.L., and Engesser, J., 1988. “An investigation of carboxymethylcellulose binders for taconite pelletization,” Society of Mining Engineers, Preprint Number 88-111.

Haas, L.A., Aldinger, J.A., and Zahl, R.K., 1989a. *Effectiveness of organic binders for iron ore pelletization*, No. 9230, US Department of the Interior, Bureau of Mines.

Haas, L.A., Aldinger, J.A., and Nigro, J.C., 1989b. *Utilization of papermill sludges as binders for iron ore concentrate*, No. 9257, US Department of the Interior, Bureau of Mines.

Halt, J.A. and Kawatra, S.K., 2014. "Review of organic binders for iron ore concentrate agglomeration," *Mining, Metallurgy, and Exploration,* Vol. 31, pp. 73-94.

Halt, J.A., Roache, S.C., and Kawatra, S.K., 2015a. "Cold bonding of iron ore concentrate pellets," *Mineral Processing and Extractive Metallurgy Review*, Vol. 36, No. 3, pp. 192-197.

Halt, J.A., Nitz, M.C, Kawatra, S.K., and Dubé, M., 2015b. "Iron Ore Pellet Dustiness Part I: Factors Affecting Dust Generation," *Mineral Processing and Extractive Metallurgy Review*, Vol. 36, No. 4, pp. 258-266.

Halt, J.A. and Kawatra, S.K., 2015. "Iron Ore Pellet Dustiness Part II: Effects of Firing Route on Fines and Dust Generation," *Mineral Processing and Extractive Metallurgy Review*, Vol. 36, No. 5, pp. 193-213.

Halt, J.A. and Kawatra, S.K., 2017a. "Does the Zeta Potential of an Iron Ore Concentrate Affect the Strength and Dustiness of Unfired and Fired Pellets?" *Mineral Processing and Extractive Metallurgy Review*, Vol. 38, No. 2, pp. 132-141.

Halt, J.A., and Kawatra, S.K., 2017b. "Can modified starch be used as a binder for iron ore pellets," *Mineral Processing and Extractive Metallurgy Review*, Vol. 38, No. 2, pp. 73-82.

Han, G. Huang, Y., Li, G., Zhang, Y., Zhou, Y., Jiang, T., 2012. “Optimizing the Mass Ratio of Two Organic Active Fractions in Modified Humic Acid (MHA) Binders for Iron Ore Pelletizing,” *ISIJ International*, Vol. 52, No. 3, pp. 378-384.

Haselhuhn, H.J., Carlson, J.J., and Kawatra, S.K., 2012. “Water chemistry analysis of an industrial selective flocculation dispersion hematite ore concentrator plant,” *International Journal of Mineral Processing*, Vol. 102-103, pp. 99-106.

Haselhuhn, H.J. and Kawatra, S.K., 2015. “Aqueous ions in process water and cake moisture during iron ore filtration,” *Mineral Processing and Extractive Metallurgy Review*, Vol. 36, pp. 370-376.

Huang, Y.-F., Han, G.-H., Jiang, T., Zhang, Y.-B., and li, G.-H., 2013. “Oxidation and sintering characteristics of magnetite iron ore pellets balled with a novel complex binder,” *Mineral Processing & Extractive Metallurgy Review*, Vol. 34, pp. 42-56.

Huttunen, M., Nygren, L., Kinnarinen, T., Häkkinen, A., Lindh, T., Ahola, J., and Karvonen, V., 2017. “Specific energy consumption of cake dewatering with vacuum filters,” *Minerals Engineering*, Vol. 100, pp. 144-154.

Iveson, S.M., Litster, J.D., Hapgood, K., and Ennis, B.J., 2001. “Nucleation, growth and breakage phenomena in agitated wet granulation processes: a review,” *Powder Technology*, Vol. 117, pp. 3-39.

Iveson, S.M., 2002. “Limitations of one-dimensional population balance models of wet granulation processes,” *Powder Technology*, pp. 219-229.

Lelis, D.F., da Cruz, D.G., and Lima, R.M.F., 2019. “Effects of calcium and chloride ions in iron ore reverse cationic flotation: fundamental studies,” *Mineral Processing and Extractive Metallurgy Review*, Vol. 40, No. 6, pp.402-409. DOI: 10.1080/08827508.2019.1666122

Li, C., Bai, Y., Ren, R., Liu, G., and Zhao, J., 2019. “Study of the mechanism for improving green pellet performance with compound binders,” *Physicochem. Probl. Miner. Process.*, Vol. 55, No. 1, pp. 153-162.

Lu, S., Yuan, Z., and Zhang, C., 2018. “Binding mechanism of polysaccharides adsorbing onto magnetite concentrate surface,” *Powder Technology*, Vol. 340, pp. 17-25.

Kakela, P.J., 1981. “Iron Ore: From Depletion to Abundance,” *Science*, Vol. 212, pp. 132-136.

Kapur, P.C. and Fuerstenau, D.W., 1964, “Kinetics of green pelletization,” *Trans. AIME,* Vol. 229, pp. 248-355.

Kapur, P.C. and Fuerstenau, D.W., 1969, “A coalescence model for granulation,” *Ind. Eng. Chem. Process Des. Dev.*, Vol. 8, No. 1, pp. 56-62.

Kawatra, S.K., Eisele, T.C., and Banerjee, D.D., 1998. “Binding iron ore pellets with fluidized-bed combustor fly ash,” *Mining, Metallurgy & Exploration*, Vol 15, No. 2, pp. 20-23.

Kawatra, S.K., Eisele, T.C., Ripke, S.J., and Ramirez, G., 1999. *High-carbon fly-ash as a binder for iron ore pellets*, (No. DE-FG26-97FT97271-01). Federal Energy Technology Center Morgantown (FETC-MGN), Morgantown, WV (United States); Federal Energy Technology Center Pittsburgh (FETC-PGH), Pittsburgh, PA (United States).

Kawatra, S.K. and Ripke, S.J., 2002a. "Pelletizing steel mill desulfurization slag," *International Journal of Mineral Processing*, Vol. 65, No. 3-4, pp. 165-175.

Kawatra, S.K. and Ripke, S.J., 2002b. "Effects of bentonite fiber formation in iron ore pelletization," *International Journal of Mineral Processing*, Vol. 5, No. 3-4, pp. 141-149.

Kawatra, S.K. and Ripke, S.J., 2003. "Laboratory studies for improving green ball strength in bentonite-bonded magnetite concentrate pellets," *International Journal of Mineral Processing*, Vol. 72, No. 1-4, pp. 429-441.

Kawatra, S.K. and Claremboux, V., 2021a. "Iron Ore Pelletization: Part I. Fundamentals," *Mineral Processing and Extractive Metallurgy Review*, pp. 1-16.

Kawatra, S.K. and Claremboux, V., 2021b. "Iron Ore Pelletization: Part II. Inorganic Binders," *Mineral Processing and Extractive Metallurgy Review*, pp. 1-20.

Kawatra, S.K. and Halt, J.A., 2011. "Binding effects in hematite and magnetite concentrates," *International Journal of Mineral Processing*, Vol. 99, No. 1-4, pp. 39-42.

Kotta, A.B., Patra, A., Kumar, M., and Karak, S.K., 2019. “Effect of molasses binder on the physical and mechanical properties of iron ore pellets,” *International Journal of Minerals, Metallurgy and Materials,* Vol. 26, No. 1, pp. 41-51.

Li, C., Bai, Y., Ren, R., Liu, G., and Zhao, J., 2019. “Study of the mechanism for improving green pellet performance with compound binders,” *Physicochem. Probl. Miner. Process.*, Vol. 55, No. 1, pp. 153-162.

Makino, K. and Ohshima, H., 2010. “Electrophoretic mobility of a colloidal particle with constant surface charge density,” *Langmuir*, Vol. 26, No. 23, pp. 18016-18019.

Matuttis, H.G. and Chen, J., 2014. “Understanding the discrete element method: simulation of non-spherical particles for granular and multi-body systems,” John Wiley & Sons, pg. 165.

Meritt, P.C., 1965. “Mesabi enters a New Era,” *Mining Engineering*, Vol. 17, pp. 93-108.

Meyer, K., 1980. *Pelletizing of Iron Ores*, Berlin, Springer-Verleg, pp. 1-302.

McDonald, J.E.D. and Kawatra, S.K., 2017. “Agglomeration of hematite concentrate by starches,” *Mineral Processing and Extractive Metallurgy Review*, Vol. 38, No. 1, pp. 1-6.

Miriyala, S.S. and Mitra, K., 2020. “Multi-objective optimization of iron ore induration process using optimal neural networks,” *Materials and Manufacturing Processes*, Vol. 35, No. 5, pp. 537-544.

Mourão, J.M., 2008. “The growing importance of pelletizing for iron ore mining and iron production,” *2nd International Symposium on Iron Ore,* São Luis, Brazil, pp. 1-13.

Najafabadi, A.H.M., Masoumi, A., and Allaei, S.M.V, 2018. “Analysis of abrasive damage of iron ore pellets,” *Powder Technology*, Vol. 331, pp. 20-27.

Ooi, T.C., Campbell-Hardwich, S., Zhu, D., and Pan, J., 2014. “Sintering performance of magnetite-hematite-goethite and hematite-goethite iron ore blends and microstructure of products of sintering,” *Mineral Processing and Extractive Metallurgy Review*, Vol. 35, No. 4, pp. 266-281.

Pal, J., Arunkumar, C., Rajshekhar, Y., Das, G., Goswami, M.C., and Venugopalan, T., 2014. “Development on Iron Ore Pelletization Using Calcined Lime and MgO Combined Flux Replacing Limestone and Bentonite,” *ISIJ International*, Vol.54, No. 10, pp. 2169-2178.

Poon, J.M.-H, Immanuel, C.D., Doyle, F.J., III, and Litster, J.D., 2008. “A three-dimensional population balance model of granulation with a mechanistic representation of the nucleation and aggregation phenomena,” *Chemical Engineering Science*, Vol. 63, pp. 1315-1329.

Ponomar, V., Yliniemi, J., Adesanya, E., Ohenoja, K., and Illikainen, M., 2022. “An overview of the utilization of Fe-rich residues in alkali-activated binders: Mechanical properties and state of iron,” *Journal of Cleaner Production*, Vol. 330, pp. 129900.

Qiu, G., Jiang, T., Li, H., and Wang, D., 2003. "Functions and molecular structure of organic binders for iron ore pelletization," *Colloids and Surfaces A: Physicochemical and Engineering Aspects,* Vol. 224, No. 1-3, pp. 11-22.

Qiu, G., Jiang, T., Fa, K., Zhu, D., and Wang, D., 2004. "Interfacial characterizations of iron ore concentrates affected by binders," *Powder Technology*, Vol. 139, pp. 1-6.

Quon, D.H.H., and Kuriakose, A.K., 1990. "Pelletizing of iron ore by partial or full substitution of bentonite by organic binders," *Process Mineralogy IX* (eds. Petruk, W., Hagni, R.D., Pignolet-Brandom, S., and Hausen, D.M.), The Minerals, Metals & Materials Society, pp. 119-132.

Ramkrishna, D., 1985. "The status of population balances," *Reviews in Chemical Engineering*, Vol. 3, No. 1, pp. 49-95.

Ripke, S.J. and Kawatra, S.K., 2000. "Can fly-ash extend bentonite binder for iron ore agglomeration?" *Int. J. Miner. Process.*, Vol. 60, pp. 181-198.

Ripke, S.J. and Kawatra, S.K., 2002a. "Effect of cations on iron ore concentrate pellet strength," *2002 SME Annual Meeting*, Feb. 25-27th, Phoenix, Arizona. Society of Mining, Metallurgy & Exploration.

Ripke, S.J., and Kawatra, S.K., 2003. "Effects of cations on unfired magnetite pellet strength," *Miner. Metall. Process.*, Vol 20, pp.153-159.

Rumpf, H., 1962. “The Strength of Granules and Agglomerates,” in *Agglomeration* (ed. Knepper, W.A.), AIME, New York, pp. 379-418.

Sastry, K.V.S. and Fuerstenau, D.W., 1970. “Size distribution of agglomerates in coalescing dispersed phase systems,” *I&EC Fundamentals*, Vol. 7, No. 1, pp. 145-149.

Sastry, K.V.S. and Fuerstenau, D.W., 1971. “A laboratory method for determining the balling behavior of taconite concentrates,” *AIME Trans.*, Vol. 250, pp. 64-67.

Sastry, K.V.S. and Fuerstenau, D.W., 1972. “Ballability index to quantify agglomerate growth by green pelletization,” *AIME Trans.*, Vol. 252, pp. 254-258.

Sastry, K.V.S., and Fuerstenau, D.W., 1975. “Laboratory simulations of closed-circuit balling drum operation by locked-cycle experiment,” *AIME Trans.*, Vol. 258, pp. 335-340.Sastry, K.V.S. and Fuerstenau, D.W., 1977a. “Kinetic and process analysis of the agglomeration of particulate materials by green pelletization,” *Agglomeration* 77, Vol. 1, pp. 381-402.

Sastry, K.V.S. and Fuerstenau, D.W., 1977b. “Kinetics of green pellet growth by the layering mechanism,” *AIME Trans.*, Vol. 272, pp. 43-46.

Sastry, K.V.S. and Gaschignard, P., 1981. “Discretization procedure for the coalescence equation of particulate processes,” *Industrial & Chemical Engineering Fundamentals*, Vol. 20, No. 4, pp. 355-361.

Society of Mining Engineering, 1966. “Iron ore in quiet revolution,” *Mining Engineering*, pp. 48-52.

Sivrikaya, O., Arol, A.I., Eisele, T.C., and Kawatra, S.K., 2013. “The effect of calcined colemanite addition on the mechanical strength of magnetite pellets produced with organic binders,” *Mineral Processing and Extractive Metallurgy Review*, Vol. 34, No. 4, pp. 210-222.

Sposito, G., Holtzclaw, K.M., Charlet, L., Jouany, C., and Page, A.L., 1983. “Sodium-Calcium and Sodium-Magnesium Exchange on Wyoming Bentonite in Perchlorate and Chloride Background Media”, *Soil Science Society of America Journal*, Vol. 47, No. 1, pp. 51-56.

Srivastava, U., Kawatra, S.K., and Eisele, T.C., 2013. “Study of Organic and Inorganic Binders on Strength of Iron Oxide Pellets,” *Metallurgical and Materials Transactions B*, Vol. 44B, pp. 1000-1009.

Stetler, J.J., 1970. “The Pelletizing of Itabira Fines and Blue Dust at Tubarão in Brazil,” Society of Mining Engineers of AIME, Preprint Number 70-L-85, pp. 1-48.

Sze, A., Erickson, D., Ren, L., and Li, D., 2003. “Zeta-potential measurement using the Smoluchowski equation and the slope of the current-time relationship in electroosmotic flow,” *Journal of Colloid and Interface Science*, Vol. 261, pp. 402-410.

Tavares, L.M., and de Carvalho, R.M., 2012. “Modeling ore degradation during handling using continuum damage mechanics,” *International Journal of Mineral Processing*, Vol. 112-113, pp. 1-6.

Tavares, L.M., Cavalcanti, P.P., de Carvalho, R.M., da Silveira, M.W., Bianchi, M., and Otaviano, M., 2018. “Fracture probability and fragment size distribution of fired iron ore pellets by impact,” *Powder Technology*, Vol. 336, pp. 546-554.

Van der Meer, F.P., 2015. “Pellet feed grinding by HPGR”, *Minerals Engineering*, Vol. 73, pp. 21-30.

Verkoeijen, D., Pouw, G.A., Meesters, G.M., and Scarlett, B., 2002. “Population balances for particulate processes – a volume approach,” *Chemical Engineering Science*, Vol. 57, No. 12, pp. 2287-2303.

Wang, D., Servin, M., Berglund, T., Mickelsson, K.O., and Rönnbäck, S., 2015. “Parametrization and validation of a nonsmooth discrete element method for simulating flows of iron ore green pellets,” *Powder Technology*, Vol. 283, pp. 475-487.

Wang, R., Zhang, J., Liu, Z., and Li, Y., 2020. “Effect of lime addition on the mineral structure and compressive strength of magnesium containing pellets,” *Powder Technology*, Vol. 376, pp. 222-228.

Yamaguchi, S., Fujii, T., Yamamoto, N., and Nomura, T., 2010. “KOBELCO Pelletizing Process,” *KOBELCO Technology Review*, No. 29, pp. 58-68.

Yang, R.Y., Yu, A.B., Choi, S.K., Coates, M.S., and Chang, H.K., 2008. "Agglomeration of fine particles subjected to centripetal compaction," *Powder Technology*, Vol. 184, pp. 122-129.

Zhou, Y., and Kawatra, S.K., 2017a. "Pelletization Using Humic Substance-based Binder," *Mineral Processing and Extractive Metallurgy Review*, Vol. 38, No. 2, pp. 83-91.

Zhou, Y., and Kawatra, S.K., 2017b. "Humic Substance-based Binder in Iron Ore Pelletization: A Review," *Mineral Processing and Extractive Metallurgy Review*, Vol. 38, No. 5, pp. 321-337.

Zhou, Y., Zhang, Y., Li, G., Wu, Y., and Jiang, T., 2015. "A further study on adsorption interaction of humic acid on natural magnetite, hematite and quartz in iron ore pelletizing process: Effect of the solution pH value," *Powder Technology*, Vol. 271, pp. 155-166.

Zhou, Y., Zhang, Y., Li, G., and Jiang, T., 2016. "Effects of metal cations on the fulvic acid (FA) adsorption onto natural iron oxide in iron ore pelletizing process," *Powder Technology*, Vol. 302, pp. 90-99.

Zhou, Y., Wattanaphan, P., and Kawatra, S.K., 2017. "Application of Modified Humic Acid (MHA) Binder in the Pelletizing of Fluxed Hematite Concentrate," *Mineral Processing and Extractive Metallurgy Review*, Vol. 38, No. 2, pp. 126-131.

Zhou, Y., Wu, W., Chen, T., and Song, S., 2018. “A case study on large-scale production for iron oxide pellets: Ezhou pelletization plant of the BAOWU,” *Mineral Processing and Extractive Metallurgy Review*, Vol. 39, No. 3, pp. 211-215.

A Copyright documentation

Figure 2.3: Based on Figure 9 from my M.S. thesis, which is my own work which I retain copyright for.

Figure 2.4: Figure 8 from my M.S. thesis, which is my own work which I retain copyright for.

I prepared all other figures utilized in this work.

B Other Works

The following is a list of references for other publications which I have written or contributed significantly to the writing of:

- Zhang, X., Gu, X., Han, Y., Parra-Álvarez, N., Claremboux, V., and Kawatra, S.K., 2021. "Flotation of iron ores: A review," *Mineral Processing and Extractive Metallurgy Review*, Vol. 42, No. 3, pp.184-212.
- Valluri, S., Claremboux, V., and Kawatra, S., 2022. "Opportunities and challenges in CO_2 utilization," *Journal of Environmental Sciences*, Vol. 113, pp. 322-344.
- Kawatra, S.K., and Claremboux, V., 2022. "Iron ore pelletization: Part II. Inorganic binders," *Mineral Processing and Extractive Metallurgy Review*, Vol. 43, No. 7, pp. 813-832.
- Copeland, C.R., Claremboux, V., and Kawatra, S.K., 2019. "A comparison of pellet quality from straight-grate and grate-kiln furnaces," *Mineral Processing and Extractive Metallurgy Review*, Vol. 40, No. 3, pp. 218-223.
- Kawatra, S.K. and Claremboux, V., 2019. "Application of surface chemical fundamentals to improving industrial filtration rates," *Mineral Processing and Extractive Metallurgy Review*, Vol. 40, No. 4, pp. 292-297.
- Claremboux, V., 2020. "Role of flocculation and dispersion in pelletization of iron ore," M.S. Thesis, Michigan Technological University, Houghton, MI.

- Claremboux, V. and Kawatra, S.K., 2022. “Iron ore pelletization: Part III. Organic binders,” *Mineral Processing and Extractive Metallurgy Review*, pp. 1-17.
- Kawatra, S.K. and Claremboux, V., 2022. “Iron ore pelletization: Part I. Fundamentals,” *Mineral Processing and Extractive Metallurgy Review*, Vol. 43, No. 4, pp. 529-544.
- Parra-Álvarez, N., Haselhuhn, H.J., Claremboux, V., and Kawatra, S.K., 2021. “Specifically adsorbed ions in the reverse cationic flotation of iron ore,” *Mineral Processing and Extractive Metallurgy Review*, pp. 1-9.

To-date, these publications together have received 131 citations, resulting in an h-index of 5 and an i10-index of 4.